2009

Surface Water and Groundwater Exchanges in Fine and Coarse Grained River Bed Systems and Responses to Initial Stages of Dam Removal, Milltown, Montana

Anthony Joseph Farinacci

SURFACE WATER AND GROUNDWATER EXCHANGES IN FINE AND COARSE GRAINED RIVER BED SYSTEMS AND RESPONSES TO INITIAL STAGES OF DAM REMOVAL, MILLTOWN, MONTANA

By

Anthony Joseph Farinacci

B.A. Communication Studies, University of Kansas, Lawrence, Kansas, 2001

Thesis

Presented in partial fulfillment of the requirements

for the degree of

Master of Science

The University of Montana
Missoula, MT

May, 2009

Approved by:

Chairman

Dean, Graduate School

Date 4/30/09

SURFACE WATER AND GROUNDWATER EXCHANGES IN FINE AND COARSE GRAINED RIVER BED SYSTEMS AND RESPONSES TO INITIAL STAGES OF DAM REMOVAL, MILLTOWN, MONTANA

By

Anthony Joseph Farinacci

B.A. Communication Studies, University of Kansas, Lawrence, Kansas, 2001

Thesis

Presented in partial fulfillment of the requirements
for the degree of

Masters of Science

The University of Montana
Missoula, MT

May, 2009

Approved by:

Associate Provost of Graduate Education Perry Brown

William Woessner, Chair
Department of Geosciences

Johnnie Moore
Department of Geosciences

Donald Potts
Department of Forestry and Conservation

Farinacci, Anthony, M.S, May 2009 Geosciences

Surface Water and Groundwater Exchanges in Fine and Coarse Grained River Bed Systems and Responses to Initial Stages of Dam Removal, Milltown, Montana

Chair: Dr. William Woessner WWW

More than 620,000 miles of rivers are affected by over 79,000 dams in the United States. The dams are a valuable asset, however dams block fish passage, and disrupt the physical and biological systems, and alter hyporheic exchange. In efforts to remediate rivers impacted by dams, dam removal is being proposed. Changes in the location and timing of groundwater and river water exchanges in post dam remediated river systems are typically not identified. The goal of this study was to examine the factors controlling surface water and groundwater exchange rates and locations in river systems during dam removal. Specific tasks included establishing a river elevation and groundwater elevation monitoring network, defining riverbed properties and exchange rates using in-riverbed measurements, developing a site conceptual model for different river reaches, and constructing and calibrating a finite difference numerical groundwater model representing site conditions. Results of monitoring indicate that the Clark Fork River above the dam and reservoir is connected to the aquifer system, containing losing and gaining and parallel flow reaches. The Clark Fork River below the dam appears to be gaining approximately 600 ft below the dam and then becomes a perched losing river that at times throughout the year may become linked to the underlying water table. The reservoir pool and its Blackfoot River arm are losing systems with pool elevations well above the local water table. In-river measurements indicate the river and groundwater exchange water at a rate of 0.02 to 13 $ft^3/(dayft^2)$. A calibrated numerical groundwater model was used to examine how pre-dam removal groundwater, river and reservoir exchanges were likely to change once the dam is removed. Simulations suggest that historically (with the dam) the reservoir contributed approximately 21% of the recharge to the local Milltown aquifer system. Once the dam is removed this recharge contribution may be reduced to less than 1%. As a result water table elevations will decrease locally and exchange locations and rates above the dam location will be altered. Reducing uncertainty of the modeling results and predictions could be improved by further data collection and evaluation of various conceptual models.

ACKNOWLEDGEMENTS

Funding for this project was provided by the Montana State Department of Environmental Quality and the Missoula County Water Quality District. I would like to thank Dr. William Woessner for his superb guidance and support throughout this project. I would like to thank my committee members Dr. Johnnie Moore and Dr. Donald Potts for being on my committee. Christine Foster and Loreene Skeel provided budget and office support that kept the project rolling. Without the additional support and partnership with Tony Berthelote many aspects of this project would not have happened. Tony was there for the majority of the project and contributed in many ways ranging from floating the river with to help collect in-river measurements, to taking over the monitoring network to continue the project, to spending long hours on the computer to with me to assist with model construction and calibration. Additionally, I would like to thank Meryll Storb for also continuing the water level monitoring and providing additional project support. Of course, none of this would have been possible without the help from my many field assistants: Andy Bookter, Toby Meierbachtol, Antony Berthelote, Meryl Storb, Joeseph Gortzen, Benson Cooke, and Brennan. Ongoing encouragement from my friends, family and my wife, Joni, helped provide the motivation necessary to complete this project. Thank you to all who helped.

TABLE OF CONTENTS

Tables

CHAPTER 1
INTRODUCTION

The 3.6 million miles ($5.79x10^6$ km) of rivers in the United States (EPA, 1998) provide society with transportation routes, hydroelectric power, water for agricultural, industrial and municipal supplies (NRC, 1992), and areas for recreation. River ecosystems cycle and chemically transform nutrients, attenuate floods, and respond to river flows and temperatures (Kauffman et. al, 1997). Unfortunately, river systems have become degraded as demands for services increase. One cause for degradation is the installation of dams. More than 620,000 miles of rivers are affected by over 79,000 dams in the United States (Echeverria et. al, 1989; USACE, 1999). Dams store water manipulate flow regimes, generate energy (Giesecke, 2006), and disrupt the associated physical and biological systems (Battala et. al., 2004; Doyle et al., 2005; Graf, 2006; lytle and Poff, 2004; Magilligan and Nislow, 2006; Poff et. al, 2006, Petts, 1984). In addition to affecting surface water systems, dams alter the rates and locations of hyporheic exchange (Alexander and Caissie, 2003; Dahm et. al, 1998; Hayashi and Rosenberry, 2002; Hendricks and White, 1991; Palmer, 1993; Pusch et. al, 1998; Stanford, 1998; Standford and Ward, 1993; Valett et al., 1990).

In efforts to remediate river systems impacted by dams, dam removals are being proposed (Pedjar and Warner, 2001, Pohl, 2002). Following dam removal, a river system undergoes changes. The driving force of these changes is the new hydrologic regime (Power et al., 1995, Poff et al., 1997); a regime that modifies channel morphology (William and Wolman, 1984), and ground water, river, and floodplain exchange processes (Kondolf, G.M., 1998; Graf, 2006). Attempts to determine the river and groundwater exchange processes, and the changes that take place during dam removal are not well documented and needs further elucidation especially at the floodplain scale.

The first challenge in documenting surface water and groundwater exchange rates is choosing an appropriate technique to determine spatial and temporal changes in surface water and groundwater exchange (Scanlon et al., 2002). This study attempted to spatially and temporally define the principal drivers of surface water and groundwater exchanges before and after a pre- dam removal drawdown.

Scope and Objectives

The purpose of this study was to monitor and forecast the changes in groundwater flow and surface water and groundwater exchanges during initial phases of dam removal. Of particular interest was to determine the key drivers of surface water and groundwater exchange rates and patterns and how they are or will likely be impacted by river and reservoir stage alterations. Though an investigation evaluating the impact of dam removal on river-groundwater exchange would be best initiated prior to any disturbance or change in the hydrologic system, this project received support 1 month after a pre-dam removal 12 feet drawdown occurred, thus limiting the direct comparison of impacts with baseline conditions.

Data were collected and evaluated for a site where a 30 ft high dam is located at the confluence of two major gravel-bedded rivers in western Montana. Specific project objectives included: 1) defining aquifer boundaries and hydrogeologic properties; 2) establishing river/reservoir stage-groundwater relationships; 3) quantifying river/reservoir exchange rates and locations; 4) developing and testing a conceptual groundwater model; 5) evaluating the appropriateness of the conceptual model and identifying the key drivers that control and dominate observed aquifer responses to allow for the prediction of future aquifer and exchange responses in a dam removal setting.

Site History and Setting

The 30 feet high Milltown Dam and Milltown Reservoir are located about 5 miles east of Missoula, Montana at the confluence of the Clark Fork and Blackfoot rivers (Figure 1). The communities of West Riverside, Milltown, and Bonner are located adjacent to the reservoir. Residents in these communities rely on over 400 shallow domestic wells penetrating the valley unconsolidated unconfined aquifer for water supply

The mean annual temperature and mean annual precipitation (records 1971-2000) are 44.8^{o}F and 13.82 inches, respectively (http://www.ncdc.noaa.gov)). The Clark Fork River at Turah (USGS station #12334550) has a mean annual flow of 1,182 cfs based on 22 years of record and 2,902 cfs above Missoula based on 77 years of record (USGS station #12340500). The Blackfoot River mean annual discharge based on 71 years of record is 1,562 cfs at a gauging station located 7 miles up river of the confluence (USGS station #12340000). Historical flows of the Clark Fork and Blackfoot Rivers show that the rivers peak flows usually occur in late May to early June and base flow conditions usually begin in August to September and end at the onset of runoff which occurs in March (Figure 2).

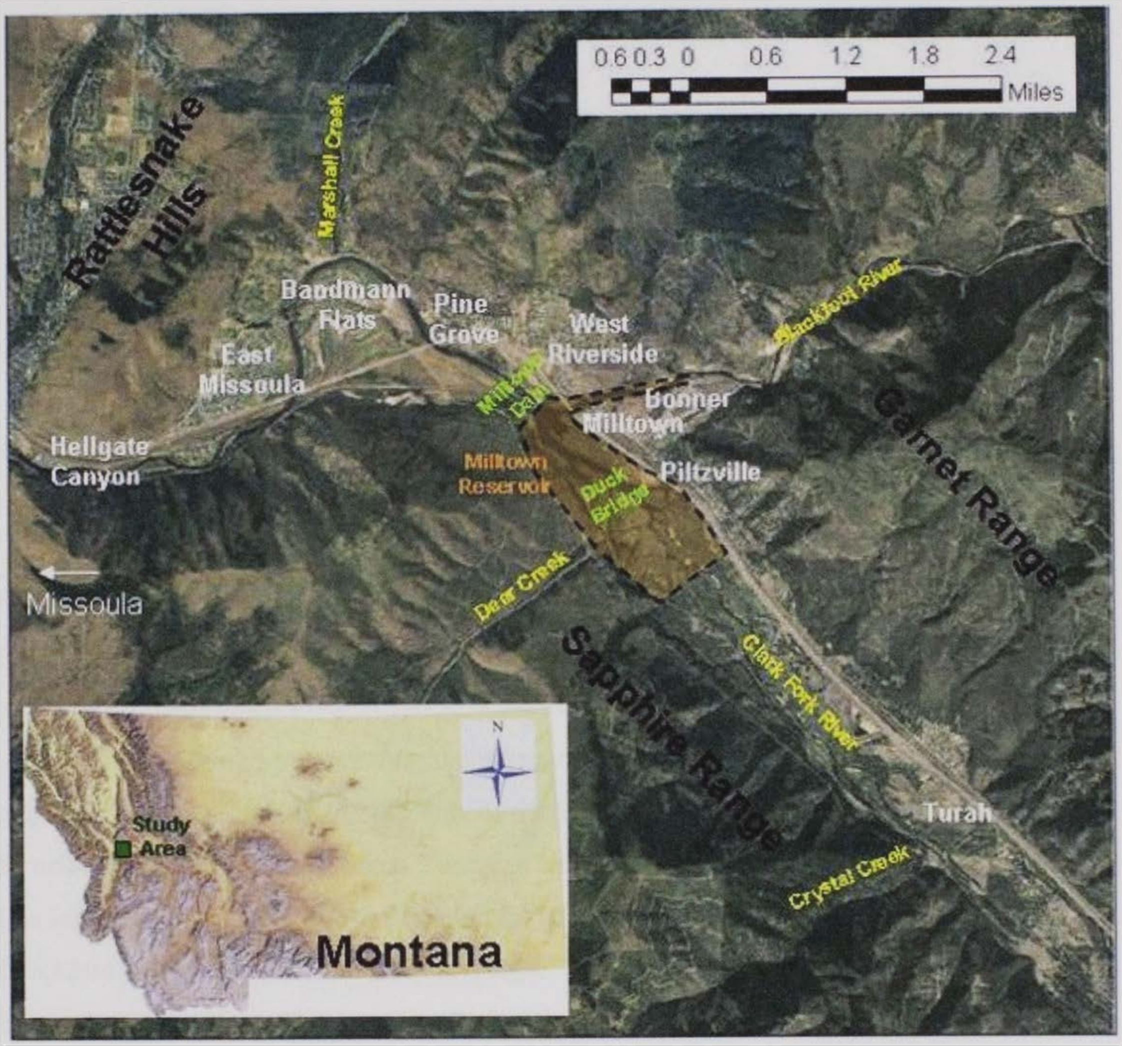

Figure 1 Vicinity map and site map of the area surrounding the Milltown Reservoir Superfund Site.

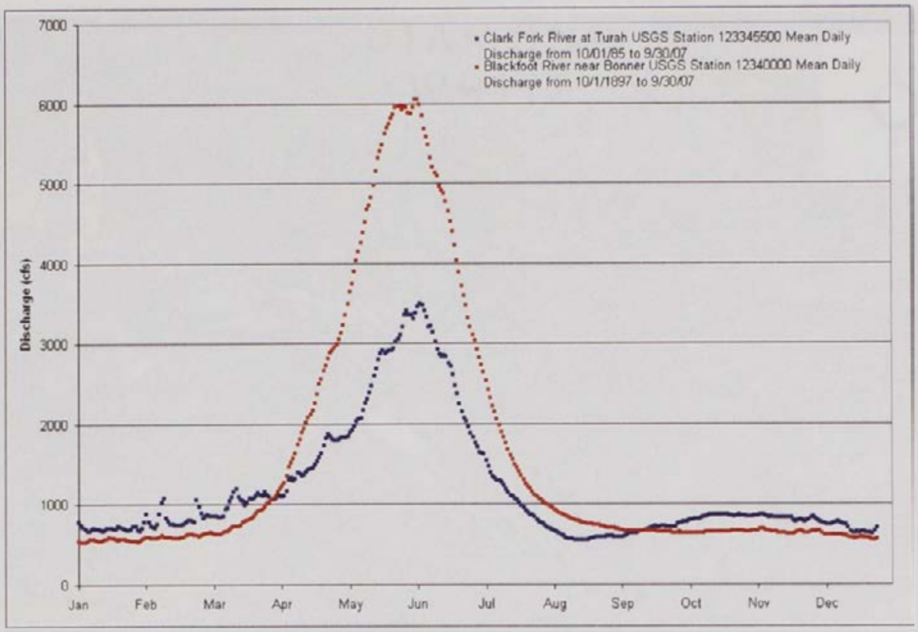

Figure 2 Mean daily discharge recorded at USGS river gauging stations at the Clark Fork River at Turah Bridge (blue) and the Blackfoot River near Bonner, MT (red).

Historically, the Milltown Reservoir elevation was maintained at 3260 ft (NAVD 88). The level would typically fluctuate with river stage no more than a few feet. From time to time reservoir drawdowns would occur and last for about 1 month, but were only temporary.

The mountains surrounding the narrow river valleys are composed of argillite, quartzite and limestone metasediments of the Precambrian Belt Series (Figure 3). Structurally, the Clark Fork Shear Zone can be traced along the Clark Fork River valley. It is intersected in the Milltown area by the Blackfoot thrust that is coincident with the Blackfoot Valley (Nelson and Dobell, 1961). The valley sediments overlying the Precambrian Belt Series bedrock are Pleistocene to Recent fluvial sand, gravel, cobbles and boulders.

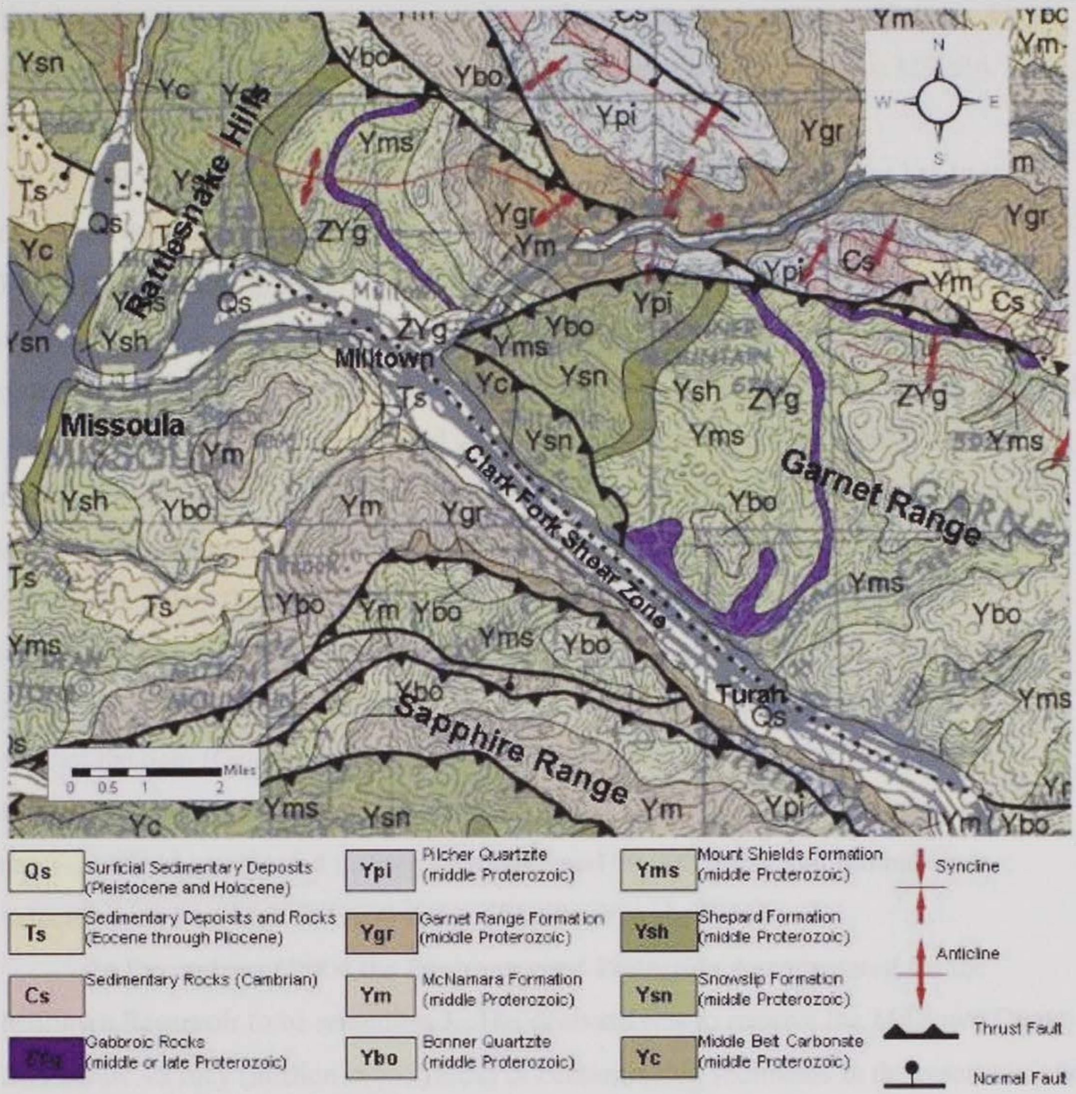

Figure 3 Geologic map of the study area after (Lewis R.S., 1998). This map shows the geologic complexity of the area.

Milltown dam was built in 1907. In 1908, a +100 year flood damaged the dam and it was repaired. Since that time up river sediment has been accumulating in the reservoir. In 1981, the Montana Department of Health and Environmental Sciences discovered ground water from four wells located in the community of Milltown contained elevated concentrations of dissolved arsenic (100 to 500 ug/l)(Woessner et al., 1984). After several hydrogeologic investigations of the sand, gravel, cobble and boulder dominated unconfined groundwater system (Woessner and Popoff, 1982; Woessner et al.,

1984) the source of contamination was determined to be the reservoir sediment. These sediments had become impacted by up river mining and smelting wastes. USEPA designated the reservoir sediments as a CERCLA site in 1983.

The bedrock bounded 20 to 200 ft thick unconfined valley aquifer has been described by a number of investigators from the 1980's through the 1990's (Arco, 1995; Brick, 2003; Gestring, 1994; Moore and Woessner, 2002; Tallman, 2005 and Woessner et al., 1984, Udaloy, 1988; Arco 2002, Western Consultants et al., 2005). Generally, groundwater levels fluctuate from 2 to 10 ft with the highest elevations in the spring and lowest in the winter. The dominated groundwater flows down valley and from the reservoir to the north and northwest (Woessner et al., 1984). A plume of arsenic and metal rich groundwater originates from the reservoir sediments, moves vertically downward, enters the underlying old floodplain gravel and flows to the north and northwest (Moore and Woessner, 2002). The rivers leak water to the aquifer and are principal sources of recharge in the vicinity of the reservoir and the valley area down river of the dam (Gestring, 1994). Groundwater discharges as underflow through Hellgate Canyon (Gestring, 1994; Tallman, 2005). Hydraulic conductivities of the aquifer have been reported to vary between 2 and 60,000 ft/day and groundwater velocities can be a high as 1,900 ft/day (Woessner et al., 1984).

In December of 2004 the Environmental Protection Agency opted for the Milltown Reservoir to be remediated. The decision was to remove the Milltown Dam, 2.51 of the +8 mcy (million cubic yards) of contaminated sediments in the reservoir, and remediate portions of the river channels. As planned, the dam will be removed in a series of three phases. During each phase the reservoir will be drawn down to prepare for the dam removal and reestablishment of the two "free flowing" river channels. The three planned phases are: phase 1 a 10 ft drawdown(June 1st, 2006) ; phase 2 a 12 ft drawdown (March, 2008); phase 3 a 3 to 8 ft drawdown (dam out).

Removing the Milltown dam is anticipated to lower groundwater levels, change flow directions in portions of the aquifer, and alter the magnitude and locations of surface water and groundwater exchanges.

Prior to this investigation, two groundwater modeling efforts were conducted to evaluate groundwater conditions in the Milltown area. These efforts used two dimensional numerical groundwater models to understand what factors control the groundwater system in the vicinity of the reservoir (Gestring, 1994) and how dam and reservoir removal would likely impact the adjacent groundwater system (Figure 4) (Brick, 2003). Gestring (1994) suggested that the northward flowing contaminated groundwater leaving the reservoir likely discharges to the Clark Fork River immediately down river of the dam. He also suggested leakage of water through the river beds contributed up to 50 percent of the aquifer recharge. Brick's (2003) work suggested that after dam removal and river restoration (as planned in 2003) the water table would decline about 10 to 15 ft in the area currently occupied by the reservoir, about seven feet of north of the reservoir in the Milltown area, 3-5 ft in West Riverside, and 2-3 ft in the Piltzville area (Figure 5).

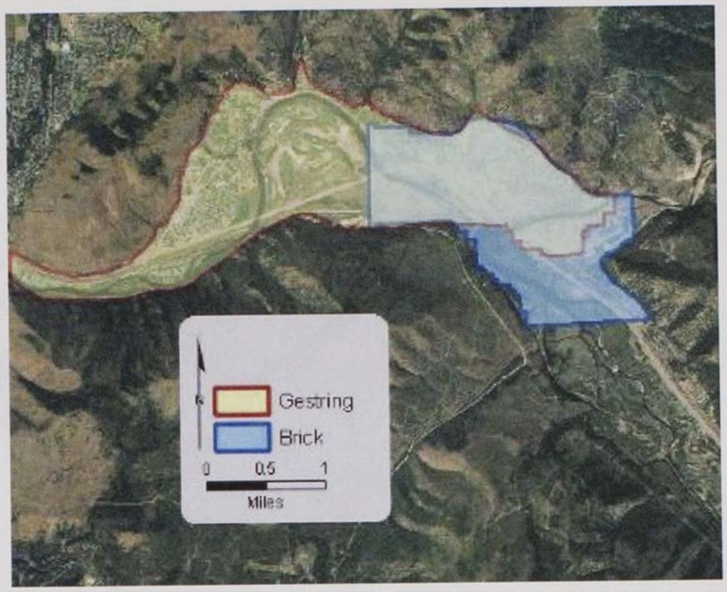

Figure 4 Representation of the areas previously modeled. The yellow region was previously modeled by (Gestring, 1994) and the blue region was previously modeled by (Brick, 2003) , with the green area being overlap from both models.

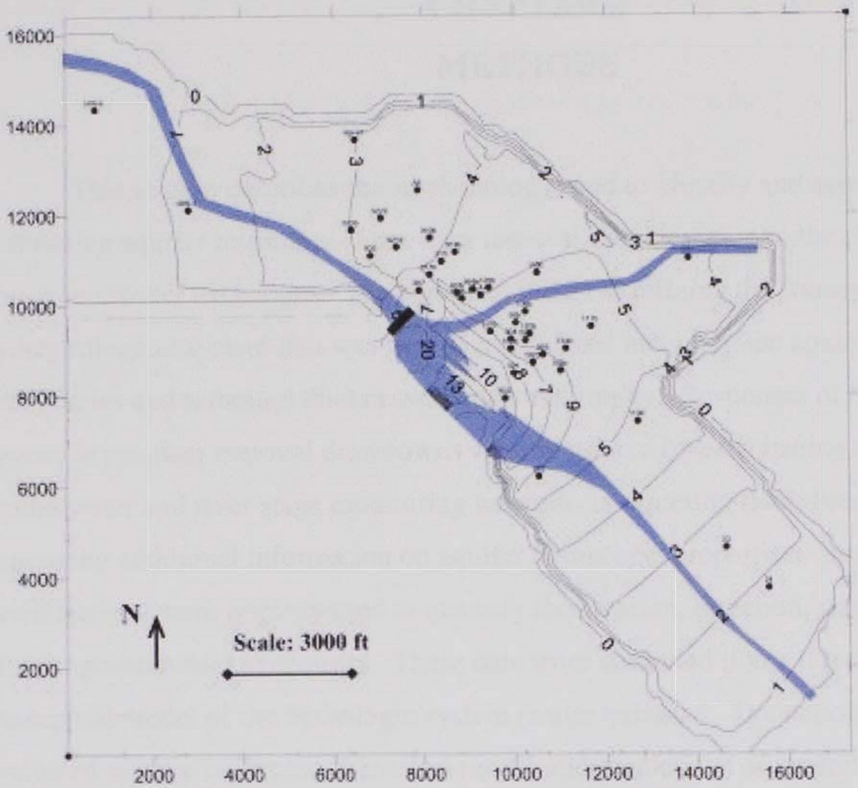

Figure 5 Contour map of predicted water table decline (ft) after dam and sediment removal (Brick, 2003).

CHAPTER 2

METHODS

This section describes the methodology used to identify and assess the processes controlling aquifer responses to pre-dam removal drawdowns, and the changes to river and groundwater exchanges. The approach included refining the framework of the hydrogeological system that was previously defined including the aquifer geometry (boundaries and saturated thicknesses) and stratigraphy. Responses of the groundwater system to pre-dam removal drawdowns were measured by establishing an extensive groundwater and river stage monitoring network, interpreting flow directions, and generating additional information on aquifer hydrologic properties. Specific investigations were implemented to quantify the location, direction, rates and magnitude of river groundwater exchanges. These data were compiled into a three-dimensional conceptual model of the hydrologic system (water balance). The conceptual model was evaluated using a calibrated numerical model and predictions of groundwater level impacts from previous and future pre-dam removal drawdowns were evaluated

Refinement of the Aquifer Framework

Aquifer boundaries were delineated by mapping the alluvial surface and bedrock contacts, examining water table maps, and estimating the location of the bedrock and elevations of subsurface valley sides from geophysical studies, and bore hole and well log data.

The bedrock base and sides of the valley aquifer were refined using previous surface geophysical studies (Blackhawk Geophysical that used depth to bedrock seismic lines (Arco, 1995), constrained gravity (Nyquist, 2001)), and new gravity studies and data analyses preformed by Berthelote et al. (2007). These studies were calibrated using borehole data produced by Montana Power Company (dam repair data) and new construction boring data (Envirocon, 2006). Previously reported bedrock boundary mapping (Nyquist, 2001; Brick 2003) was combined with new gravity data sets and interpreted to generate a three-dimensional bedrock elevation surface in GIS (Berthelote et al., 2007). These interpretations were then used to generate an aquifer thicknesses map and surface.

A hydrostratigraphic framework of the valley fill aquifer was developed by gathering well and borehole logs (Brick, 2003; Gestring, 1994; Woessner et al., 1984, Montana's Ground-Water Information Center (http://mbmggwic.mtech.edu/)), entering the geologic data into a data base (RockWorks® Borehole Software), and constructing geologic cross-sections and fence diagrams. These cross-sections were then interpreted by lumping similar zones into three principle hydrostratigraphic units: Unit 1 (coarse sand and gravel), Unit 2 (silty sand to sandy silt) and Unit 3 (sand and gravel with clay) after Woessner (1988) and Tallman (2005).

Groundwater Conditions

A network of monitoring wells was established in March 2006 to monitor groundwater elevation responses to reservoir drawdowns and to describe general properties of the alluvial groundwater system. The selection of wells to be included in the monitoring network was based on extensive review and compilation of historical data (Gestring, 1994; Harding Lawson Associates (HLA), 1987; Arco, 2005; Tallman, 2005; Woessner et al., 1984), a plan to both re-occupy wells with historical water level data, the need to establish a higher resolution of observations proximal to the reservoir, and coverage of a large study area. Initially, 51 wells formed the groundwater monitoring network that extended from Hellgate Canyon to Turah Bridge on the Clark Fork River and about 3 miles up river on the Blackfoot River (Figure 6). This monitoring network was set up in cooperation with the Montana Department of Environmental Quality and the Missoula County Water Quality District as part of the Milltown Reservoir Sediments Operable Unit Remedial Action Monitoring Plan (Envirocon, 2006).

Groundwater levels at 22 of these wells were recorded at intervals no greater than 60 minutes using Solinst® continuous water level recorders (recording pressure transducers corrected for barometric pressure changes with readings from separate Solinst® barologgers). At all network wells from June 1st to about July 15th, 2006 weekly hand measurements were collected using an electric water level tape. After July 15th, 2006 monthly manual monitoring was conducted.

To tie river stage with ground water elevations, a network of surface water stage gauges was established (Figure 6). Surface water elevations were obtained from USGS gauging locations on the Blackfoot River at Bonner (#12340000), Clark Fork River at Turah (#12334550) and Clark Fork River above Missoula (#12340500)). This river stage data was supplemented with project installed staff gauges and a continuous water level recorder operated at the Milltown dam (Figure 6). Initially, the staff gauge spacing was set up at approximate equal distant intervals along the river channels or where access was attainable. Both river stage gauges and wells that did not have previously established elevations were surveyed using a real-time kinematic survey-grade Trimble 5800 GPS surveyor using standard techniques. Water level data were analyzed by constructing well hydrographs, flow nets and regional water table maps.

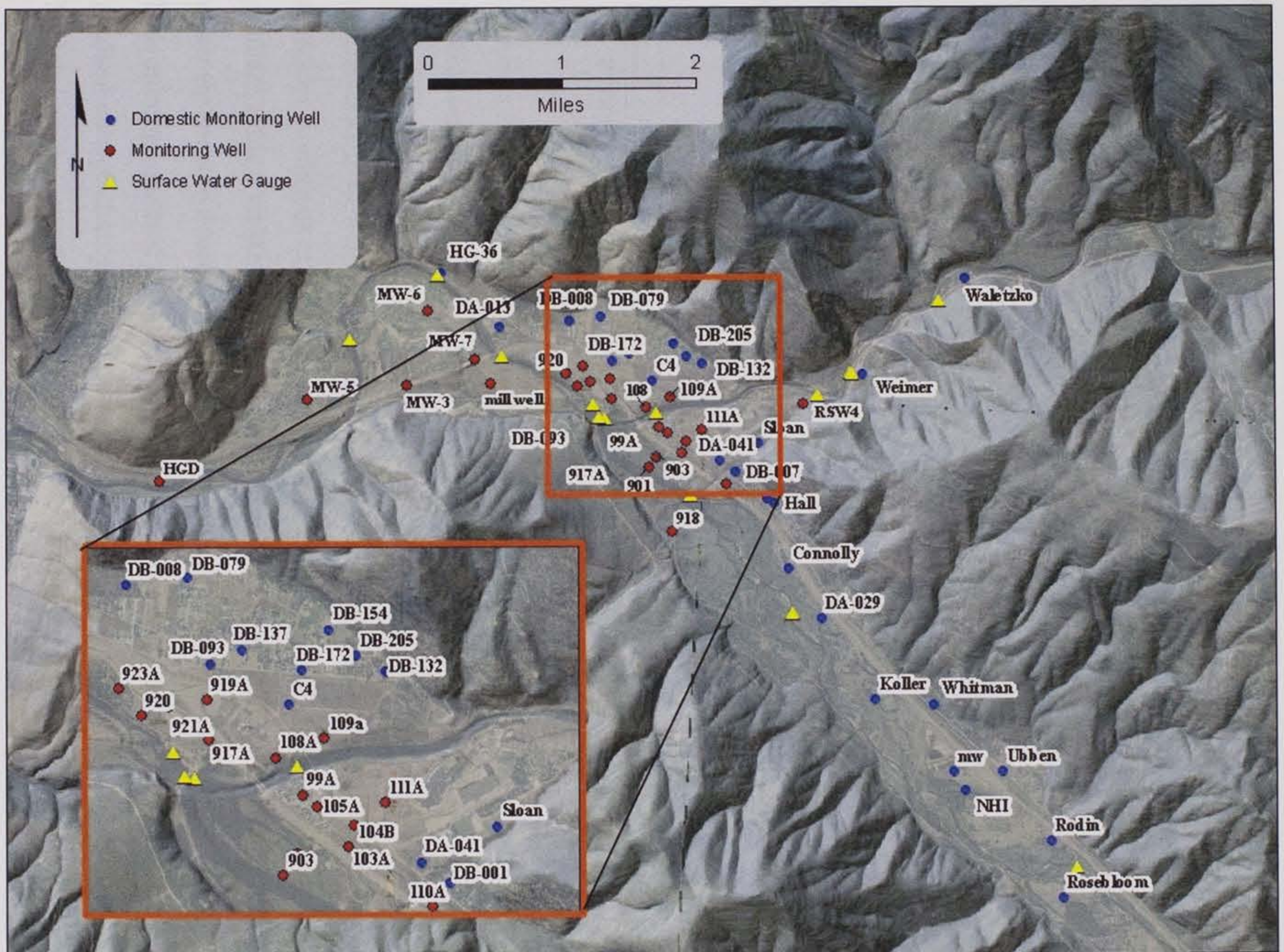

Figure 6 Monitoring Network. (Map created in Arc Map with DEM from www.mapmart.com and 1-meter resolution state wide color aerial photo from the Natural Resource Information System 2005).

Aquifer property information, including hydraulic conductivity and specific yield, were complied from existing studies (Woessner et al., 1984; Arco, 1995; and Newman, 1996). The hydraulic conductivity data sets were supplemented by analyzing well hydrograph data using stage peak lag time methods (Pinder et al., 1969), and flow net analyses (Fetter, 2006). Pinder et al. (1969) derived a method to use river stage and corresponding groundwater level changes to estimate intervening hydraulic conductivities. The method was applied to evaluate the lag response between up-gradient wells and down-gradient wells along a common flow path:

$$h_p = \sum_{m=1}^{p} \Delta H_m \left\{ erfc \frac{u}{2\sqrt{p-m}} \right\} \tag{1}$$

where: the change in hydraulic head is represented by h_p; the change in the up gradient well water level for every time interval as ΔH_m; u can be calculated by the equation:

$$u = \frac{x}{\sqrt{v\Delta t}} \tag{2}$$

where: x is the distance between the wells ; Δt is the time interval; v is the diffusivity (transmissivity divided by the aquifer storativity).

A second approach to examine the likely spatial variation of hydraulic conductivity used water table maps with flow lines added, flow nets. These flow nets represent conditions at a single time (steady state). Mapped changes in the hydraulic gradient along a single flow tube were interpreted to represent proportional changes in either the local hydraulic conductivity or saturated cross sectional area, or both. Determining saturated thickness from bedrock boundary and water table data resolved gradient changes likely caused by variations in the flow tube cross sectional area. Hydraulic conductivities were then estimated using Darcy's Law:

Q=KIA

where: Q = Discharge; K = hydraulic conductivity; I = hydraulic gradient; A = saturated cross sectional area.

Determining the rates, locations and magnitudes of the exchange of surface water and groundwater

The river and reservoir influences on the adjacent aquifer system were evaluated by documenting the observed response of the groundwater system to the planned initial pre-dam removal drawdown of 12 ft, physically instrumenting river channel bed sediments to derive vertical hydraulic gradients, groundwater velocities and hydraulic conductivities. These data were then used to compute groundwater-river exchange rates.

As the intense hydrologic data collection was initiated just after the initial stage of the first pre-dam removal reservoir drawdown , quantitatively determining the response of the adjacent aquifer required a comparison of historical water level data with observed post drawdown water levels. Groundwater level data collected by Gestring (1994) was selected for comparison as it was the most spatially extensive and appeared to represent a similar climate/runoff period (1992-1993) (Figure 7). Drawdown water level impacts were illustrated by plotting hydrographs of wells using Gestring's data and if available other historical water level data collected at that well to show both recorded 1992-1993 water level variation and the likely range of historical water level changes at a particular location. Water table maps constructed from post drawdown data were compared to Gestring's maps for similar time periods. This qualitative analyses yielded ranges of water level changes at historical well sites.

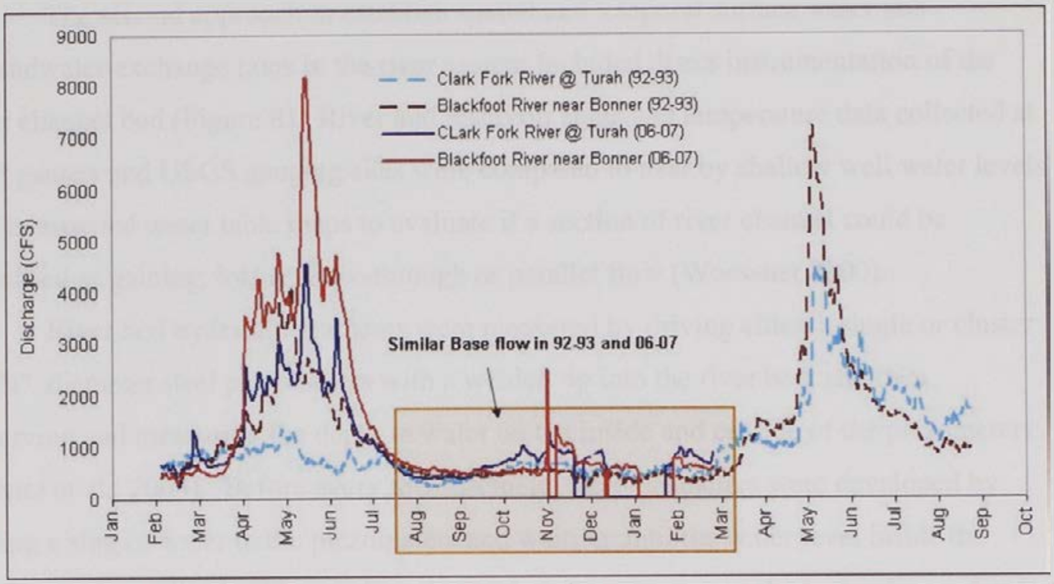

Figure 7 River hydrographs for the Clark Fork River and the Blackfoot River for 1992-1993 and 2006 to 2007. The shaded block indicates base flow periods.

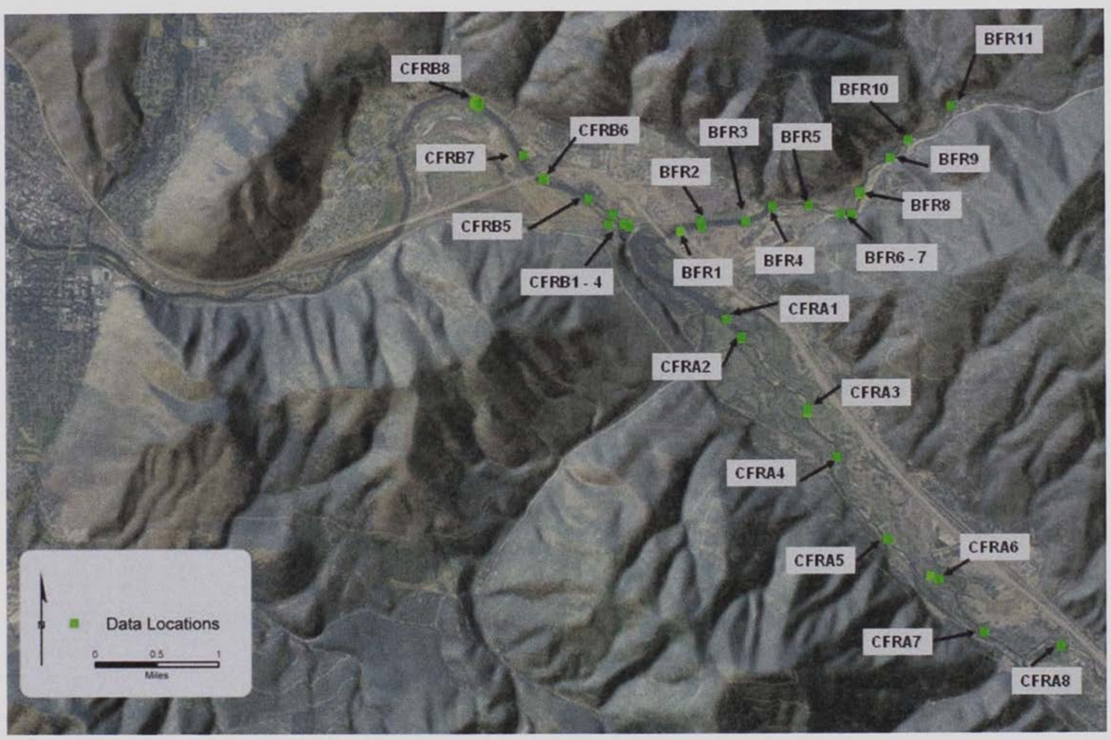

Figure 8 A map illustrating the locations where river VHG's and seepage rates were investigated.

The second approach to establish spatial and temporal surface water and groundwater exchange rates in the river system included direct instrumentation of the river channel bed (Figure 8). River and reservoir stage and temperature data collected at staff gauges and USGS gauging sites were compared to near by shallow well water levels and interpreted water table maps to evaluate if a section of river channel could be classified as gaining, losing, flow-through or parallel flow (Woessner 2000).

River bed hydraulic gradients were measured by driving either a single or cluster of ¾" diameter steel piezometers with a welded tip into the river bed, and then observing and measuring the depth to water on the inside and outside of the piezometers (Baxter et al., 2003). Before every measurement, the piezometers were developed by adding a slug of water to the piezometers and waiting until the water level inside the piezometers stabilized. When only a single piezometer was used the hydraulic gradients were measured at three different depths in the river bed (Figure 9). All gradients were estimated using the following equation:

$$i_v = \Delta h / \Delta l \qquad (3)$$

Where

i_v = vertical hydraulic gradient

Δh = difference between the river level and the head inside the piezometer

ΔL = depth to the center of the 3 in long perforated interval located just above the drive tip below the river bed

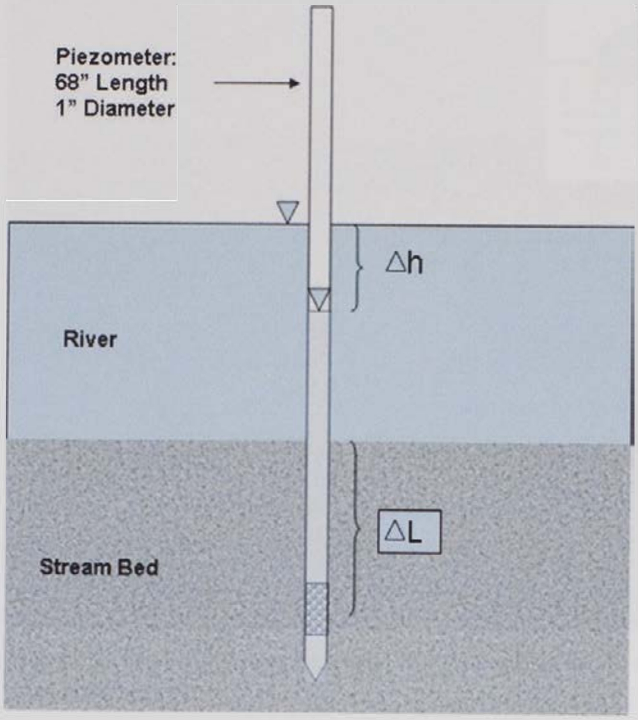

Figure 9 Schematic showing the measurements needed to estimate the vertical hydraulic gradient (VHG).

Three dimensional vertical hydraulic gradients were determined in the Clark Fork and Blackfoot river channels using clusters of in-river mini piezometers located every ~3000 ft down river from site boundaries (Tallman, 2005). At each location 6 piezometers were driven into the river bed at three different depths (ranged from 1 ft to 3 ft below the river bed)(Figure 10). The hydraulic heads at each depth were used to generate a two dimensional surface of hydraulic head. Each surface was then scaled vertically and the gradient and flow direction estimated. Gradient data sets provide information on the three-dimensional direction of exchange at a site. The exchange rate was then computed using gradient values, and a measurement of bed hydraulic conductivity.

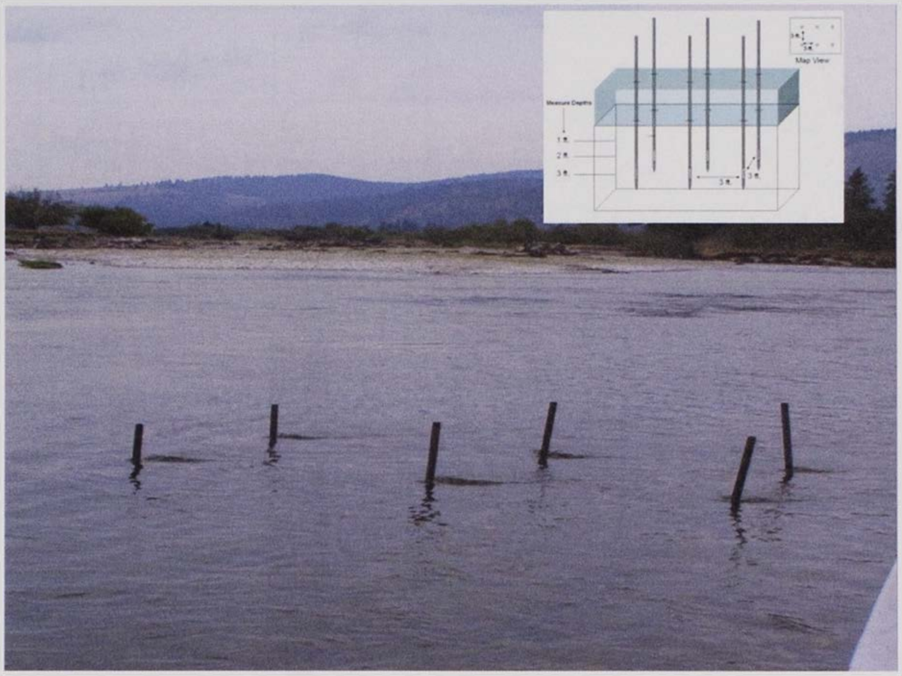

Figure 10 Photograph and schematic illustrating how the three dimensional riverbed gradients were investigated.

River bed hydraulic conductivity values were established by conducting falling head tests in piezometers installed in the river bed throughout the study area (Bouwer and Rice, 1989). A small diameter piezometer was driven into the river bed and outfitted with a larger diameter riser that was filled completely with river water. At the start of the analyses the elevation was recorded, and then again at a later time. The falling head tests were analyzed using the Bouwer and Rice slug test method (1989) to determine horizontal hydraulic conductive values. The vertical hydraulic conductivity was estimated by assuming the horizontal to vertical ratio is 10/1 (Anderson and Woessner, 1992).

$$K = \frac{r_c^{\,2} \ln(\frac{R_e}{R_w})}{2L_e} \frac{1}{t} \ln(\frac{y_o}{y_t}) \qquad (4)$$

where:

$$\ln\left(\frac{R_e}{R_w}\right) = \left[\frac{1.1}{\ln\left(\frac{Lw}{rw}\right)} + \frac{A + B\ln\left[\frac{(H - Lw)}{rw}\right]}{\frac{L_e}{rw}} \right]^{-1} \tag{5}$$

The terms A and B are dimensionless values determined from a chart and are a function of L_e/rw. All other terms are defined in Figure 11.

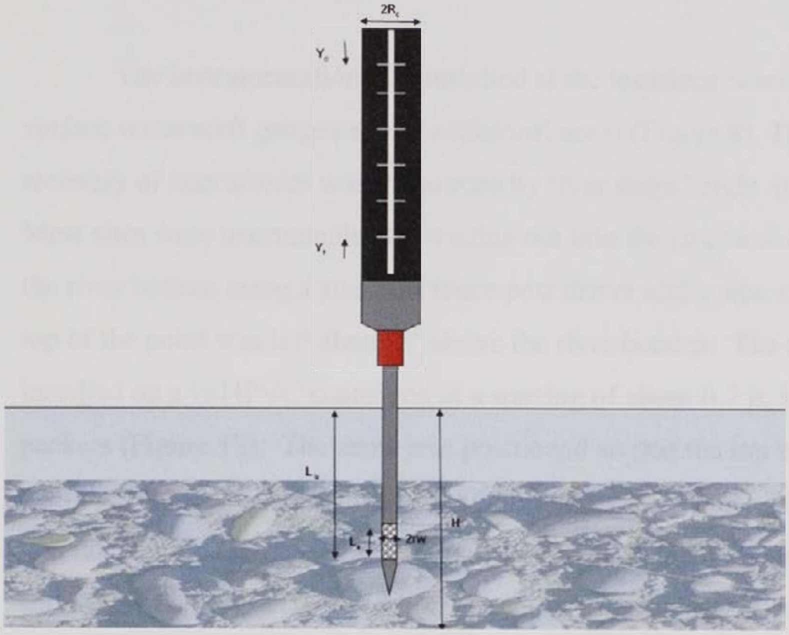

Figure 11 Schematic showing permeameter used to conduct slug test and measured variables necessary to compute horizontal hydraulic conductivity with the Bouwer and Rice slug test method (1989).

The vertical hydraulic conductivity estimates were combined with the vertical gradient data to compute river bed fluxes and discharges per unit river bed area using Darcy's Law (Scanlon et al., 2002).

Temperature profile monitoring techniques were also applied to determine in bed exchange direction and rates (Constantz et al., 2003). One and a quarter inch diameter four feet long well points (Campbell Manufacturing, LLC) were driven into the river bed and outfitted with a string of isolated temperature monitors. River and bed water temperatures were recorded with Thermocron iButton® temperature recording devices (Johnson et al., 2005). Table 1 presents the duration of temperature monitoring at each location. Temperatures were recorded at 15 minute intervals.

Data Collection Locations	Temperature Collection Dates
CFRA2, CFRA5, CFRA8, CFRB6	8/24/06 to 11/12/06
CFRA3	5/18/06 to 7/8/06
CRRB8a and CFRB8d	6/20/06 to 8/6/06
BFR2	7/31/06 to 10/10/06

Table 1 The dates and locations at which in-river bed temperatures were collected.

The instrumentation was installed at the locations coincident with project installed surface water staff gauges and in additional areas (Figure 8). The installation and recovery of instruments was influenced by river stage height and river bed accessibility. Most sites were instrumented by wading out into the river and driving the sandpoint into the river bottom using a standard fence post driver and a pipe extension. The threaded top of the point was left about 2" above the river bottom. The temperature array was installed on a ½ HPVC center rod at a spacing of about 0.7 ft, isolated by duct tape packers (Figure 12). The array was positioned so that the top temperature monitor sensed the river temperature. The top of the point was then sealed with a galvanize cap. At several locations where the sandpoint was driven in the river bed so that the top button was below the river bed, an additional temperature button was attached to the outside of the sandpoint with a piece of wire to record the river temperature. At sites BFR1 and BFR2 the depth of water was approximately 9 ft and the sand point and instrument array was installed using a raft (Figure 8). The raft was anchored to the river bottom and pipe extensions were added to the end of the sandpoint so the top of the casing would reach the surface. The sand point was instrumented prior to installation in the river bed and a diver was used to control the depth to which the sandpoint was driven. Pipe extensions were then removed and the point was capped by an underwater diver. A diver was also used to then retrieve the instrumentation after data collection.

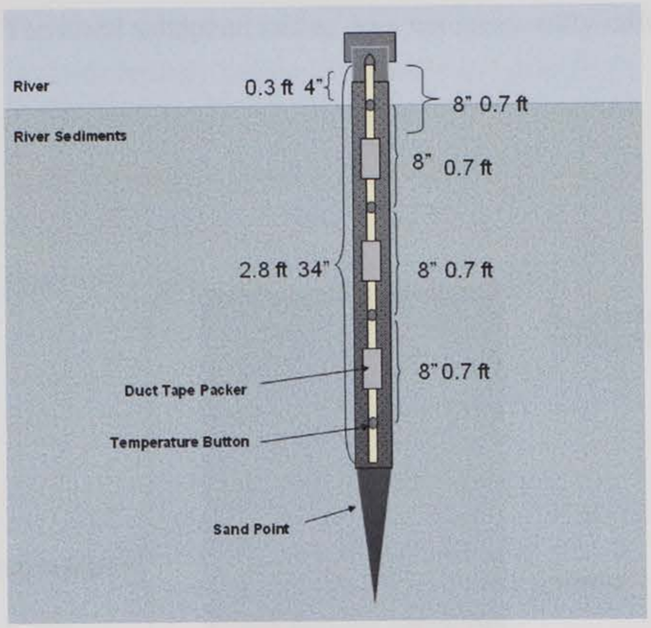

Figure 12 Schematic showing the general installation of temperature buttons

Analyses of these time varying vertical temperature profiles were performed using observed lags in temperature to interpret either upward or downward vertical movement of water. In addition, two-dimensional heat flow modeling was used to establish hydrologic properties of the bed sediments and rates of water flow. The USGS heat transport model VS2DHI (Hsieh et. al, 2000) was used to represent a 2D vertical column (1D transport). The sides of the column were assigned as no flow boundaries, the top boundary was used to represent the river bed (river head), and the lower boundary was set as a head value (estimated from in-river piezometers). Initial temperature conditions were assigned using temperature data for near by shallow wells (water table connected to the river) or from the lowest instrument in the vertical river bed array (river is perched above the local water table). Model discretization used a grid spacing of 0.065 ft (Figure 13).

Assumptions made using the VS2DHI heat transport model included:

1. Water enters and leaves the river only in a vertical direction
2. Sediments in the riverbed have uniform hydraulic and thermal properties
3. Vertical hydraulic gradients do not vary with time

4. The metal sandpoint casing does not measurably influence heat conduction

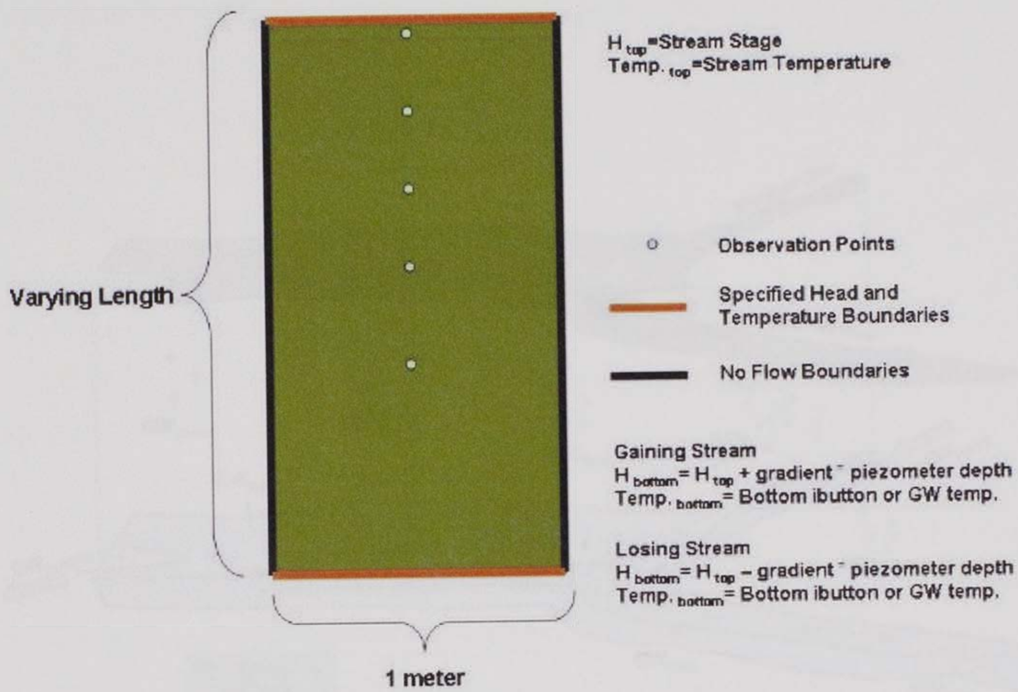

Figure 13 Two dimensional vertical profile of the temperature model constructed using USGS heat transport model VS2DHI.

A site wide groundwater balance was derived in an effort to estimate the overall quantity of exchange between the river/reservoir and groundwater. This water balance required estimates of exchange and provided estimates at the order of magnitude scale. This water budget is also a component used to help calibrate the numerical groundwater model that required field determined locations, directions and magnitudes of exchanges to be appropriately reproduced. It also suggests how exchange rates are distributed throughout the study area.

The development of the site conceptual model can be thought of as an interpretation of the site hydrogeology based on the interpreted hydrostratigraphy, aquifer boundaries and properties, flow directions and groundwater sources and sinks. A water balance schematic can be seen in Figure 14.

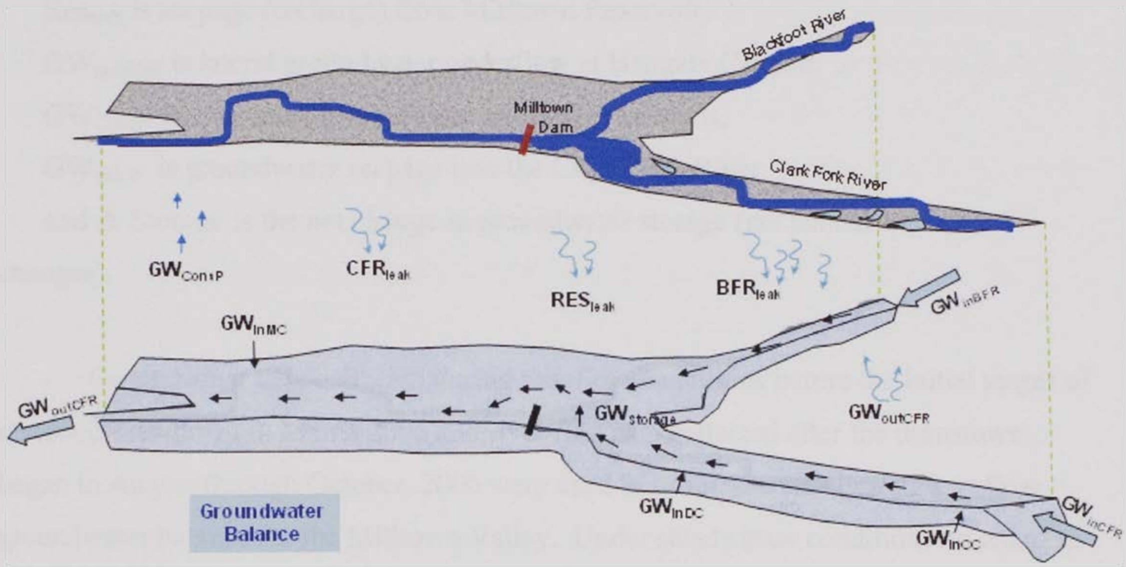

Figure 14 Generalized conceptual model.

A steady state groundwater balance for the project area (Table 4) was formulated as follows:

$$In = Out \pm \Delta Storage$$

$$In = GW_{inCFU} + GW_{inBFU} + GW_{inDC} + GW_{inSC} + GW_{inBFR} + CFR_{leak} + Res_{leak}$$

$$Out = GW_{outHGU} + GW_{ConsP} + GW_{outCFR} \pm \Delta Storage$$

Where:

GW_{inCFU} is lateral groundwater underflow at Turah Bridge

GW_{inBFU} is lateral groundwater underflow from the Blackfoot River valley,

GW_{inSC} is lateral groundwater underflow from side canyons including Deer Creek (DC), Marshall Creek (MC) and Crystal Creek (CC)

GW_{inMC} is lateral groundwater underflow from Marshall Creek,

GW_{inBFR} is seepage (recharge) from the Blackfoot River channel,

CFR_{leak} is seepage (recharge) from the Clark Fork River Channel,

Res_{leak} is seepage (recharge) from Milltown Reservoir,

GW_{outHGU} is lateral groundwater underflow at Hellgate Canyon,

GW_{ConsP} is consumed groundwater pumped from wells,

GW_{outcfr} is groundwater seepage into the Clark Fork River,

and Δ Storage is the net change in groundwater storage (net annual water level changes).

Groundwater data collected during baseflow conditions before the initial stages of reservoir drawdown in March 2006 and river flux data collected after the drawdown began in August through October, 2006 were used to estimate a steady state low flow groundwater balance for the Milltown Valley. Under steady state conditions no changes occur in groundwater storage in the study area therefore changes in storage were not estimated. As mentioned above, though an investigation evaluating the impact of dam removal on river-groundwater exchange would be best initiated prior to any disturbance or change in the hydrologic system, this project received support 1 month after a pre-dam removal 12 feet drawdown occurred.

One of the principal contributions of water to the valley aquifer is underflow from the Clark Fork Canyon, the Blackfoot Canyon and smaller side canyons including Deer Creek, Marshall Creek and Crystal Creek. Underflow estimates were determined using Darcy's Law. Cross sectional areas were derived from bedrock surface interpretations and water table elevations taken from March 2006 measurements (Berthelote et al., 2007).

Another important contribution to aquifer recharge is river leakage. As discussed above, river leakage was estimated using the exchange rates determined from the temperature modeling and a conceptual distribution of the areas of exchange. The areas were broken up into different reaches and exchange rates were multiplied by the corresponding reach bed area. Data used to estimate river leakage was collected between August and October 2006 during baseflow conditions. The reservoir leakage was estimated by using and assumed historical downward vertical gradient data (Udaloy, 1986), established hydraulic conductivity values (Woessner 2002) and the reservoir area.

All domestic water consumption, storm drain or direct precipitation recharge, and local evapotranspiration were considered negligible when compared to the magnitude of the other water balance components and therefore were not included.

Based on the conceptual model, a numerical groundwater model was constructed to test and interpret how the surface water and groundwater system exchanged water. It was further used to build upon the identified exchange processes and predict the likely effects of the phase 2 reservoir drawdown on exchange rates. First pre-dam removal conditions were simulated and calibrated to both steady state and transient conditions. A detailed description of the model framework, the calibration process and the calibration results can be found in (Berthelote et al., 2007). A summary of these results is presented in Appendix I. The numerical model was developed using Ground Water Vistas graphical user interface to the USGS MODFLOW code (Environmental Simulations Inc. (ESI), 2004; Harbaugh et al., 2000). The constructed numerical groundwater model contains 1,052,800 cells of which 53,192 are active (Figure 15).

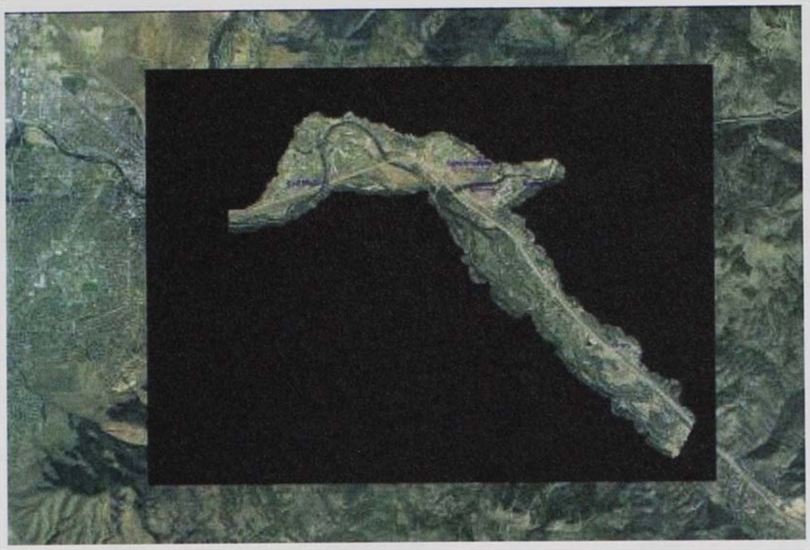

Figure 15 Illustrates the extent of the modeled area.

The large model area was designed so modeling results could be linked to the modeling work of Tallman (1995) (a numerical model extending from the Hellgate area west into the Missoula valley) if desirable. The study area was discretized into 150 ft by 150 ft cells (Figure 16.) and 7 layers.

Figure 16 Illustrates spatial discretization of model area.

Each layer was laterally constrained by no flow cells which represented the locations of valley slope bedrock. The bedrock topography was used to create a no-flow model base (Figure 17). Initially, two specified head boundaries formed the boundaries of the aquifer at Turah and in Hellgate Canyon. A variable head flux boundary was used for the Blackfoot Canyon boundary. The specified head boundaries represent equipotential lines at these locations for either steady state or transient conditions. Additional groundwater underflow was simulated as injection wells where side surface water drainages intersect the valley and underflow is likely (Marshall Creek and Deer Creek).

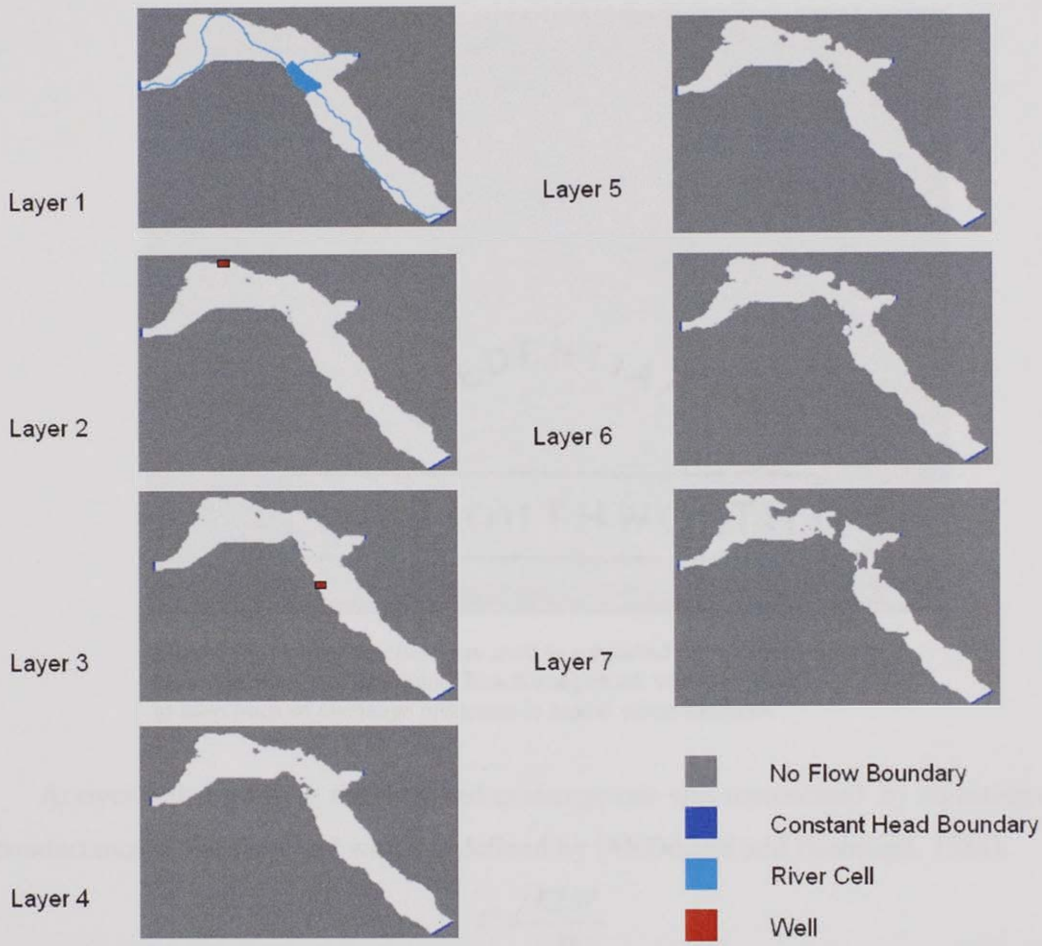

Figure 17 Illustration of boundary conditions for each layer of the numerical groundwater model. Initial model runs used constant head boundaries representing single equipotential lines at the southeastern Turah Bridge, northeastern Blackfoot River valley and western Hellgate Canyon boundaries. Remaining boundaries were simulated as no flow except where small yield river cells were used to allow exchange of water between the river and groundwater in Layer 1. Note as the layer bases encountered bedrock highs portion of layers would become inactive (no flow gray areas).

Aquifer parameterization of the model cells was based on the location of field tests, interpretations of the geologic cross sections, and likely distributions of sediment types based on perceived depositional environments. Adjustments were made to these aquifer properties during model calibration however the changes were constrained by the conceptual model.

The unconfined valley aquifer and the rivers were allowed to exchange water at 808 river cells representing 11 different reaches (Figure 18). The reaches began and ended at field river stage monitoring sites.

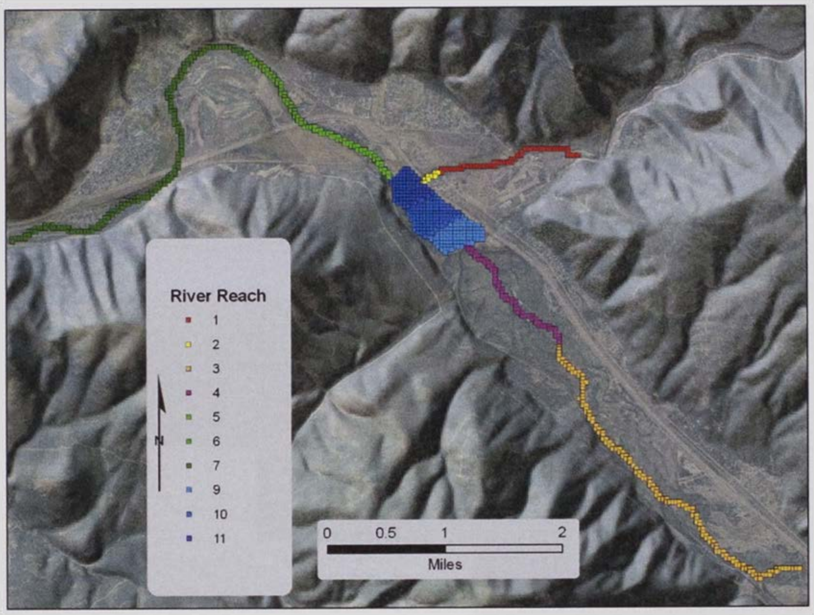

Figure 18 11 river reaches were used to simulated river/groundwater exchange rates and locations. Reach assignment was also used to keep track of exchange processes in model water balances.

At river cells locations, the river bed exchange rate was represented by adjusting the conductance of the river bed which is defined by (McDonald and Harbaugh, 1984):

$$C = \frac{KLW}{M}$$

Where

C = River Conductance
K = Riverbed hydraulic conductivity
L = Length of river cell

W = Width of river cell
M = Thickness of river cell

The exchange rate within a groundwater model cell was determined using the conductance term and the head difference between the assigned river stage and the computed groundwater head. When a river cell becomes disconnected from the groundwater (the elevation of the assigned base of the river bed sediments is greater than the simulated groundwater head in the cell) a constant exchange (river bed leakage rate) is assigned (MODFLOW 2000 River Package). The river bed conductance term is usually poorly known and during model calibration it is fitted to derive observed groundwater conditions. However, for this work, initial riverbed conductances were assigned based on river bed measurements. The leakage of water from the Milltown Reservoir was simulated using river cells (River Design Group, 2007)(Figure 19).

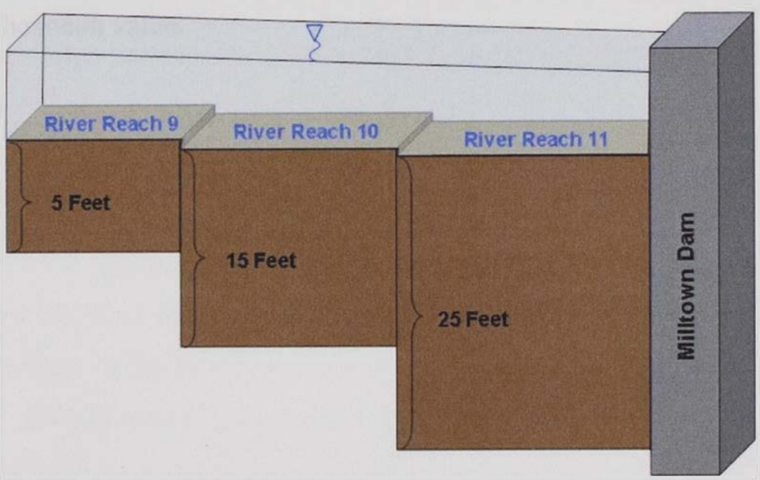

Figure 19 Illustration of increasing riverbed thickness used within the river cells for reach 9 – 11 to simulate the reservoir sediment wedge (Figure 27). The length of reach 9 is ~1450 ft, reach 10 is ~ 1600 ft, and reach 11 is ~ 1500 ft.

Once the model was calibrated to initial steady state and transient conditions the reservoir and river stage were varied in an attempt to represent Phase1 and planned Phase II pre-dam removal drawdowns. Results were then compared with simulated unimpacted conditions, and field measurements. Changes in the exchange process were then compared and contrasted, and the response of the groundwater evaluated.

Error and Uncertainty

Errors and uncertainties were estimated for the methods used in this study. Errors are attributed to measurement instrumentation and techniques such as the single point survey, river stage elevations, and groundwater level measurements. These types of errors were estimated independently. Errors in bedrock were estimated by comparing the estimated bedrock surface to known bedrock elevations. To estimate the error of vertical hydraulic gradient calculations, a range of values were determined from the various measurements taken at each river location and the maximum range used as the error. Uncertainties were estimated for analyses including falling head tests, peak lag analyses, flow tube analyses and historical pump test analyses. The error was estimated as half the range of the reported values and is presented as a percentage calculated as half of the range divided by the mean value.

CHAPTER 3
RESULTS

This section presents the observations made and the results of the analyses performed during the investigation. The first section will describe the refined aquifer framework. This section will be followed by a description of the observed aquifer responses to the Phase 1 reservoir drawdown. The next sections will present the interpretations of groundwater response to reservoir stage and river stage where in-river investigations were conducted to estimate areas where the rivers were gaining and losing, and their corresponding exchange rates. The final section will describe the calibration and execution of the three dimensional groundwater model developed to test the conceptual model and calibrate the likely spatial and temporal river exchange rates. The calibrated model was then used to forecast reservoir stage drawdowns would likely impact the identified river/groundwater exchange processes

Refinement of Aquifer Framework

To determine the three dimensional configuration of the valley groundwater system the sides and base of the fluvial deposits needed refinement as aquifer thicknesses are key aspects of valley groundwater system (Berthelote et al, 2007). Aquifer boundaries were defined using boring and geophysical techniques. The revised bedrock elevation map produced shows the valley bedrock boundary is complex (Berthelote et al. 2007) (Figure 20). The pre-existing interpolated bedrock surface was refined by conditioning the interpolation with 173 bore holes and well completion data sets, and interpolations of data from a micro gravity survey providing 198 new data locations (Cordell, L., and R.G. Henderson, 1968; Berthelote et al., 2007).

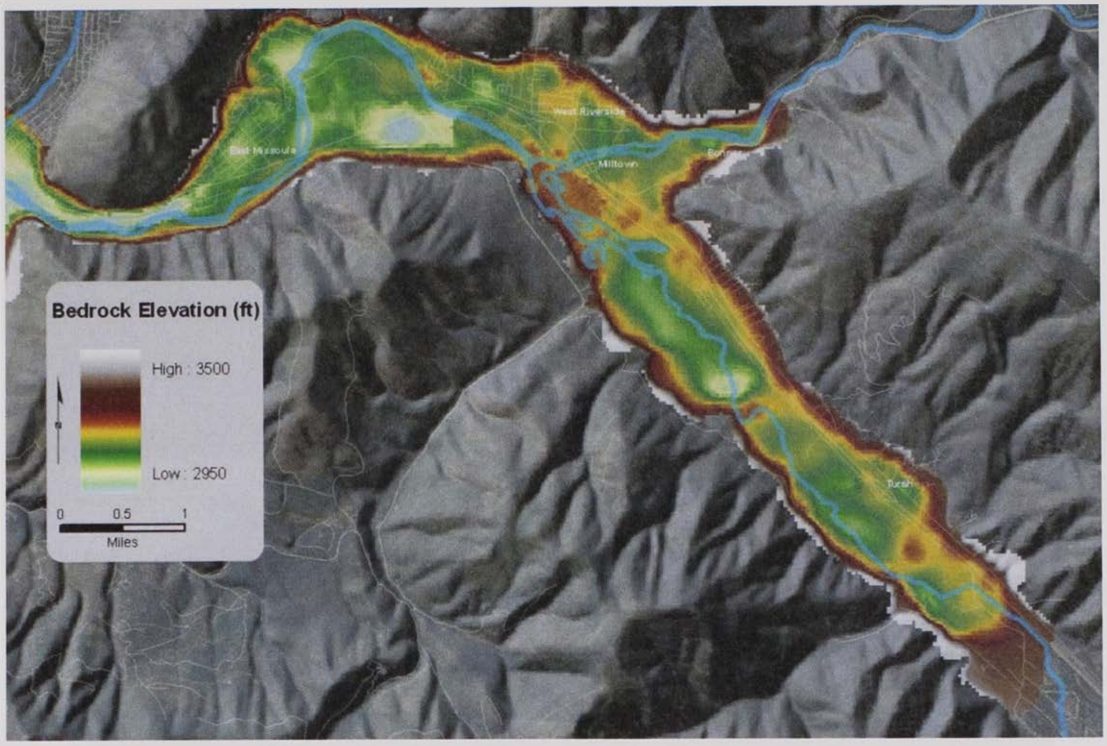

Figure 20 Bedrock elevations derived from a compilation of gravity data, four seismic lines processed by Gradient Geophysics (1991), historical borehole data, well logs, and topographic projections into the subsurface. Known depth to bedrock was used to condition the data. However, bedrock depth may actually vary up to + or – 35 feet in areas outside of the area immediately adjacent to the reservoir area.

The nature and extent of geologic units that make up the unconsolidated valley fill sediments were interpolated from available borehole and drillers logs. A total of 89 of logs were reviewed and 3 cross sections were prepared for analyses. An example of a cross section in which the detailed geology was generalized into like hydrostratigraphic units is presented in Figure 21. The valley fill sediments are characterized by a heterogeneous mix of fluvial sediments and colluvium with an upper sand and gravel package that overlies a discontinuous interval dominated by more silt and sand. The finer faction of the sediments has been reported in well logs completed in Hellgate Canyon, in areas just up river of Milltown, and in portions of West Riverside. The lower hydrostratigraphic unit is composed of what drillers report as a heterogeneous mix of sand, gravel and clay and is utilized as the primary water yielding unit. Due to the small number of wells drilled in Bandmann Flats and in areas of the Clark Fork flood plain above Milltown Dam, the stratigraphy is less well interpreted and it is often extrapolated based on a single well log or distal well information.

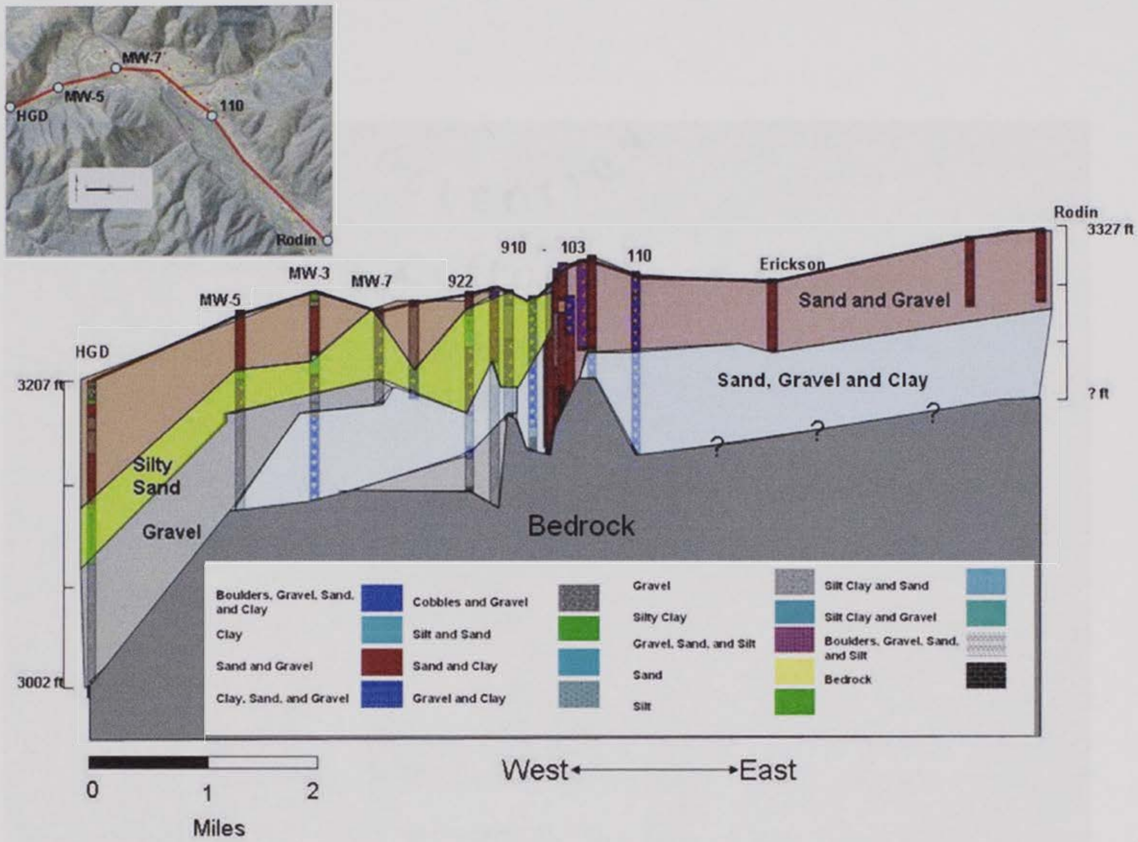

Figure 21 Hydrostratigraphic cross section interpreted from well logs.

Establishment of Groundwater Conditions

The bedrock boundary presented in Figure 20 was combined with the interpolated position of the valley water table (November 7, 2007) and an aquifer saturated thickness map was generated (Figure 22). Groundwater interpolated surfaces based on individual water table measurements have measurement, instrument, survey, and spatial and temporal interpolation errors which were determined and estimated. This results in the sum of the individual errors to be about 0.6 ft. When errors are all assumed to be independent the error is ~ 0.33 ft. The bedrock geophysical boundary elevation was considered to be +/- 35 ft except in the reservoir and Milltown area where boring to bedrock resolved elevations are within 1 ft. Review of Figure 22 reveals a complex saturated thickness of the valley aquifer. The aquifer is the thinnest along the valley sides, in the Milltown Reservoir area, and just east of West Riverside. The analyses suggest the bedrock surface is quite irregular with sizable areas containing thick saturated sequences (dark colors).

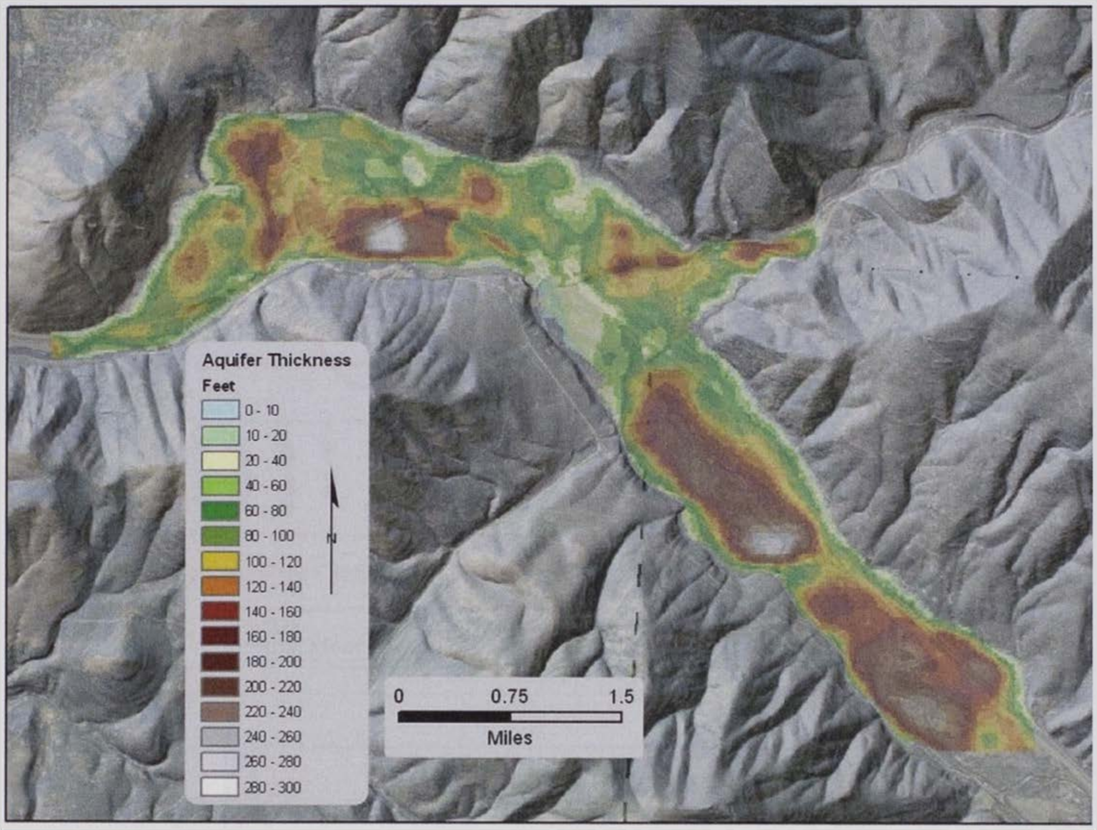

Figure 22 General aquifer thickness derived from water table map in November, 2007 and Berthelote's bedrock elevation Grid.

The valley groundwater system water table generally rises in response to the spring snow melt and then declines gradually for the remainder of the year. Hydrographs of wells Rodin and 99a and MW-6 (Figure 6) show this trend with water levels fluctuating up to 10 ft annually in wells located in Milltown and the area down valley to Hellgate Canyon, and wells up river of the reservoir varying between 4 to 5 ft (Figure 23, 24, 25). The initial work of Woessner et al. (1984) and later research by Gestring (1994), Arco (1995) and Brick (2002) linked water level changes to river discharge, and river and reservoir stages. The Blackfoot River, Milltown Reservoir and Clark Fork River below the Milltown dam leak or recharge water to the valley groundwater system with the exception of a short section for river channel (about 600 ft) located directly below Milltown dam (Gestring, 1994).

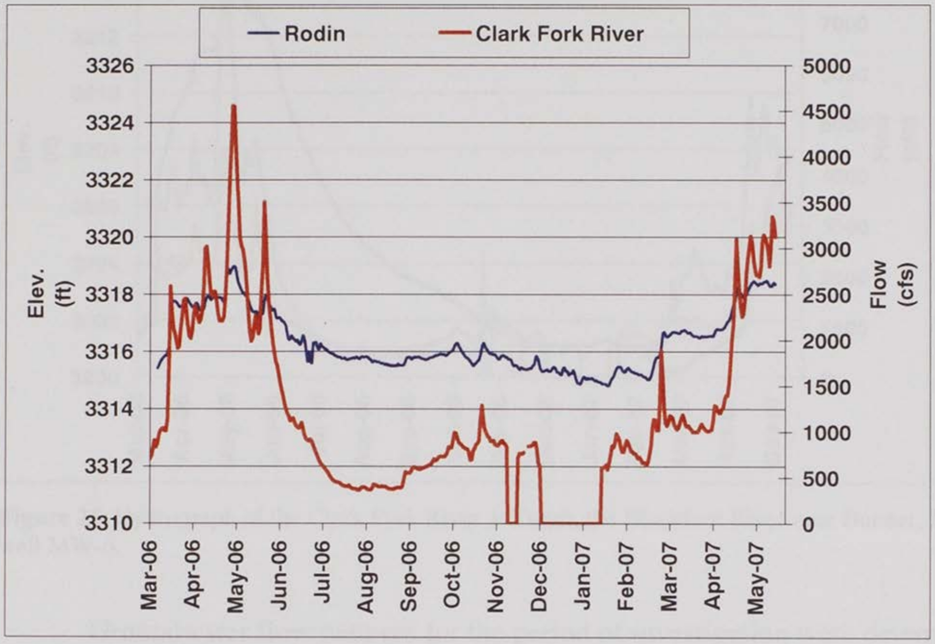

Figure 23 Hydrograph of the Clark Fork River at Turah and the Rodin Well.

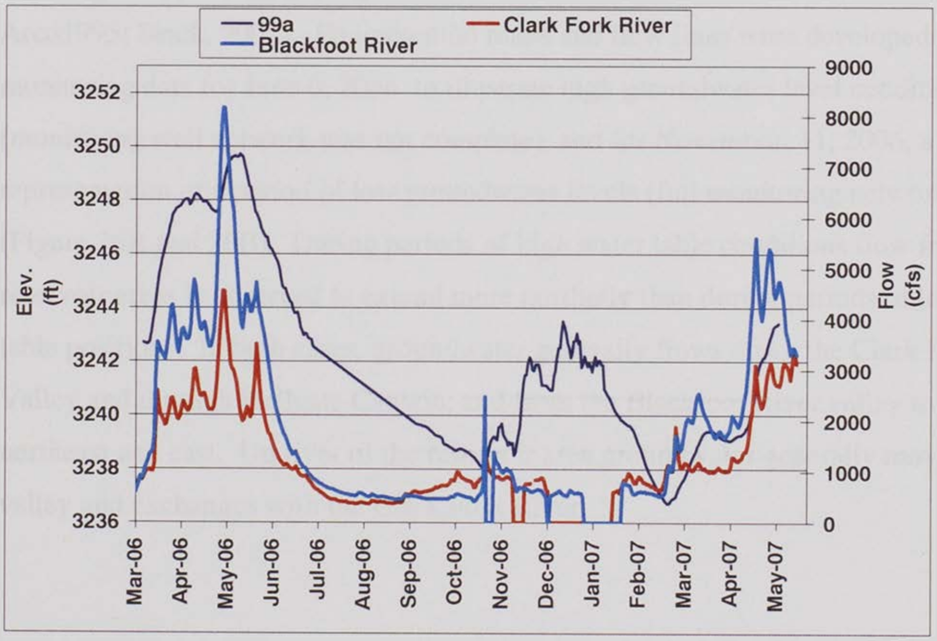

Figure 24 Hydrograph of the Clark Fork River at Turah, the Blackfoot River near Bonner, MT and the well 99a.

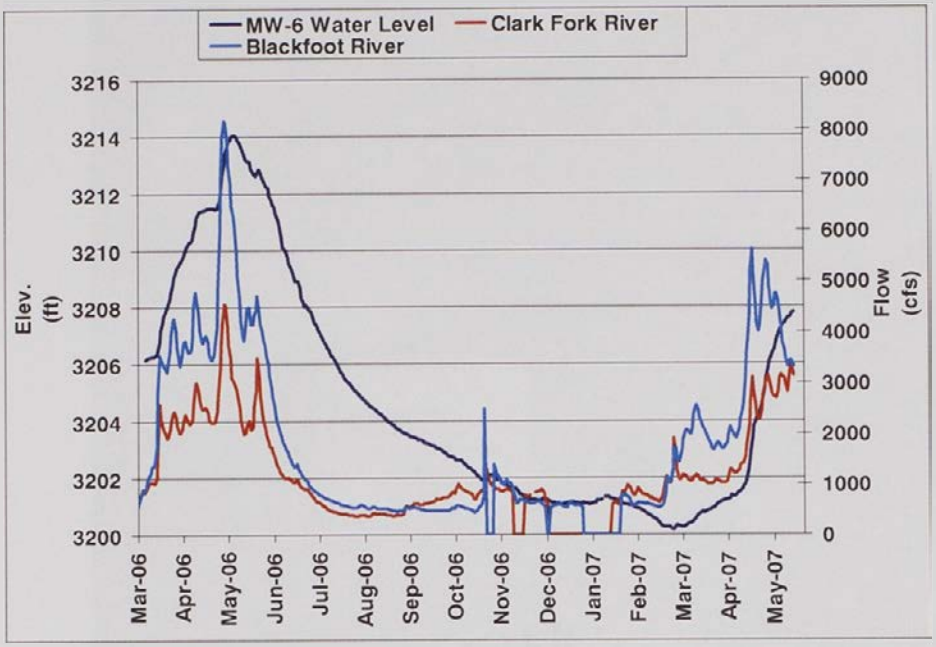

Figure 25 Hydrograph of the Clark Fork River at Turah, the Blackfoot River near Bonner, MT and the well MW-6.

Groundwater flow patterns for the period of investigation were determined to be similar to those described by pervious researchers (e.g. Gestring, 1994; Woessner, 1984; Arco1995; Brick, 2002). Equipotential maps and flow lines were developed from the monitoring data for June 6, 2006 to illustrate high groundwater level conditions (monitoring well network was not complete) and for November, 11, 2006, a representation of a period of low groundwater levels (full monitoring network data) (Figure 26A and 26B). During periods of high water table conditions flow from the reservoir areas is observed to extend more northerly than during periods of low water table positions. In both cases, groundwater generally flows down the Clark Fork River Valley and through Hellgate Canyon, and from the Blackfoot River valley to the northeast and east. Up river of the reservoir area groundwater generally moves down valley and exchanges with the Clark Fork River.

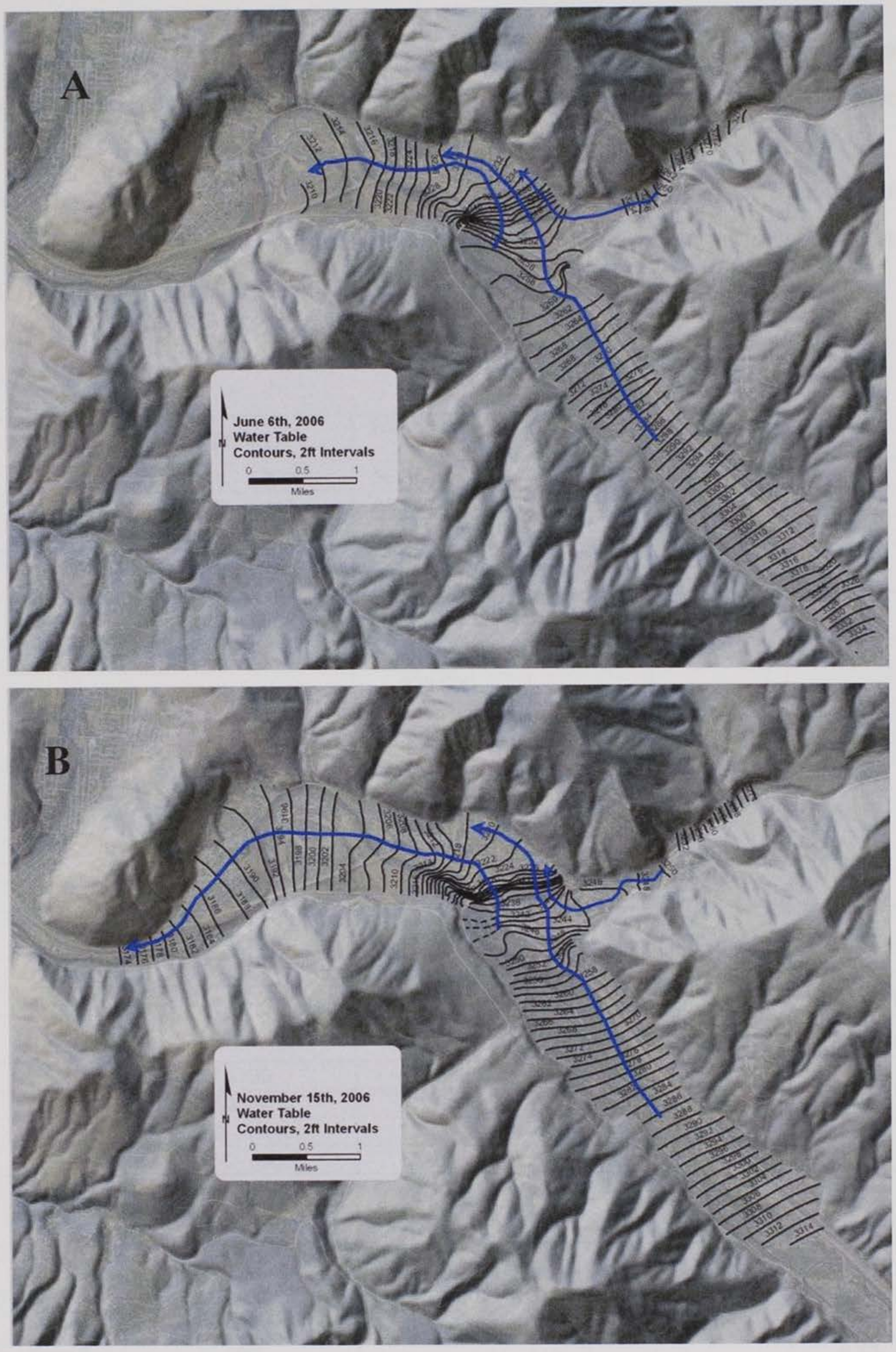

Figure 26 Water table maps A) June 6, 2006 and B) November 15, 2006. The data for June reflects a developing well network, where November data includes the complete network of monitoring wells. Flow is generally down valley from the east to the west and from the Blackfoot River canyon to the west.

Aquifer properties were evaluated by assembling published values from numerous studies, and flownet and peak lag analyses performed as part of this investigation. These values were also used to provide ranges that allowed the assignment of values to the interpreted aquifer geologic framework. The ranges of values reported in the literature are large and generally supported by studies conducted in similar geologic settings (Hsieh et al., 2007) (Table 2). All coordinates (locations) for each well are presented in the Appendix A.

	well #	K (ft/day)	Transmissivity (ft^2/day)	Kz (ft/day)	Sy	S
1	102	3,710 - 3,720	96,400-96,600			
1	103	1,770 - 2,100	65,200-55,000			
1	105a	290	18,230			
3	105b	1,580 - 1,890	882,680-1,041,000			0.0477 - 0.006
3	105c	1,510 - 1,700	834,220			0.028 - 0.026
1	106	56,700 - 59,400	4,140,100			
1	107	13,600 - 14,200	573,000-595,100			
1	108	6,500 - 6,800	539,800-595,200			
1	109	15,100 - 16,900	1,600,000-1,800,000			
1	110	2,200 - 2,580	242,100-208,500			
3	906	1,730 - 2,190			0.24 - 0.10	0.0005 - 0.001
3	99b	1,870 - 3,070			0.36 - 0.12	0.001 - 0.0008
4	west well	1500	9,160 - 34,030			
4	east well		46,580 - 89,900			2.54E-14
5	R-75	1,270 - 1,290		230-240	0.12	.00119 - .00012
2	HG-32	16,730	903,640			
2	HG-33	9,010	877,820			
6	mw-6	3,900 - 11,000				
6	Mw-7	300 - 400				
6	Turah Bridge - Rodin	9000 - 5000 @ 150' thickness	1,400,000 - 780,000			
6	West-Riverside	14,000 - 83,000				
7	West-Riverside	1,830 – 89,200				
8	Smw-3	600				0.13
9	Canyon river Well	608-5,080	55,290 - 462,170			
10	HGD	4,500				

Table 2 The collected compilation of hydraulic conductivity values determined throughout the study area.

[1] (Woessner et al., 1984)
[2] (Gestring, 1994)
[3] (Atlantic Richfield Company (ARCO), 1995)
[4] (Newman, 1996)
[5] (Newman, 2005)
[6] (Peak Lag Analysis)
[7] (Flow Tube Analysis)
[8] (Land and Water Consulting, 2004)
[9] (Land and Water Consulting, 2005)
[10] (Tallman, 2005)

The distribution of estimated hydraulic conductivity values shows that values range from 350 to 59,000 ft/day and the general distribution is highly variable (Figure 27).

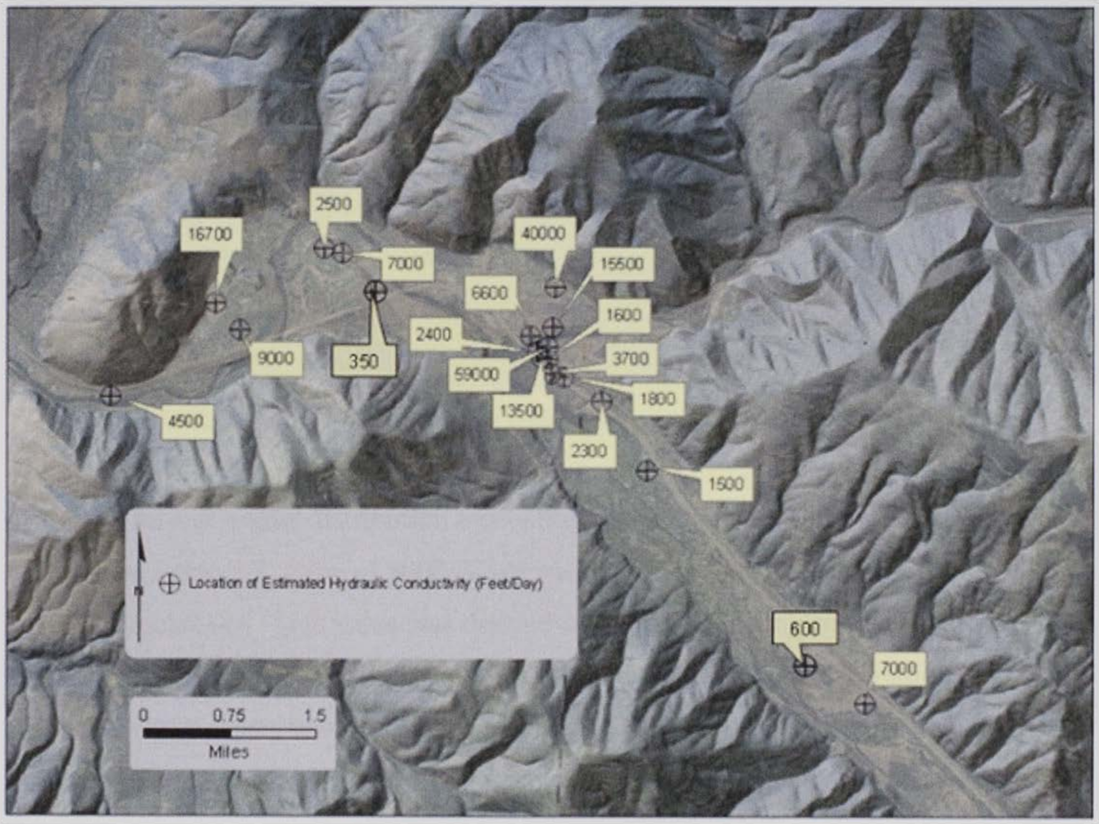

Figure 27 Aquifer hydraulic conductivity (ft/day) distribution of the alluvial material.

The reported wide range in aquifer property values in the Milltown and West Riverside area prompted additional analyses that attempted to assess the likely spatial distribution of local hydraulic conductivities. Results of stage peak analysis using water level fluctuation data from well DB-205 and responses in wells HG-23, DB-079 and HG-27 (Appendix B) yielded a range of 19,000 to 82,000 ft/day (Figure 28).

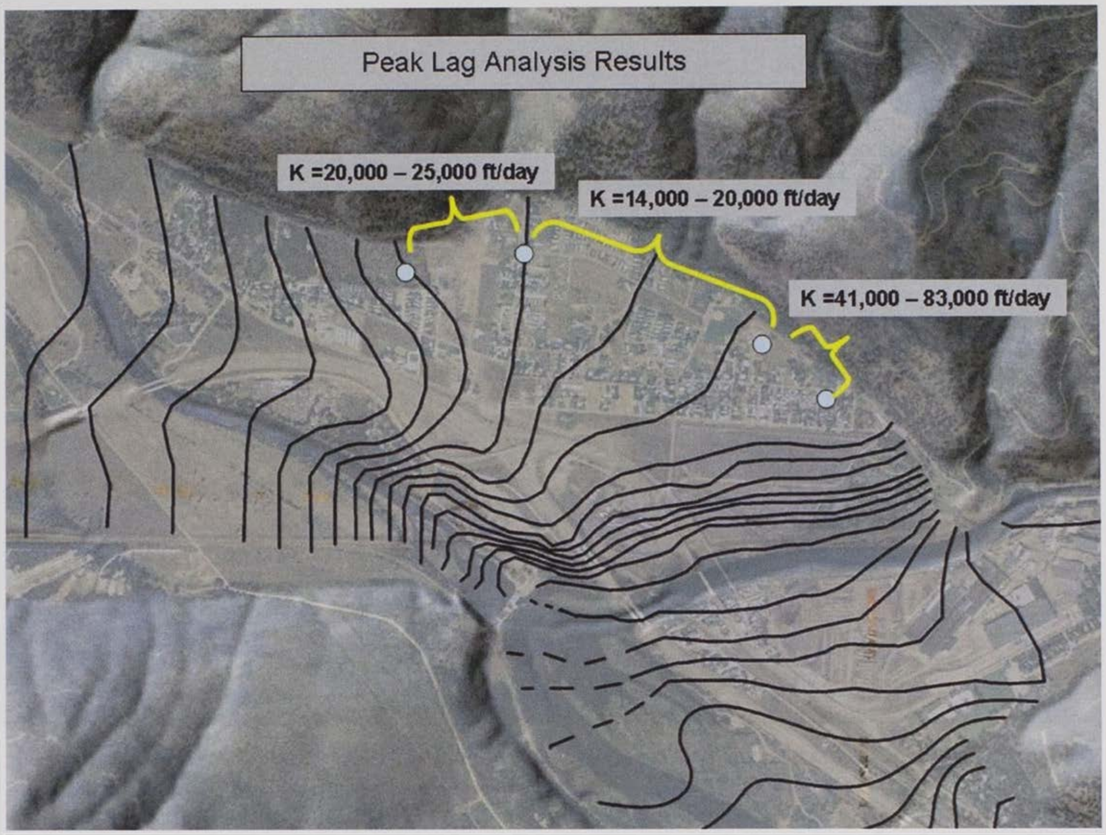

Figure 28 Estimations of hydraulic conductive from peak lag analyses in the West Riverside area..

A second spatial distribution evaluation was attempted using flownet analyses. It was assumed that a K value of 5000 ft/day was representative of the conditions used to initiate the analyses. This value was derived from aquifer testing conducted at well 108. Using the bedrock depth map and aquifer saturated thickness, the distribution of hydraulic conductivity was estimated (Figure 29). Results suggest a very high hydraulic conductive zone is present in the West Riverside area and that values decrease slightly to the west.

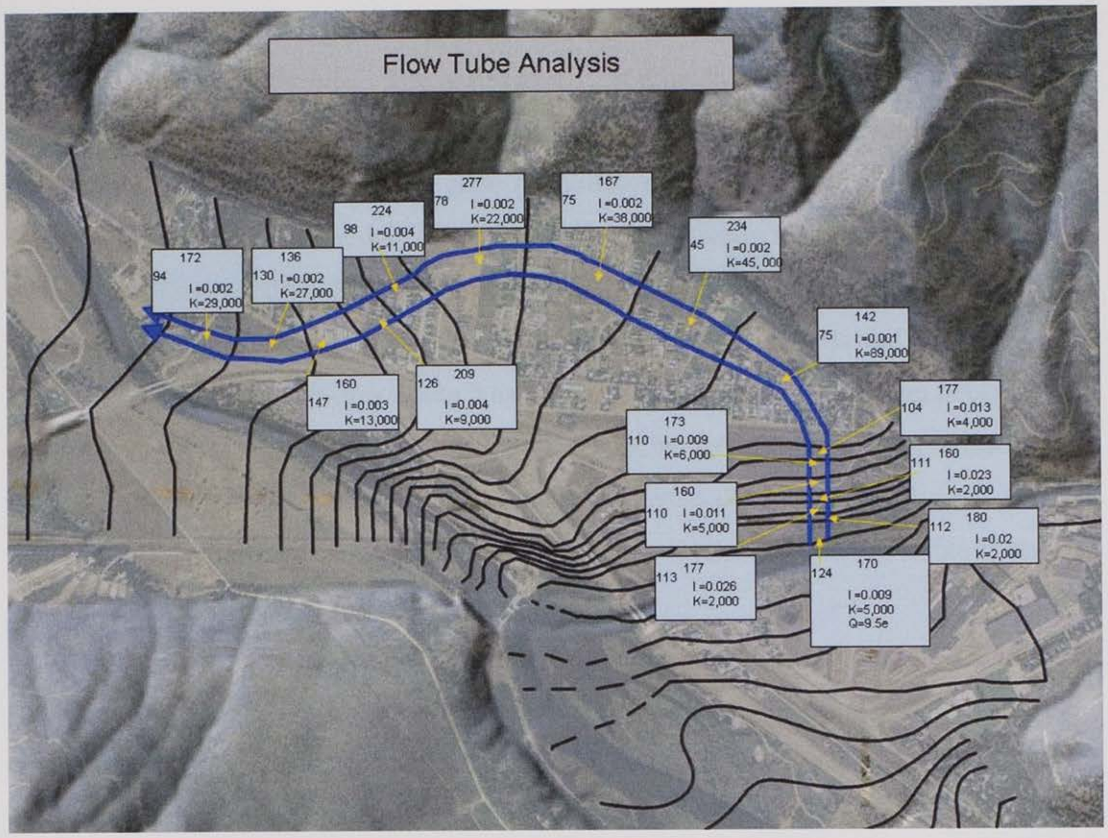

Figure 29 An illustration of the flow tube used to determine the hydraulic conductivity values and treads in neighborhood of West Riverside and Pine Grove. Water table map is contoured from 3/31/06 water level measurements. Units are reported as follows: i is dimensionless, K ft/d, Q ft^3/d. The numbers on the left hand side and top of each box are the estimated dimensions of each cross section.

Examining the rates, locations and magnitudes of the exchange of surface water and groundwater

This investigation and previous investigations in Milltown and down valley documented the contrast between the river and reservoir stages and the position of the water table (Gestring, 1994; Woessner et al., 1984) and suggested where losing and gaining river reaches occurred. The addition of river stage monitoring sites, the groundwater monitoring network, identification of the presence or absence of the response of groundwater temperature to changes in-river temperatures, and measurements of in bed hydraulic gradients, hydraulic conductivities and temperature derived flux rates expanded the resolution of interpreted river groundwater exchange locations and magnitudes in the study area.

During this investigation a groundwater level change induced by a 12 ft reservoir drawdown was also observed. The permanent 12 ft drawdown was the first of a series of three drawdowns that will total a maximum of 30 ft, the final dam out condition. The initial drawdown began on June 1st, 2006 (turquoise line on Figure 30). The reservoir stage was lowered approximately 9 ft by the end of June when the drawdown was stopped to lessen the perceived stress to fish populations below the dam (pink line on Figure 30). Down-river stress was defined as high river temperatures and high sediment loads. In September a 3 ft drawdown was initiated, however reservoir stage became controlled by river stage and a 3 ft drawdown was achieved only for a short period of time in January (purple line on Figure 30). The reduction of the reservoir stage and related Clark Fork River and Blackfoot River stage reduction had a measurable impact on near reservoir and valley groundwater levels.

In an attempt to evaluate the degree of change and the spatial distribution of the impacts, a baseline or pre-drawdown groundwater condition was needed. As this work was initiated just as this drawdown was initiated, no project data could be used to establish starting conditions. Thus, previous water level data were compiled and a generalized pre-drawdown set of conditions was suggested based mainly on Gestring's (1994) data (Berthelote et al., 2007). The Phase 1 drawdown was completed on November 12th when the river flows became the only factor controlling reservoir stages. The maximum drawdown from full pool was ~12 ft which occurred for a brief time in January when the river level was low. River discharge and reservoir elevations that occurred during the study are presented in Figure 30.

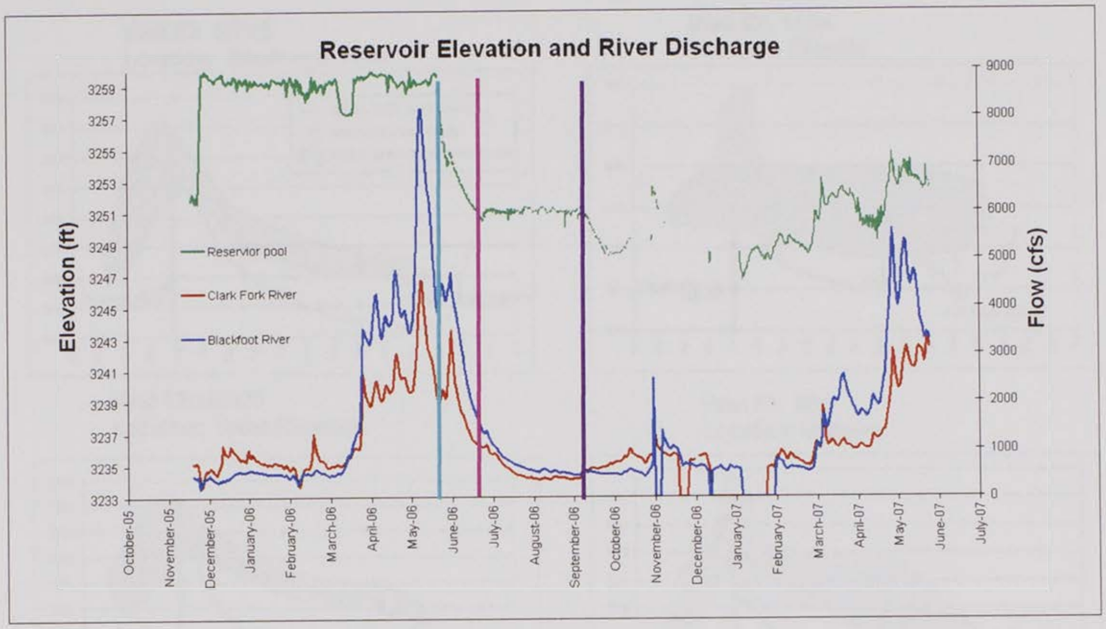

Figure 30 A hydrograph illustrating the timing of the Clark Fork River and Blackfoot River discharge and the elevation of the Milltown Reservoir pool during prior to, during, and after stage 1 drawdown. The turquoise line indicates the start of the initial 9 ft drawdown, the pink line indicates the end of the initial drawdown and the purple line indicates the start of the final 3 ft drawdown.

Gestring's (1994) groundwater level data (similar river flows with the reservoir at full , (Berthelote et al. 2007) and all historical data for a given monitoring well (some 1982 to 2005) were plotted along with the observed 2006-2007 water levels (Figure 31). The difference between water levels in February was used as to estimate the likely water level decline as a result of the 12 feet reservoir drawdown.

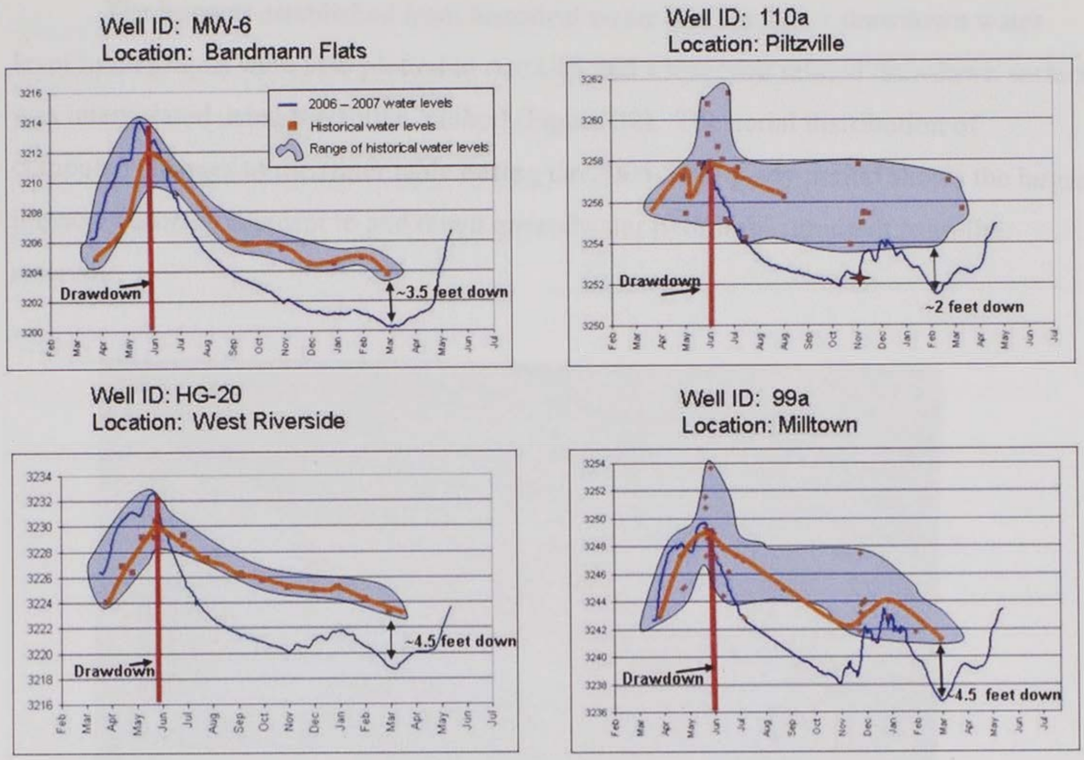

Figure 31 Hydrographs of selected wells showing measured water table response during this project (2006-2007), the timing of the 2006 reservoir and river Stage 1 drawdown (red line), the historical response to full reservoir conditions (Gestring, 1992, orange line), and the historical range of values measured using data sets from 1982 to 2005. The observed drawdown difference between historical (Gestring, 1992) and this project's water levels at low water in March 2007 is indicated by the double arrow.

Post drawdown water levels (March 2007) where compared to the historical ranges of water levels measured when the Milltown Reservoir was at full pool (historical), and an estimate of observed Stage 1 drawdown impact was established. The post phase 1 drawdown water levels reached a low during March, 2007. The largest groundwater level impacts where seen slightly north and west of Milltown with about 5 to 6 ft of water level decline. West Riverside and Milltown had water levels decrease about four feet below historical measurements where water levels in the Piltzville area were reduced by about 2 ft. The Bandmann Flats area experienced about 3 to 4 ft water level decline. Water level comparisons were not performed for the areas near Turah Bridge because no historical data were available.

The impacts established from historical water level and post drawdown water level hydrographs were also plotted in Arc GIS and a reservoir related drawdown surface was interpolated using the spline method (Figure 32). The aerial distribution of computed changes to the water table during the 2006-2007 study period shows the largest impacts occurred adjacent to and down groundwater hydrologic gradient from the reservoir.

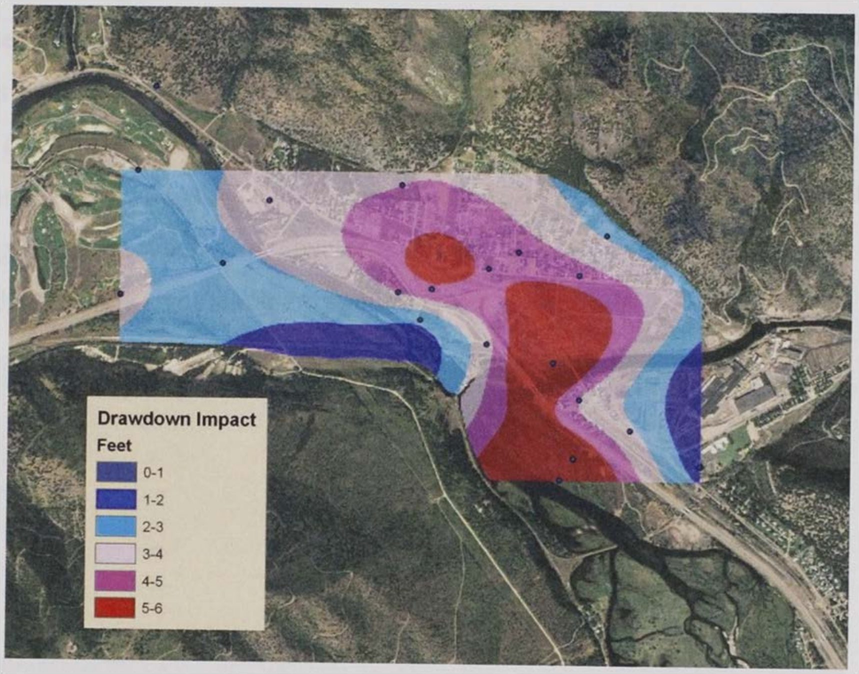

Figure 32 Computed impacts of lowering water levels below March historical levels as a result of Stage 1 remediation drawdowns. March 2007 data were compared with March 1993 data.

To evaluate the position of the water table in relation to the river stage a series hydrogeologic cross sections were created (Figure 33). The cross sections show the relationship between the river stage elevations, groundwater elevations, land surface elevations, bedrock elevations and river channel elevations. These can be used to help illustrate the river channel position and river stage in relation to the position of the water table. They were then used to identify likely the direction of surface water and groundwater exchanges. The hydrogeologic cross sections were created from interpolated water table surfaces and a land surface digital elevation grid, and Berthelote's derived bedrock elevation grid (Berthelote et al, 2007).

The first cross section A-A' illustrates how the Blackfoot River above Milltown Dam and the Clark Fork River stages above Milltown dam are higher than adjacent groundwater levels (Figure 34). The Blackfoot River appears to be a losing perched river when local ground water levels are lowest and a losing river with the water table connected during periods of time when groundwater levels are their highest. The cross section also indicates that the Clark Fork River below the dam east of Bandmann Flats is likely a losing perched river when groundwater levels are low and becomes losing with a connected water table during high flow periods. The Clark Fork River in East Missoula is likely a losing river through most of the year however may sometimes have gaining segments when groundwater levels are highest, although water level and river stage data for this river reach are sparse.

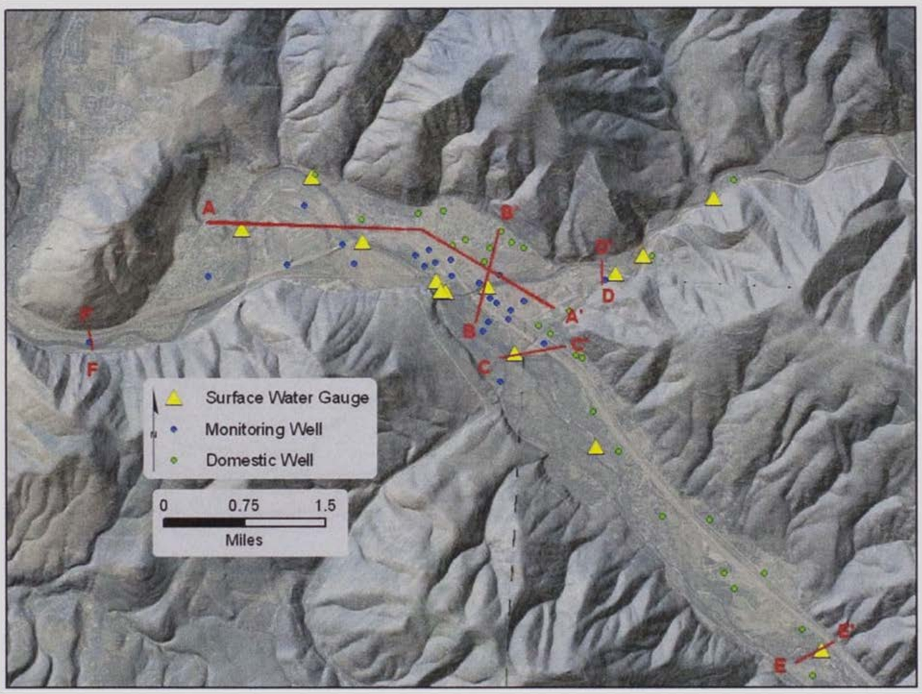

Figure 33 Map view showing the locations of the created hydrogeologic cross sections show n in figures 34, 35, 36, 37, 38 and 39.

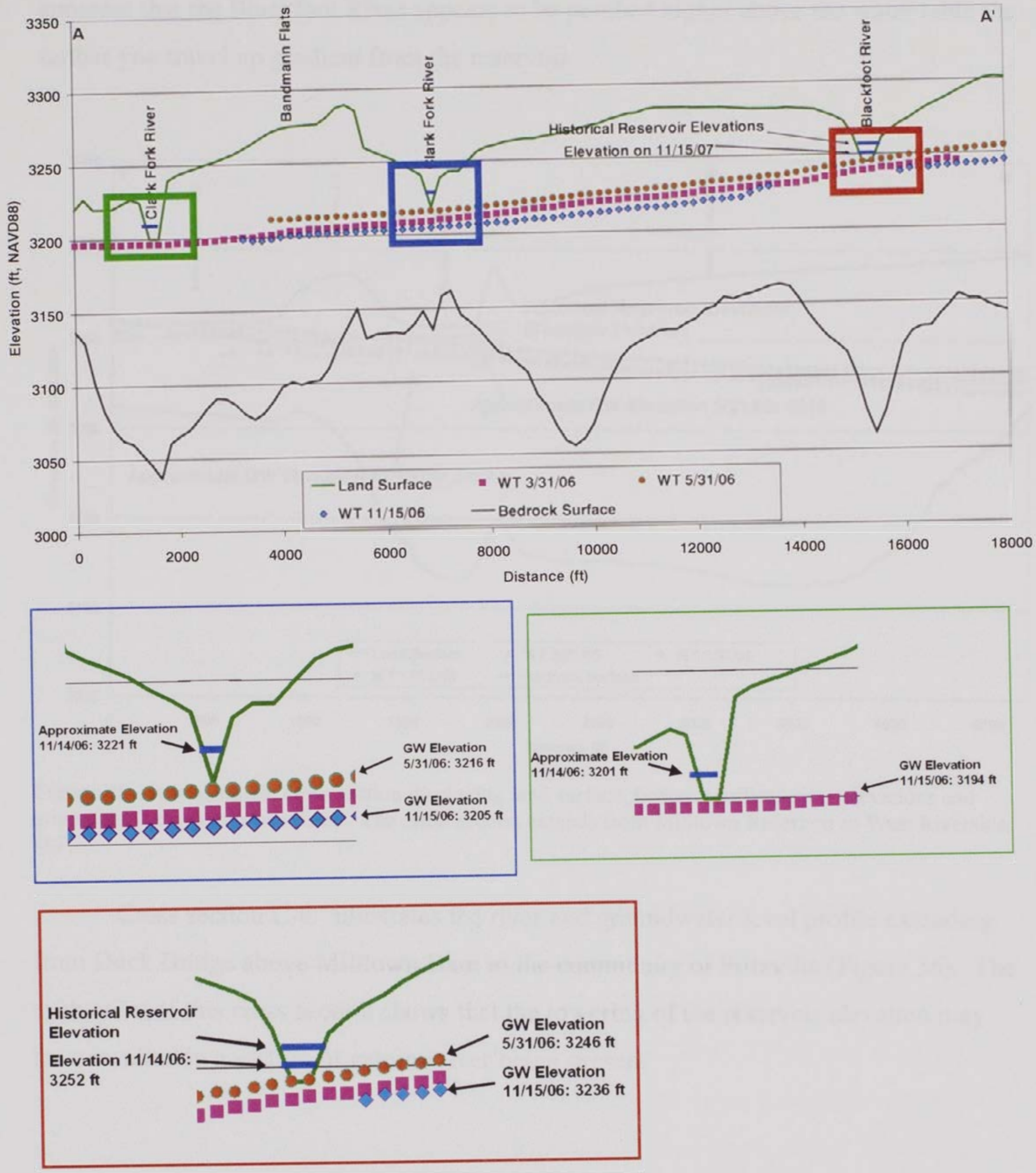

Figure 34 Hydrogeologic cross section displaying land surface, bedrock surface, river elevations and groundwater elevations over time. The cross section extends from East Missoula to Milltown, MT.

Cross section B-B' extends from the Milltown Reservoir into the community of West Riverside (Figure 35). This cross section shows how the groundwater elevations slope from reservoir into West Riverside. When comparing this cross section to A-A' it is apparent that the Blackfoot River appears to be perched higher above the water table the farther you travel up gradient from the reservoir.

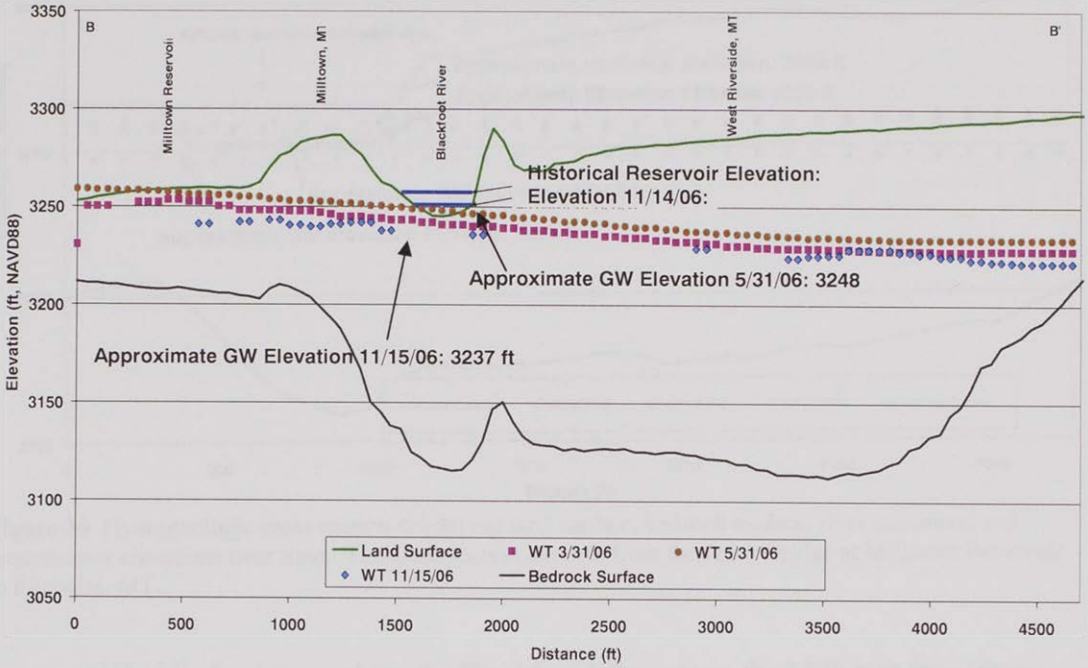

Figure 35 Hydrogeologic cross section displaying land surface, bedrock surface, river elevations and groundwater elevations over time. The cross section extends from Milltown Reservoir to West Riverside, MT.

Cross section C-C' illustrates the river and groundwater level profile extending from Duck Bridge above Milltown Dam to the community of Piltzville (Figure 36). The evaluation of this cross section shows that the lowering of the reservoir elevation may have resulted in a section of gaining river being present

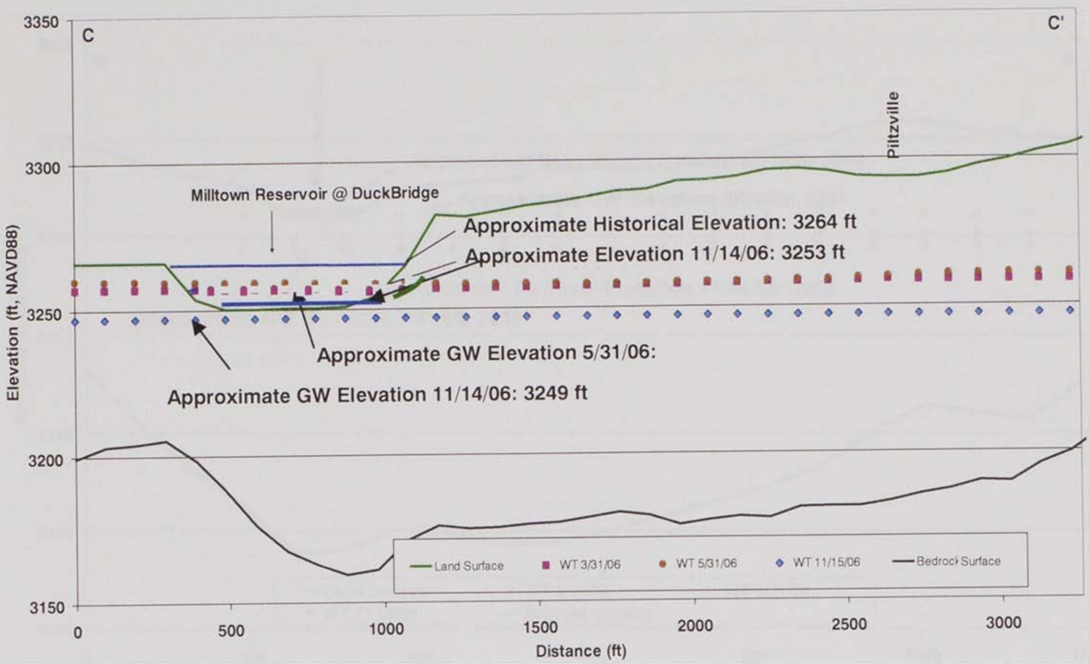

Figure 36 Hydrogeologic cross section displaying land surface, bedrock surface, river elevations and groundwater elevations over time. The cross section extends from the Duck Bridge at Milltown Reservoir to Piltzville, MT.

At the site boundary where the Blackfoot River enters the Milltown area (cross section D-D') the river is losing and possibly perched during baseflow conditions (Figure 37). Where the Clark Fork River enters the site up at Turah Bridge (cross section E-E') the surface water elevation and groundwater elevations are similar. The hydrogeologic cross section created in this area shows the river may be a losing reach (Figure 38). However, it is possible that this area goes from a losing to a gaining river during high flow. At Hellgate Canyon (cross section F-F') the river is a losing river and is perched throughout most of the year (Tallman, 2005). However, the hydrogeologic cross section created indicates that the bottom of the riverbed may become physically connected to the river during high flow periods (Figure 39).

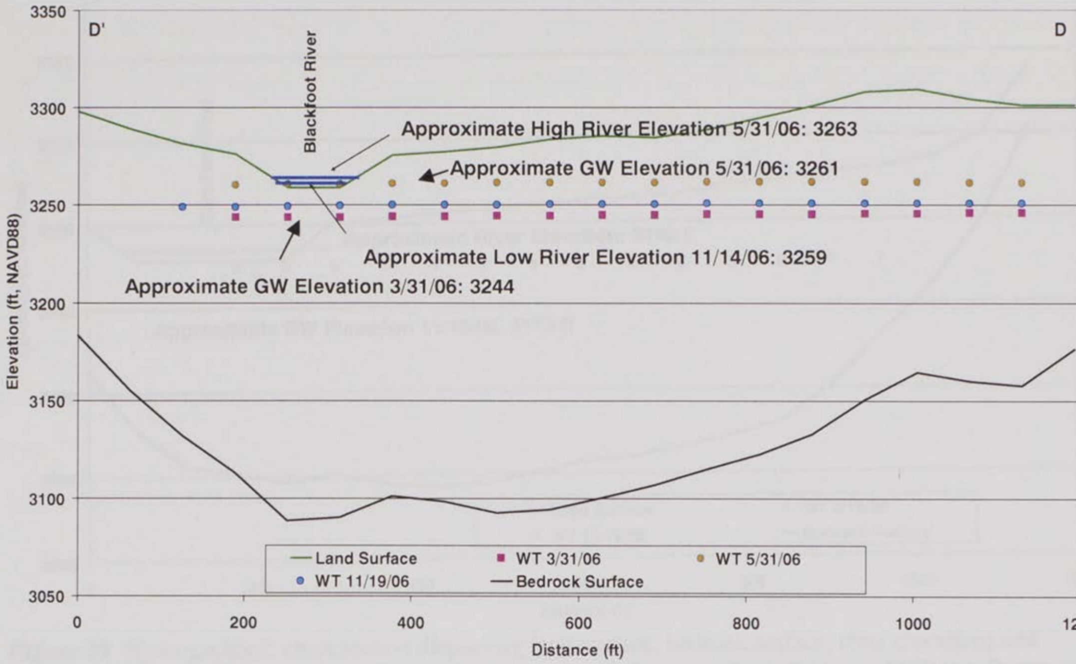

Figure 37 Hydrogeologic cross section displaying land surface, bedrock surface, river elevations and groundwater elevations over time. The cross section extends across the Blackfoot River in the northern area of Bonner, MT.

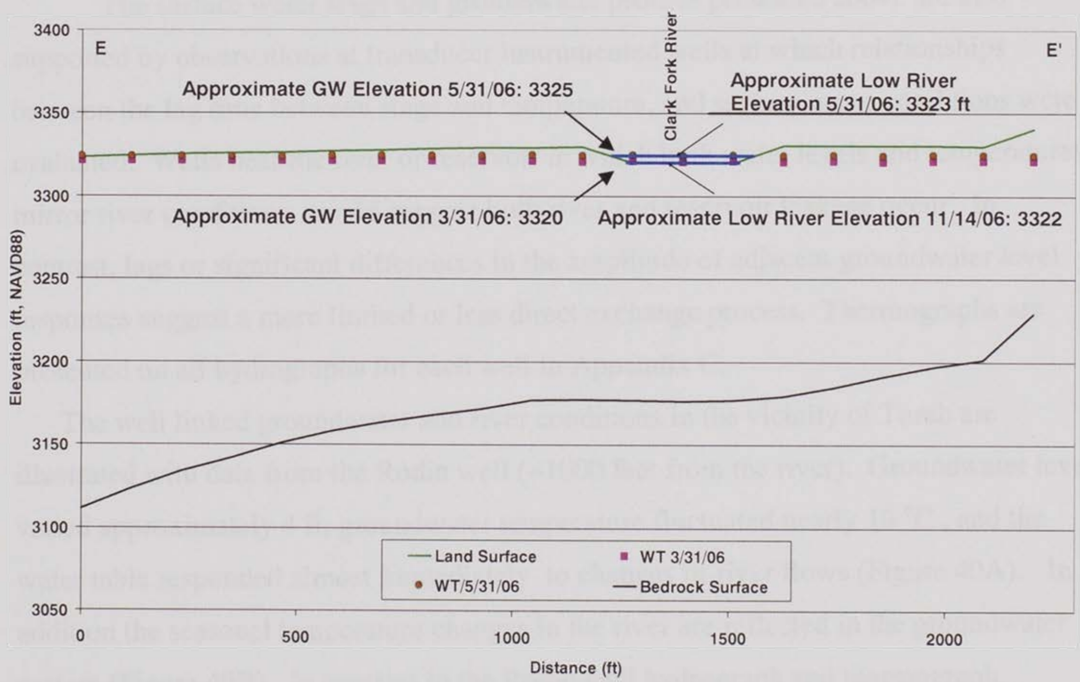

Figure 38 Hydrogeologic cross section displaying land surface, bedrock surface, river elevations and groundwater elevations over time. The cross section extends from across the Clark Fork River Valley across Turah Bridge in Turah, MT.

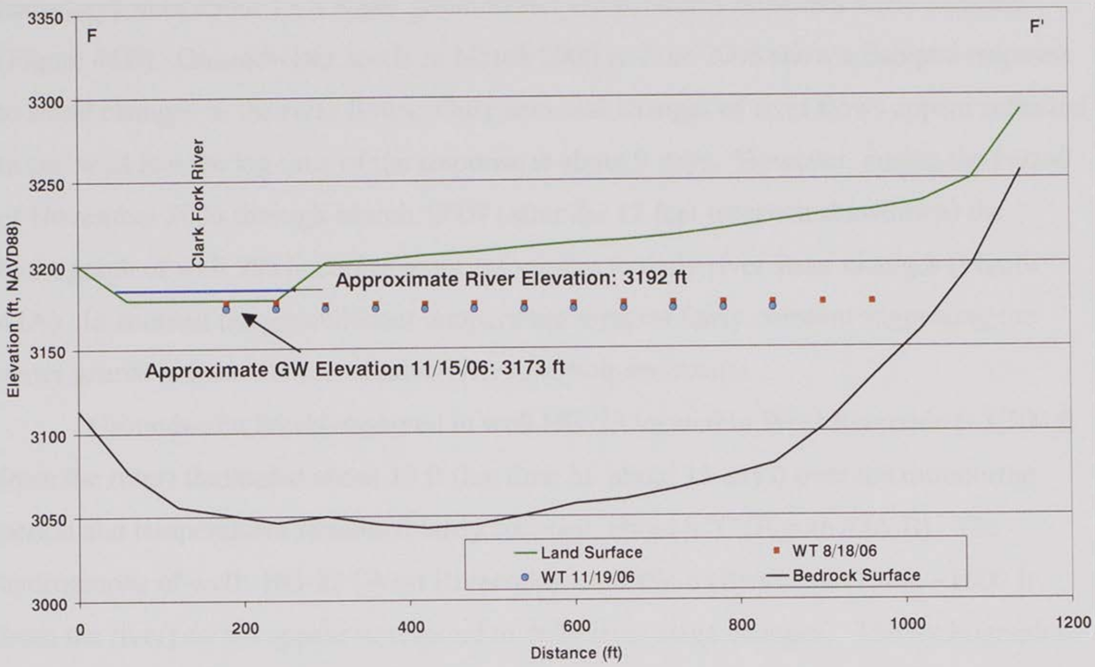

Figure 39 Hydrogeologic cross section displaying land surface, bedrock surface, river elevations and groundwater elevations over time. The cross section extends from the Duck Bridge at Milltown Reservoir to Piltzville, MT.

The surface water stage and groundwater profiles presented above are also supported by observations at transducer instrumented wells at which relationships between the lag time between stage and temperature, and surface water conditions were evaluated. Wells near the river or reservoir in which both water levels and temperatures mirror river conditions would suggest both river and reservoir leakage occur. In contrast, lags or significant differences in the amplitude of adjacent groundwater level responses suggest a more limited or less direct exchange process. Thermographs are presented on all hydrographs for each well in Appendix C.

The well linked groundwater and river conditions in the vicinity of Turah are illustrated with data from the Rodin well (~1000 feet from the river). Groundwater levels varied approximately 4 ft, groundwater temperature fluctuated nearly 16 °C , and the water table responded almost immediately to changes in-river flows (Figure 40A). In addition the seasonal temperature changes in the river are reflected in the groundwater system (Figure 40B). In contrast to the Rodin well hydrograph and thermograph, seasonal water level changes at well 99a (about 1000 ft from the northern reservoir boundary) were about 13 ft while groundwater temperatures remained fairly constant (Figure 41B). Groundwater levels in March 2006 to June 2006 show a damped response to small changes to the river flows. Only seasonal changes of river flows appear reflected in this well and the lag time of the response is about 9 days. However, during the period of November 2006 through March, 2007 (after the 12 feet reservoir drawdown) the hydrograph of well 99a becomes more responsive to daily river stage changes (Figure 41A). In contrast the groundwater temperature remains fairly constant suggesting the water source is from the low conductivity reservoir sediments.

Groundwater levels observed in well HG-23 located in West Riverside (~3,500 ft from the river) fluctuated about 13 ft (lag time of about 13 days) over the monitoring period and temperatures remained fairly constant, about 8 ^{o}C (Figure 42A,B). The hydrographs of wells HG-23 (West Riverside) and MW-6 (Bandmann Flats, ~1600 ft from the river) do not appear to respond to daily river stage changes. The hydrograph of well MW-6 in located in Bandmann Flats shows water levels in this area fluctuated almost 14 feet and temperatures fluctuated about 1 C during the study (Figure 43A,B). This is likely a result of the perched river conditions that exist below the dam and long flow paths from the river to the well (Gestring, 1994). The lag time of response to river flow changes in this well is 7 days.

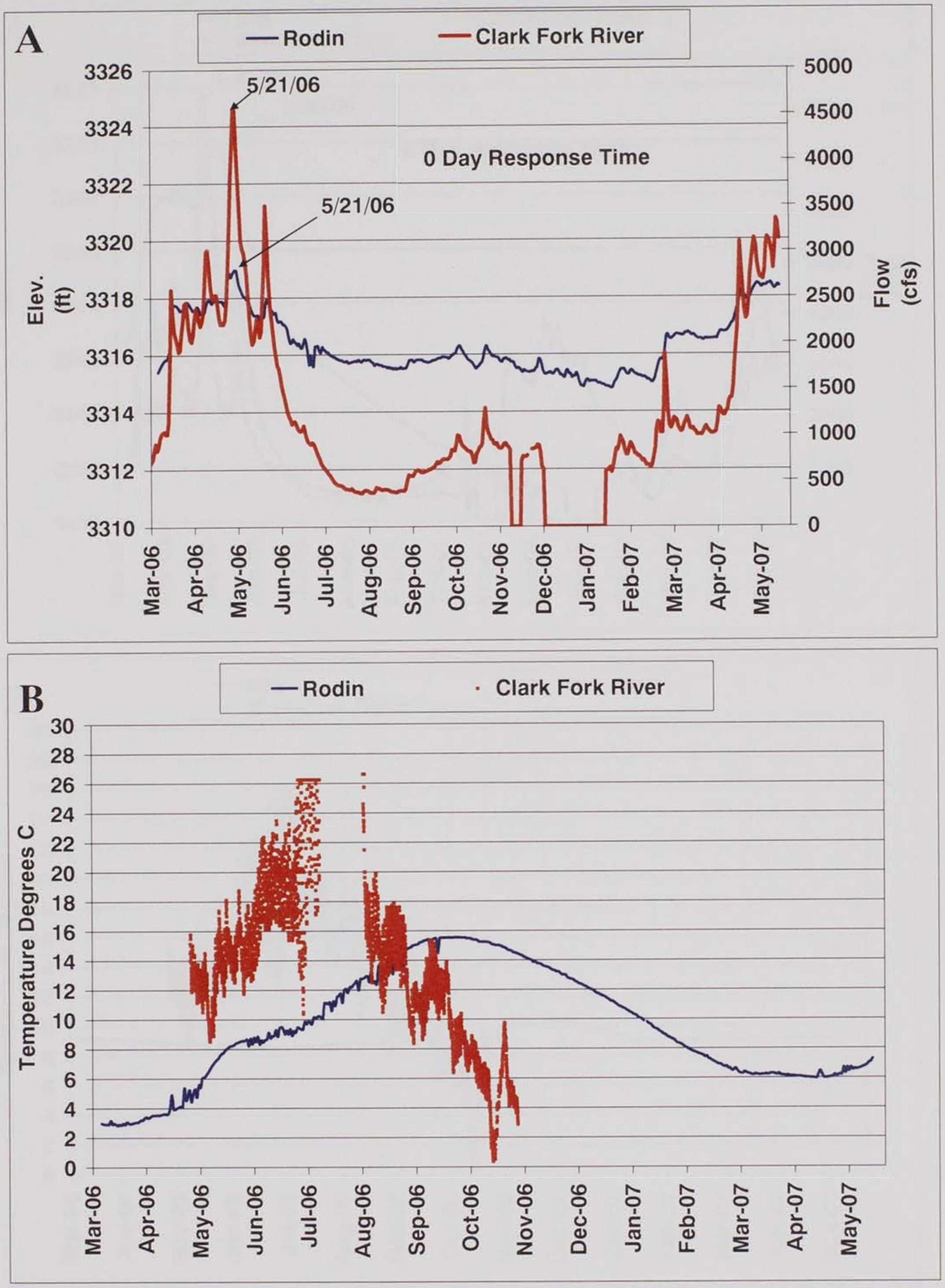

Figure 40. **A**) The Clark Fork River, Blackfoot River and Rodin well hydrographs. This figure illustrate that daily river stage changes are reflected in the adjacent aquifer system near Turah, MT. **B**) This figure shows that the seasonal temperature changes in the river are reflected in the adjacent aquifer system near Turah, MT.

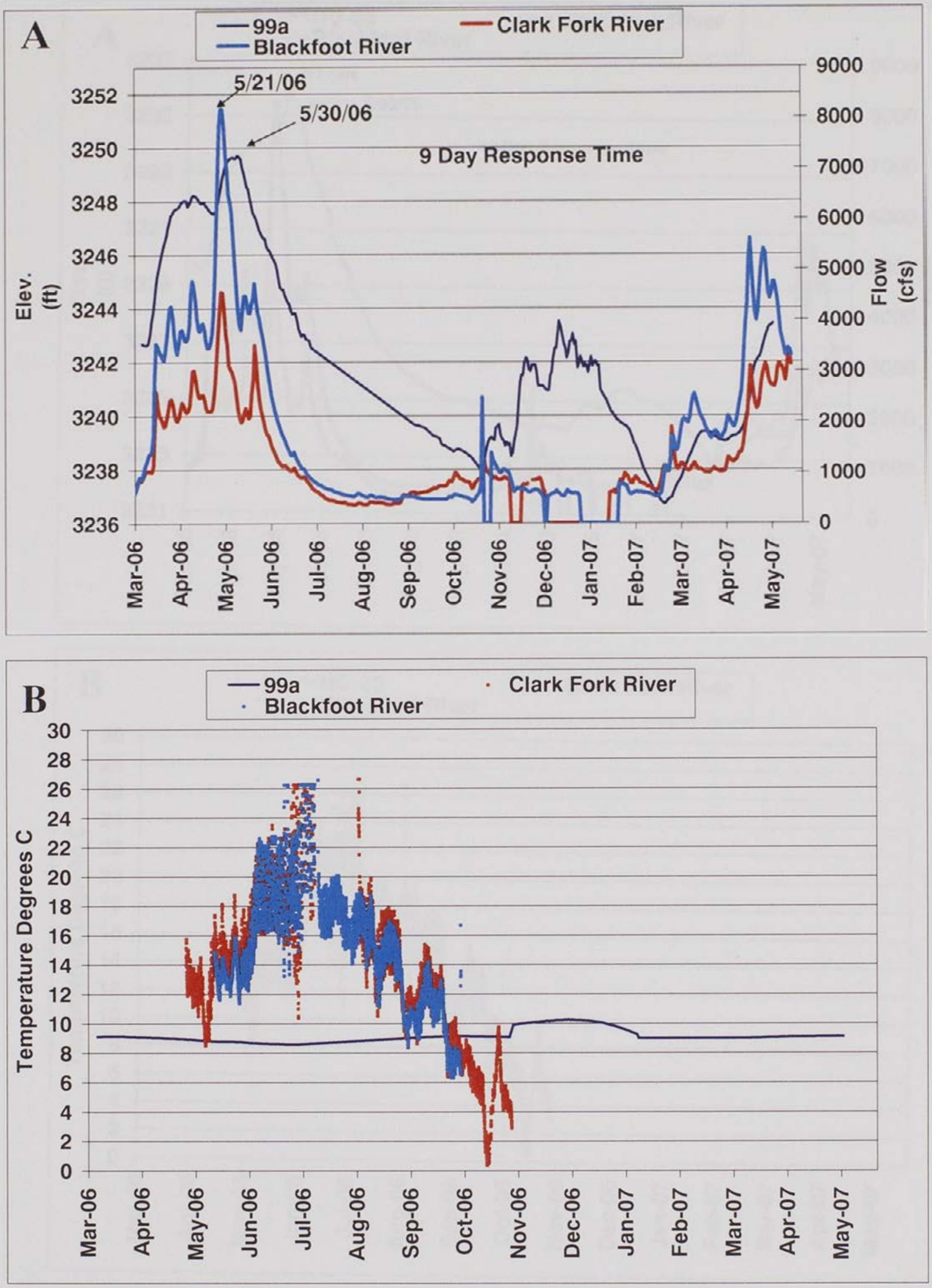

Figure 41 A) The Clark Fork River, Blackfoot River and well 99a hydrographs. This figure illustrates that daily river stage changes are not reflected in the adjacent aquifer before the drawdown of the reservoir but are after near Milltown, MT. **B)** This figure shows that the seasonal temperature changes in the river are not necessarily reflected in the adjacent aquifer system near Milltown, MT.

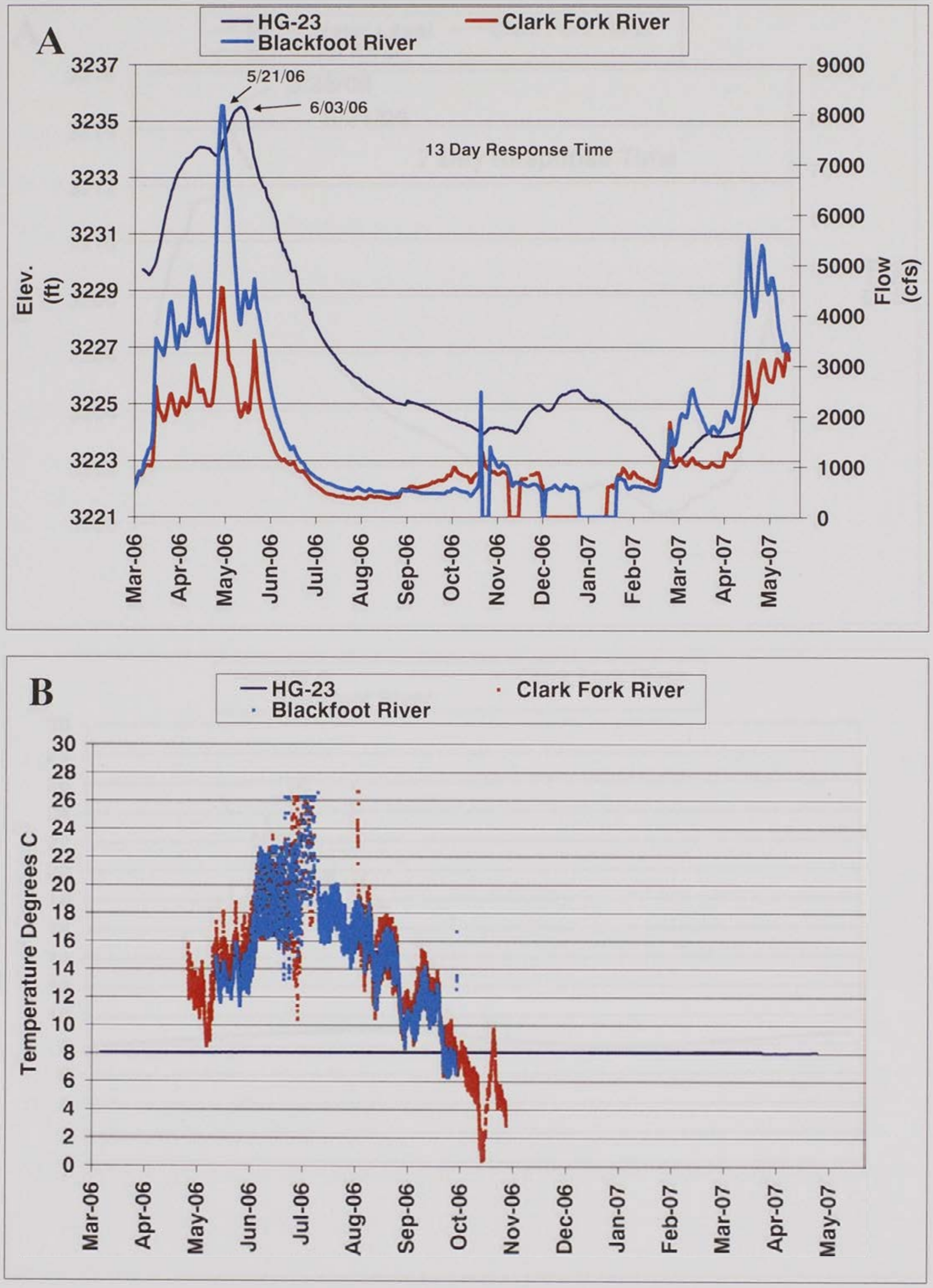

Figure 42 A) The Clark Fork River, Blackfoot River and HG-23 hydrographs. This figure illustrates that daily river stage changes are not reflected in the aquifer in West River Side, MT. **B)** This figure shows that the seasonal temperature changes in the river are not necessarily reflected in the adjacent aquifer system in West Riverside, MT.

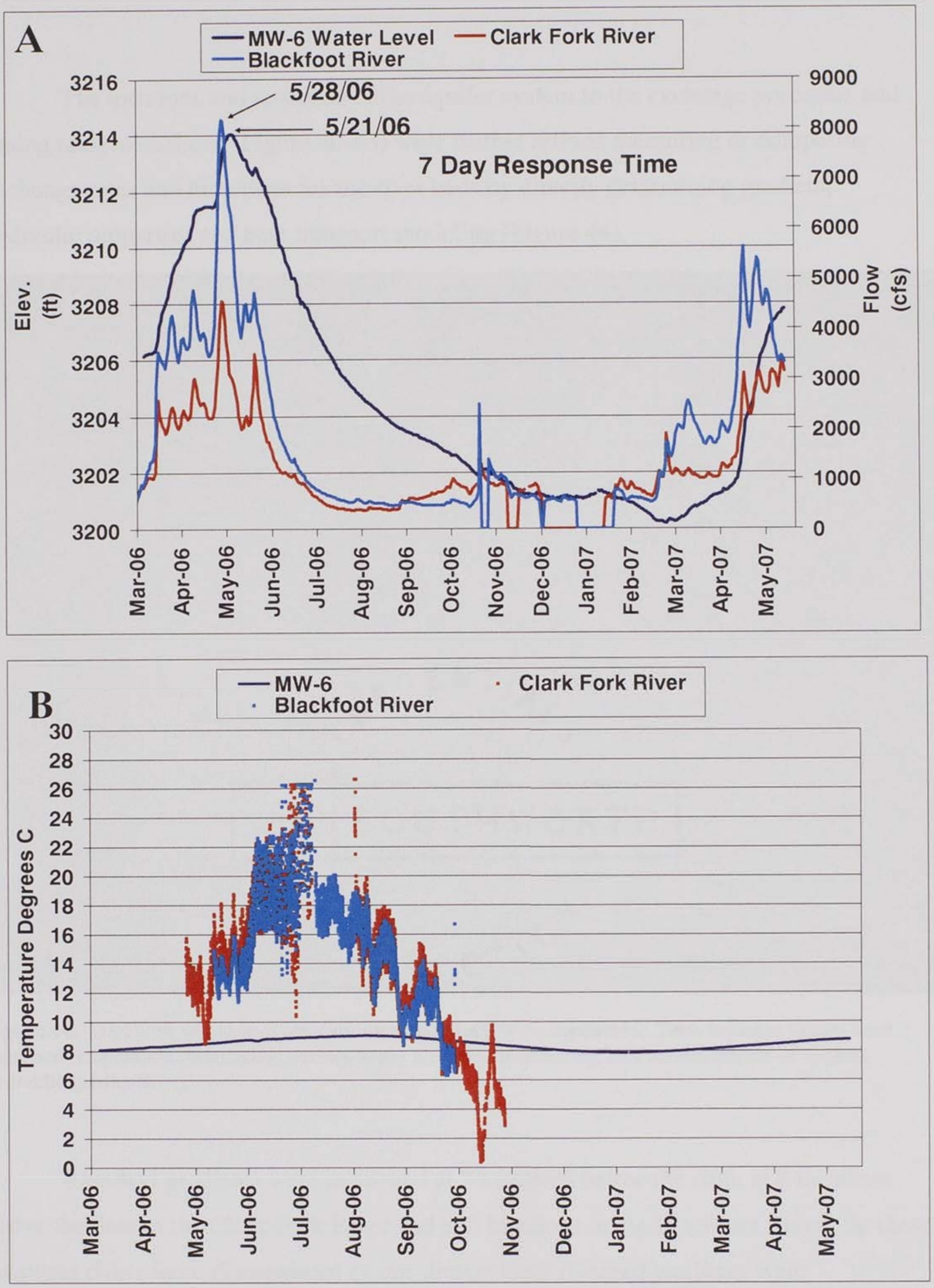

Figure 43 **A**) The Clark Fork River, Blackfoot River and well MW-6 hydrographs. This figure illustrates that daily river stage changes are not reflected in the aquifer in Bandmann Flats. **B**) This figure shows that the seasonal temperature changes in the river are not necessarily reflected in the adjacent aquifer system near Bandmann Flats.

The locations and response of the aquifer system to the exchange processes and timing presented above (Figure 40-43) were further refined measuring or computing exchange rates and directions for the river beds by directly determining gradient, hydraulic properties and heat transport modeling (Figure 44).

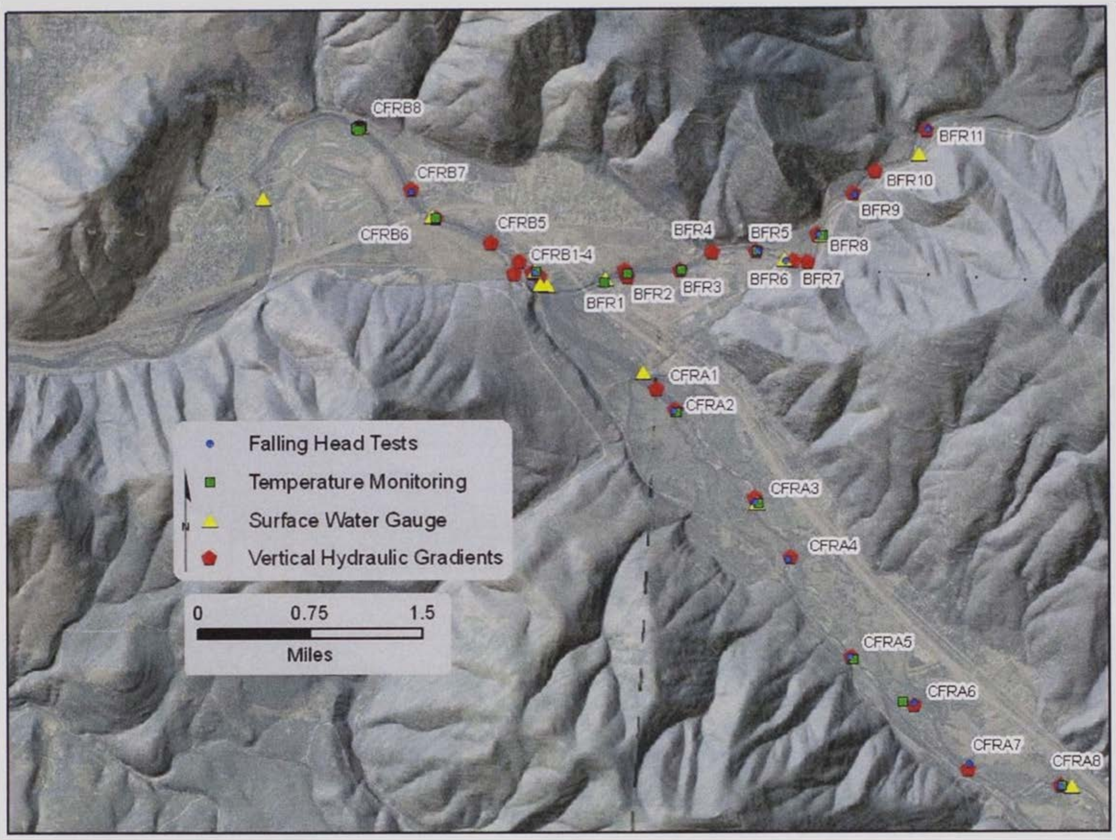

Figure 44. Locations where in-river instrumentation tests were conducted. Tests included falling head tests, bed temperature monitoring, surface water elevation monitoring, and measurements of vertical hydraulic gradients.

Riverbed gradients were measured at 7 locations below the dam, at 8 locations above the dam in the Clark Fork River and at 8 locations in the Blackfoot River. At these locations either three-dimensional or one dimensional riverbed gradients were determined. Three dimensional in-river gradients were measured at locations CFRA2, CFRA3, CFRA4, CFRA5, CFRA6, CFRA 7 and CFRA 8. The three dimensional gradients were only defined in the Clark Fork River above the dam for the following reasons: 1) The Clark Fork River below the dam is perched (near vertical flow is assumed) and in many instances the unsaturated zone below the river bed extended to a depth of less than 2 feet; 2) several attempts were made to evaluate three dimensional gradients on the Blackfoot River, however the coarse make up of the riverbed limited instrument penetration; 3) the depth of water in the Blackfoot arm of the reservoir made instrumentation impractical. Flow direction trends in instrumented locations in the Clark Fork River above the reservoir were identified as upward as well as slightly downward and towards the river bank (Figure 45). All derived surfaces for three dimensional gradients are presented in Appendix D.

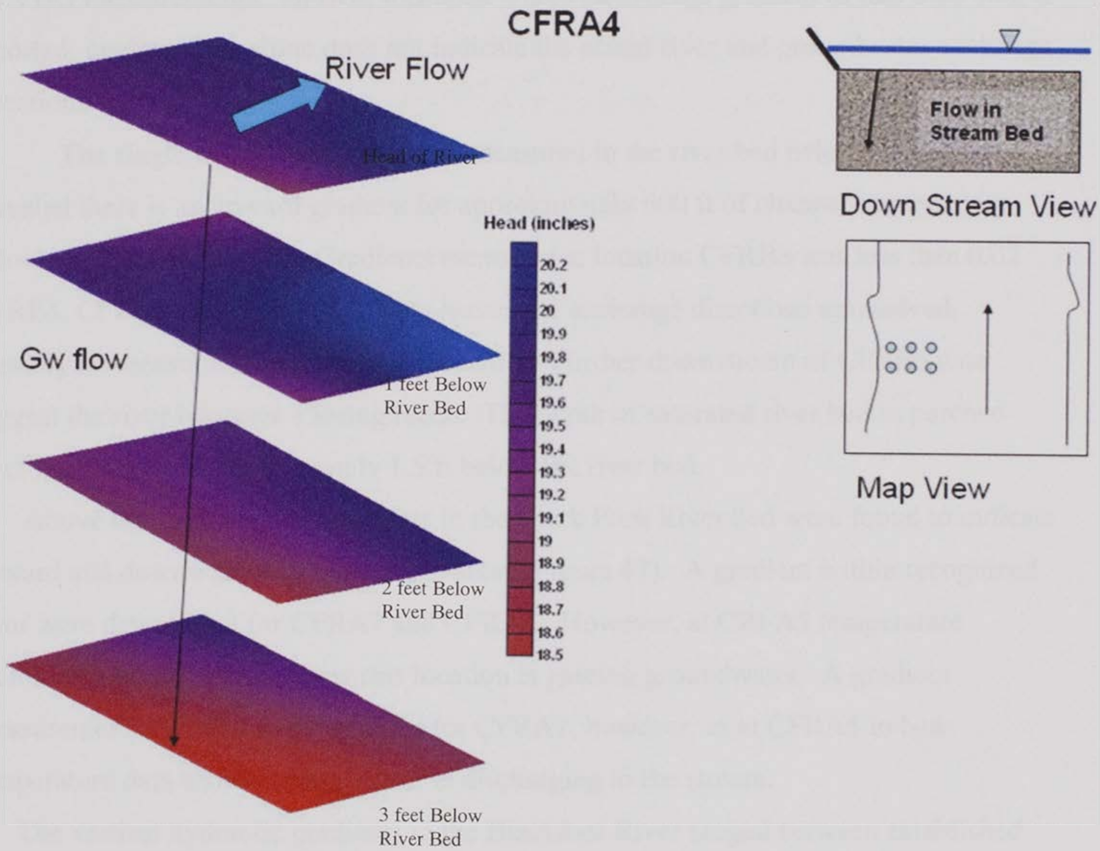

Figure 45 The 2-dimensional surfaces in this figure show the measured hydraulic total head at four discrete locations; 1) the river surface, 2) 1 ft below the river bed, 3) 2 ft below the river bed, 4) 3 ft below the river bed. The hydraulic head of the river and just below the river bed is higher that the hydraulic head measured at 2 and 3 ft below the river bed suggesting a downward flow of the river water into the bed sediments. The arrow indicates the interpreted direction of flow.

The vertical hydraulic gradients were measured in the summer and fall of 2006 following the initial drawdown and/or at the time of installation of temperature monitoring instrumentation. Vertical gradients were also measured at the time of installation of temperature monitoring instrumentation. Vertical hydraulic gradient measurements have an estimated error of 0.02. The gradient is a dimensionless parameter. An error was determined at each river station as half of the estimated range of the measured gradients at that station. Typically, three to eighteen vertical hydraulic gradients were measured at each river station. The reported value is the average estimated gradient. The maximum range estimated for all locations is the reported error for VHG measurements. At river locations where an average gradient of less than 0.02 is reported, gradient data alone does not indicate the actual river and groundwater exchange directions.

The single depth piezometer data measured in the river bed below the dam revealed there is an upward gradient for approximately 600 ft of channel immediately below the dam (Figure 46). Gradients measured at location CFRB3 was less than 0.02 CFRB4, CFRB5 were 0.02, these data leaves the exchange directions unresolved, possibly no measurable exchange is occurring. Further downstream of CFRB5 data suggest the river becomes a losing reach. The depth of saturated river bed in perched river locations was approximately 1.5 ft below the river bed.

Above the dam, vertical gradients in the Clark Fork River bed were found to indicate upward and downward water exchange areas (Figure 47). A gradient within recognized error were determined for CFRA7 and CFRA5. However, at CRFA5 temperature monitoring results clearly show this location is gaining groundwater. A gradient measurement of 0.02 was determined for CFRA2, however, as at CFRA5 in bed temperature data shows ground water is discharging to the stream.

The vertical hydraulic gradients in the Blackfoot River ranged between established errors and -0.1 indicating reaches are generally losing water and recharging the groundwater (Figure 48).

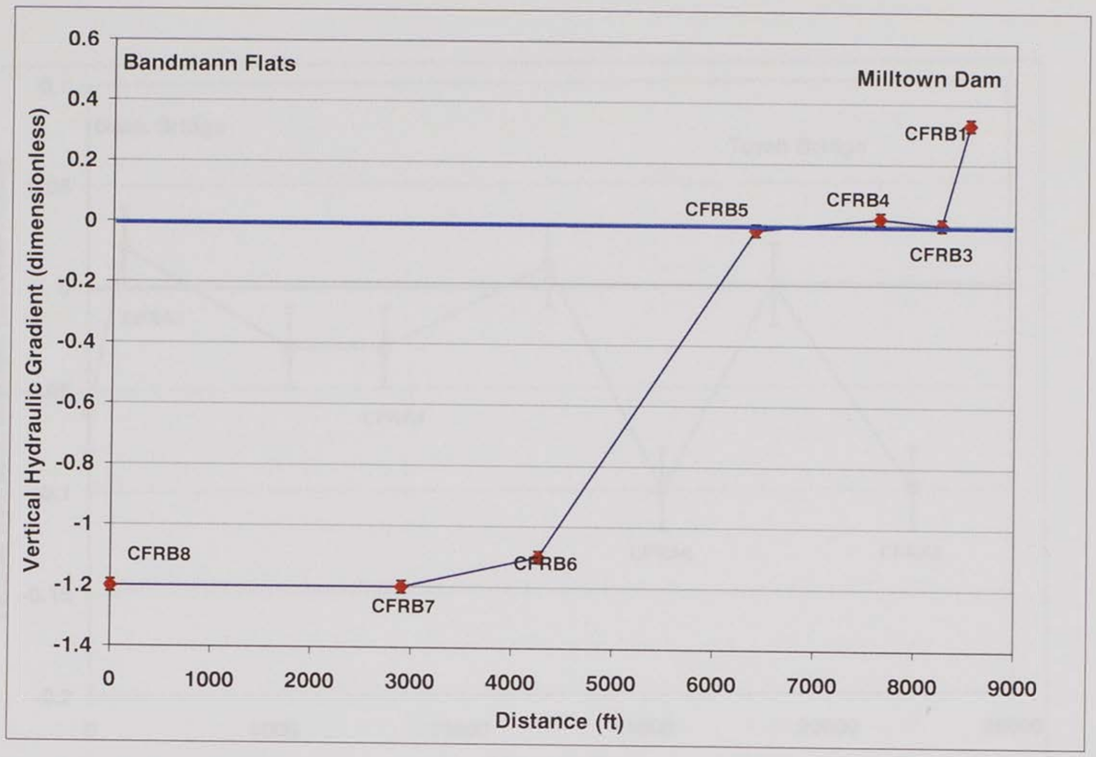

Figure 46 The distribution of vertical hydraulic gradients below Milltown Dam. Negative gradients indicate zones of river water seepage to the underlying groundwater systems. Positive gradients are present when groundwater is discharging to the river bed. Areas with no measurable upward or downward gradients suggest no measurable exchange of water between systems is occurring. The gradients were collected between August and October 2006. The error bars show the measurement error.

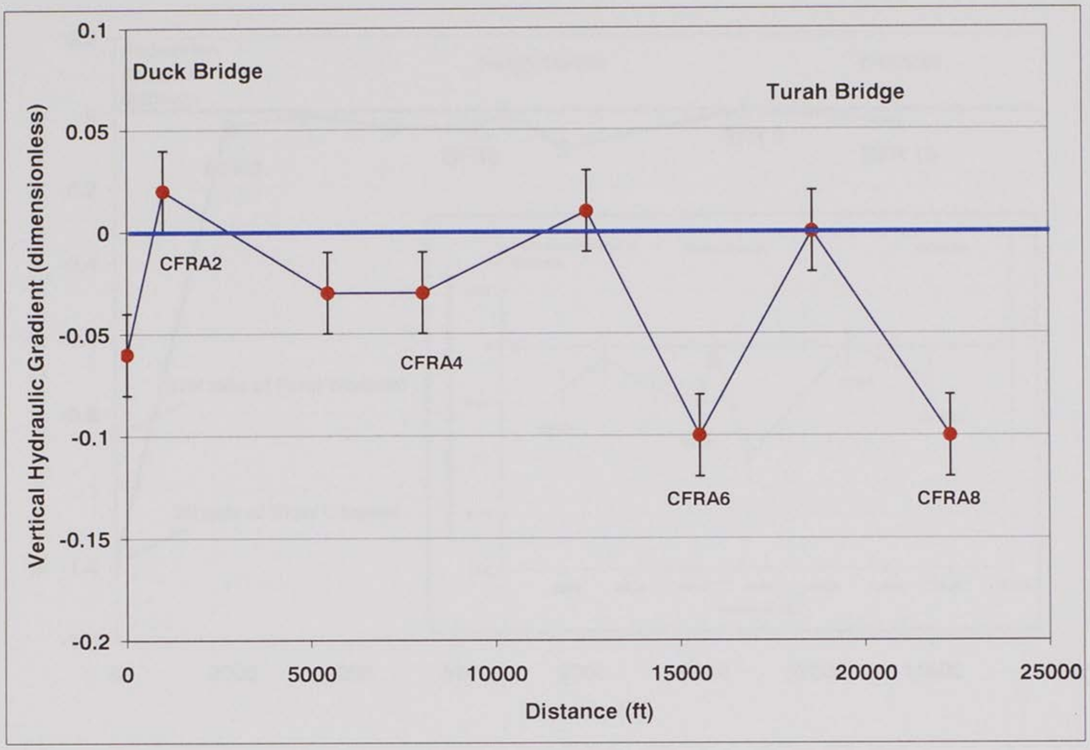

Figure 47 The distribution of vertical hydraulic gradients between Turah Bridge and Milltown Dam. Negative gradients indicate zones of river water seepage to the underlying groundwater systems. Positive gradients are present when groundwater is discharging to the river bed. Areas with no measurable upward or downward gradients suggest no measurable exchange of water between systems is occurring. The gradients were collected between August and October 2006. The error bars show the measurement error. The error bars show the measurement error.

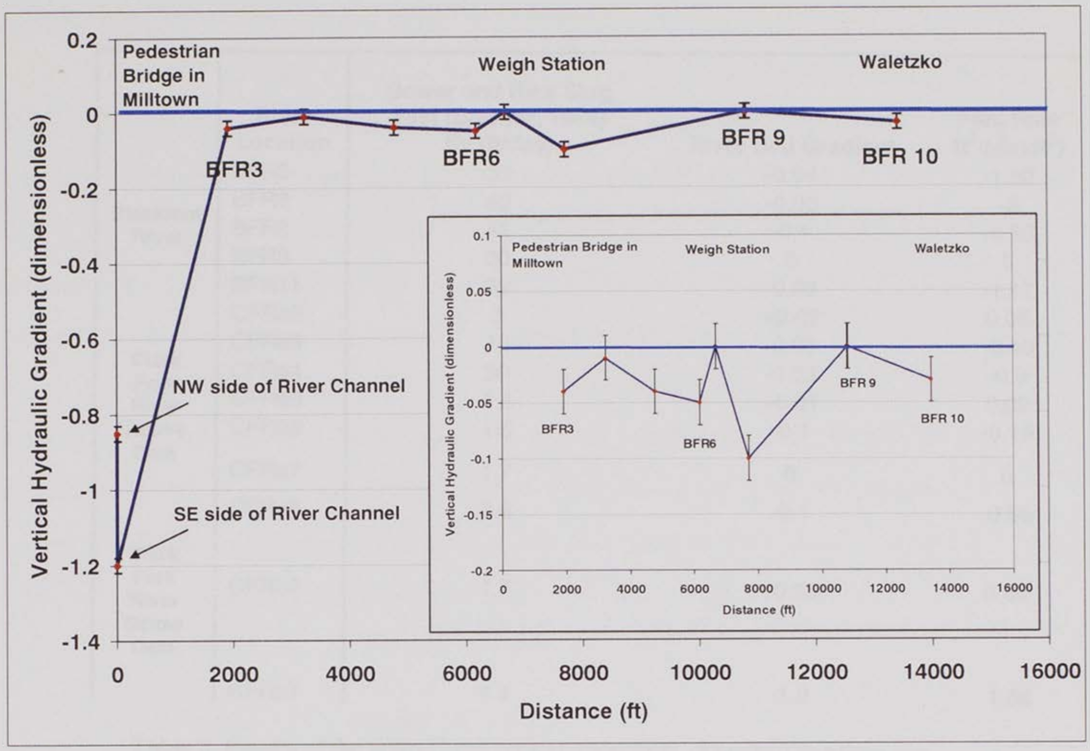

Figure 48 The distribution of vertical hydraulic gradients on the Blackfoot River above Milltown Dam. Negative gradients indicate zones of river water seepage to the underlying groundwater systems. Positive gradients are present when groundwater is discharging to the river bed. Areas with no measurable upward or downward gradients suggest no measurable exchange of water between systems is occurring. The gradients were collected between August and October 2006. The error bars show the measurement error. The error bars show the measurement error.

Riverbed horizontal hydraulic conductivity values (Kh) were determined by conducting falling head permeameter tests throughout the study area (Bouwer, 1989), and the vertical hydraulic conductivity (Kv) were computed from field measured horizontal hydraulic conductivity values Kv = 0.1* Kh. The vertical bed hydraulic conductivities ranged from 1.4 to 42 ft/day (Table 3). The hydraulic conductivity values for the bed of the Blackfoot River and the Clark Fork River above the dam tend to be higher than the values in the Clark Fork River channel below the dam. There is an estimated 3% error for the reported values. All data and calculations related to falling head test are presented in Appendix E.

	River Location	Bower and Rice Slug Test (Bouwer, 1989) Kv (ft/day)	River Bed Gradient	Flux Rate $ft^3/(dayft^2)$
Blackfoot River	BFR5	30	-0.04	-1.20
	BFR6	40	-0.05	-2
	BFR8	42	-0.1	-4.20
	BFR9	30	0	0
	BFR11	39	-0.03	-1.17
Clark Fork River Above Dam	CFRa2	3	+0.02	0.06
	CFRa3	16	-0.03	-0.48
	CFRa4	30	-0.03	-0.9
	CFRa5	1.5	+0.01	0.02
	CFRa6	1.5	-0.1	-0.15
	CFRa7	1.7	0	0
	CFRa8	3.6	-0.1	-0.36
Clark Fork River Below Dam	CFRb2	1.7	+0.33	0.56
	CFRb7	1.4	-1.2	-1.68

Table 3 Results of the falling head permeameter tests. Riverbed locations can be viewed in Figure 44.

The gradient measurements and hydraulic conductivity values were combined to compute flux rates at monitored locations in units of discharge per square foot of channel bottom. Flux rates were highest in the Blackfoot River bed test sites upriver from the mill area. On the Clark Fork River flux rates were typically higher at test locations below the dam (a combination of a lower hydraulic conductivity values than measured in the river bed above the reservoir with larger downward hydraulic gradient values at instrumented sites).

Riverbed temperature monitoring and modeling provided additional evidence of the locations of gaining and losing river reaches and site exchange rates. Plots of river and river bed temperatures at CFRA2 (up gradient from the Milltown Reservoir) shows that this area of the river is a gaining reach. The lower thermistor (depth of 1.0 ft into the river sediments) shows water temperatures at that depth remained fairly constant and cooler that more shallow bed water (thermistor located 0.5 feet below the bottom of the river bed).. This temperature distribution is interpreted to represent conditions were cooler groundwater is discharging into the river as the surface water temperature is not evident at depth.

The riverbed temperature profile collected at CFRA4 from May 17th, 2007 to July, 10th, 2006 shows trends typical of a profile of a losing river. River temperatures at this site are transmitted so that almost no temperature lag is recorded at a depth of 1.0 ft below the river bed. The temperature profile recorded below the dam (CFRB8) also indicates the river is losing at this site, however, the observed temperature lag (timing between changes in-river temperatures in in-bed temperatures) is greater than at CRFA4 suggesting a reduced seepage rate. It is also known from measuring the hydraulic gradients with in-river piezometers that there is an unsaturated zone below the riverbed at this location. The profile at 1.3 feet below the bottom of the riverbed appears not to reflect the diurnal temperature variations, data that support the presence of a vadose zone. Temperature and depth time series plots can be seen in Figures 49, 50 and 51.

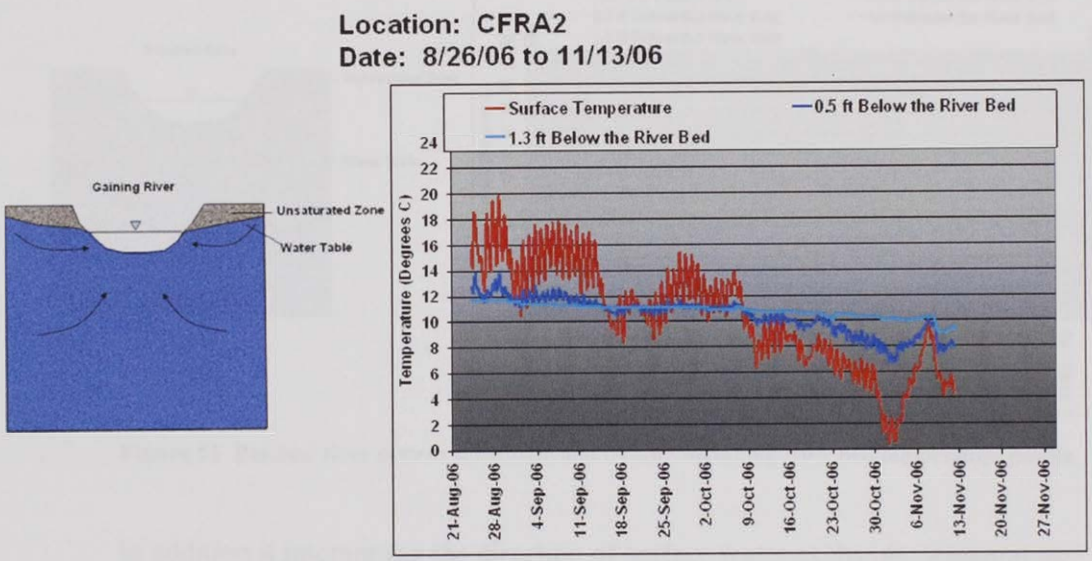

Figure 49 Gaining river system schematic and its corresponding river bed temperature profile.

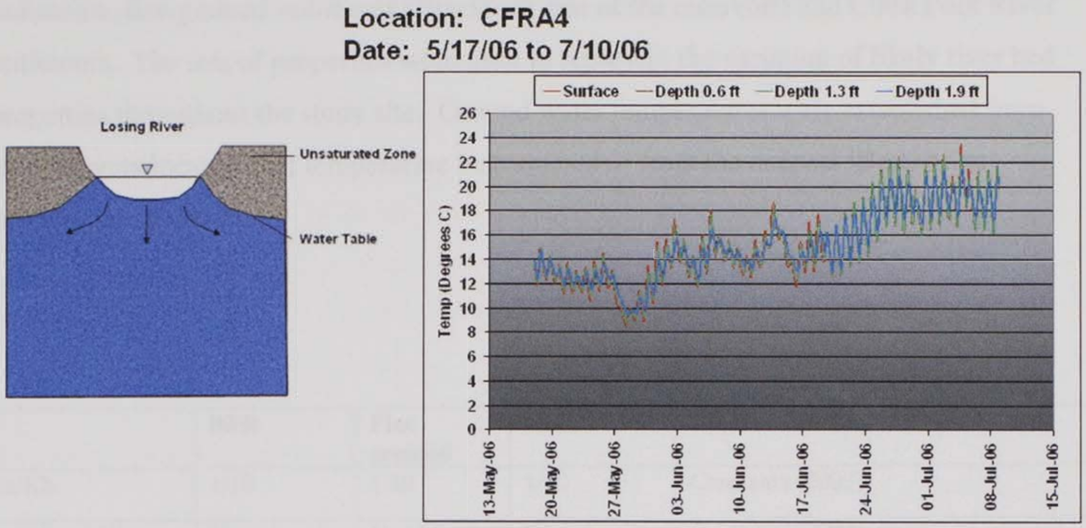

Figure 50 Losing river system schematic and its corresponding river bed temperature profile.

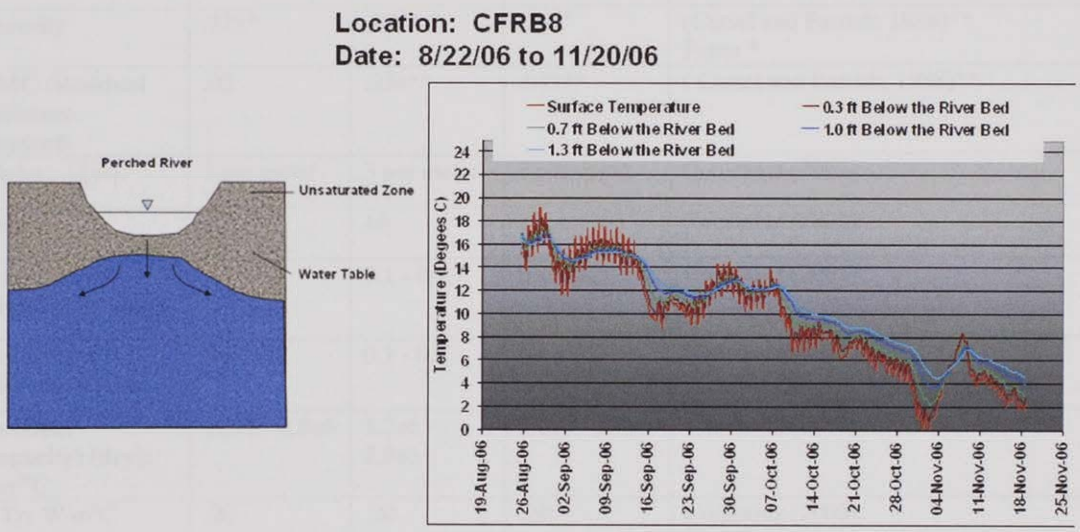

Figure 51 Perched river system schematic and its corresponding river bed temperature profile.

In addition it interpreting the direction of surface water exchange, temperature flux modeling was used to compute leakage rates (VS2DHI USGS). The exchange rates are determined by matching observed versus simulated riverbed temperature gradients. Matches are obtained by adjusting the hydraulic properties in the model until the best fit is reached. Table 4 presents a list of the sediment parameters used in the models. Hydraulic conductivity and riverbed porosity were the parameters adjusted to find the best fit. Three different riverbed sediment properties settings were used, Blackfoot River sediments, fine grained sediments (Blackfoot arm of the reservoir) and Clark Fork River sediments. The sets of properties were used to represent the variation of likely river bed properties throughout the study site. Ground water temperatures were established from level loggers located near temperature instruments or from the deepest iButtons on temperature arrays.

	BFR	Fine grained	CFR	Source
Kz/Kh	1/10	1/10	1/10	Constantz (2003)
Saturated Kh (m/min)	Varied	Varied	Varied	Constantz (2003)
Specific Storage	1e-6	1e-6	1e-6	Constantz (2003)
Porosity	.275*	.46**	.41**	(Carsel and Parrish, 1988)** Fetter *
RMC (Residual Moisture Content)	.02	.034**	.045**	(Carsel and Parrish, 1988)**
Alpha : 1/[m].	3 per meter	3 per meter	3 per meter	Constantz (2003)
Beta	10	10	10	Constantz (2003)
Longitudinal Dispersivity (m)	0.1 - 0.2	0.1 - 0.2	0.1 - 0.2	Constantz (2003)
Transverse Dispersivity (m)	0.1 - 0.2	0.1 - 0.2	0.1 - 0.2	Constantz (2003)
Cs (Heat Capacity) (dry): $J/m^{3o}C$	1.2e6 - 2.8e6	1.2e6 - 2.8e6	1.2e6 - 2.8e6	Constantz (2003)
KTr: W/m^oC	.20	.20	.20	Constantz (2003)
KTs: $[Q/mT^oC]$	1.8	1.8	1.8	Constantz (2003)
Cw (Heat Capacity) (water): $[Q/m^{3o}C]$	4186000	4186000	4186000	Constantz (2003)

Table 4 Parameters used to define sediment properties for temperature modeling.

Kz/Kh: Ratio of saturated hydraulic conductivity in the vertical (z) direction to that in the horizontal (x or r) direction.
Saturated Kh: Saturated Khh: [L]/[T]. Saturated hydraulic conductivity in the horizontal (x or r) direction.
Specific Storage: Specific Storage (Ss): 1/[L]. Fluid storage due to fluid and porous medium
Porosity: Defined in the usual way--volume of pore space per bulk volume of soil or porous medium.

Alpha : 1/[L]. Parameter in van Genuchten model. Must be positive.
Beta Parameter in van Genuchten function.
Cs (Heat Capacity) (dry): Heat capacity of dry solids, [Q/L^{3o}C], where Q is energy or ML^2T^{-2}. For SI units the conductivities are in J/m^{3o}C
KTr: Thermal conductivity of water-sediment at residual moisture content [Q/LT^{o}C]. For SI units their conductivities are in W/m^{o}C
KTs: Thermal conductivity of water-sediment at full saturation, [Q/LT^{o}C]
Cw (Heat Capacity) (water): Heat capacity of water, which is the product of density * specific heat of water, [Q/L^{3o}C]

		Date	Dispersivity (assigned transport parameter)	RMS ERROR	Gradient	River bed Vertical Conductivity (ft/day)	Computed flux rate $ft^3/(day ft^2)$
Clark Fork River Above the Dam	CFRA2 (above duck bridge)	8/24/06-11/12/06	0.2	.49	+0.02	1.0	0.8-0.7
	CFRA3 (CE)	5/18/06 – 7/8/06	0.2	.94 - .42	-0.03	13.1	11.3 – 13.0
	CFRA5 (CCR)	8/24/06 – 11/12/06	0.2	1.17	+0.01	1.3	2.9 – 3.2
	CFRA8 (Turah Bridge)	8/24/06 – 11/13/06	0.15	.67 - .17	-0.1	3.3	2.9 – 2.3
Blackfoot River	BFR2	7/31/06 – 10/10/06	0.2	0.1 – 0.13	-0.85	0.7	0.9 – 1.2
	BFR8 (in middle of channel)	10/10/06 – 10/31/06	0.2	0.01	-0.85	98.4	13.0 – 10.4
Clark Fork River Below the Dam	CFRB6	8/26/06 – 11/17/06	0.2	0.1 - 1	-1.2	0.7	0.7 – 1.1
	CFRB8a	6/20/06 – 8/6/06	0.2	0.7 – 0.12	-1.2	2.3	2.9 – 3.2
	CFRB8d	6/20/06 – 8/6/06	0.15	1.14 – 0.1	-1.2	2.1	3.7 – 2.8

Table 5 Results of temperature modeling. Locations are identified in Figure 44.

Heat transport modeling simulated flow in the vertical direction. As a result, hydraulic conductivity estimates are representative of the vertical hydraulic conductivity of riverbed sediments. The difference between the simulated and measured temperatures is presented as the root mean squared error. The assumptions made in the modeling effort consisting of: 1) water entering and leaving the river only in a vertical direction; 2) sediments in the riverbed having uniform hydraulic and thermal properties; 3) vertical hydraulic gradients not varying with time and; 4) the metal sandpoint casing not influence heat conduction, all increase the uncertainty in the estimates and may have contributed in part to this error. The uncertainties could be significantly reduced by measuring the vertical hydraulic gradients and temperatures simultaneously. Modeling the heterogeneity of the thermal properties of the river bed sediments will not largely influence the results because the modeling results are less sensitive to the assigned thermal properties of the soil and are most sensitive to the hydraulic conductivity and flow into and out of the river bed is controlled by the lowest hydraulic conductivity unit (Tallman, 2005; Stonestrom et al., 2003)). The measured temperature profiles and simulated results are presented in Appendix F.

The results of the temperature modeling show vertical hydraulic conductivity values that range from 0.8 to 98.0 ft/day and exchange rates that range from 0.7 to 13.0 $ft^3/(dayft^2)$(Table 5). Temperature instruments at locations CFRB1, BFR3 and BFR5 were not recovered.

Figure 52 A picture of the riverbed sediments below Milltown dam. The photo shows the coarse river bed armored with fine grained reservoir sediments.

The Clark Fork River bed above Milltown Dam and the Blackfoot River bed have hydraulic conductivities that range from 3 to 98.4 ft/day and seepage rates that range from 0.7 to 13.0 $ft^3/(dayft^2)$. The highest measured seepage rates are present in historic portions of the channels where gravel is transported. The in bed temperature signal in these areas is illustrated by the recorded at CFRA4. The majority of lower hydraulic conductivity values were found to be associated with portions of the river that were previously overlain by the reservoir pool and contain fine-grained sediment. The in bed temperatures measured in these areas are shown in Figure 51. The coarse grained Clark Fork River bed below the dam has become in-filled with fine grained reservoir sediments (Figure 52). Such areas appear to have lower river bed hydraulic conductivities but higher than expected exchange rates which appear to be driven by measured large vertical hydraulic gradients found in these perched sections of streams (Gestring, 1994). The temperature signature measured at CFRB8 is interpreted to also reflect these conditions.

An initial conceptual model of possible distributions gaining and losing reaches of river was developed using the vertical hydraulic gradient data, the temperature monitoring data and by comparing river stage elevations to adjacent groundwater elevations. Based of the location of vertical gradient measurements the distribution gaining, losing and parallel flow reaches were estimated to extend half of the distance between monitoring locations (Figure 53, 54 and 55).

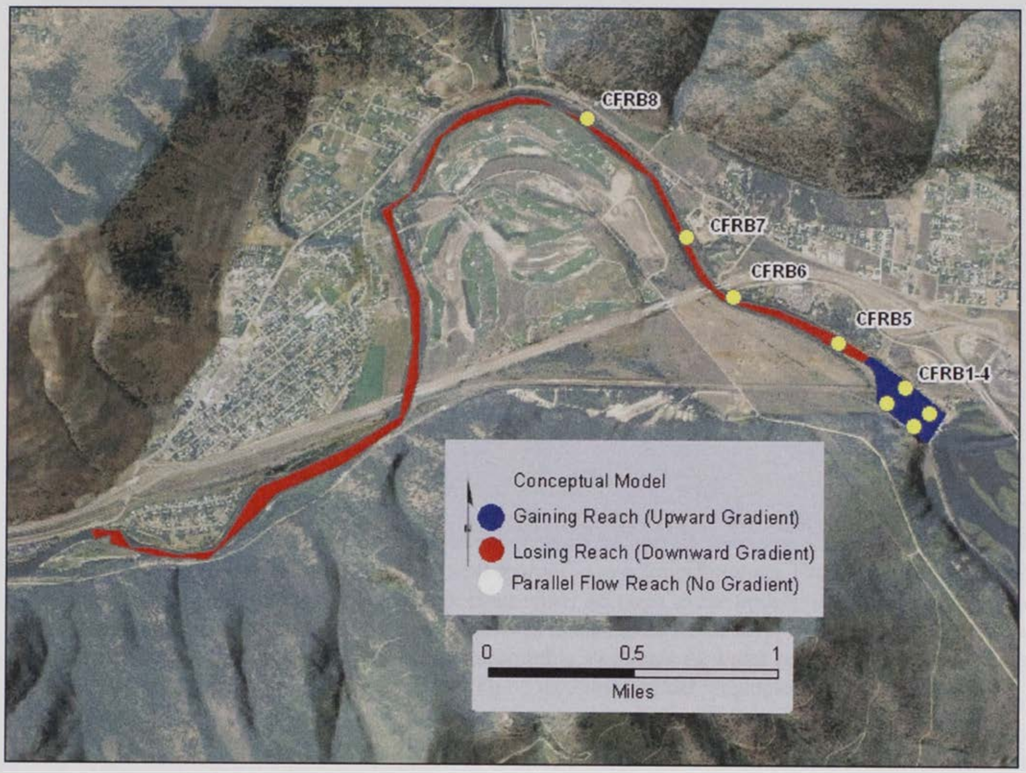

Figure 53 Conceptual distribution of vertical hydraulic gradients below Milltown Dam. Negative gradients indicate zones of river water seepage to the underlying groundwater systems. Positive gradients are present when groundwater is discharging to the river bed. Areas with no measurable upward or downward gradients suggest no measurable exchange of water between systems is occurring. These are considered areas of parallel flow. The conceptual model was determined for low water conditions.

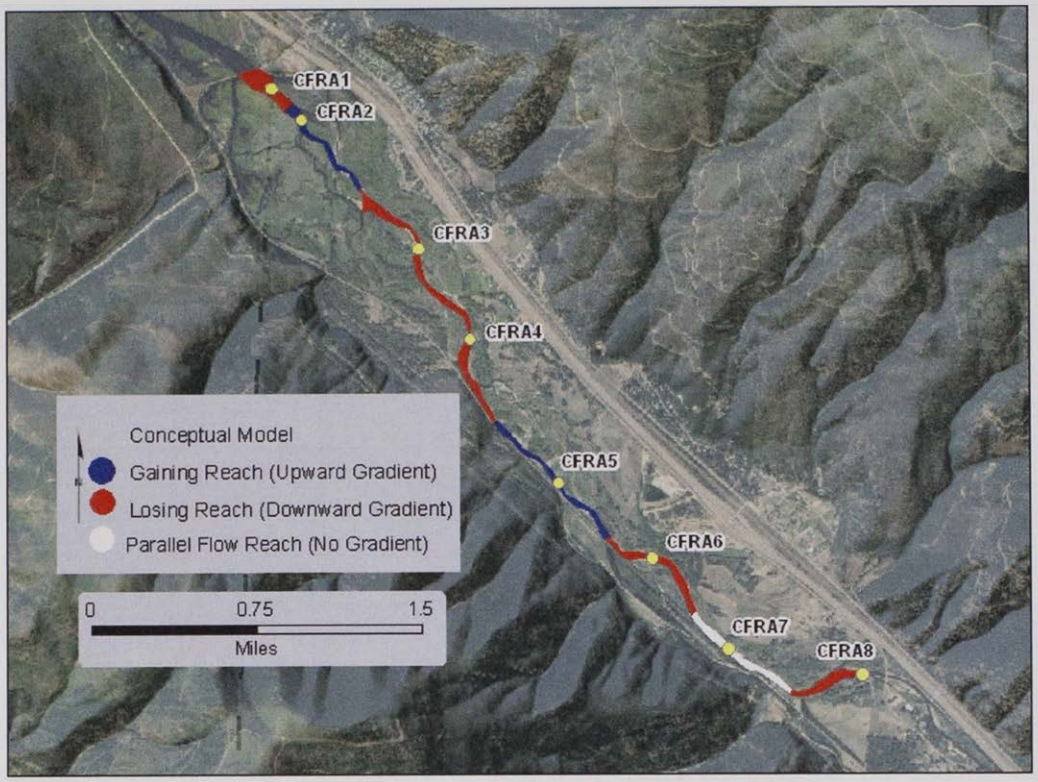

Figure 54 Conceptual distribution of vertical hydraulic gradients between Turah Bridge and Milltown Dam. Negative gradients indicate zones of river water seepage to the underlying groundwater systems. Positive gradients are present when groundwater is discharging to the river bed. Areas with no measurable upward or downward gradients suggest no measurable exchange of water between systems is occurring. These are considered areas of parallel flow. The conceptual model was determined for low water conditions.

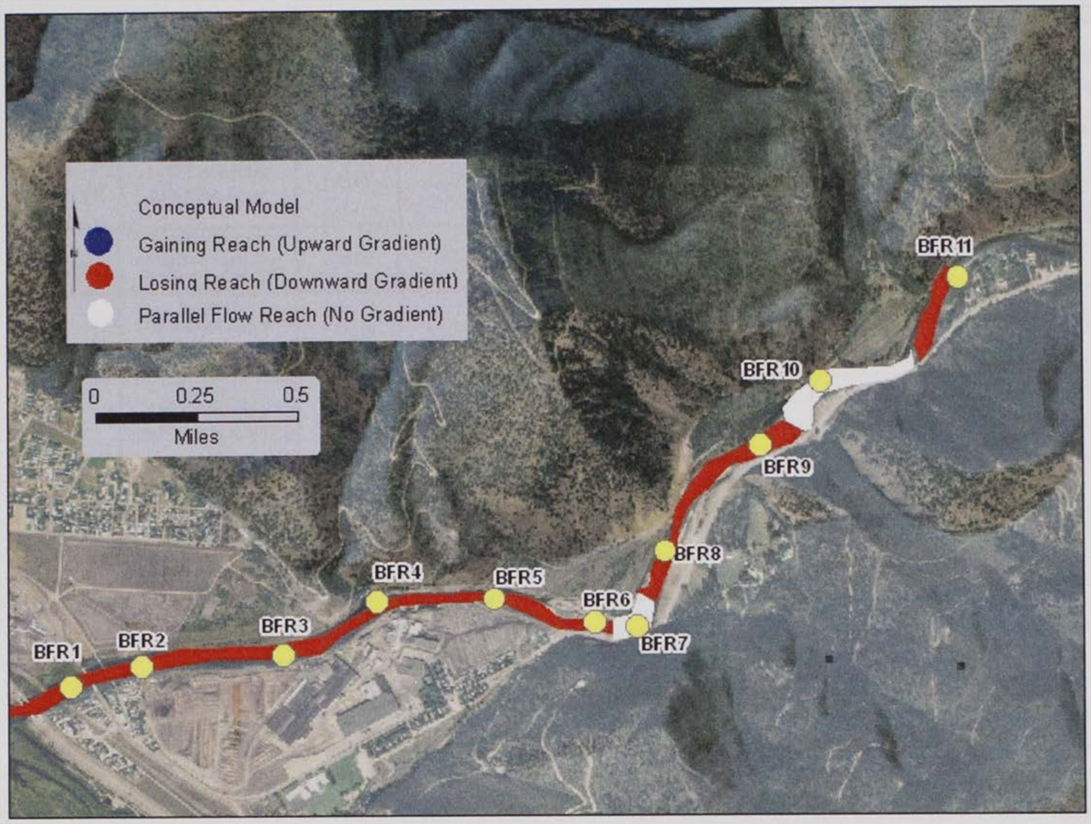

Figure 55 Conceptual distribution of vertical hydraulic gradients on the Blackfoot River above Milltown Dam. Negative gradients indicate zones of river water seepage to the underlying groundwater systems. Positive gradients are present when groundwater is discharging to the river bed. Areas with no measurable upward or downward gradients suggest no measurable exchange of water between systems is occurring. These are considered areas of parallel flow. The conceptual model was determined for low water conditions.

In addition to examining the general relationship of the water table and river stage, measuring and extrapolating exchange locations, rates and directions at key river channel locations, the exchange process was placed in the context of a site area water balance.

Based on the proposed site wide conceptual model a steady state site-wide groundwater balance was estimated for historical (pre-drawdown) site conditions. The water balance was computed for baseflow conditions that typically occur between mid-august and mid-march (Figure 2). This analysis included field based estimates of exchanges between the rivers, and the reservoir and the aquifer (Table 6a and 6b). An explanation of how each component was estimated can be found in Appendix G.

Water Balance Parameter	Inflow source	Average Daily ft^3/day	Average Daily Acre ft/yr	Minimum ft^3/day	Maximum ft^3/day	Possible Error	Percent Contribution	Previously Determined Values ft^3/day
GW_{inCFU}	GW Underflow Clark Fork River	$1.0x10^6$	8,400	$5.2x10^5$	$1.5x10^6$	49%	7%	
GW_{inBFU}	GW Underflow Blackfoot River	$3.4x10^5$	2,520	$8.6x10^4$	$6.0x10^5$	75%	2%	$2.7x10^5$ (Brick, 2003) $2.4x10^4$(Popoff M.A., 1985)
GW_{inSD}	Marshall Creek underflow and Dear Creek Underflow	$2.2x10^4$	190	$2.8x10^3$	$4.2x10^4$	89%	0.1%	
BFR_{leak}	Leakage Blackfoot River (I-90 Bridge to BFR6)	$1.7x10^6$	14,280	$1.5x10^6$	$1.9x10^6$	12%	10%	$6x10^5$-$1.8x10^6$(Gestring, 1994)
CFR_{leak}	Leakage Clark Fork river Below dam to well HGD	$6.2x10^6$	74,690	$2.4x10^6$	$1.0x10^7$	60%	61%	$2.4x10^6$-$7.2x10^6$(Gestring, 1994)
	Leakage Clark Fork river CFRA3 to CFRA4	$3.9x10^5$	3,280	$1.2x10^5$	$6.6x10^5$	69%	3%	
	Leakage Clark Fork river Above dam CFRA8	$2.4x10^6$	20,160	$2.3x10^6$	$2.4x10^6$	2%	17%	
Res_{leak}	Leakage Reservoir	$1.7x10^6$	14,280	$1.8x10^5$	$3.2x10^6$	89%	12%	$2x10^6$(Gestring, 1994) $1.9x10^6$-$2.6x10^6$(Popoff M.A., 1985) $3.2x10^6$(Moore and Woessner, 2002)
	Average Total Inflow	**$1.4x10^7$**	**117,600**					

Table 6a Groundwater inflow balance table results. Individual river leakage and discharge locations can be located in figure 44.

Water Balance Parameter	Outflow Source	Average Daily ft^3/day	Average Daily Acre ft/yr	Minimum ft^3/day	Maximum ft^3/day	Possible Error	Percent Contribution	
GW_{outHGU}	GW under Hellgate Canyon	6.0×10^6	77,280	2.7×10^6	9.3×10^6	55%	55%	3.8×10^6-7.6×10^6(Gestring, 1994) 4.2×10^6(Brick, 2003) 3.3×10^6-6.6×10^6(Tallman A.A., 2005)
GW_{outCFR}	GW discharge: Clark Fork River CFRA2	1.4×10^6	11,760	1.2×10^6	1.5×10^6	11%	13%	
	GW discharge: Clark Fork River CFRA5	9.6×10^5	8,060	9.2×10^5	1.0×10^6	4%	9%	
	GW discharge: Clark Fork River (CFRB1 to CFRB4)	2.1×10^6	17,640	3.9×10^5	3.9×10^6	84%	19%	4.2×10^6 (Brick, 2003) 3.8-7.6×10^6(Gestring, 1994)
GW_{ConsP}	Pumping Wells	6.3×10^4	530	5×10^4	7.6×10^4	41%	0.1%	(Gestring, 1994)
	Total Outflow	**1.1×10^7**	**92,345**					

Table 6b Groundwater outflow balance table results. Individual river leakage and discharge locations can be seen in Figure 44.

This water budget formed the template for developing a numerical groundwater model that was used to estimate the likely spatial distribution and magnitudes of the historical/pre drawdown river groundwater exchanges. In addition, the calibrated model was then modified and used to forecast how the exchange process changes once the Phase 1 reservoir drawdown was completed and how it is likely to change after the planned Phase 2 drawdown. The calibration process is summarized in Appendix I and presented in Berthelote (2007).

The modeling approach describing the exchange process was initially simplified lumping the net exchange into the following four reaches: 1) Clark Fork River (CFR)Above the Dam; 2) Clark Fork River (CFR) Below the Dam; 3) Blackfoot River (BFR) arm of the Reservoir ; 4) Milltown Reservoir. The conceptualization of the historical surface water and groundwater exchanges can be defined by Figure 53; where the CFR above the dam is a gaining and losing river, the reservoir is mainly conceived to be a recharge source to the underlying aquifer (losing reach), the BFR arm of the reservoir is a losing reach, and the CFR within 600 ft below the dam is a gaining reach and then becomes losing to the Hellgate Canyon boundary. The magnitude of the reach scale exchanges were estimated as an overall percent of water contributing total groundwater flow discharging as underflow at Hellgate Canyon. A negative percent indicates a net loss of groundwater flow (Table 7).

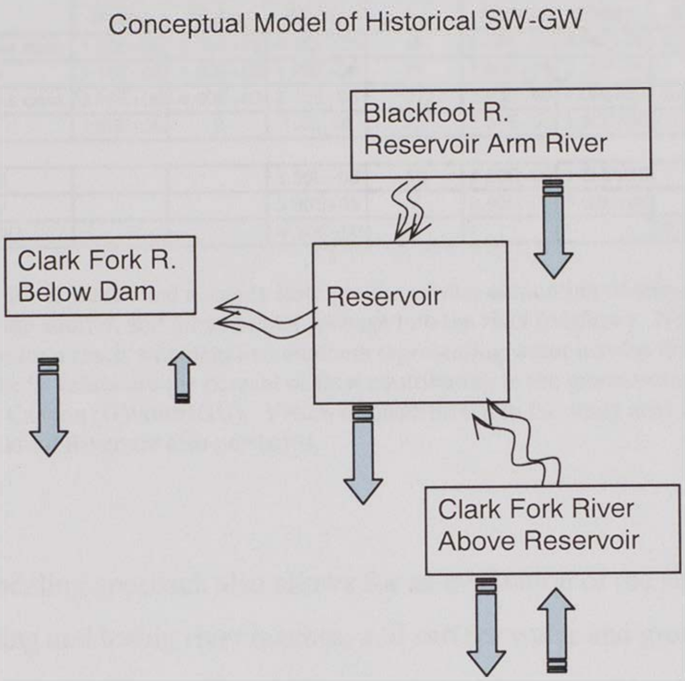

Figure 56 Schematic showing the general conceptual surface water and groundwater exchange directions (upward and downward arrow) and magnitudes (size of arrow) within the described reaches.

Overall, the historical (pre drawdown) steady state simulated seepage rates for each reach were within range of the estimated values (Table 7). The seepage rate of the CFR above the dam is -6.8 E+05 ft^3/day (the negative value indicates a net discharge of the groundwater to the river over the reach length). The reservoir area in the model contributes 1.7E+06 ft^3/day to the underlying aquifer which is 21% of the total volume of groundwater that discharges through Hellgate Canyon. The BFR arm of the reservoir in the model contributes 1.8E+06 ft^3/day or 22% to the underlying aquifer, and the CFR below the dam contributes the majority of recharge 3.7E+06 or 37% of recharge to the underlying aquifer. Underflow from the CFR (at Turah) and BFR contribute 16% and 7%, respectively, to the groundwater discharging through Hellgate Canyon. For this analysis the simulated underflow contribution from Mill Creek and Deer Creek are assumed to be less than one percent of the total and not included in the analyses.

	Steady State Model Value				Estimated Range					
	inflow ft³/day	outflow ft³/day	Netflow ft³/day	%	min inflow ft³/day	max inflow ft³/day	min outflow ft³/day	max outflow ft³/day	min netflow ft³/day	max netflow ft³/day
CFR above dam	1.60E+06	-2.00E+06	-6.80E+05	-8	2.42E+06	3.06E+06	-2.80E+05	-2.50E+06	-8.00E+04	3.34E+06
Reservoir	2.10E+06	-1.60E+05	1.70E+06	21	1.80E+05	3.20E+06			1.80E+05	3.20E+06
CFR below dam	3.10E+06	-4.60E+03	3.10E+06	37	2.40E+06	1.00E+07	-3.90E+05	-3.90E+06	2.01E+06	6.10E+06
BFR arm	1.80E+06	0	1.8E_06	22	1.50E+06	1.90E+06			1.50E+06	1.90E+06
GWinCFU			1.30E+06	16	5.20E+05	1.50E+06			5.20E+05	1.50E+06
GWinBFU			5.80E+05	7	8.60E+04	6.00E+05			8.60E+04	6.00E+05
GWoutHGU			-8.30E+06				-2.70E+06	-9.30E+06	-2.70E+06	-9.30E+06

Table 7 River Reach and a steady state pre drawdown accounting of seepage from the river reach into (inflow) the aquifer, and groundwater seepage into the river (outflow). Net flow represents the net discharge for a reach with negative numbers representing water leaving the aquifer and discharging to the river. The % values are the percent of flow contributing to the groundwater underflow discharging through Hellgate Canyon (GWoutHGU). Values of underflow into the study area for the upper Clark Fork River and Blackfoot River are also presented.

The modeling approach also allows for an evaluation of the simulated spatial distribution of gaining and losing river reaches, and surface water and groundwater exchange rates and directions (Figure 57 and 58). A gaining river condition is defined as a river cell receiving groundwater discharge. A losing river conditions refers to a river cell in which surface water is leaking water into the groundwater system. The seepage rates per ft^2 were estimated for each cell by dividing the seepage rate for an individual cell by the cell area (150 ft x150 ft) to establish the seepage rate per square foot of riverbed ($ft^3/(day ft^2)$).

Simulation of conditions in the CFR above the dam show a variety of gaining and losing reaches (Figure 54). Computed seepage rates in this river reach vary widely as observed in the field and range from 3.3 to -5.0 $ft^3/(day ft^2)$.

The steady state model shows the reservoir as an area that contributes water to groundwater except in the upper portion where two small areas of groundwater discharge (<0 to -0.4 $ft^3/(day ft^2)$) are indicated. Computed exchange rates within the reservoir range from >0 to 3.3 $ft^3/(day ft^2)$. Rates along the northern boarder may be slightly higher.

The steady state model results simulate the BFR arm of the reservoir as a losing reach that has seepage rates ranging between 0.4 and 3.3 $ft^3/(day ft^2)$. Higher seepage rates (3.3 to 5.0 $ft^3/(day ft^2)$) are shown in the area immediately adjacent to the main reservoir. The model results for the CFR below the dam shows an area of approximately 150 ft (one cell) where groundwater is discharging to the river. Below this point, model results simulate the river as a losing reach. The modeled gaining portion of the river is smaller than the reach length (600 ft) documented under field conditions. River leakage rates to the aquifer are highest in the losing reach closest to the dam (5.0 to 0.4 $ft^3/(dayft^2)$) and they decrease further down river (>0 to 0.4 $ft^3/(dayft^2)$) (Figure 55).

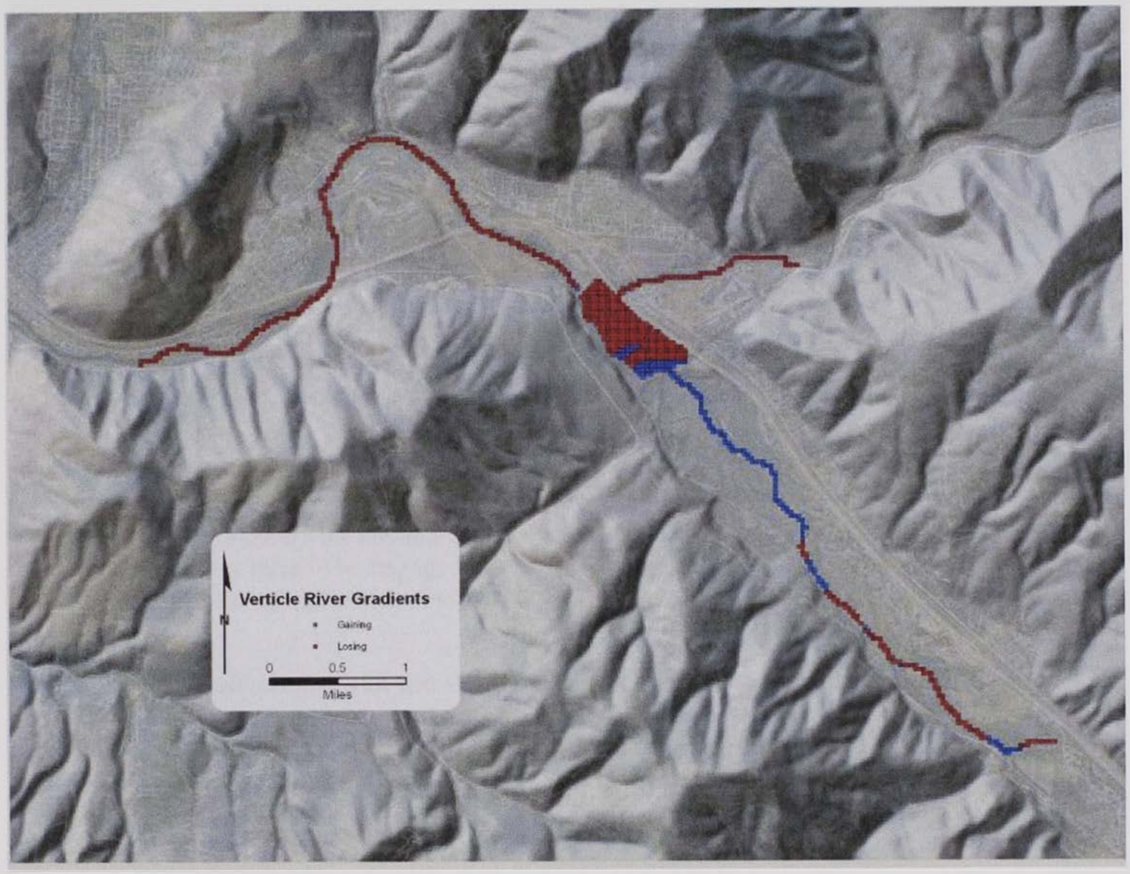

Figure 57 The figure shows the pre dam removal steady state model results of river and groundwater exchange directions.

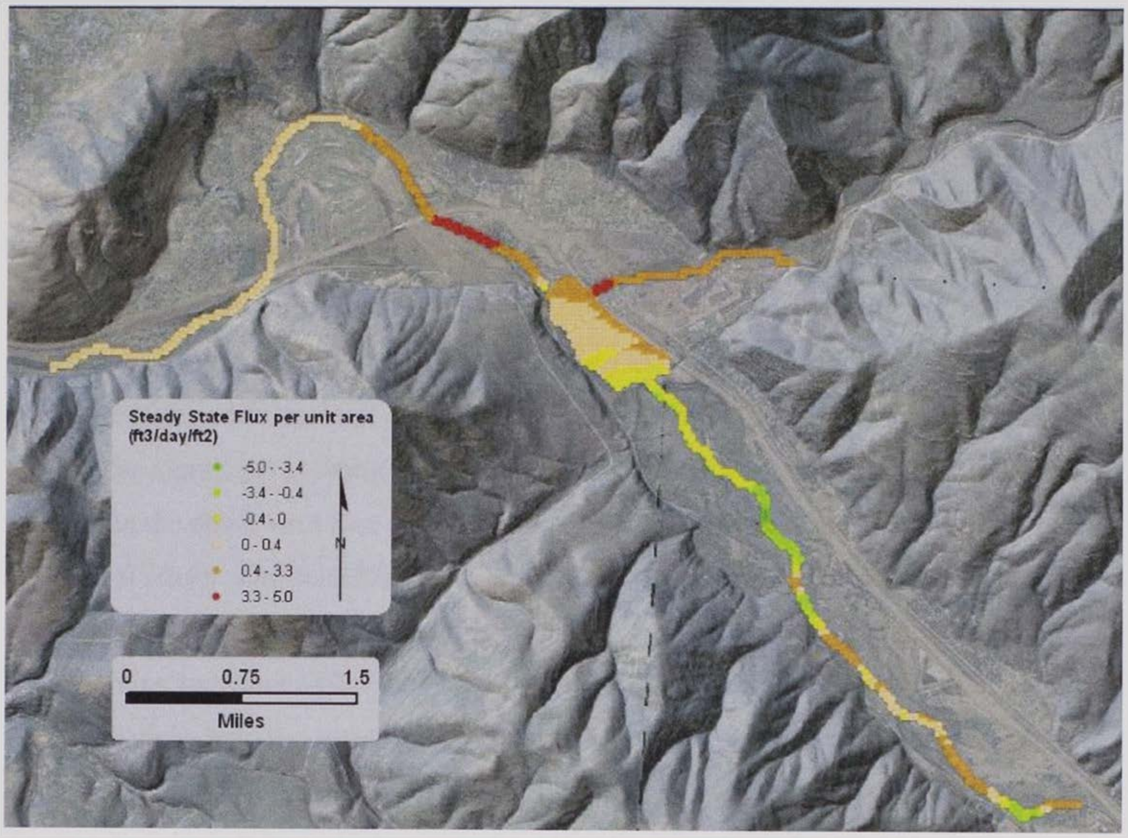

Figure 58 The figure show s the pre-dam removal steady state model calibration to condition of river and groundwater exchange rates. The seepage rates for each cell were divided by the cell area (150 ft x150 ft) to establish the seepage rate per square foot of riverbed ($ft^3/dayft^2$)).

Reach scale changes in the steady state pre drawdown conditions during the Phase 1 drawdown were evaluated through use of a calibrated transient model. The transient simulation was run from March 31, 2006 and through April 17, 2007. The time period was divided into 12 stress periods and the river flux for each river cell was reported for the last time step in each stress period (Table 8). Throughout the transient simulations all riverbed properties remained constant and only the river elevations and groundwater head boundary elevations were varied.

The data show that throughout most of the simulation the overall flux for the CFR above the dam reach was from the groundwater into the river. As the reservoir stage was lowered the net discharge of groundwater to the river decreased. During stress period 9 and stress period 10 (January 24, 2007 and February 17, 2007) the overall flux rate reversed and the net flow was from the river into the groundwater.

The simulated flux rate from the reservoir decreased as the reservoir stage was lowered, 1.7E+06 ft^3/day on May 9, 2007 to 1.0E+06 ft^3/day on February 17, 2007. The overall contribution of reservoir seepage to the groundwater underflow at Hellgate Canyon decreased from 22% to 15%. The BFR arm of the reservoir acted much like the CFR portion of the reservoir. The net reservoir leakage changed from 2.3E+06 to 1.4E+06 ft^3/day as the reservoir was lowered. The contribution of this reach to the underlying groundwater discharge changed from 30% to 23%. In each case, the percentage changes were estimated by comparing the flow of the individual reach at a given stress period to the total groundwater outflow for that same stress period.

The simulated exchange in the CFR below the dam showed an overall slight increase in the downward flux of water as the reservoir was lowered (3.4E+06 to 3.7E+06 ft^3/day). The contribution of this reach to groundwater recharge and underflow at Hellgate Canyon was initially 41% of that flow; simulated post drawdown contributions are about 51% while the flow out of the canyon decreased by 6%. Figures 59 and 60 show how the seepage rates and percent contribution to the groundwater discharge through Hellgate Canyon changed throughout the simulation. The data displayed was taken from the last time step of each stress period.

Flux Rates	**Transient Model Stress Period 1**	**Stress Period 2**	**Stress Period 3**	**Stress Period 4**	**Stress Period 5**	**Stress Period 6**
	Day 40	Day 76	Day 105	Day 140	Day 171	Day 206
River Area	**Net flow**	**Net flow**	**Net flow**	**Net flow**	**Net flow**	**Net flow**
Flux Rate	**ft^3/day**	**ft^3/day**	**ft^3/day**	**ft^3/day**	**ft^3/day**	**ft^3/day**
CFR above dam	-7.8E+05	-5.2E+05	-4.5E+05	-6.1E+05	-5.2E+05	-2.7E+05
Reservoir	1.7E+06	1.2E+06	1.2E+06	1.3E+06	1.5E+06	1.5E+06
CFR below dam	3.1E+06	3.2E+06	3.1E+06	2.7E+06	2.7E+06	2.8E+06
BFR arm	2.3E+06	1.8E+06	1.5E+06	1.5E+06	1.4E+06	1.5E+06
GWinCFU	1.4E+06	1.2E+06	1.1E+06	1.3E+06	1.3E+06	1.1E+06
GWinBFU	5.4E+04	8.6E+04	7.7E+04	8.9E+04	9.1E+04	6.8E+04
GWoutHGU	-7.6E+06	-7.6E+06	-7.5E+06	-7.8E+06	-7.4E+06	-7.1E+06

Percent Contribution to Groundwater Discharge	%	%	%	%	%	%
CFR above dam	-10	-7	-6	-8	-7	-4
Reservoir	22	16	16	17	20	21
CFR below dam	41	42	42	35	37	40
BFR arm	30	24	19	19	18	21
GWinCFU	19	16	15	17	17	15
GWinBFU	1	1	1	1	1	1

Flux Rate River Reach	Transient Model Stress Period 7 Day 229 Net flow ft^3/day	Stress Period 8 Day 259 Net flow ft^3/day	Stress Period 9 Day 300 Net flow ft^3/day	Stress Period 10 Day 324 Net flow ft^3/day	Stress Period 11 Day 351 Net flow ft^3/day	Stress Period 12 Day 386 Net flow ft^3/day
CFR above dam	-1.2E+05	-8.5E+04	1.4E+05	3.4E+05	-2.5E+05	-1.5E+05
Reservoir	1.4E+06	1.5E+06	1.4E+06	1.0E+06	1.4E+06	1.1E+06
CFR below dam	3.1E+06	3.1E+06	3.1E+06	3.4E+06	3.3E+06	3.7E+06
BFR arm	1.6E+06	1.6E+06	1.5E+06	1.4E+06	1.4E+06	1.5E+06
GWinCFU	8.9E+05	8.0E+05	6.3E+05	5.1E+05	1.1E+06	1.0E+06
GWinBFU	7.3E+04	1.1E+05	1.2E+05	9.1E+04	8.1E+04	7.6E+04
GWoutHGU	-7.1E+06	-7.2E+06	-7.3E+06	-7.3E+06	-7.4E+06	-7.2E+06
Percent Contribution to Groundwater Discharge	%	%	%	%	%	%
CFR above dam	-2	-1	2	5	-3	-2
Reservoir	20	21	19	14	19	15
CFR below dam	43	43	43	47	44	51
BFR arm	23	22	21	19	19	20
GWinCFU	13	11	9	7	14	14
GWinBFU	1	2	2	1	1	1

Table 8 River reach and underflow transient simulated water balance estimates and the estimated ranges for each component. The % indicates the percent of flow contributing to the groundwater discharging through Hellgate Canyon (GWoutHGU).

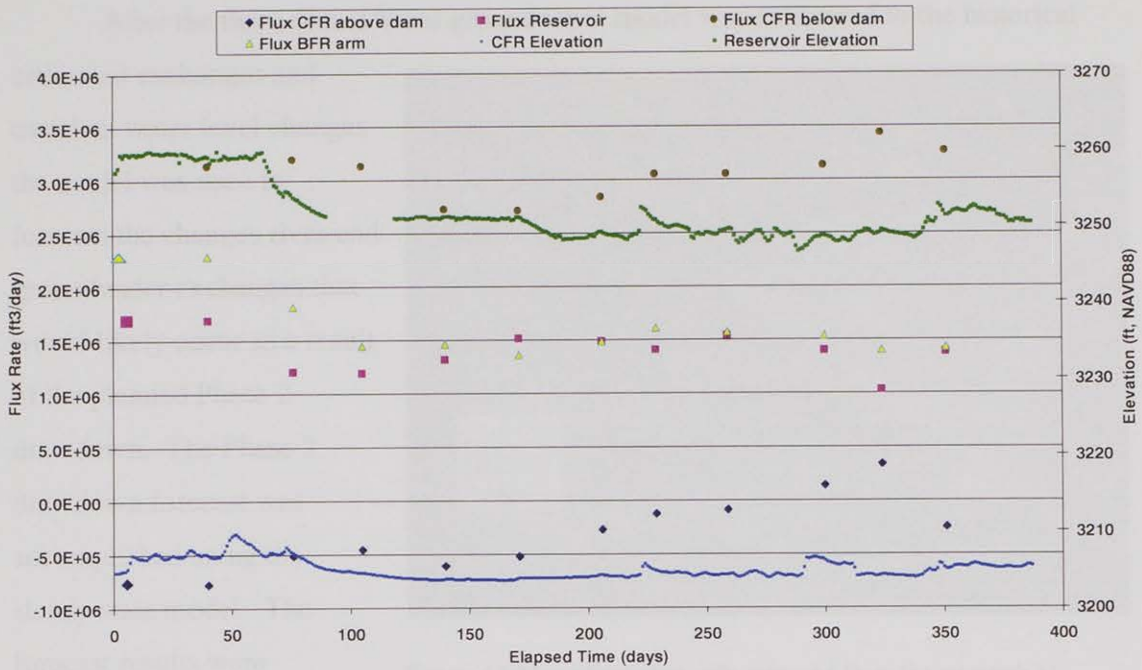

Figure 59 This graph shows how seepage rates of each river reach changed at the end of each stress period in response to Phase 1 drawdown. These reservoir stage (green) and the CFR stage is in blue (right hand scale)is illustrated The transient run started on March 31, 2006 and ended on April 17, 2007. A negative rate represents groundwater discharge to the river reach.

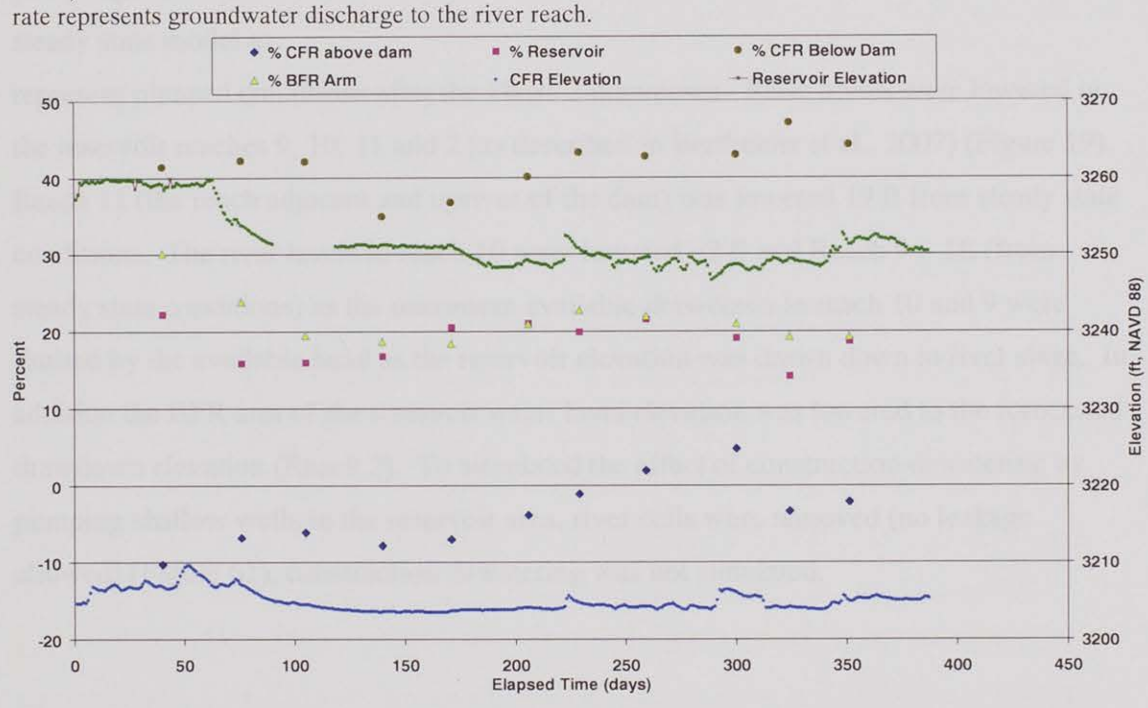

Figure 60 This graph shows the contribution of water to the groundwater discharge through Hellgate Canyon (as computed from the transient water balance) and how it changed in each river reach as the river stage and reservoir stage varied during transient simulations. The transient run started on March 31, 2006 and ended on April 17, 2007. A negative percentage indicates a net from the ground to the river.

After the three dimensional groundwater model was calibrated to the historical estimated exchanges and transient water level changes the model was used to forecast the changes river and groundwater exchanges that would likely occur as a result of the planned Phase 2 drawdown. The Phase 2 drawdown forecast was accomplished using the steady state model. The forecast results were derived by adjusting the river stage elevations in the steady state model to represent planned conditions after the Phase 2 drawdown. River levels were lowered in the reservoir reaches 9, 10, 11 and 2 (as described in Berthelote et al., 2007) (Figure 19). Reach 11 (the reach adjacent and upriver of the dam) was lowered 19 ft from steady state conditions. The river levels in reach 10 were lowered ~2 ft and Reach 9 ~ 1ft (from steady state conditions) as the maximum available drawdown in reach 10 and 9 were limited by the available head as the reservoir elevation was drawn down to river stage. In addition the BFR arm of the reservoir water level elevation was lowered to the forecasted drawdown elevation (Reach 2). To simulated the effect of construction dewatering by pumping shallow wells in the reservoir area, river cells were removed (no leakage allowed) (Figure 61), construction dewatering was not simulated.

Figure 61 Map of the river cells removed from the reservoir to simulate lower leakage from construction sediment dewatering and sediment removal.

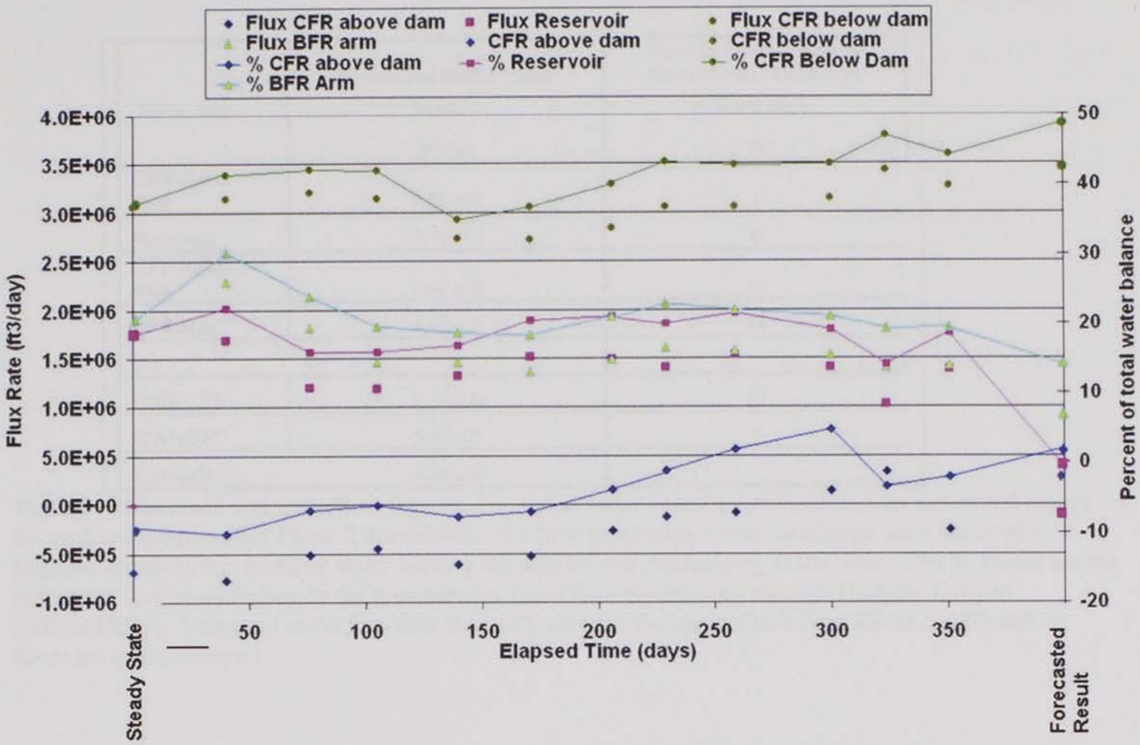

Figure 62 A graph showing the river flux rates and percent contribution to gw discharge through Hellgate Canyon for each time step during transient simulations. The transient simulations began on March 31, 2006 and ended April 21, 2007. This graph also exhibits the steady state initial condition and the steady state forecasted (final condition) flux rates and percent contribution in and out of each river reach.

The model results indicate that under the Phase 2 drawdown conditions it is possible that the CFR above the dam may end up contributing a flow into the valley aquifer of 9.5E+04 ft^3/day, about 1% of the water leaving Hellgate Canyon as underflow (Figure 62; Table 9). The modeling suggests that the reservoir area will convert into an area receiving groundwater discharge, a netflow of -5.9E+03 ft/day (again less than 1% of the volume of groundwater leaving through Hellgate Canyon). The net flow from the BFR arm of the reservoir into the aquifer is predicted to decrease to 9.6E+05 ft^3/day, a discharge representing nearly 14% of Hellgate Canyon underflow. Under Phase 2 conditions, the CFR below the dam will potentially provide recharge to the underlying aquifer of about 3.4E+06 ft^3/day, nearly 50% of the groundwater underflow at Hellgate Canyon. A bar graph summarizing the simulated pre-drawdown water balance and the post phase 2 drawdown water balance is presented on Figure 63.

River Area	Forecasted Model Value Netflow ft^3/day	Percent Contribution to Groundwater Discharge GWout HGU %
CFR above dam	9.5E+04	1
Reservoir	-5.9E+03	0
CFR below dam	3.4E+06	49
BFR arm	9.6E+05	14
GWinCFU	1.3E+06	19
GWinBFU	5.8E+05	8
GWoutHGU	-6.9E+06	

Table 9 River reach and underflow forecast simulated water balance estimates and the estimated ranges for each component after Phase 2 drawdown. Net flow represents the net discharge for a reach with negative numbers representing water leaving the aquifer and discharging to the river. The % values are the percent of flow contributing to the groundwater underflow discharging through Hellgate Canyon (GWoutHGU). Values of underflow into the study area for the upper Clark Fork River and Blackfoot River are also presented.

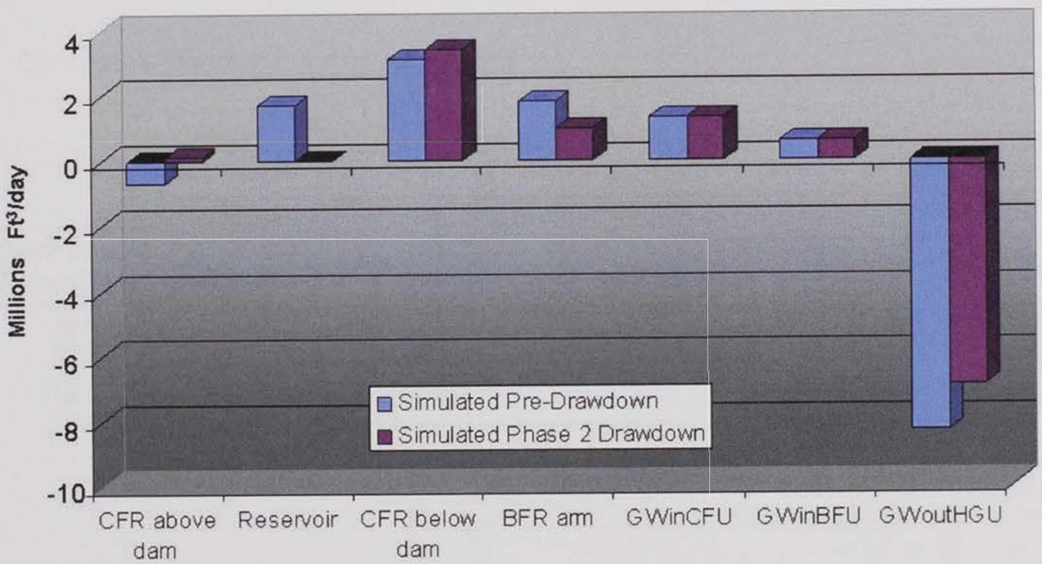

Figure 63 A bar graph comparing the simulated pre-drawdown water balance and the post Phase 2 drawdown water balance. Positive values indicate an overall flux of water into the ground and negative values indicate an overall flux of water from the ground water to the surface water.

These results present a new conceptual understanding of the river and groundwater exchange processes that could occur as a result of the Phase 2 drawdown and/or dam removal. The new conceptual model has less seepage coming from the BFR arm of the reservoir and slightly more seepage coming from the CFR below the dam.

The river and groundwater exchanges for the CFR above the dam remained a series of gaining and losing reaches. Seepage directions in a large area of the CFR above the dam reach transitioned from gaining to losing conditions. The reservoir area now contributes less water to the underlying aquifer and has more groundwater discharging to the river. Overall, the net change of seepage into the valley aquifer. The overall simulated reduction of seepage from the river channel into the groundwater system (groundwater recharge) was 1.8E+06 ft^3/day (21 cubic feet per second). It needs to be noted that modeling assumed river bed characteristics after the Phase 2 drawdown remained in pre-drawdown conditions and that changes in river bed characteristics as a result of increased deposition of fine grained sediments in the river channel below the dam, rerouting of the river channel, and changes in river bed elevations as a result of head cutting were not evaluated. A post Phase 2 drawdown conceptual model can be seen on Figure 64. Changes in gradient can be seen by comparing Figures 65 A and B. Changes in seepage rates can be seen by comparing Figures 66 A and B.

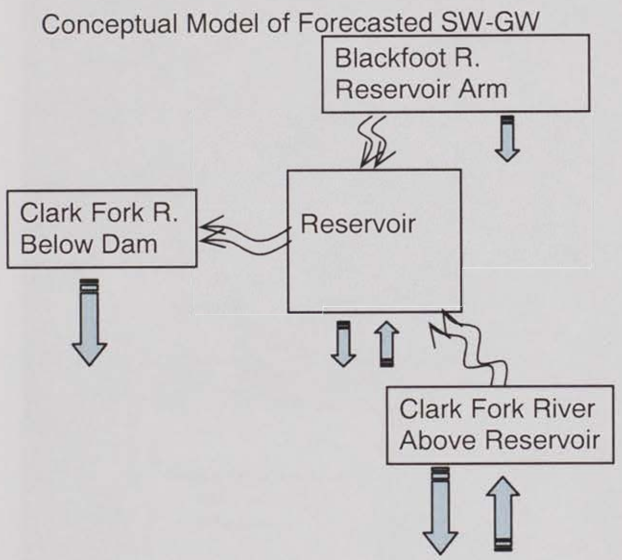

Figure 64 Schematic showing the new post Phase 2 drawdown conceptual surface water and groundwater exchange directions (upward and downward arrow) and magnitudes (size of arrow) within the described reaches.

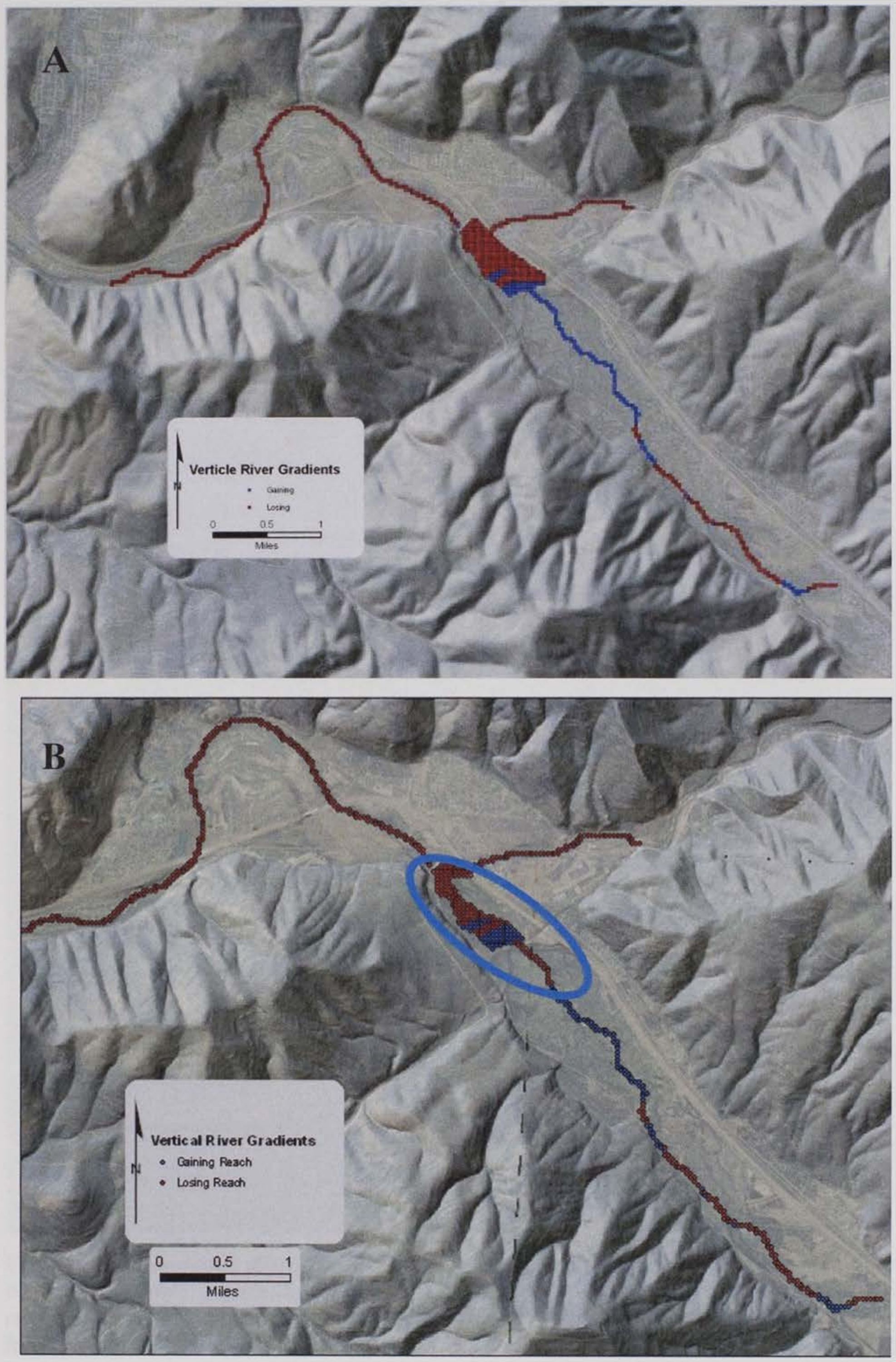

Figure 65 A) The figure shows the forecasted model results of river and groundwater exchange directions. The blue circle identifies the vertical river gradients changed by the Phase 2 drawdown. **B**) For comparison, this figure shows the pre-drawdown (historical) steady state model results of river and groundwater exchange directions.

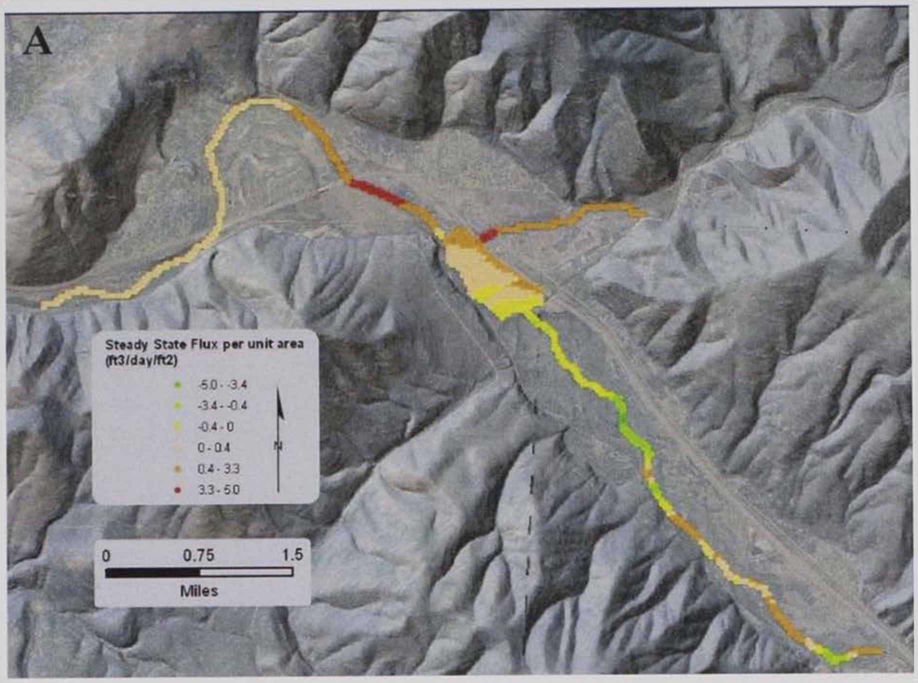

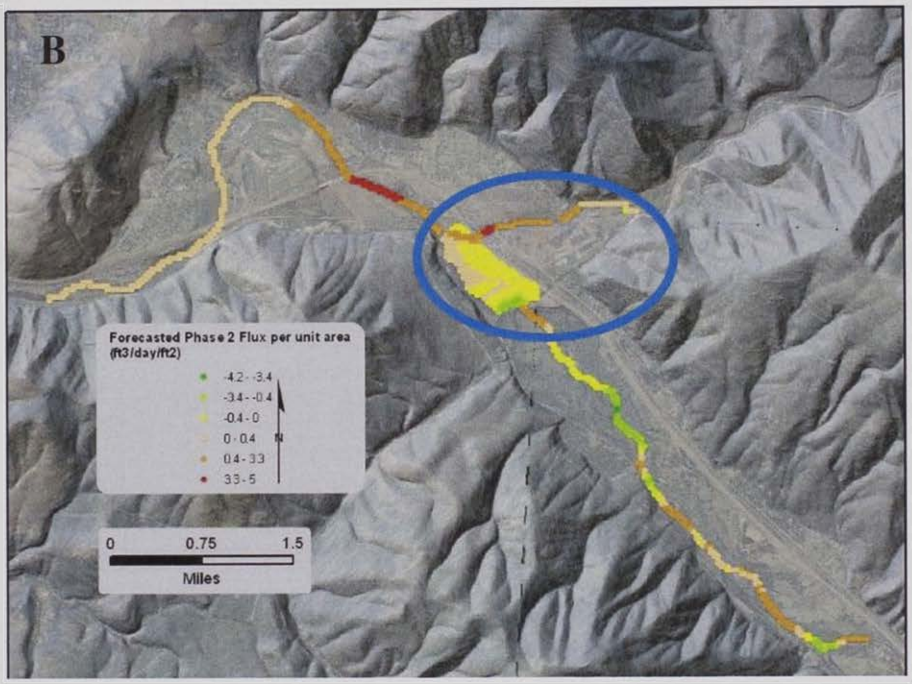

Figure 66 A) The figure shows the forecast model results of river and groundwater exchange rates after Phase 2 drawdown. The seepage rates for each cell were divided by the cell area to establish the seepage rate per square foot of riverbed ($ft3/(dayft^2)$). The blue circle shows the area which exchange rates changed from the initial pre-drawdown (historical) steady state conditions. **B)** For comparison, this figure shows the pre-drawdown (historical)steady state model results of the river and groundwater exchange rates.

CHAPTER 4
DISCUSSION

This work attempted to monitor and forecast groundwater flow patterns a highly conductive unconfined aquifer and gravel bedded river system and spatial and temporal variations in surface water and groundwater exchanges that were likely to result as a dam/reservoir removal project progressed in western Montana. Efforts became focused on understanding identifying the locations and rates of exchange sites and the factors controlling the river channel/reservoir-groundwater exchange process, a dominate recharge mechanism to the underlying aquifer over most of the study site.

River and Groundwater Exchange Processes

The position of the water table and corresponding river level data supports the interpretation that both the BFR and CFR below the dam are perched and losing river water to the underlying and adjacent groundwater system. Perched reaches on the CFR have a bed sediment saturated zone about 1.5 ft thick as measured the north side of the channel. Tallman (2005) measured a saturated thickness of 2.9 ft on the north river bank of the Clark Fork River at locations in Hellgate Canyon and a thickness of 1.3 ft in the channel near Madison Street Bridge in Missoula. The thickness of the un-saturated zone beneath the BFR arm of the reservoir and the distance between the water table and the saturated sediments is reduced as the mouth of the river at the reservoir is approached. It appears the water table connects to the saturated river bed sediments in the Milltown area. It is also likely that portions of both the Blackfoot River and Lower Clark Fork River reaches become connected to the underlying groundwater system during seasonal periods of during which the water table is highest. This is supported by the influence of river stage and temperature changes on closely associated wells.

The original monitoring in the reservoir showed a saturated continuum of fine sediment that was hydrologically connected to the underlying original pre-dam coarse grained floodplain aquifer. Though in reservoir groundwater level data during this study was sparse because data for reservoir wells were mostly absent during this study because of construction restrictions, adjacent monitoring well levels and responses suggest the reservoir groundwater connection condition was maintained during this study. Moore and Woessner (2002) suggested that the leakage rate into the underlying aquifer from the full reservoir was 2.3E+06 ft^3/day. This computed discharge was most certainly impacted during this work by both a Phase 1 lowering of the reservoir (12 ft stage reduction), and construction pumping designed to dewater the sediments in the Clark Fork arm of the reservoir so a bypass channel could be constructed. However, water levels and temperature data collected at wells located just north of the reservoir area continued to suggest the reservoir remained connected to the underlying coarse grained valley aquifer during the construction and drawdown phases (Figure 41).

The CFR above the reservoir was observed to contain well connected reaches that were both gaining and losing during the study. Both groundwater levels and temperature data collected in near river wells support this. Water level changes in wells located in the nearby floodplain sediments also reflected seasonal river stage fluctuations and river temperatures variations (Figure 40).

In addition to the water table and river stage and temperature interpretation, general analyses, in channel bed measurements also supported the interpreted river – groundwater exchange locations and magnitudes. In-river vertical hydraulic gradient measurements indicated that approximately 600 feet below the dam the river channel was a gaining reach. In contrast, vertical hydraulic gradient measurements made from in the BFR arm of the reservoir indicated losing conditions as the vertical hydraulic gradients of -1.2 to -0.85 on the right and left banks were recorded. These large gradients were interpreted to illustrate the presence of an unsaturated zone below the river at the measured locations Attempts to measure the vertical gradient in the middle of the channel in the Blackfoot arm of the reservoir were unsuccessful (water depth, current and fine sediment).

In channel measurements collected in the CFR above the dam supported the interpretation of the presence of gaining, losing and parallel flow reaches. At two separate locations (CFRA5 and CFRA2) distinguishable upward VHG gradients were observed to depths of 3 ft fell with in the measurement error range (0.02 and 0.01) and fluxes were observed to depths of 3 ft below the river bed. River bed temperature data collected at these river locations (CFRA5 and CFRA2) support the interpretation of local upwelling of groundwater. In portions of the CFR above the dam downward gradients in this reach were observed and recognized to be an order of magnitude less than the downward gradients observed in the other reaches (CFR below the dam, and in the BFR arm of the reservoir). The head differential between the floodplain aquifer system and river is also less pronounced suggesting the channel is hydraulically connected to the water table (Sophocleous, 2002). At location CFRA7 established measurement errors precluded flow direction determination, suggesting gradients were small and possibly a parallel flow condition was occurring.

The conceptual understanding of river and groundwater connectivity was used in conjunction with in field measurements to estimate river channel and groundwater exchange rates, values incorporated used in an overall water balance.

Seepage rates derived for the river channel below the dam appear to vary less than in other study channel reaches. This may reflect the presence of a more uniform bed sediment condition, a condition possible impacted as a result of the river bottom sediment being impacted from the down river mobilization of finer grained reservoir sediments (Brunke et al., 1997). All computed exchange rates for the entire study area were found to be fairly comparative in all similar reaches with the exception of areas of high flux rates (10 to 13 $ft^3/(dayft^2)$) found at locations of reach sections with coarse grained deposits such as the CFR above the dam and the BFR above the influence of the reservoir of areas of high flux rates (10 to 13 $ft^3/(dayft^2)$).

	River Location	River Bed Gradient	Temperature Modeling Vertical Hydraulic Conductivity ft/day	Temperature Modeling Flux Rate $ft^3/(day ft^2)$	Falling Head Test Vertical Hydraulic Conductivity ft/day	Darcy's Law Flux Rate $ft^3/(day ft^2)$
Blackfoot River	BFR2	-0.85	0.7	-0.9--1.2		
	*BFR5	-0.04	-	-	30	-1.20
	*BFR6	-0.05	-	-	40	-2
	*BFR8	-0.1	98	-13.0--10.4	42	-4.20
	*BFR9	0	-	-	30	0
	*BFR11	-0.03	-	-	39	-1.17
Clark Fork River Above Dam	CFRa2	+0.02	1	0.8-0.7	3	0.06
	CFRa3	-0.03	13	-11.3--13.0	16	-0.48
	CFRa4	-0.03	-	-	30	-0.9
	CFRa5	+0.01	1.3	2.9-3.2	1.5	0.02
	CFRa6	-0.1	-	-	1.5	-0.15
	CFRa7	0	-	-	1.7	0
	CFRa8	-0.1	3.3	-2.9--3.2	3.6	-0.36
Clark Fork River Below Dam	CFRb2	+0.33	-	-	1.7	0.56
	CFRB6	-1.2	0.7	-0.7--1.1	-	-
	CFRb7	-1.2	-	-	1.4	-1.68
	CFRB8	-1.2	-2.3	-2.9--3.2	-	-

Table 10 Summary of in-river measurements and estimates made. *Locations that were investigated just upriver of project area.

Overall, the temperature modeling derived river bed hydraulic conductivity values and the falling head test values results compared well at locations where both tests were performed (Table 10). These results are comparable also similar to river bed vertical hydraulic conductivities estimated by Tallman (2005) for the Clark Fork River bed below Hellgate Canyon (2.6 to 111 ft/day). The study results show that the river bed vertical hydraulic conductivity varies throughout the site (Figure 67). The highest hydraulic conductivities were measured in Blackfoot River bed sediments at locations up gradient of the fine grain sediments deposited from the reservoir. Hydraulic conductivities measured in the Clark Fork River above the dam show more variability and slightly higher values of hydraulic conductivity than values for the Clark Fork River channel below the dam. Overall, it appeared the river bed hydraulic conductivity estimates for this study varied widely with the majority of derived values being below 5 ft/day (Figure 67).

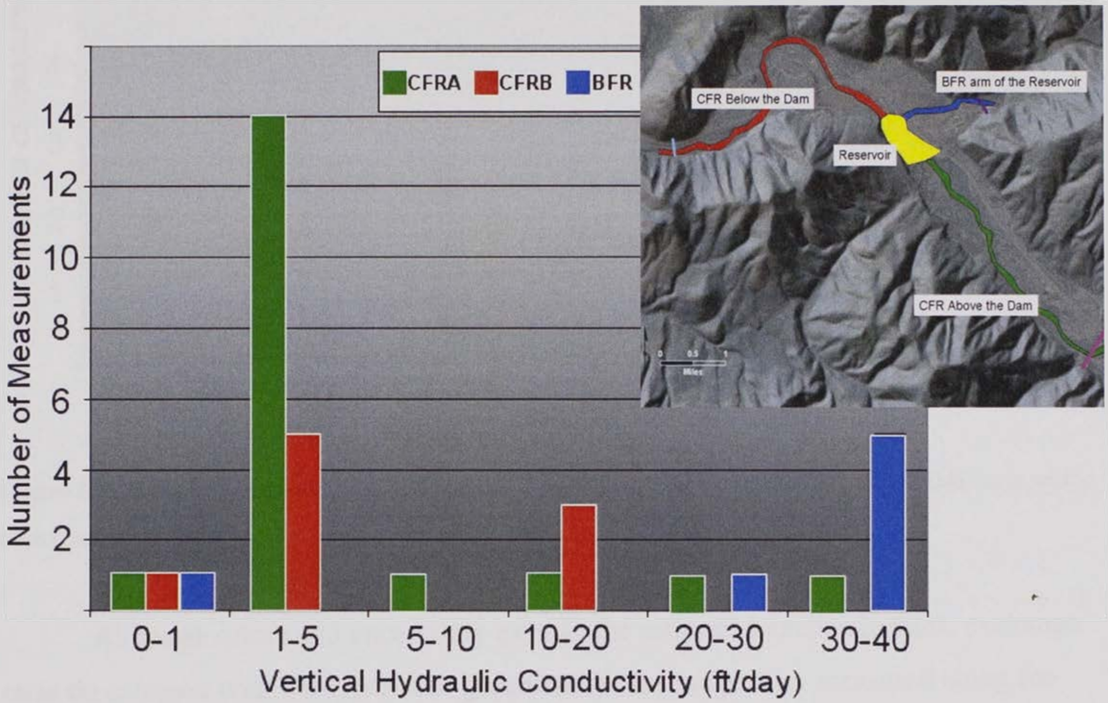

Figure 67 Histogram illustrating the distribution of river bed sediment vertical hydraulic conductivity values within each river reach.

Estimated river bed flux rates based on the results of temperature modeling were close to an order of magnitude higher than the estimates made using computed hydraulic conductivity values from slug tests and field measured gradients (Table 10). It is not clear why values vary so widely, possibly, they are integrating more of the local heterogeneities and provide more average values. Additional insight into local seepage rates would be gained from the combined use of geochemical tracers and temperature data and would help to reduce uncertainties in estimates (Scanlon et al., 2002; Tallman, 2005)). Overall, it appeared the flux rates for this study varied widely with the majority of derived fluxes being below 2 ($ft^3/day/ft^2$) (Figure 68).

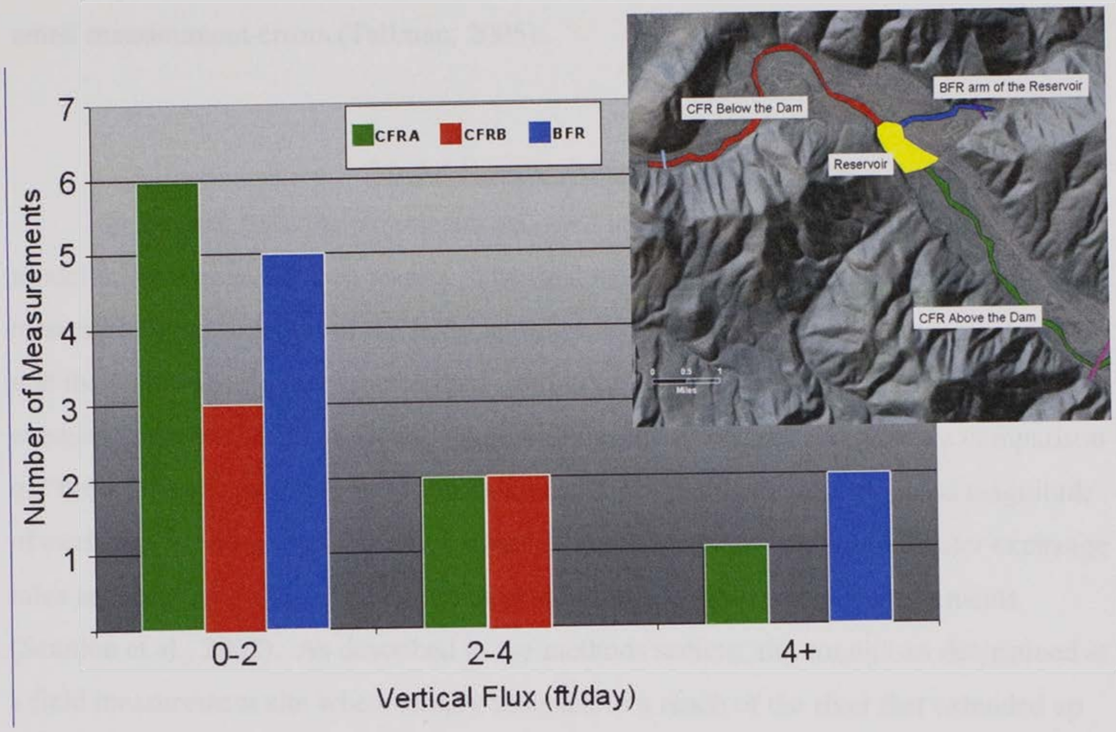

Figure 68 Histogram illustrating the distribution of estimated river bed sediment vertical flux rates within each river reach.

Although errors and uncertainty exist in the estimated exchange rates, exchange rates do compare well with river and groundwater exchange rates measured along the Lemhi River in Idaho (Konrad, 2006). The Lemhi River is a tributary of the Salmon River, which in turn is tributary to the Snake River and Columbia River. The Lemhi River has been described to have a similar hydrogeologic and riverine setting as the Clark Fork River and Blackfoot River (Haws et al., 1977). This study investigated the spatial temporal and magnitude of trends for river and groundwater exchanges of tributaries of the Columbia River. Rates were estimated per unit length of river bed. Estimated exchange rates ranged from 0.7 (into the aquifer) to 5.9 (out of the aquifer) $ft^3/(dayft^2)$ of riverbed. Konrad (2006) reported seepage values of 12.7 to 0.3 $ft^3/(dayft^2)$ in gaining reaches and 0.3 to 5.6 $ft^3/(dayft^2)$ in losing reaches of the Lemhi River. These seepage rates were estimated using seepage runs. Seepage estimates are calculated by looking at the difference in river flow at one river location to the next. Seepage runs were not used in this study as the method requires significant differences in river flow from one site to the next, good river access (bridges in a river the size of either the BFR or CFR), and small measurement errors (Tallman, 2005).

Model Results versus Field Estimates

In general, both the parameters assigned to the model and the calibration of the model influence the forecast results. The final model parameters should reflect a reasonable representation of the hydrogeologic setting outlined by the conceptual model and the model should meet established calibration criteria. As this work focused on examining the exchange of groundwater with the site rivers and reservoirs, a comparison of "field derived" data sets and simulated results describing the location, and magnitude of exchange is addressed. Clearly, estimates of surface water and groundwater exchange rates are sensitive to the number, location and timing of in-channel measurements (Scanlon et al., 2002). As described in the methods section, the conditions determined at a field measurement site where simply assigned to a reach of the river that extended up and down stream one half the distance to the next measurement point. It is recognized that this process most likely incorrectly designated some portions of the channel as gaining or losing. Despite this approach simulated reach scale exchange rates fell within range of the field based estimated reach scale exchange rates (Figure 69; Table 11).

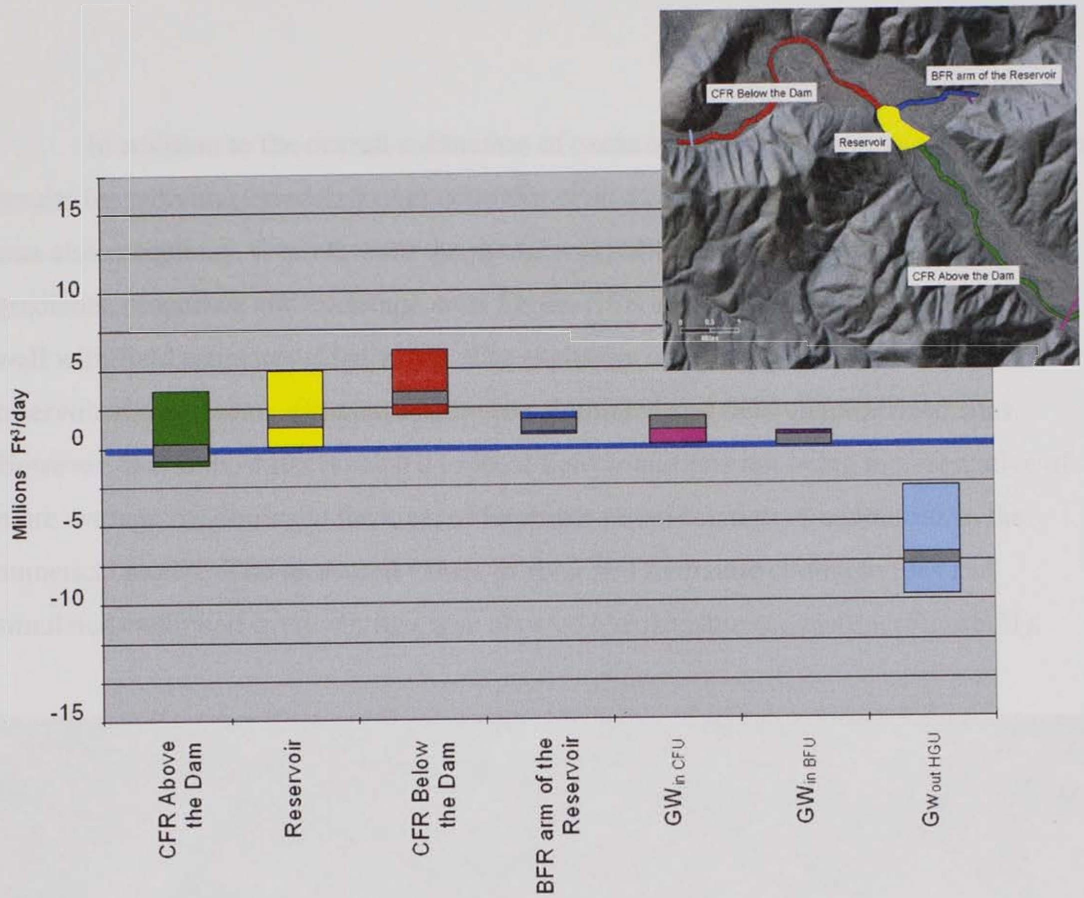

Figure 69 This graph illustrates how the modeled river flux values for each reach fell within the estimated range of river flux for each reach. The gray bars represent the simulated steady state values while the colored bars show the estimated range of values.

	Steady State Model Value		Estimated Range	
			min	max
	Net flow ft³/day	%	Net flow ft³/day	Net flow ft³/day
CFR above dam	-6.8E+05	-8	-8.00E+04	3.34E+06
Reservoir	1.7E+06	21	1.80E+05	3.20E+06
CFR below dam	3.1E+06	37	2.01E+06	6.10E+06
BFR arm	1.8E+06	22	1.50E+06	1.90E+06
GWinCFU	1.3E+06	16	5.20E+05	1.50E+06
GWinBFU	5.8E+05	7	8.60E+04	5.20E+05
GWoutHGU	-8.3E+06		-2.70E+06	-9.30E+06

Table 11 Summary of the simulated steady state water balance and estimated range. The % values are the percent of flow contributing to the groundwater underflow discharging through Hellgate Canyon (GWoutHGU). The % values are the percent of flow contributing to the groundwater underflow discharging through Hellgate Canyon (GWoutHGU). Values of underflow into the study area for the upper Clark Fork River and Blackfoot River are also presented.

In addition to the overall calibration of exchange rates, a comparison of simulated results for individual modeled river cells that correspond with field measurement sites was also completed. Overall, once the model was calibrated, simulated riverbed gradients, properties and exchange rates for the BFR and lower CFR regions compared well with field estimates (Figure 70). The exchange complexity in the CFR above the reservoir showed some differences between simulated and field characterized sites. However, this is most likely related to local field conditions not being representative of more average conditions in the area, or improper representation of conditions in the numerical model. The measured values of river bed hydraulic conductivities and simulated calibrated conductivities also showed a reasonable correlation (Figure 71).

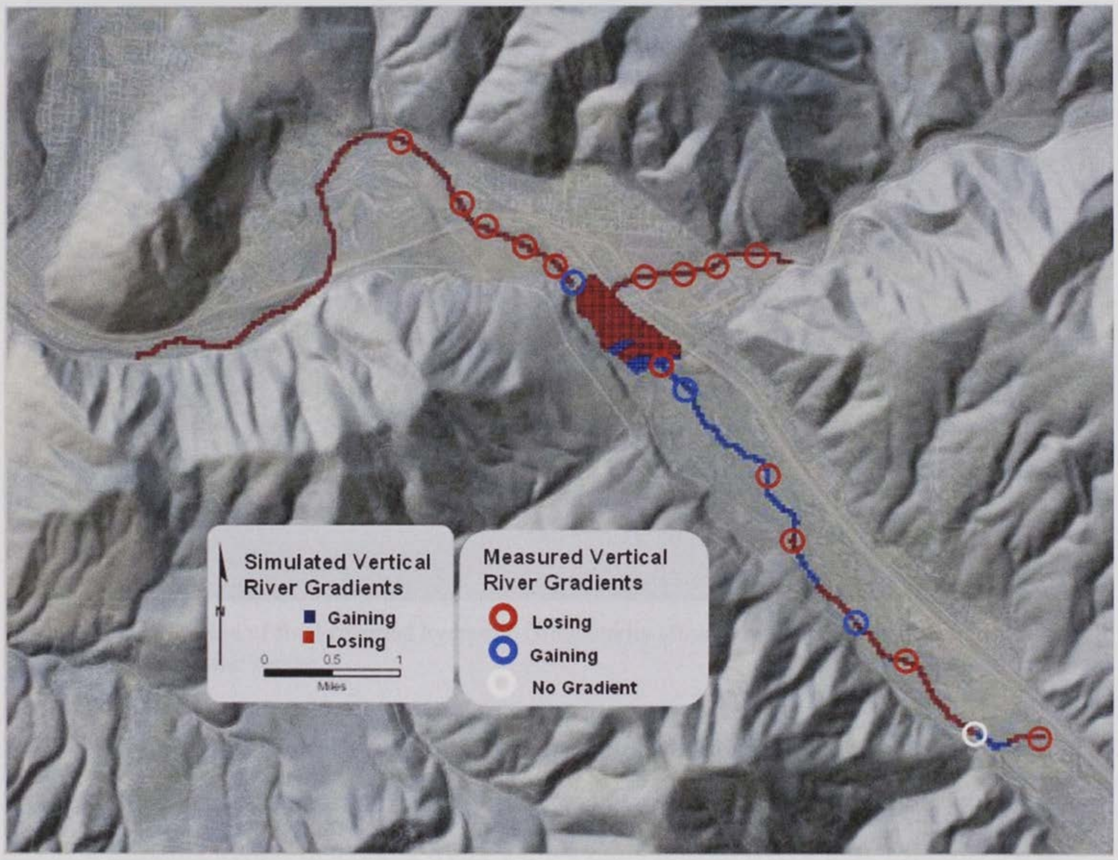

Figure 70 Distribution of final riverbed gradients of the calibrated numerical groundwater model.

More specifically, overall, field hydraulic conductivity values in the CFR reach above the reservoir compared well with the conductivity values used in the model. The hydraulic conductivity results from the temperature modeling and falling head tests ranged from 13 to 0.9 ft/day and 30 to 1.5 ft/day, respectively. The modeled river cell hydraulic conductivity for the CFR in this reach ranged from 10 to 0.2 ft/day. Final model hydraulic conductivity values assigned to the bed of the CFR below the dam ranged from 0.01 to 1.6 ft/day. Field estimates from temperature modeling and falling head test data ranged from 0.7 to 2.0 ft/day and 1.4 to 1.7 ft/day, respectively.

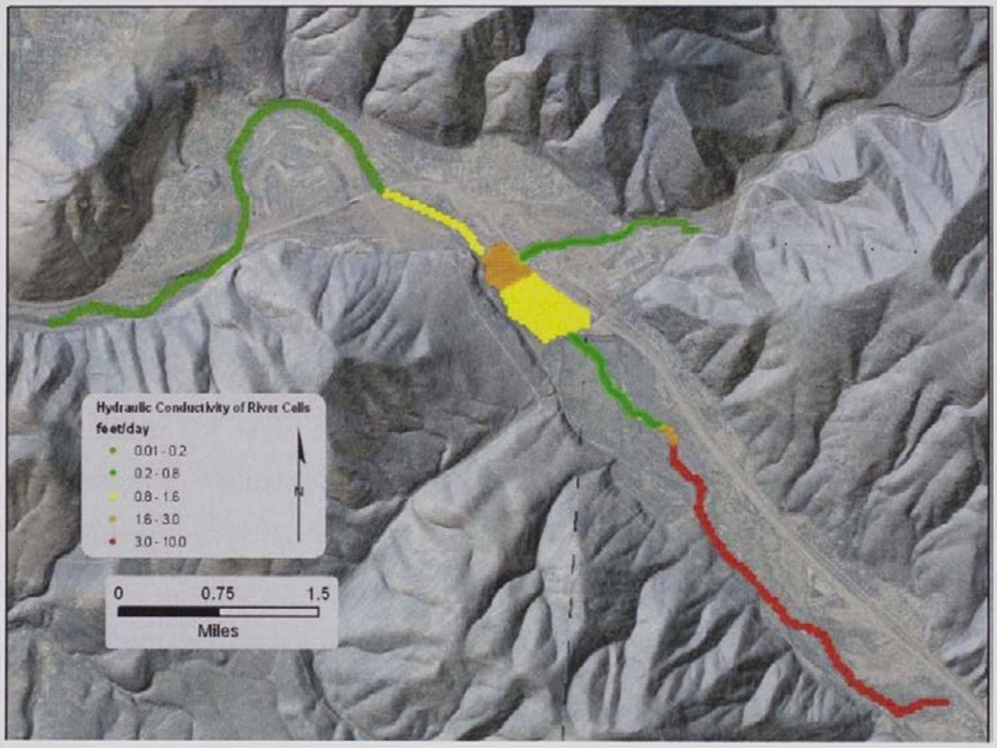

Figure 71 Distribution of final riverbed hydraulic conductivity (ft/day) of the calibrated numerical groundwater model.

No field observations were made in the reservoir sediments during the course of this study because of construction activities, however historical conductivity values report sediments hydraulic conductivity values ranged from 0.019 to 0.2 ft/day (Arco, 2005). The final hydraulic conductivity values used in the numerical model in the reservoir area ranged from 1.5 to 2 ft/day. These values are on the order of one to three orders of magnitude higher than reported values. Some of this difference is most likely an artifact of the model discretization process. The large cell size and the simulated stepped representation of the sediment thickness (reach 9 = 5 ft, reach 10 = 15 ft, reach 11 = 25 ft) may have required assignment of higher values than reported for point measurements collected in the field (Figure 19). In MODFLOW, the river cell conductance is decreased with increasing assigned river bed thickness (see equation 6). To increase the conductance and seepage out of the reservoir the hydraulic conductivity values had to be increased to greater than measured values to compensate for the assigned thicknesses. In contrast, modeled river cell hydraulic conductivity values in the BFR arm of the reservoir (3 ft of bed thickness) range from 0.01 ft/day in the upper section to 0.8 ft/day in the lower section with the majority of the reach being 0.3 ft/day. Temperature monitoring and modeling conducted within this reach resulted in an estimated hydraulic conductivity of 0.7 ft/day, comparable to the model values.

A comparison of surface water and groundwater exchange rates per square foot of riverbed estimated from field observations and from temperature modeling results to simulated model results was also made. In general, the results are similar.

Simulated flux rates at CFR below the dam indicate rates that vary with values as high as 5 to as low as 0.4 $ft^3/(day/ft^2)$ of riverbed and measured values range from 0.7 to 3.7 $ft^3/(dayft^2)$. Tallman (2005) estimated leakage rates from the CFR below the dam to be 4 $ft^3/(dayft^2)$ in Hellgate Canyon to 8.1 $ft^3/(dayft^2)$ in Missoula, MT. The modeled seepage rate distribution below the dam (Figure 58) (higher near the dam and lower down gradient from dam) is not fully supported by field measurements. Unfortunately no data were collected between CFRB8 and the study sites of Tallman (2005) in Hellgate Canyon.

Simulated and estimated exchange rates in CFR above the dam are quite variable. The steady state model results show that the upper section of the CFR above the dam is primarily a losing reach and closer toward the upper reaches of the reservoir the river becomes primarily a gaining river. Simulated rates from the river into the groundwater in the upper reaches range from 0 to 5 $ft^3/(dayft^2)$. Estimates based on field observations range from 0.06 to 3.2 $ft^3/(dayft^2)$ during low water season.

The simulated exchange rates in the BFR arm ranged from 0.4 to 3.3 $ft^3/(dayft^2)$. Field estimated exchange rates ranged from 0.9 to 1.2 $ft^3/(dayft^2)$.

Model Forecasts

The model predictions of the impact to groundwater levels from Phase 2 reservoir drawdowns were made using the assumption that physical river bed hydraulic properties remained constant and that future dewatering efforts intended to dry up a portion of the reservoir sediments for removal were successful. Adjustments made to the river elevations in the groundwater model resulted in changes in seepage rates (generally lowering) and a subsequent decline in groundwater elevations.

The predictions show that after the Phase 2 reservoir drawdown the reservoir area leakage will change from1.7 E+06 ft^3/day (2.3E+06 ft^3/day calculated by Moore and Woessner, 2002) to the underlying aquifer to -5.9E+03 ft^3/day, seepage from the underlying aquifer to the river/reservoir. The reservoir will go from contributing 21% of the recharge to the groundwater leaving through Hellgate Canyon to being a potential groundwater discharge area (gaining river reach) where less than 1 % of the groundwater leaving through Hellgate Canyon is discharging back to the river (Table 12). The model also forecasts lower seepage rates in the BFR arm of the reservoir. The rates were predicted to be 9.6E+05 ft^3/day compared with the original rates of 1.8E+06 ft^3/day. This leakage of water from the river to the groundwater is predicted to be 14% of the volume of groundwater discharge leaving through Hellgate Canyon down from 22% (Table 12).

The extent of the area where changes in surface water groundwater exchanges are forecasted to occur extends as far up as 1.5 miles upriver of the Milltown Dam (Figure 66). No changes in seepage rates were predicted to occur below the dam. This portion of the river system is modeled as maintaining the same stage as the river prior to the Phase 2 drawdown. However, model results suggest that groundwater levels in the aquifer below the dam location will decline as a result of the reduction of aquifer recharge that will occur in the vicinity of the reservoir. Peterson and Wilson (1988) report, based on unsaturated flow theory, the that the further lowering of a water table below a perched river system may in fact influence the seepage rates; however, at some point the lowering of the water table has no further influence on exchange rates (Bouwer et al., 1997). This process is not directly represented in the MODFLOW model code.

	Pre-Drawdown Steady State Simulation		Phase 2 Forecast Simulation	
	Net flow		Net flow	
	ft^3/day	%	ft^3/day	%
CFR above dam	-6.8E+05	-8	9.5E+04	1
Reservoir	1.7E+06	21	-5.9E+03	0
CFR below dam	3.1E+06	37	3.4E+06	49
BFR arm	1.8E+06	22	9.6E+05	14
GWinCFU	1.3E+06	16	1.3E+06	19
GWinBFU	5.8E+05	7	5.8E+05	8
GWoutHGU	-8.3E+06		-6.9E+06	

Table 12 Comparison of pre-drawdown steady state water balance and phase 2 drawdown forecasted water balance.

Post Phase 2 groundwater levels are shown to decline below historical pre dam drawdown levels in the area surrounding the reservoir and down valley as a result of the reservoir drawdown. This was also illustrated during modeling efforts using transient simulations and model forecasts documented in (Berthelote et al., (2007). Impacts to groundwater levels are likely to increase as the reservoir drawdown continues prior to a new steady state dam out river-groundwater configuration. However, other factors such as drought periods and changes to river bed morphology are likely to also have an effect on exchange rates and locations, factors not directly evaluated during this study. Forecasts of long term hydrologic changes are further limited by uncertainty in-river bed values of hydraulic conductivity and final restored river bed configurations.

Processes Controlling River Groundwater Exchange

Overall, field studies showed that surface water and groundwater exchange rates were driven by river bed characteristics, and groundwater and surface water stage relationships. Similar controls on surface water and groundwater exchanges were found by Konrad (2006) and Sophocleous (2002). Additional factors such how the aquifer conductivity and unsaturated conditions impact exchanges and changing bed characteristics (Rassam and Werner, 2008; Rushton and Tomlinson, 1979) impact the exchange process were not evaluated.

Simulated exchange rates were controlled by modeler assigned constant river bed characteristics and simulated groundwater and surface water stage relationships. Model calibration was used to adjust assigned values to assist in matching aquifer heads, groundwater fluxes and river groundwater exchange rates and locations. The bed scale exchange process is at best generally represented in the modeling process. Application of additional representations of this process in the MODFLOW model (Stream Package, new exchange functions) may improve model calibrations.

Though this work appears to satisfactorily describe both pre-dam and post Phase 2 groundwater conditions and exchange sites and rates, it is likely that the bed character, a parameter assumed to remain at pre-dam removal conditions, will change during the removal process. Increase sedimentation in the channel bed below the dam area may impact seepage rates by reducing bed hydraulic conductivities and changes in river stages (Sophocleous, 2002). Exchange rates in the area of the reservoir have largely been controlled by the pool elevation since the dam was built and fine grained sediments were deposited in the pool. Lowering of the reservoir head should decrease the exchange rate with the underlying and adjacent valley aquifer. Model simulations indicate final groundwater levels associated with the post dam in reservoir river channel may create a gaining and losing river reach.

Factors controlling seepage rates in the CFR above the dam appear to be river bed morphology, bed properties and groundwater and river elevations. Changes in the exchange locations and rates will most likely occur in planned restored stream reaches upstream of the reservoir location and un-restored sections of the stream immediately adjacent to this area to some degree as the river channel gradient is modified during river restoration efforts following dam removal.

Study Limitations

An analysis of the impacts of dam removal activities on historical groundwater river exchange processes would be best initiated well in advance of any reservoir drawdown activity. Extensive hydrologic data sets and exchange investigations should be completed. This work, however, was initiated after an initial drawdown phase and without a continuous few years of complete groundwater and surface water data. This investigation did not extensively examine the transient nature of seepage rates during seasonal changes in river conditions, a factor that likely influences the annual groundwater budget. Instrumentation should be designed to measure transient temperature and stages of the river and river bed water transiently at various depths below the river bottom (data that would allow flux calculations). These data could then be analyzed to evaluate if exchange rates are simply linearly related to river and groundwater stages or require a more complex function to properly represent exchange rates. The interpolation of the location of gaining and losing reaches from point measurement data is a simple approach to distributing parameter assignments. Possibly field data could be correlated with remote sensing data such as a thermal analyses or other methods that would suggest how gaining and losing reaches are distributed in areas that lack field measurements.

Numerical modeling consisted of calibration to a single conceptual model. Such an approach does not allow for the characterization of the likely uncertainty in model forecasts. Alternative conceptual models should be developed and calibrated to establish some degree of confidence in model predictions. To remove some model bias, parameter estimation calibration methods should also be evaluated to determine if an improved model calibration can be achieved.

CHAPTER 5

CONCLUSION

This work has refined the hydrogeologic framework in the Milltown area and supplied additional information regarding the locations and rates of surface water and groundwater exchanges within the reservoir and river systems. It also catalogued changes that occurred to groundwater levels and exchange processes during reservoir drawdowns related to on going dam removal activities. Specific project objectives included: 1) defining aquifer boundaries and hydrogeologic properties; 2) establishing river/reservoir stage-groundwater relationships; 3) quantifying river/reservoir exchange rates and locations; 4) developing and testing a conceptual groundwater model; 5) evaluating the appropriateness of the conceptual model and identifying the key drivers that control and dominate observed aquifer responses to allow for the prediction of future aquifer and exchange responses during in a dam removal setting process.

Based on the extensive field investigation the aquifer boundaries were refined by adding additional bedrock depth data, boreholes, and completion of a geophysical survey which were used to generate a bedrock surface. The Results show that the bedrock boundary was more complex than previously represented. These data formed the foundation of groundwater discharge calculations and constrained the groundwater modeling effort. The existing data sets that reported hydraulic conductivities were compiled and assessed with geologic log interpretations. These data sets were used to help constrain numerical model calibration. Final estimates ranged from 290 to greater than 80,000 ft/day suggesting the valley aquifer is heterogeneous and has portions that are highly conductive.

Groundwater stage and river/reservoir stage data were collected by establishing an extensive monitoring network consisting of 51 groundwater wells and 13 river staff gages. Hydrogeologic cross sections and water table maps were created from the data and were and were used as a tool to help develop and support the conceptual understanding of river/reservoir stage and groundwater stage relationships. By comparing surface water and groundwater stages, the exchange directions and scope of hydraulic connection connections were established for certain areas. Groundwater and surface water data were also used to construct and calibrate the numerical groundwater model.

Direct river bed measurements conducted at 26 locations were used to examine the river and groundwater exchange rates. River bed measurements consisted of the measurement of vertical hydraulic gradients, thermal profiles of the riverbed over time, and falling head tests to measure hydraulic conductivity. Thermal profiles were evaluated with a temperature model to estimate bed exchange rates. River bed hydraulic conductivity data were used to estimate the exchange of water using Darcy's Law. Estimated flux measurements ranged from 0.02 to 12 $ft^3/(dayft^2)$. From these data a conceptual model was developed that detailed the surface water and groundwater interactions.

To construct the initial conceptual model, measurements within the river bed were interpolated across areas where the river channel bed characteristics and the river and groundwater exchanges were undefined. To evaluate reach scale surface water and groundwater exchanges, the river was broken up into 4 reaches that consisted of the CFR above the dam, the reservoir, the CFR below the dam and the BFR arm of the reservoir and net exchanges were estimated for each reach. The resultant conceptual model suggested that the CFR above the dam reach contained both gaining and losing river reaches, and the reservoir, the CFR below the dam and the BFR arm of the reservoir were identified as are net losing reaches. The conceptual model was tested with the numerical groundwater model. Measured hydraulic conductivities, estimated fluxes, and vertical river and groundwater exchange directions compared favorably with values used and computed in the fairly well with the calibrated final steady state numerical groundwater model results.

Estimates made at the specific locations in the river were used to develop and constrain the conceptual model. However, the constraints of the conceptual model were not sufficient enough to establish a detailed account of surface and groundwater exchanges above the dam in the Clark Fork River. The number of measurements and interpretation of measurements could lead to the construction of many conceptual models. However, various conceptual models were not investigated. Investigating multiple conceptual models would improve the uncertainty of the modeled results. Study results suggest that reservoir drawdowns during the dam removal process impact the exchange of surface water and groundwater. The rates of leakage from losing portions of the reservoir are decreased so that the water table is lowered adjacent to and downstream of the reservoir location. Little change in conditions is predicted in the river above the reservoir or in the losing stream reach below the dam area. At this site the key drivers controlling the observed responses appear to be river bed characteristics, and groundwater and surface water stage relationships and the hydraulic conductivity of the underlying aquifer.

References

Alexander, M.D., and Caissie, Daniel, 2003. Variability and comparison of hyporheic water temperatures and seepage fluxes in a small Atlantic Salmon stream. Ground Water vol. 41, no. 1, 72-82.

Allan J.D, and Flecker A.S., 1993. Biodiversity Conservation in running waters. Bioscience 43: 32-43.
Arco, 1995. Milltown Reservoir Sediments Operable Unit, Final Draft Remedial Investigation Report. Report prepared for Arco by Titan Environmental Corp., February, 1995.

Arco, 2002. Milltown Reservoir Sediments Site Final Combined Feasibility Study. Report prepared for Arco by EMC2, Bozeman, MT, December 6, 2002.

Battala, R.J., Gomez, C.M., and Kondolf, M., 2004. Reservoir-induced hydrological changes in the Ebro River basin (NE Spain). Journal of Hydrology 290, 117-136.

Baxter, Colden, F. R. Hauer, and W.W. Woessner, 2003. Measuring Groundwater-Stream Water Exchange: New Techniques for Installing Minipiezometers and Estimating Hydraulic Conductivity. Transactions of the American Fisheries Society. Pp 493 – 502.

Bencala, K.E., 1993. A perspective on Stream-catchment connections. The North American Benthological Society 12(1), 44-47.

Berthelote, T., A.J. Farinacci, and W.W. Woessner, 2007. Determining the Impact of Milltown Reservoir Drawdowns on the Adjacent Unconfined Aquifer: Remediation Stage 1 Observed and Stage 2 Forecasted. Prepared for Montana Department of Environmental Quality. July, 2007.

Boulke, E.L., Vaccaro, J.J., 1981. Digital-model simulation of the hydrologic flow system, with emphasis on ground water, in the Spokane Valley, Washington and Idaho. U.S. Geological Survey Open-File Report 80-1300, pp. 43.

Bower, Herman, 1989. The Bower and Rice Slug Test – An update. Groundwater. Vol. 27. No. 3, 304-309.

Brick, Christine, 2003. Preliminary groundwater modeling to estimate effects of dam and sediment removal on the alluvial aquifer in Milltown, Montana. Clark Fork Coalition. Report.

Brunke, M., E. Grieder, 1997. The ecological significance of exchange processes between river and ground-water. Freshwater Biology. 37. pp 1-33.

Caldwell, R.R., and Bowers, C.L., 2003. Surface-water/Ground-water interaction of the Spokane River and the Spokane Valley/Rathdrum Prairie Aquifer, Idaho and Washington. Water-Resources Investigations Report 03-4239.

Constantz, J., S.W. Tyler, E. Kwicklis, 2003. Temperature-Profile Methods for Estimating Percolation Rates in Arid Environments. Vadose Zone Journal. 2:12-24

Dahm, C.N., Grimm, N.B., Marmonier, P., Valett, H.M., Vervier, P., 1998. Nutrient dynamics at the interface between surface waters and groundwaters. Freshwater Biology 40, 427-451.

Doyle, M.W. et al., 2005. Stream ecosystem response to small dam removal: Lessons from the Heartland. Geomorphology 71, 227-244.

Echeverria J.D., Barrow P., Roos-Collins R., 1989. Rivers at risk: the concerned citizens guide to hydropower. Washington (DC): Island Press.

Envirocon, 2006. Stage 1A Element 1 – Stage 1 Reservoir Drawdown and Scour Mitigation Milltown Reservoir Sediments Site, Final Design Report. May, 2006.

Envirocon, 2006. Milltown Reservoir Sediments Operable Unit Remedial Action Monitoring Plan.

Environmental Simulations Inc., 2004. Guide to Using Groundwater Vistas, Version 4.

Fetter, C.W., 1994. Applied Hydrogeology, 3rd edition, Prentice Hall, Englewood Cliffs, NJ.

Freeman, L.A., Carpenter, M.C., Rosenberry, D.O., Rousseau, J.P., Unger, R., and Mclean, J.S., 2004. Use of Submersible Pressure Transducers in Water-Resources Investigations. USGS Techniques of Water-Resources Investigations 8-A3.

Gestring, S.L., 1994. The interaction of the Clark Fork River and the Hellgate Valley Aquifer near, Milltown, Montana. M.S. Thesis, Geology Department, University of Montana.

Graf, William, 2006. Downstream hydrologic and geomorphic effects of large dams on American Rivers. Geomorphology 79, 336-360.

Harding Lawson Associates, 1987. Milltown Reservoir data report, supplemental investigations conducted under the feasibility study. Report to Montana DHES, Appendix D, March, 1987.

Haws, F. W., J. Fletcher and E. Israelsen, 1977. Hydrologic Consideration for the Proposed Finding of Water Rights in the Lemhi River Basin, Idaho. Report prepared for the water users at the request of Kent W. Foster, Holden, Holden, Kidwell, Hahn and Crapo, Idaho Falls, Idaho and James C. Herndon, Attorney at Law, Salmon, Idaho. April 8th.

Hayashi, M. and Rosenberry, D.O., 2002. Effects of Ground water exchange on the hydrology and ecology of surface water. Ground Water vol. 40, no. 3, 309-316.

Hsieh, P.A., W. Wingle, and R.W. Healy, 2000. VS2DHI- A graphical software package for simulating fluid flow and solute or energy transport in variably saturated porous media, 16 pp., USGS Water Resources Investigations Report 9.

Hsieh, P.A., M.E. Barber, B.A. Contor, M.A. Hossain, G.S. Johnson, J.L. Jones, and A.H. Wylie. 2007. Ground-Water Flow Model for the Spokane Valley-Rathdrum Prairie Aquifer, Spokane County, Washington, and Bonner and Kootenai Counties, Idaho. U.S. Geological Survey Scientific Investigations Report 2007-5044.

Hendricks, S.P., and D.S. White, 1991. Physiochemical patterns within a hyporheic zone of a northern Michigan River, with comments on surface water patterns. Can. J. Fish. Aquat. Sci. 48, 1645-1654.

Huntsman, B.E., and R.W. McCready, 1995. Passive monitoring to determine aquifer diffusivity. Proceedings of the International Association of Hydrogeologists Congress, Edmonton, Alberta.

Johnson, A.N., B.R. Boer, W.W. Woessner, J.A. Standord, G.C. Poole, S.A. Thomas, and S.J. O'Daniel. Evaluation of an inexpensive small-diameter temperature logger for documenting ground water-river interactions. Ground Water Monitoring and Remediation 25, no.4, 68-74.

Kondolf, G.M., 1998. Lessons learned from river restoration projects in California. Aquatic Conservation: Marine and Freshwater Ecosystems 8, 39-52.

Konrad, C.P. 2006. Location and timing of river-aquifer exchanges in six tributaries to the Columbia River in the Pacific Northwest of the United States. Journal of Hydrology. Accepted February 24, 2006. Article in Press. Elsevier.

Kauffman, J.B., R.L. Beschta, N. Otting, D. Lytjen, 1997. An Ecological Perspective of Riparian an Stream Restoration in the Western United States. Watershed Restoration vol. 22., no. 5.

Landon, M.K. et al, Rus, D.L., and Harvey, F.E., 2002. Comparison of Instream Methods for Measuring Hydraulic Conductivity in Sandy Streambeds. Ground Water 39(6), 870-885.

Lewis R.S., 1998. Geologic map of the Butte 1o x 2o Quadrangle. Montana Bureau of Mines and Geology.

Lytle, D. A., and Poff, N.L., 2004. Adaptation to natural flow regimes. Trends in Ecology and Evolution, vol. 19 no. 2.

Magilligan, F.J., and Nislow, K.H., 2005. Changes in hydrologic regime by dams. Geomorphology 71, 61-78.

Mickey, J.W., 1998. The effects of discharge variation on dissolved element concentration through Milltown Reservoir, Montana. M.S. Thesis. Department of Geology, University of Montana.

Moore, J.N. and Woessner, W.W., 2002. Arsenic contamination in the water supply of Milltown, Montana. In: A.H. Welch and K.G. Stollenwerk (editors), Arsenic in Ground Water: Geochemistry and Occurrence. Kluwer Academic Publishers, Boston.

[NRC] National Research Council, 1992. Restoration of aquatic systems: science, technology, and public policy. Washington (DC): National Academy Press.

Nyquest, D.L., 2001. A depth-to-bedrock model of the Hellgate Canyon and Bandmann Flats area, East Missoula, Montana using constrained inversion of gravity data. M.S. thesis, Geology Department, University of Montana.

Palmer, M.A., 1993. Experimentation in the hyporheic zone: challenges and prospectus. Journal of the North American Benthalogical Society 12(1), 84-93.

Pinder, G.F., J.D. Bredehoeft, and H.H. Cooper Jr., 1969. Determination of aquifer diffusivity from an aquifer response to fluctuations in-river stage. Water resources Research, 5, 850-855.

Poff, N.L. et al., 2006. Hydrologic variation with land use across the contiguous United States: Geomorphic and ecological consequences for stream ecosystems. Geomorphology 79, 264-285.

Pohl, M.M., 2002. Bringing down our dams: Trends in American dam removal rationales. Journal of American Water Resources Association, (Dec. 2002).

Pusch, M., Fiebig, D., Brettar, I., Eisenmann, H., 1998. The role of micro-organisms in the ecological connectivity of running waters. Freshwater Biology 40, 453-495.

Rassam, David and A. Werner. 2008. Review of groundwater-surface water interaction modeling approaches and their suitability for Australian conditions. eWater Technical Report. eWater Cooperative Research Centre, Canberra. http://ewatercrc.com.au/reports/Rassam_Werner-2008-Groundwater_Review.pdf

Rushton, K.R. and L.M. Tomlinson, 1979. Possible mechanisms for leakage between aquifers and rivers. Journal of Hydrology. Vol 40. pp 49-65.

Scanlon, B.R., R.W. Healy and P.G. Cook, 2002. Choosing appropriate techniques for quantifying groundwater recharge. Hydrogeology Journal, 10, 18-39.

Sophocleous, M., 2002. Interactions between groundwater and surface water: the state of the science. Hydrogeology Journal. Vol. 10. pp52-67.

Stanford, J.A., 1998. Rivers in the landscape: introduction to the spatial issue on riparian and groundwater ecology. Freshwater Biology 40, 402-406.

Stanford, J.A., Ward, J.V, 1993. An ecosystem perspective of alluvial rivers: connectivity and the hyporheic corridor. Journal of the North American Benthological Society 12(1), 48-60.

Stonestrom, D.A. and J. Constantz, 2003. Heat as a Tool for Studying the Movement of Ground Water Near Streams. U.S. Geological Survey Circular 1260.

Tallman, Emelia A., 2005. Source of Water Captured by Municipal Supply Wells in a Highly Conductive Aquifer, Western Montana. M.S. Thesis. Geology Department, University of Montana.

Udaloy, A.G., 1988. Arsenic mobilization in response to the draining and filling of the reservoir at Milltown, Montana. M.S. Thesis. Department of Geology, University of Montana.

U.S. Army Corps of Engineers, http://crunch.tec.army.mil/nid/webpages/nid.cfm

Valett, H.M., Fisher, S.G., and Stanley, E.H., 1990. Physical and chemical characteristics of the hyporheic zone of a Sonoran Desert stream. Journal of the North American Benthological Society 9(3), 201-215.

Western Consultants, Inc., River Design Group, Inc., and Geum Environmental Consulting, Inc. 2005. Restoration Plan for the Clark Fork River and Blackfoot River near Milltown Dam – October 2005. Submitted to State of Montana Natural Resource Damage Program and Montana Fish, Wildlife and Parks In consultation with the U.S. Fish and Wildlife Service and Confederated Salish and Kootenai Tribes.

Williams, G.P., and Wolman, M.G., 1984. Downstream effects of Dams on Alluvial Rivers. U.S. Geological Survey Professional Paper, vol. 1286. U.S. Government Printing Office, Washington, D.C.

Woessner, W.W., J.N. Moore, C. Johns, M.A. Popoff, L.C. Sartor, and M. Sullivan, 1984. Arsenic Source and Water Supply Remediation Action Study, Milltown, Montana. Final Report for Solid Waste Bureau, Montana Dept. Health and Environmental Sciences.

Woessner, W.W. and Popoff, W.A., 1982. Hydrogeologic Survey of Milltown, Montana and Vicinity. Report, Water Quality Bureau, Department of Health and Environmental Sciences. Helena, MT.

Woessner, W.W., 1988. Missoula Valley Aquifer Study: Hydrogeology of the Eastern portion of the Missoula Valley Aquifer, Missoula County, Montana. Report, Water Development Bureau, Montana Department of Natural Resources and Conservation. Helena, MT.

Woessner, W.W., 1993. Clark Fork Natural Resource Damage Assessment. Milltown Groundwater Injury Report. Department of Geology, University of Montana, Missoula, MT.

Woessner, W.W., 2000. Stream and Fluvial Plain Ground Water Interactions: Rescaling Hydrogeologic Thought. Ground Water. Vol. 38, No. 3. pp 423-429.

Appendix A

Well and River Survey and Water Level Data

Well Number	99b	99c	103a	103b	104b	105a	105b	105c	108a	108b
AKA										
mtspft nad83	873409.34	873388.47	874288.30	874299.27	874414.77	873682.86	873712.78	873696.80	872848.68	872864.66
mtspft nad83	986325.64	986351.90	985272.33	985259.32	985715.84	986088.57	986088.46	986079.55	987060.84	987070.77
TOC elev.	3295.11	3293.83	3307.454	3307.26	3305.024	3299.27	3299.36	3298.79	3274.313	3274.12
Ground Elev.										
2/23/2006										
3/9/2006										
3/31/2006			3249.794		3246.754				3240.153	
5/10/2006			3252.564		3251.924	3248.86			3244.603	
5/15/2006										
5/22/2006			3253.494							
5/26/2006			3254.054		3253.854	3250.73			3246.303	
5/31/2006			3254.054		3253.874	3250.75			3246.393	
6/6/2006			3253.284		3252.524	3249.2			3244.813	
6/15/2006			3251.854		3250.984	3247.67			3243.203	
6/23/2006			3251.454		3249.774	3246.47	3246.557		3242.013	
6/30/2006			3250.754		3248.624	3245.36	3245.427		3240.903	3240.843
7/3/2006										
7/14/2006			3249.554		3247.034	3243.77	3243.827		3239.343	3239.303
7/19/2006	3242.06		3249.174	3248.714						
8/18/2006			3247.754		3244.674	3241.42	3241.457		3237.033	3237.003
9/18/2006	3239.44	3238.83	3247.194	3246.734	3243.894	3240.64	3240.727		3236.263	3236.253
10/23/2006					3242.994	3239.77	3239.817		3235.423	3235.403
11/15/2006	3239.01		3245.894	3245.484	3243.394				3234.763	3235.743
12/15/2006			3246.384		3245.514	3242.07	3242.157	3242.137		3237.353
1/25/2006	3240.8		3246.694		3245.424	3241.99	3242.087			3237.283
2/18/2007				3245.334	3243.064	3239.61	3239.677	3239.687		3235.273
3/17/2007	3238.33	3237.56	3244.764	3244.374	3241.724	3238.47	3238.567	3238.557		3234.183
4/9/2007										
4/21/2007					3243.454	3240.19	3240.257	3240.247		3235.653
5/7/2007										
5/19/2007	3243.3	3242.83	3248.964	3247.554	3247.804	3244.47	3244.597	3244.527		3239.683

Well Number	109a	109b	110a	110b	111a	111b	901	903	917A	917b
AKA										
mtspft nad83	873834.45	873821.43	875993.57	876013.56	875039.91	875069.94	873271.90	872999.60	871500.13	871530.06
mtspft nad83	987453.30	987447.35	984079.06	984066.05	986161.78	986161.68	985144.71	984714.43	987425.29	987425.29
TOC elev.	3280.01	3282.07	3294.214	3294.02	3296.814	3296.67	3264.657	3265.707	3280.16	3280.56
Ground Elev.										
2/23/2006										
3/9/2006										
3/31/2006					3246.374				3232.05	
5/10/2006			3257.164		3250.594				3236.06	
5/15/2006										
5/22/2006			3258.064		3252.314		3258.027	3259.557		
5/26/2006			3258.014		3252.114		3258.257		3237.46	
5/31/2006			3257.514		3252.314		3258.857	3259.807	3237.86	
6/6/2006			3257.184		3250.814		3257.157	3257.217	3235.99	
6/15/2006			3256.214		3249.114		3255.457	3256.137	3232.96	
6/23/2006			3255.714		3248.214		3254.657	3254.907	3232.06	
6/30/2006			3255.014		3247.114		3253.857	3254.187	3230.76	
7/3/2006										
7/14/2006	3233.44	3242.67	3254.014		3245.314		3252.957	3253.547	3228.96	
7/19/2006			3253.804		3245.114	3245.894	3252.037		3228.42	
8/18/2006	3231.53	3240.9	3252.914		3243.314		3251.657	3252.347	3226.26	
9/18/2006	3230.6	3240.03	3252.524		3242.514	3243.234	3250.997		3225.51	
10/23/2006							3250.307	3251.637		
11/15/2006	3230.01	3239.69	3252.534	3253.204	3242.174	3242.944	3247.257	3245.477	3224.88	3224.82
12/15/2006							3246.707	3244.787		
1/25/2006			3253.314		3244.064	3244.924			3225.85	3225.79
2/18/2007		3239.09								
3/17/2007		3238.07	3251.894	3252.654	3240.504	3241.324			3223.43	3223.37
4/9/2007									3224.51	
4/21/2007		3239.66							3224.71	3224.56
5/7/2007										
5/19/2007		3243.87	3254.914	3255.494	3246.654	3247.534			3228.06	3227.98

Well Number	918	919A	919B	919C	920	921A	921b	922A	922b	922C	922D
AKA											
mtspft nad83	873861.73	871474.11	871504.14	871474.11	870151.69	870699.56	870729.48	870386.59	870416.62	870386.59	870386.59
mtspft nad83	982190.14	988212.72	988212.71	988182.80	987907.65	988080.78	988080.78	988719.77	988719.66	988719.77	988719.77
TOC elev.	3265.65	3281.27	3280.69	3281.50	3275.11	3274.123	3274.35	3278.473	3278.70	3278.86	3279.93
Ground Elev.											
2/23/2006											
3/9/2006											
3/31/2006	3259.35	3228.11			3225.72			3222.333			
5/10/2006	3260.76	3232.33			3229.36	3230.403		3227.053			
5/15/2006											
5/22/2006											
5/26/2006	3261.05	3233.72			3230.91	3231.743		3228.523			
5/31/2006	3261.15	3234.05			3230.41	3232.073		3228.763			
6/6/2006	3259.75	3232.61			3229.98	3230.553		3227.733			
6/15/2006	3259.25	3230.65			3228.71	3228.613		3226.033			
6/23/2006	3259.05	3229.3	3228.62	3229.32	3227.71	3227.243		3224.663	3225.583	3225.773	
6/30/2006	3258.75	3228.06	3227.37	3228.04	3226.41	3226.013	3227.993	3222.963	3223.793	3224.003	
7/3/2006							3226.973	3222.863	3223.793	3224.003	
7/14/2006	3258.95	3226.21	3225.47	3226.18	3225.11	3224.183	3225.623	3221.533	3222.423	3222.663	
7/19/2006	3259.01				3224.73						
8/18/2006	3259.35	3223.47	3222.79	3223.47	3223.01	3221.453	3223.203	3218.693	3219.683	3219.933	
9/18/2006	3258.91	3222.51	3221.82	3222.5	3222.59	3220.473	3222.083	3217.613	3218.693	3218.913	
10/23/2006		3221.76	3221.09	3221.77		3219.753	3221.643	3216.853	3217.963	3218.183	
11/15/2006	3258.87	3221.7	3221.04	3221.7	3223.47	3219.603	3221.443	3216.683	3217.803	3218.033	
12/15/2006		3222.49	3221.79	3222.45		3220.293	3221.923	3217.183	3218.373	3218.623	
1/25/2006	3256.77	3222.52	3221.81	3222.5	3222.87	3220.333	3221.963	3217.273	3218.473	3218.753	
2/18/2007		3221.41	3220.69	3221.34		3219.343	3221.443	3216.333	3217.483	3217.713	
3/17/2007	3259.5	3220.27	3219.54	3220.19	3223.83	3218.203	3220.753	3215.273	3216.393	3216.623	3216.63
4/9/2007											
4/21/2007		3221.36				3219.273	3221.353	3216.343	3217.423	3217.673	3217.72
5/7/2007											
5/19/2007	3259.75	3225.01	3224.32	3224.97	3227.45	3222.923	3223.363	3220.063	3221.153	3221.393	3221.42

Well Number	923A	923B	923C	C-4	DA-29A	DB-001	DB-007	DB-079	DB-132	DB-205
AKA					Chuck			ROUTH	29	
mtspft nad83	869699.76	869729.79	869729.79	873090.66	879681.96	876321.60	877569.55	871081.12	875046.28	874446.77
mtspft nad83	988454.75	988454.75	988454.75	988131.88	978781.29	984560.65	983518.70	990661.90	988734.58	989099.03
TOC elev.	3270.667	3270.80	3272.63	3291.737	3287.391	3297.979	3295.52	3288.07	3307.35	3304.033
Ground Elev.										
2/23/2006						3259.209	3260.63			
3/9/2006				3230.767					3226.35	3229.633
3/31/2006	3220.777			3229.407	3278.031	3256.969	3259.12	3223.66	3229.05	3227.843
5/10/2006	3225.837			3233.587	3278.571	3260.559	3260.77	3228.48	3236.17	3232.113
5/15/2006	3225.767									
5/22/2006										
5/26/2006	3227.507			3234.537		3261.909	3261.36	3229.57	3234.3	3233.143
5/31/2006	3227.777			3235.437	3278.831	3261.859	3261.32	3229.87	3234.65	3233.423
6/6/2006	3226.777			3234.437	3278.671	3260.609	3260.63	3229.47	3233.8	
6/15/2006	3225.057			3232.337	3278.721	3259.679	3260.12	3227.27	3232.15	
6/23/2006	3223.567			3231.437	3278.301	3258.749	3259.92	3226.17	3232.6	
6/30/2006	3222.167			3230.137		3257.949	3259.42	3224.77	3229.7	
7/3/2006										
7/14/2006	3220.137			3228.237	3276.411	3256.949	3258.82	3222.67	3227.65	
7/19/2006				3227.737			3258.69	3222.1		3226.383
8/18/2006	3217.097			3225.737	3277.881	3255.379	3258.17	3219.87	3225.27	
9/18/2006	3215.967			3224.827		3254.989	3258.08	3218.79	3224.35	3223.423
10/23/2006	3215.197				3278.111	3254.519			3223.13	
11/15/2006	3214.997	3215.04		3224.677	3278.011	3254.859	3257.15	3217.81	3222.81	3222.513
12/15/2006	3215.327				3278.001	3256.179			3222.61	
1/25/2006	3215.417	3215.47	3217.02	3225.037	3277.901	3255.979	3258.4	3218.51	3224.15	3223.733
2/18/2007	3214.407				3278.091	3254.579			3223	
3/17/2007	3213.317	3213.58		3222.547	3278.191	3253.929	3257.91	3216.52	3222.15	3221.213
4/9/2007										
4/21/2007	3214.387				3278.181	3254.999			3222.65	
5/7/2007										
5/19/2007	3218.387			3227.737	3279.861	3257.979	3259.48	3221.07	3225.55	3225.423

Well Number	DA-41	HLA-2	HG-17	HG-20	HG-21	HG-23	HG-26	HG-27	HG-36
AKA	2			DB-171	DB-172			**DB-008**	
mtspft nad83	875840.761	872626.70	867085.22	871534.07	873360.27	873908.36	872134.64	**869757.08**	864770.19
mtspft nad83	985010.1552	986935.24	990264.88	988941.57	988819.03	989629.30	989280.37	**990604.34**	992533.33
TOC elev.	3309.367	3266.47	3267.037	3291.823	3301.047	3298.62	3296.65	3279.16	3252.253
Ground Elev.									
2/23/2006	3252.107		3214.987		3228.917			3222.6	
3/9/2006						3230.83			3202.123
3/31/2006	3249.877		3214.497	3226.593	3227.127	3229.88	3225.99	3222.22	3200.953
5/10/2006	3253.867		3219.087	3230.763	3232.027	3233.82	3230.73	3226.39	3210.353
5/15/2006									
5/22/2006								3227.31	
5/26/2006	3255.467		3221.017	3232.263	3232.867	3235.02	3231.97	3226.96	3215.753
5/31/2006	3255.467		3220.877	3232.663	3233.307	3235.42	3232.38	3226.46	3216.253
6/6/2006	3254.307		3220.267	3231.653	3232.377	3234.87	3231.51	3227.56	3214.453
6/15/2006	3252.967		3219.237	3229.323	3230.677	3232.82	3229.53	3225.76	3214.013
6/23/2006	3252.267		3217.887		3229.597	3231.82	3228.15	3224.66	3212.103
6/30/2006	3251.267		3216.627	3227.473	3228.027	3230.42	3226.92	3223.26	3211.593
7/3/2006									
7/14/2006	3249.967		3214.867	3224.923	3226.477	3228.72	3224.9	3221.16	3209.453
7/19/2006	3237.647			3224.403		3227.85		3220.38	
8/18/2006			3212.057	3222.323	3224.687	3225.92	3221.83	3217.96	3205.263
9/18/2006	3247.507		3210.947	3221.243	3223.537	3225.16	3221.26	3217.07	3203.803
10/23/2006			3210.447		3223.347		3220.49		3202.953
11/15/2006	3247.317		3209.857	3220.403	3222.497	3224.12	3220.5	3215.92	3202.093
12/15/2006			3209.817		3223.337		3220.98		3201.393
1/25/2006	3248.967		3210.047	3221.043	3223.757	3225.12	3221.17	3216.54	
2/18/2007			3209.367		3223.027		3220.38		
3/17/2007	3246.137	3233.393	3208.467	3218.993	3221.397	3222.96	3219.5	3214.52	
4/9/2007						3223.87		3215.47	
4/21/2007		3234.873	3209.487		3222.247		3219.79		
5/7/2007									
5/19/2007	3250.867	3238.903	3213.457	3223.563	3225.817	3226.95	3224.12	3219.41	

Well Number	HGD	HGS	M-16	MW#3	MW#5	MW#6	MW#7	Barbara	Wiemer(BFR)	Hall
AKA								BW		
mtspft nad83	**853458.06**	**853458.06**	871488.75	863279.94	859800.62	864424.18	866158.37		**881327.70**	**877882.49**
mtspft nad83	**984370.10**	**984370.10**	987215.47	987980.96	987390.36	990845.92	989001.98		**988392.55**	**983350.17**
TOC elev.	3207.247	3207.747	3277.61	3278.107	3263.317	3255.203	3265.297		3284.77	3294.95
Ground Elev.										
2/23/2006										
3/9/2006										
3/31/2006				3202.207		3205.233	3209.917			
5/10/2006				3207.717		3211.433	3214.257		3260.67	
5/15/2006										
5/22/2006							3215.637			
5/26/2006				3210.217		3214.003	3215.997		3263.87	
5/31/2006				3209.827		3213.603	3215.897		3262.67	
6/6/2006				3209.177		3213.033	3215.587		3261.72	
6/15/2006				3208.907		3212.403	3214.597		3260.87	
6/23/2006						3211.303	3213.797		3259.47	
6/30/2006				3205.917		3209.803	3212.497		3258.4	
7/3/2006				3205.917						
7/14/2006	3179.617	3179.967		3204.687	3197.347	3207.903	3210.697		3253.97	3260.12
7/19/2006						3207.383	3210.507			
8/18/2006	3175.817	3176.147		3201.457		3204.803	3208.297		3252.7	3259.52
9/18/2006	3174.597	3174.907	3225.97	3200.037	3192.547	3203.443	3207.177		3252.31	3259.54
10/23/2006	3173.247	3173.527		3199.077	3191.467				3250.87	3259.57
11/15/2006	3172.487	3172.767			3190.587	3202.023	3205.957		3251.33	
12/15/2006	3170.757	3171.017		3197.487	3188.897		3205.607		3255.29	3259.93
1/25/2006	3170.047	3170.337		3197.417	3188.587	3201.303	3205.657		3256.25	
2/18/2007	3169.007	3169.297		3196.957	3188.107				3250.01	
3/17/2007	3168.917	3169.197		3196.357	3187.417	3200.243	3204.377		3250.27	
4/9/2007							3203.397			
4/21/2007	3170.567	3170.847		3197.357	3188.807					
5/7/2007				3199.787						
5/19/2007	3179.547	3179.917			3195.937	3206.783				

Well Number	Hampton(turah)	Rodin(turah)	rsw4	Sloan	Ubben	Waletzko	Whitman	Koller	Connolly
AKA									
mtspft nad83	891310.01	888694.16	879341.30	877271.59	886822.18	885358.75	884113.3	881799.563	878430.852
mtspft nad83	963420.87	969959.16	987546.76	985692.13	972736.33	992135.58	975381.6	975536.724	980731.791
TOC elev.	3363.98	3327.56	3294.02	3298.98	3322.28	3317.51	3324.63	3295.11	3281.43
Ground Elev.									
2/23/2006									
3/9/2006	3343	3315.33			3306.61	3275.06			
3/31/2006	3343.91	3315.6		3249.33	3306.78	3276.22			
5/10/2006	3345.49	3317.86		3252.98	3308.77	3278.22			
5/15/2006									
5/22/2006		3318.82							
5/26/2006	3345.25	3318.06		3254.96	3308.66	3280.21			
5/31/2006	3344.97	3317.66	3256.17	3254.73	3308.51	3278.87			
6/6/2006	3344.4	3317.43	3254.62	3253.35	3308.07	3278.76			
6/15/2006	3344.97	3317.48	3253.72	3251.96	3308.33	3278.55			
6/23/2006	3344.5	3317.06	3252.02	3250.7	3307.71	3277.4	3293.47		
6/30/2006	3343.25	3316.56	3250.82	3249.73	3307.19	3276.76			
7/3/2006									
7/14/2006	3342.79	3316.26	3248.82	3248.01	3306.94	3276.05	3291.75	3286.609	
7/19/2006		3316.2	3248.96						
8/18/2006	3342.07	3315.86	3247.02	3245.83	3306.36	3275.29	3292.37	3286.139	3272.39
9/18/2006	3342.29	3315.73	3246.09	3245.04	3306.41	3275.14			3272.05
10/23/2006	3342.82			3243.91	3306.77	3275.06	3292.83	3286.649	3272.27
11/15/2006		3315.85	3245.88	3244.54	3306.46	3275.99	3292.82	3286.629	
12/15/2006				3246.75	3306.67	3275.55	3292.82	3286.629	3271.17
1/25/2006	3342.57	3314.94	3248.48	3246.74	3306.17	3277.07	3292.41	3286.349	3272.01
2/18/2007	3343.51			3243.98	3306.7	3275.18	3292.8	3286.689	3271.78
3/17/2007	3345.62	3316.54	3244.38	3243.03	3307.35	3276.33	3293.09	3286.939	3272.29
4/9/2007									
4/21/2007	3344.5			3244.78	3307.44	3276.76	3293.15	3286.989	3273.03
5/7/2007									
5/19/2007	3344.98	3318.4	3251.3	3249.34	3308.54	3279.05	3293.81		3272.93

Well Number AKA	rosebloom	subdivision MW	Shack IRR	RW	CCR	ST1	ST2	ST3	Davis House
mtspft nad83	889138.301	884925.24	885223.518	866664.646	882150.692	886856.06	887323.539	887502.126	884334.374
mtspft nad83	967715.964	972711.612	971987.0957	988121.007	972345.225	968771.729	968517.419	968445.839	970051.064
TOC elev.	3326.68	3320.25	3313.622333	3276.01	3307.36	3338.175	3331.694	3322.284	3308.342
Ground Elev.									
2/23/2006									
3/9/2006									
3/31/2006									
5/10/2006									
5/15/2006									
5/22/2006									
5/26/2006									
5/31/2006									
6/6/2006									
6/15/2006									
6/23/2006									
6/30/2006									
7/3/2006									
7/14/2006									
7/19/2006									
8/18/2006									
9/18/2006									
10/23/2006	3319.943								
11/15/2006	3319.843	3301.648	3304.052333						
12/15/2006		3301.498	3303.972333	3205.666					
1/25/2006	3319.243	3301.028	3303.502333	3205.726	3298.2				
2/18/2007	3319.583	3301.488	3303.992333	3205.306	3298.67				
3/17/2007	3320.073	3301.888	3304.432333	3204.556	3299.1	3317.125	3220.064	3316.164	3302.592
4/9/2007				3205.226					
4/21/2007	3320.193	3302.028	3304.652333		3299.01	3317.175		3316.634	3302.442
5/7/2007				3205.226	3299.76				
5/19/2007	3320.973	3303.088	3305.822333			3317.205		3317.644	

AKA		
mtspft nad83	884572.04	881390.958
mtspft nad83	969979.19	988445.14
TOC elev.	3302.88	3295.186
Ground Elev.		
2/23/2006		
3/9/2006		
3/31/2006		
5/10/2006		
5/15/2006		
5/22/2006		
5/26/2006		
5/31/2006		
6/6/2006		
6/15/2006		
6/23/2006		
6/30/2006		
7/3/2006		
7/14/2006		
7/19/2006		
8/18/2006		
9/18/2006		
10/23/2006		
11/15/2006		
12/15/2006		
1/25/2006		
2/18/2007		
3/17/2007	3297.83	
4/9/2007		
4/21/2007	3297.03	3253.856
5/7/2007		
5/19/2007		3259.566

Surface Water
Elevations

	BF- Bridge	BF -Stimpson	BF- weigh stn.	BF-top	Hellgate	CFRB 3	CFRB 2	CFRB 1	C.E.
	BFR1	BFR2	BFR3	BFR4	Hellgate	CFRB 3	CFRB 2	CFRB 1	C.E.
Elevation	3290.24	3259.25	3265.62	3272.04	3184.27633	3213.71	3218.4	3230.46	3272.12
Easting	986886.53	987532.41	988407.74	991219.31	984021.453	992283.82	989117.79	987177.21	978978.06
Northing	873273.46	879599.76	880918.98	884389.78	853720.306	864657.08	867187.24	870795.47	878607.56
top to ruler (in)					1.167				
Elevation (ft)									
4/2/06		3261.733122	3267.203333			3214.50167	3220.9	3232.54333	3272.90871
4/8/06	3261.54	3264.194147	3268.911667				3223.65	3234.62667	3273.89086
5/9/06	3261.24	3263.894022	3268.703333				3223.4	3234.54333	3273.99999
5/11/06		3262.213322	3267.536667						3273.80902
5/16/06	3260.74	3264.614322	3269.203333			3217.66833	3224.4	3234.54333	3274.32738
5/17/06									3274.62
5/26/06	3290.24								3274.45333
5/31/06	3260.74	3263.533872	3268.453333			3217.12667	3223.65	3234.71	3274.03667
6/6/06	3256.74	3263.293772	3268.286667			3216.87667	3223.48333	3234.54333	3273.78174
6/8/06									3273.78667
6/15/06	3255.24	3262.933622	3268.036667			3216.79333	3223.48333	3234.54333	3274.12
6/23/06	3253.74	3261.083333	3266.703333	3274.37333		3216.04333	3221.98333	3233.46	3273.03667
6/30/06	3252.34	3260.25	3266.161667	3273.70667		3215.37667	3221.23333	3232.87667	3272.53667
7/14/06	3252.34	3259.333333	3265.62	3273.20667		3214.96	3220.65	3232.37667	3272.53667
8/18/06	3252.34	3258.75	3265.036667	3272.62333		3213.87667	3219.60833	3230.46	3271.39456
9/18/06	3253.34		3265.62	3272.54		3214.37667	3219.73333	3231.21	3272.04933
10/23/06	3251.24		3265.953333	3272.54		3214.585	3219.98333	3231.71	3272.7723
11/14/06	3252.24	3259.416667	3265.786667	3273.37333		3215.04333	3220.73333	3232.12667	3272.79958
12/15/06				3272.87333		3214.62667	3220.4		3272.53667
1/25/07									
2/20/2007							3220.15	3231.79333	3272.22417
2/23/2007									
3/8/2007				3273.21	3180.95				
3/16/2007				3273.58	3181.66				
3/19/2007							3221.57	3233.21	
4/21/2007	3251.64		3265.703	3274.123	3181.82	3215.835	3221.692	3233.377	3273.370
4/25/2007									
5/7/2007									
5/18/2007	3255.83				3183.87		3223.817		3274.620

	usgs_turah	usgs_above_miss	usgs_bfr	Hellgate
	3318	3198.3	3344.76	3189
Elevation	889265.8079	861096.2044		
Easting	968806.4397	989933.6423		
Northing				
top to ruler (in)				
Elevation (ft)	3322.71	3201.7	3347.84	3192.4
4/2/06	3323.43	3203.77	3349.59	3194.47
4/8/06	3323.51	3203.9	3349.81	3194.6
5/9/06	3323.37	3203.6	3349.58	3194.3
5/11/06	3323.75	3204.52	3350.49	3195.22
5/16/06	3324.06	3205.28	3351.13	3195.98
5/17/06	3323.87	3205.39	3351.3	3196.09
5/26/06	3323.4	3204.11	3350.09	3194.81
5/31/06	3323.35	3204.1	3350.15	3194.8
6/6/06	3323.31	3203.97	3350.04	3194.67
6/8/06	3323.4	3203.94	3349.85	3194.64
6/15/06	3322.77	3202.61	3348.76	3193.31
6/23/06	3322.48	3201.98	3348.17	3192.68
6/30/06	3322.46	3201.54	3347.53	3192.24
7/14/06	3321.6		3344.67667	3191.38
8/18/06	3322.08	3200.79	3344.76	3191.49
9/18/06	3322.61	3201.14	3344.78431	3191.84
10/23/06	3322.63	3201.76	3344.78083	3192.46
11/14/06			3344.79472	3191.99
12/15/06				
1/25/07				
2/20/2007				
2/23/2007				
3/8/2007				
3/16/2007				
3/19/2007				
4/21/2007				
4/25/2007				
5/7/2007				
5/18/2007				

Historical Water Level

Well Number		99A
HLA	5/22/1985	3248.63
HLA	5/4/1986	3244.93
HLA	6/22/1986	3244.43
HLA	7/16/1986	3242.83
ENSR	6/1/1990	3250.80
ENSR	9/1/1990	3244.90
ENSR	6/1/1991	3251.55
Gestring	5/1/1992	3247.33
ENSR	5/1/1992	3247.33
Gestring	11/6/1992	3242.31
Gestring	12/7/1992	3243.93
Gestring	1/4/1993	3244.01
Gestring	2/5/1993	3241.80
Gestring	3/6/1993	3241.17
Gestring	4/6/1993	3242.88
Gestring	5/7/1993	3245.04
Gestring	6/4/1993	3248.64
Gestring	7/7/1993	3247.27
State	6/11/1998	3248.92
State	12/7/1998	3244.06
State	6/1/1999	3249.36
State	12/2/1999	3243.78
State	6/28/2000	3246.21
State	12/1/2000	3243.15
State	6/13/2001	3247.2
State	11/29/2001	3242.35
State	6/3/2002	3248.54
State	12/6/2002	3242.94
State	7/15/2003	3246.99
State	1/2/2004	3242.9
State/Tallman	6/22/2004	3247.84
State	12/1/2004	3247.4
State	6/8/2005	3253.7
State	11/30/2005	3241.83

S

Well Number		103a
Woessner 84	11/3/1983	3246.30
Woessner 84	11/21/1983	3244.62
Woessner 84	6/25/1984	3248.87
HLA	5/22/1985	3253.10
HLA	5/4/1986	3246.10
HLA	6/22/1986	3246.00
HLA	7/16/1986	3244.90
ENSR	10/1/1991	3246.48
State	6/19/1998	3253.32
State	12/15/1998	3250.26
State	6/1/1999	3253.14
State	12/10/1999	3250.19
State	7/8/2000	3250.57
State	12/8/2000	3249.99
State	6/29/2001	3252.25
State	12/6/2001	3249.63
State	6/3/2002	3253.14
State	12/6/2002	3249.60
State	1/2/2004	3250.76
State/Tallman	6/30/2004	3252.89
State	12/1/2004	3252.14
State	6/14/2005	3264.68
State	12/5/2005	3246.95

Well Number		104b
Woessner 84	11/21/1983	3243.64
Woessner 84	1/26/1984	3248.26
Woessner 84	2/21/1984	3247.24
Woessner 84	3/20/1984	3248.38
Woessner 84	5/3/1984	3248.76
Woessner 84	5/29/1984	3249.60
Woessner 84	6/26/1984	3250.68
HLA	5/22/1985	3250.13
HLA	5/4/1986	3247.13
HLA	6/22/1986	3246.83
HLA	7/16/1986	3243.23
ENSR	6/1/1990	3253.35
ENSR	9/1/1990	3247.48
ENSR	6/1/1991	3254.26
Gestring	5/1/1992	3251.85
ENSR	5/1/1992	3249.85
Gestring	4/6/1993	3245.55
Gestring	5/7/1993	3247.58
Gestring	6/4/1993	3251.22
Gestring	7/7/1993	3249.81
State	6/18/1998	3251.67
State	12/10/1998	3246.19
State	6/1/1999	3251.75
State	12/8/1999	3246.09
State	7/6/2000	3249.02
State	12/6/2000	3245.54
State	6/15/2001	3249.99
State	12/6/2001	3244.89
State	6/3/2002	3251.41
State	12/6/2002	3245.4
State	7/1/2004	3252.61
State	12/1/2004	3247.49

Well Number		105a
Woessner 84	11/3/1983	3245.81
Woessner 84	11/21/1983	3242.12
Woessner 84	6/25/1984	3249.34
HLA	5/22/1985	3248.73
HLA	5/4/1986	3245.53
HLA	6/22/1986	3245.13
HLA	7/16/1986	3243.53
ENSR	6/1/1990	3251.61
ENSR	9/1/1990	3245.89
ENSR	6/1/1991	3252.47
Gestring	11/6/1992	3243.80
Gestring	12/7/1992	3245.47
Gestring	1/4/1993	3244.99
Gestring	2/5/1993	3242.72
Gestring	3/6/1993	3242.11
Gestring	4/6/1993	3243.85
Gestring	5/7/1993	3245.99
Gestring	6/4/1993	3249.62
Gestring	7/7/1993	3248.23
State	6/15/1998	3250.01
State	12/9/1998	3244.68
State	6/1/1999	3250.09
State	12/7/1999	3244.53
State	6/30/2000	3247.46
State	12/5/2000	3244.02
State	6/18/2001	3248.37
State	12/5/2001	3248.37
State	6/3/2002	3249.6
State	12/6/2002	3243.83
State	7/21/2003	3248.62
State	1/2/2004	3244.92
State	6/28/2004	3248.78
State	12/1/2004	3244.47
State	6/15/2005	3251.17
State	12/1/2005	3239.12

Well Number		108a
Woessner 84	11/21/1983	3238.25
Woessner 84	6/25/1984	3245.10
HLA	5/22/1985	3244.33
HLA	5/4/1986	3241.53
HLA	6/22/1986	3241.13
HLA	7/16/1986	3239.53
ENSR	6/1/1990	3247.05
ENSR	9/1/1990	3241.61
ENSR	6/1/1991	3247.89
Gestring	5/1/1992	3244.11
ENSR	5/1/1992	3244.11
Gestring	10/8/1992	3240.41
Gestring	11/6/1992	3241.78
Gestring	12/7/1992	3242.48
Gestring	1/4/1993	3240.58
Gestring	2/5/1993	3238.64
Gestring	3/6/1993	3237.97
Gestring	4/6/1993	3239.18
Gestring	5/7/1993	3241.33
Gestring	6/4/1993	3245.12
Gestring	7/7/1993	3243.85
State	6/11/1998	3245.49
State	12/7/1998	3240.74
State	6/1/1999	3245.86
State	12/1/1999	3240.39
State	6/28/2000	3242.99
State	11/30/2000	3240.04
State	6/13/2001	3243.51
State	11/29/2001	3238.93
State	6/3/2002	3244.58
State	12/6/2002	3240.24
State	7/15/2003	3243.68
State	1/2/2004	3239.31
State	6/21/2004	3244.31
State	12/1/2004	3240.53
State/Tallman	6/7/2005	3246.53
State	11/28/2005	3235.19

Well Number		109a
Woessner 84	11/21/1983	3240.04
Woessner 84	6/25/1984	3239.15
HLA	5/22/1985	3238.73
HLA	5/4/1986	3236.03
HLA	6/22/1986	3235.43
HLA	7/16/1986	3233.93
ENSR	6/1/1990	3241.38
ENSR	9/1/1990	3235.95
ENSR	6/1/1991	3241.51
Gestring	5/1/1992	3237.91
ENSR	5/1/1992	3237.91
Gestring	10/8/1992	3234.57
Gestring	11/6/1992	3234.06
Gestring	12/7/1992	3234.41
Gestring	1/4/1993	3234.58
Gestring	2/5/1993	3233.42
Gestring	3/6/1993	3233.22
Gestring	4/6/1993	3233.11
Gestring	5/7/1993	3235.33
Gestring	6/4/1993	3239.04
Gestring	7/7/1993	3237.91

Well Number		110a
Woessner 84	11/21/1983	3253.89
Woessner 84	3/20/1984	3257.01
Woessner 84	6/26/1984	3261.29
HLA	5/22/1985	3257.83
HLA	5/4/1986	3255.43
HLA	6/22/1986	3255.13
HLA	7/16/1986	3254.23
ENSR	6/1/1990	3260.77
ENSR	9/1/1990	3256.23
ENSR	6/1/1991	3259.32
Gestring	5/1/1992	3257.34
ENSR	5/1/1992	3257.14
Gestring	4/6/1993	3255.63
Gestring	5/7/1993	3256.27
Gestring	6/4/1993	3257.87
Gestring	7/7/1993	3257.20
State	6/18/1998	3258.06
State	12/14/1998	3255.41
State	6/1/1999	3257.64
State	12/8/1999	3255.49
State	7/7/2000	3257.68
State	12/7/2000	3255.4
State	6/28/2001	3254.94
State	12/5/2001	3254.94
State	6/3/2002	3257.91
State	12/6/2002	3254.95
State	7/15/2003	
State	1/2/2004	
State	6/29/2004	3257.51
State	12/1/2004	3257.78
State	6/13/2005	3258.68
State	12/1/2005	3252.28

Well Number		111a
Woessner 84	11/21/1983	3243.95
Woessner 84	3/21/1984	3248.9
Woessner 84	6/26/1984	3251.15
HLA	5/22/1985	3250.73
HLA	5/4/1986	3247.73
HLA	6/22/1986	3247.03
HLA	7/16/1986	3245.23
ENSR	6/1/1990	3253.56
ENSR	9/1/1990	3247.82
ENSR	6/1/1991	3254.52
Gestring	5/1/1992	3250.14
ENSR	5/1/1992	3250.14
Gestring	4/6/1993	3245.42
Gestring	5/7/1993	3246.88
Gestring	6/4/1993	3251.5
Gestring	7/7/1993	3250.05
State	6/29/2001	3253.65
State	11/29/2001	3248.65
State	6/3/2002	3256.33
State	12/6/2002	3249.15
State	7/17/2003	3253.08
State	1/2/2004	3249.53
State	6/23/2004	3254.07
State	12/1/2004	3249.95
State	6/8/2005	3256.55
State	11/30/2005	3244.67

Well Number		901.00
ENSR	9/1/1990	3256.51
ENSR	6/1/1991	3259.77
ENSR	10/1/1991	3255.76
ENSR	5/1/1992	3257.65

Well Number		903.00
ENSR	9/1/1990	3258.69
ENSR	6/1/1991	3260.21
ENSR	10/1/1991	3257.96
ENSR	5/1/1992	3259.47

Well Number		917a
ENSR	6/1/1991	3237.61
ENSR	8/1/1991	3233.41
ENSR	10/1/1991	3232.33
Gestring	5/1/1992	3234.87
ENSR	5/1/1992	3234.87
Gestring	10/8/1992	3230.87
Gestring	11/6/1992	3232.21
Gestring	12/7/1992	3230.36
Gestring	1/4/1993	3232.33
Gestring	2/5/1993	3229.41
Gestring	3/6/1993	3228.38
Gestring	4/6/1993	3229.00
Gestring	5/7/1993	3231.23
Gestring	6/4/1993	3235.35
Gestring	7/7/1993	3234.13
State	6/12/1998	3236.39
State	12/15/1998	3230.94
State	6/1/1999	3235.88
State	12/10/1999	3230.53
State	7/7/2000	3232.87
State	12/8/2000	3230.05
State	6/28/2001	3229.05
State	12/7/2001	3229.05
State	6/3/2002	3233.95
State	12/6/2002	3230.59
State	7/15/2003	3234.5
State	1/2/2004	3230.39
State/Tallman	6/30/2004	3235.01
State	12/1/2004	3231.77
State	6/14/2005	3237.8
State	12/6/2005	3223.59

Appendix B
Peak Lag Results

Peak Lag analyses calculations are presented in the attached CD-ROM.

Pinder et al. (1969) derived a method to use river stage and corresponding groundwater level changes to estimate intervening hydraulic conductivities. The method was applied to evaluate the lag response between up-gradient wells and down-gradient wells along a common flow path:

$$h_p = \sum_{m=1}^{p} \Delta H_m \left\{ erfc \frac{u}{2\sqrt{p-m}} \right\} \quad (1)$$

where: the change in hydraulic head is represented by h_p; the change in the upgradient well water level for every time interval as ΔH_m; u can be calculated by the equation:

$$u = \frac{x}{\sqrt{v\Delta t}} \quad (2)$$

where: x is the distance between the wells; Δt is the time interval; v is the diffusivity (transmissivity divided by the aquifer storativity).

Water Level Elevation Data (ft, NAVD 88) for wells in the West Riverside Area

	Db-205	HG-23	Routh_db-079	HG-27
12/3/06 0:00	3222.50671	3218.80061	3217.67951	3212.17481
12/4/06 0:00	3222.5824	3218.8715	3217.7285	3212.2192
12/5/06 0:00	3222.65888	3218.94538	3217.78808	3212.27758
12/6/06 0:00	3222.76655	3219.05525	3217.88915	3212.37185
12/7/06 0:00	3222.86826	3219.14646	3217.95026	3212.42886
12/8/06 0:00	3222.9607	3219.2328	3218.01	3212.4757
12/9/06 0:00	3223.03865	3219.30285	3218.05815	3212.51955
12/10/06 0:00	3223.1194	3219.3836	3218.1314	3212.6001
12/11/06 0:00	3223.17479	3219.44259	3218.19119	3212.64399
12/12/06 0:00	3223.24443	3219.49993	3218.21113	3212.66033
12/13/06 0:00	3223.27666	3219.53086	3218.22716	3212.67136
12/14/06 0:00	3223.32129	3219.57479	3218.27129	3212.71099
12/15/06 0:00	3223.37105	3219.60655	3218.26805	3212.71655
12/16/06 0:00	3223.38169	3219.64169	3218.35299	3212.79789
12/17/06 0:00	3223.39315	3219.64505	3218.34585	3212.79415
12/18/06 0:00	3223.36218	3219.62018	3218.34018	3212.77748
12/19/06 0:00	3223.3184	3219.5682	3218.2691	3212.7199
12/20/06 0:00	3223.26142	3219.51362	3218.22862	3212.66722
12/21/06 0:00	3223.22575	3219.47645	3218.18055	3212.62195
12/22/06 0:00	3223.19338	3219.44478	3218.15368	3212.59238
12/23/06 0:00	3223.20016	3219.44996	3218.15106	3212.58696
12/24/06 0:00	3223.04073	3219.47653	3218.18463	3212.61393
12/25/06 0:00	3223.28875	3219.52195	3218.17875	3212.61155
12/26/06 0:00	3223.35976	3219.59136	3218.23636	3212.67886

Groundwater Hydrographs for wells used in the analysis for wells in the West Riverside area.

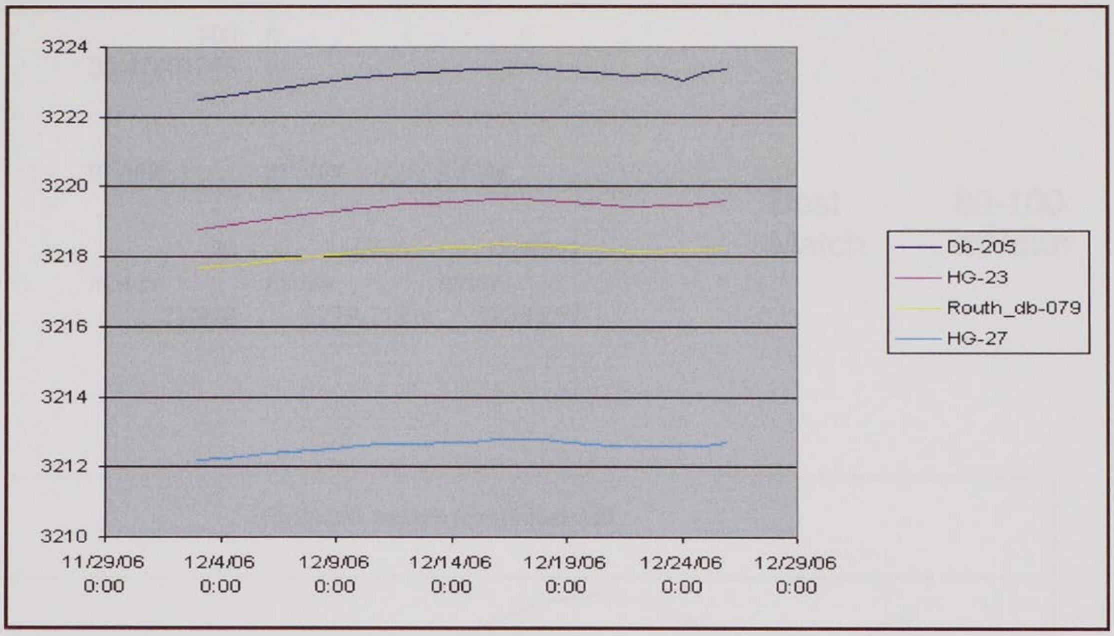

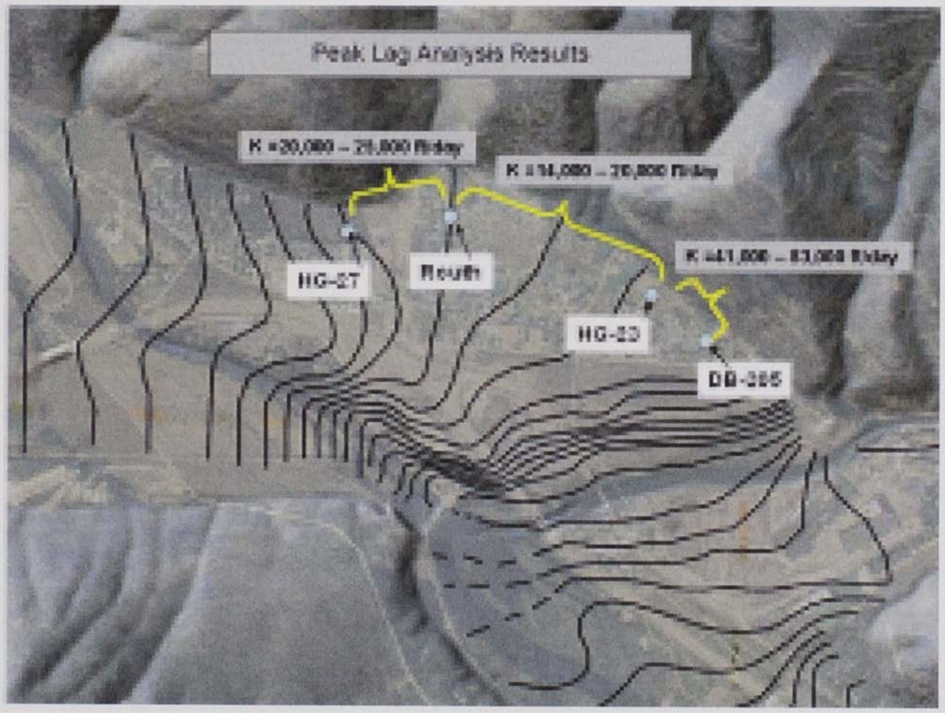

Well HG-23

Aquifer Thickness (b)=	100	ft	
	30.47851265	m	
	m^2/min	m^2/day	ft^2/day
T=	80	115200	1239552
	m/min	m/day	ft/day
K=	2.6248	3779.712	12395.52

Best Match 80-100 **m^2/min**

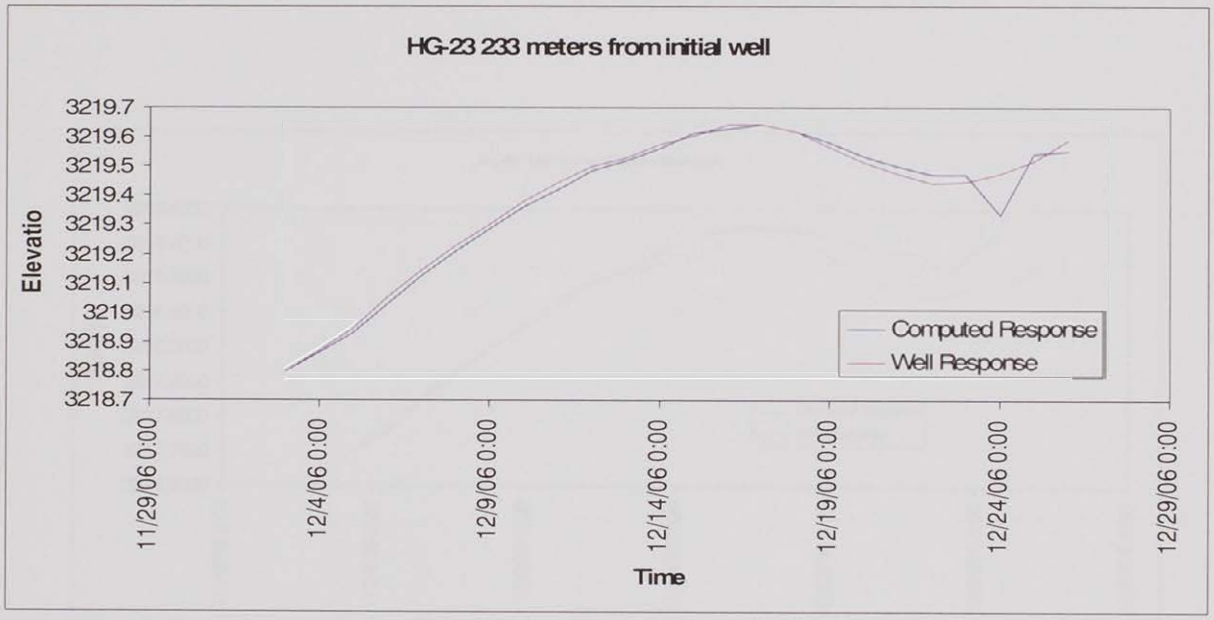

Well: Routh

Aquifer Thickness (b)=	100	ft	
	30.47851265	m	
	m^2/min	m^2/day	ft^2/day
T=	80	115200	1239552
	m/min	m/day	ft/day
K=	2.6248	3779.712	12395.52

Best Match **60-80 m^2/min**

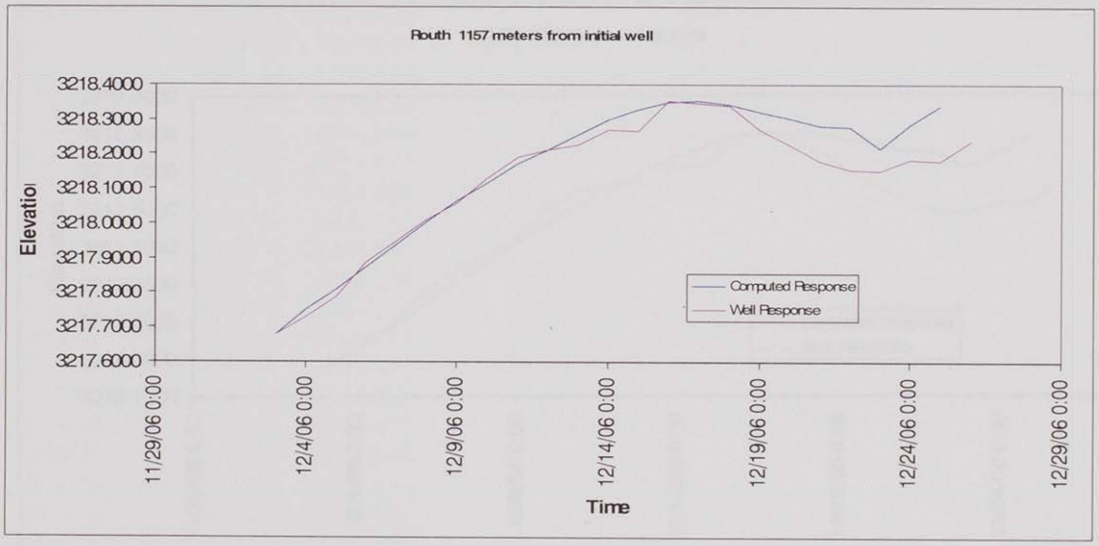

Well: HG-27

Aquifer Thickness (b)=	100	ft	
	30.47851265	m	
	70-90		
	m^2/min	m^2/day	ft^2/day
T=	90	129600	1394496
	m/min	m/day	ft/day
K=	2.9529	4252.176	13944.96

Best Match **70-90 m^2/min**

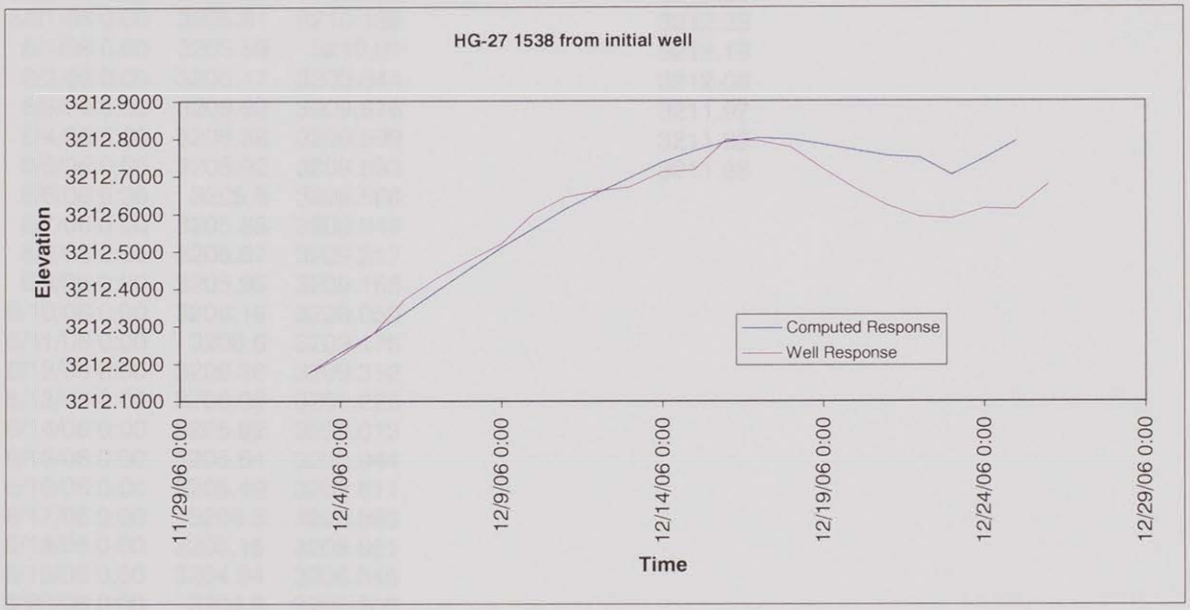

Water Level Elevation Data (ft, NAVD 88) for wells in the Bandman Flats area

date	river	mw-6	mw-7
5/13/06 0:00	3205.34	3207.915	3210.69
5/14/06 0:00	3205.44	3207.907	3210.69
5/15/06 0:00	3205.7	3207.919	3210.72
5/16/06 0:00	3206.22	3208.011	3210.81
5/17/06 0:00	3206.98	3208.226	3211.01
5/18/06 0:00	3207.66	3208.631	3211.25
5/19/06 0:00	3208.09	3209.08	3211.51
5/20/06 0:00	3208.32	3209.506	3211.76
5/21/06 0:00	3208.37	3209.863	3211.99
5/22/06 0:00	3208.11	3210.116	3212.11
5/23/06 0:00	3207.79	3210.267	3212.21
5/24/06 0:00	3207.6	3210.371	3212.34
5/25/06 0:00	3207.23	3210.48	3212.44
5/26/06 0:00	3207.09	3210.509	3212.50
5/27/06 0:00	3207.04	3210.502	3212.53
5/28/06 0:00	3206.76	3210.48	3212.48
5/29/06 0:00	3206.45	3210.367	3212.43
5/30/06 0:00	3206.18	3210.25	3212.36
5/31/06 0:00	3205.81	3210.138	3212.28
6/1/06 0:00	3205.59	3210.01	3212.19
6/2/06 0:00	3205.47	3209.844	3212.08
6/3/06 0:00	3205.62	3209.676	3211.97
6/4/06 0:00	3205.88	3209.599	3211.93
6/5/06 0:00	3205.92	3209.593	3211.88
6/6/06 0:00	3205.8	3209.568	
6/7/06 0:00	3205.65	3209.348	
6/8/06 0:00	3205.67	3209.217	
6/9/06 0:00	3205.95	3209.168	
6/10/06 0:00	3206.16	3209.059	
6/11/06 0:00	3206.6	3209.175	
6/12/06 0:00	3206.36	3209.312	
6/13/06 0:00	3206.02	3209.225	
6/14/06 0:00	3205.82	3209.013	
6/15/06 0:00	3205.64	3208.944	
6/16/06 0:00	3205.49	3208.811	
6/17/06 0:00	3205.3	3208.693	
6/18/06 0:00	3205.15	3208.661	
6/19/06 0:00	3204.94	3208.349	
6/20/06 0:00	3204.8	3208.208	
6/21/06 0:00	3204.64	3208.092	
6/22/06 0:00	3204.45	3207.953	
6/23/06 0:00	3204.31	3207.757	
6/24/06 0:00	3204.17	3207.64	
6/25/06 0:00	3204.06	3207.492	
6/26/06 0:00	3203.95	3207.257	
6/27/06 0:00	3203.86	3206.875	
6/28/06 0:00	3203.78	3206.569	
6/29/06 0:00	3203.7	3206.471	
6/30/06 0:00	3203.68	3206.405	
7/1/06 0:00	3203.66	3206.183	

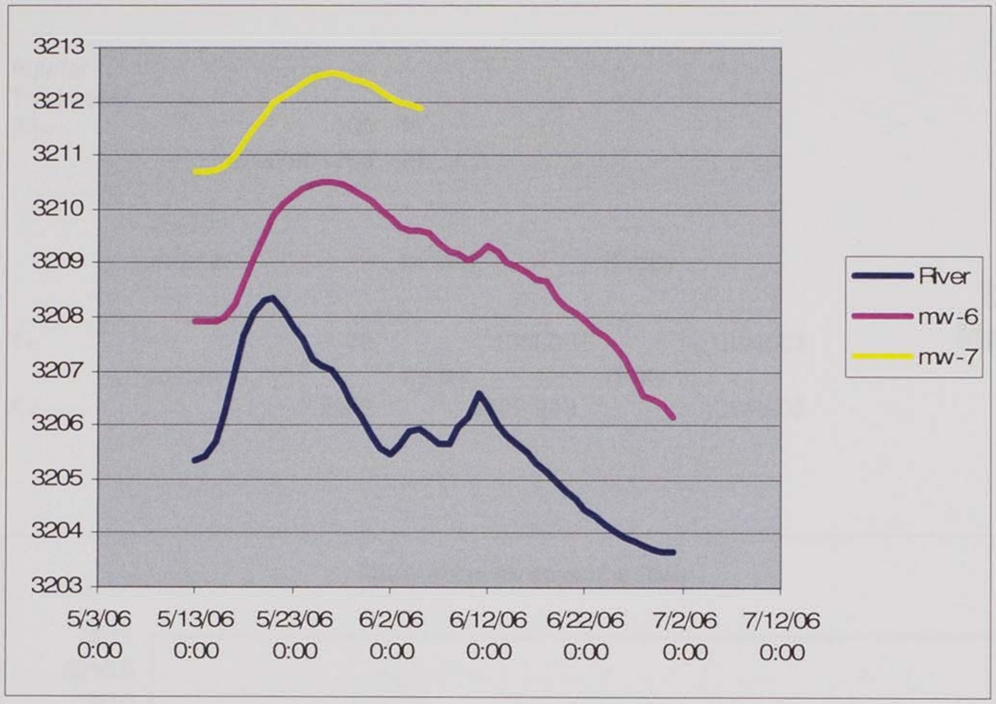

3213
3212
3211
3210
3209
3208
3207
3206
3205
3204
3203
5/3/06 0:00
5/13/06 0:00
5/23/06 0:00
6/2/06 0:00
6/12/06 0:00
6/22/06 0:00
7/2/06 0:00
7/12/06 0:00
River
mw-6
mw-7

Well: MW-6

Aquifer Thickness (b)=		100	ft	
		30.47851265	m	
	25-70			
	m^2/min		m^2/day	ft^2/day
T=		70	100800	1084608
	m/min		m/day	ft/day
K=		2.2967	3307.248	10846.08

Best Match 25-70 m^2/min

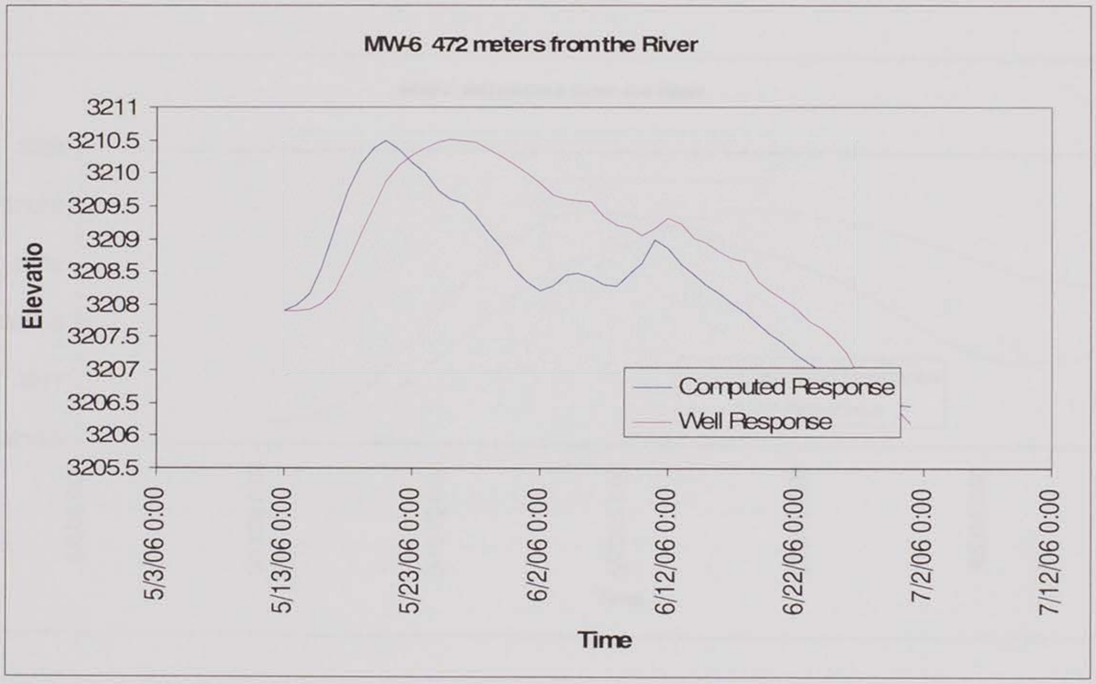

Well: MW-7

Aquifer Thickness (b)=	100		ft	
	30.47851265		m	
	2-2.5			
	m^2/min		m^2/day	ft^2/day
T=		2	2880	30988.8
	m/min		m/day	ft/day
K=		0.06562	94.4928	309.888

Best Match 2-2.5 m^2/min

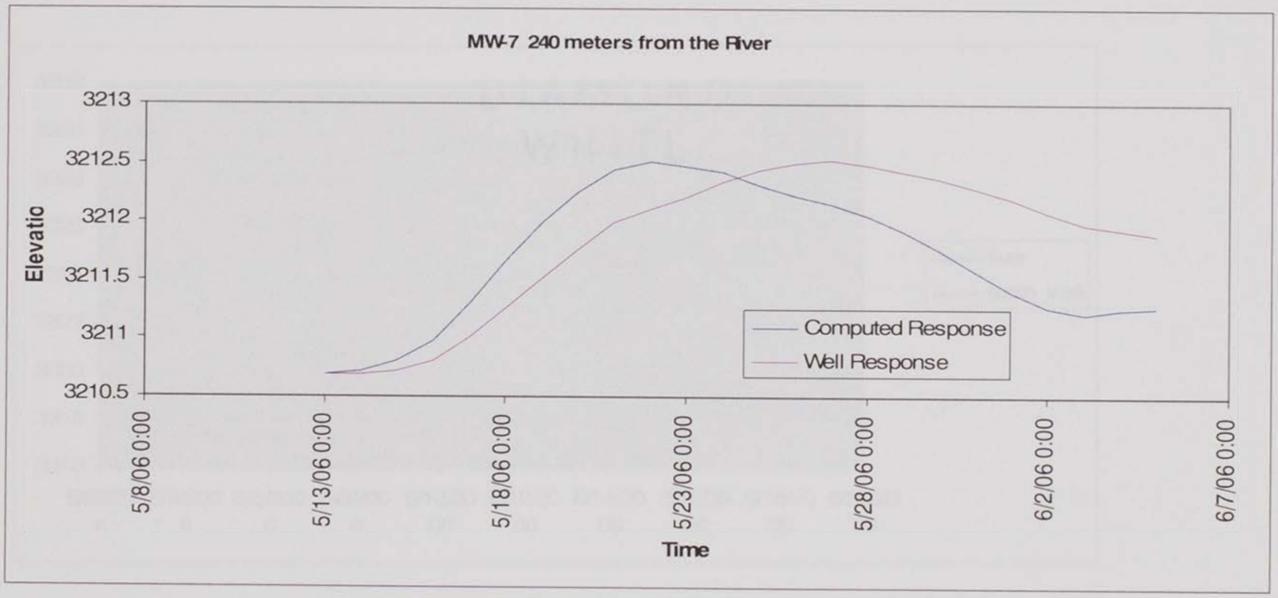

Water Level Elevation Data (ft, NAVD 88) for wells in the Turah area

date	River	Rodin
6/3/2006	3328.74	3317.398
6/4/2006	3328.84	3317.364
6/5/2006	3328.91	3317.369
6/6/2006	3328.85	3317.406
6/7/2006	3328.77	3317.28
6/8/2006	3328.81	3317.16
6/9/2006	3329.08	3317.32
6/10/2006	3329.27	3317.34
6/11/2006	3329.61	3317.73
6/12/2006	3329.44	3317.92
6/13/2006	3329.2	3317.85
6/14/2006	3329.01	3317.65
6/15/2006	3328.9	3317.57
6/16/2006	3328.81	3317.51
6/17/2006	3328.7	3317.42
6/18/2006	3328.61	3317.47

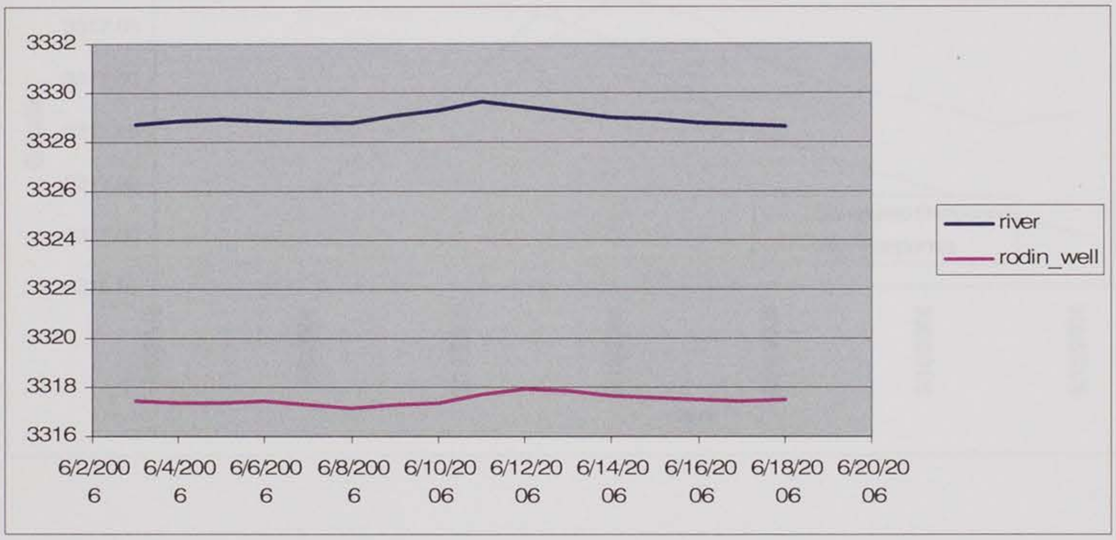

Well: Routh

Aquifer Thickness (b)=	200		ft
	60.9570253		m
	m^2/min	m^2/day	ft^2/day
T=	50	72000	774720
	m/min	m/day	ft/day
K=	0.82025	1181.16	3873.6

Best Match 50 m^2/min

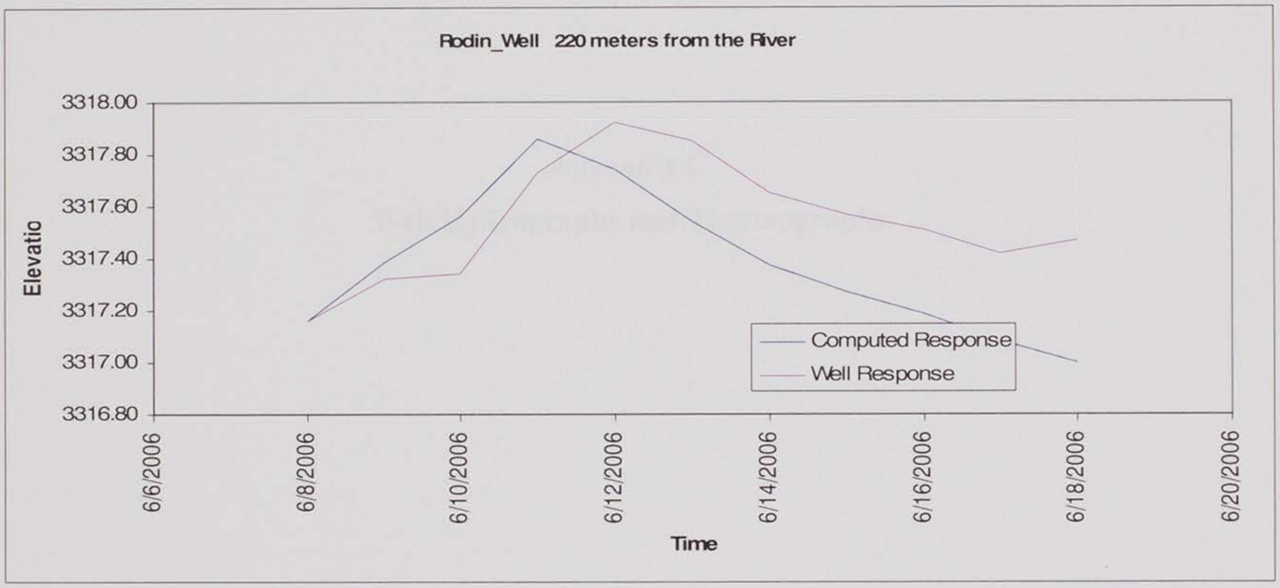

Appendix C

Well Hydrographs and Thermographs

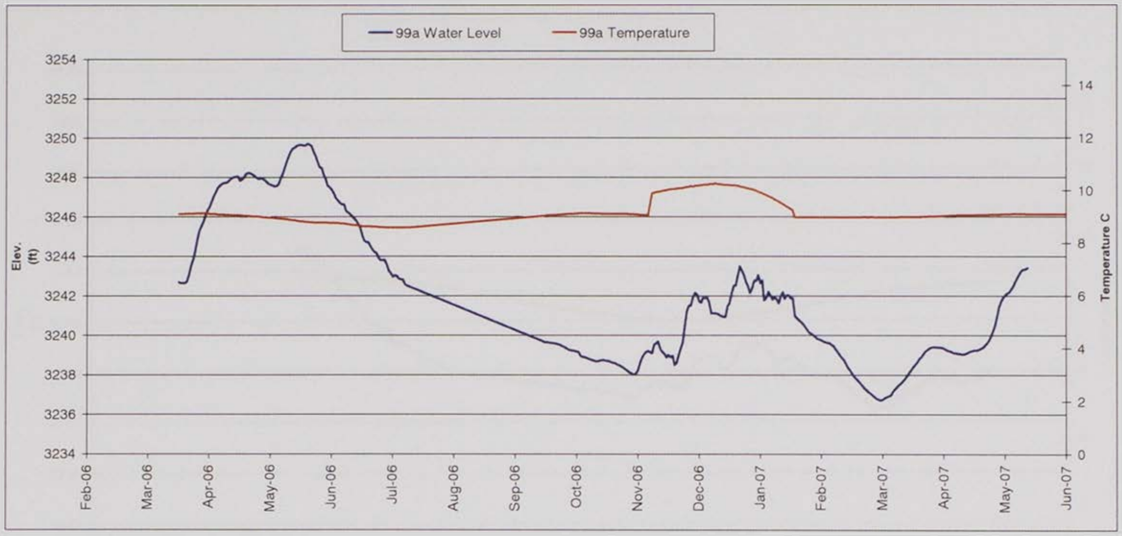

99a Water Level
99a Temperature
Elev. (ft)
Temperature C
3254
3252
3250
3248
3246
3244
3242
3240
3238
3236
3234
14
12
10
8
6
4
2
0
Feb-06
Mar-06
Apr-06
May-06
Jun-06
Jul-06
Aug-06
Sep-06
Oct-06
Nov-06
Dec-06
Jan-07
Feb-07
Mar-07
Apr-07
May-07
Jun-07

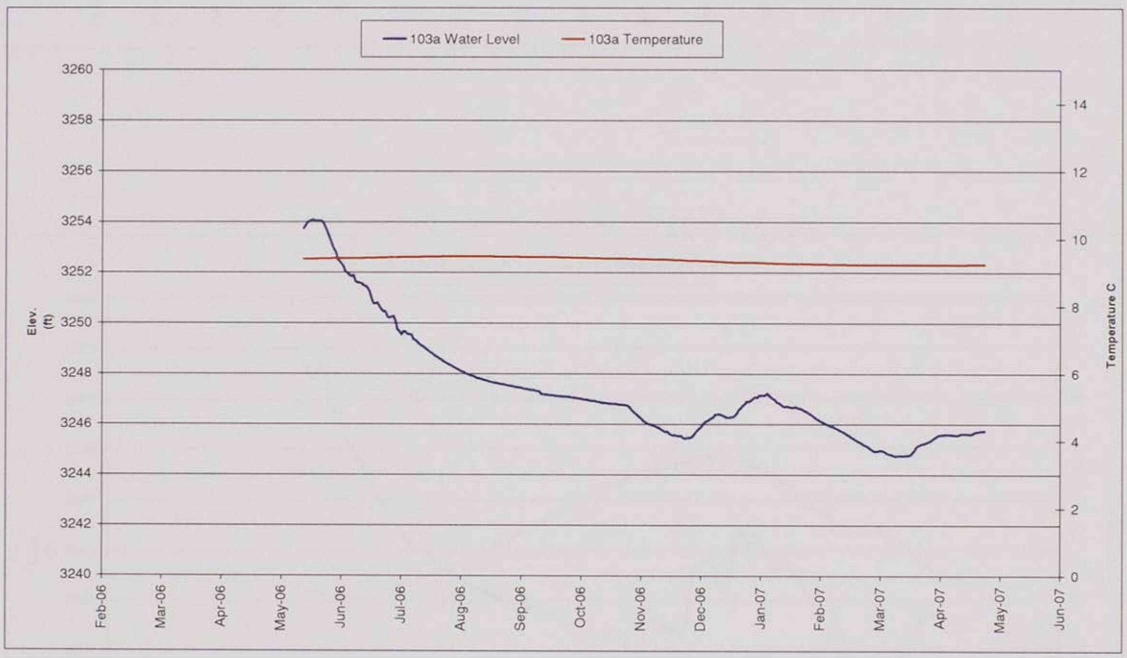

103a Water Level
103a Temperature
Elev. (ft)
Temperature C
3260
3258
3256
3254
3252
3250
3248
3246
3244
3242
3240
14
12
10
8
6
4
2
0
Feb-06
Mar-06
Apr-06
May-06
Jun-06
Jul-06
Aug-06
Sep-06
Oct-06
Nov-06
Dec-06
Jan-07
Feb-07
Mar-07
Apr-07
May-07
Jun-07

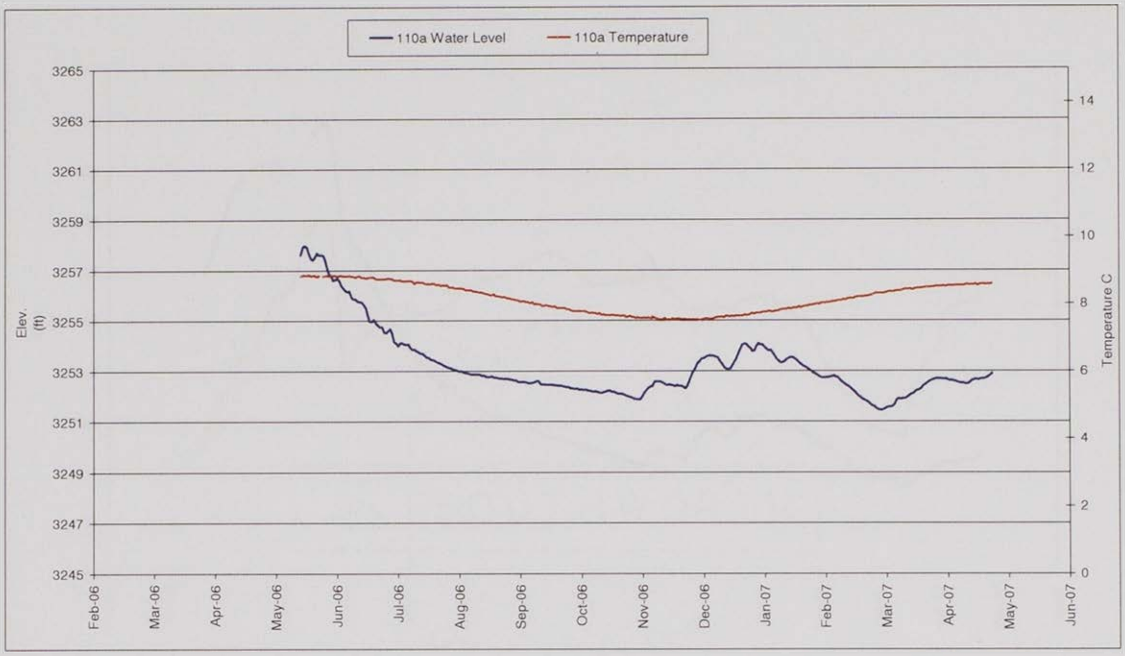
110a Water Level
110a Temperature
Elev. (ft)
Temperature C
3265
3263
3261
3259
3257
3255
3253
3251
3249
3247
3245
14
12
10
8
6
4
2
0
Feb-06
Mar-06
Apr-06
May-06
Jun-06
Jul-06
Aug-06
Sep-06
Oct-06
Nov-06
Dec-06
Jan-07
Feb-07
Mar-07
Apr-07
May-07
Jun-07

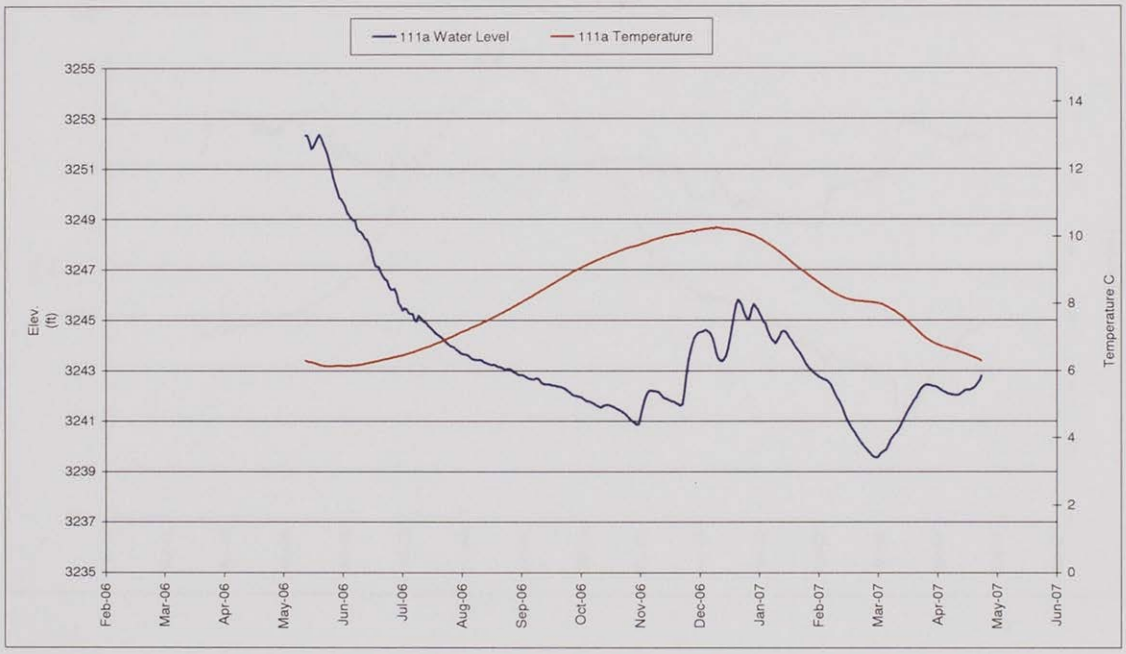
111a Water Level
111a Temperature
Elev. (ft)
Temperature C
3255
3253
3251
3249
3247
3245
3243
3241
3239
3237
3235
14
12
10
8
6
4
2
0
Feb-06
Mar-06
Apr-06
May-06
Jun-06
Jul-06
Aug-06
Sep-06
Oct-06
Nov-06
Dec-06
Jan-07
Feb-07
Mar-07
Apr-07
May-07
Jun-07

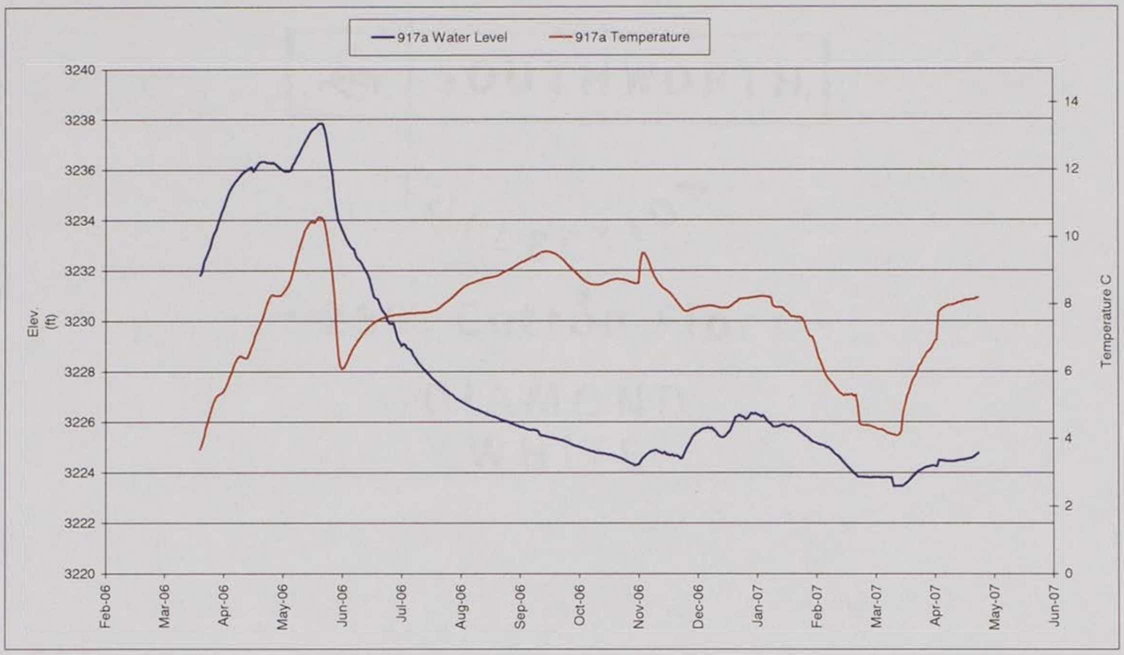

917a Water Level
917a Temperature
Elev. (ft)
Temperature C
3240
3238
3236
3234
3232
3230
3228
3226
3224
3222
3220
14
12
10
8
6
4
2
0
Feb-06
Mar-06
Apr-06
May-06
Jun-06
Jul-06
Aug-06
Sep-06
Oct-06
Nov-06
Dec-06
Jan-07
Feb-07
Mar-07
Apr-07
May-07
Jun-07

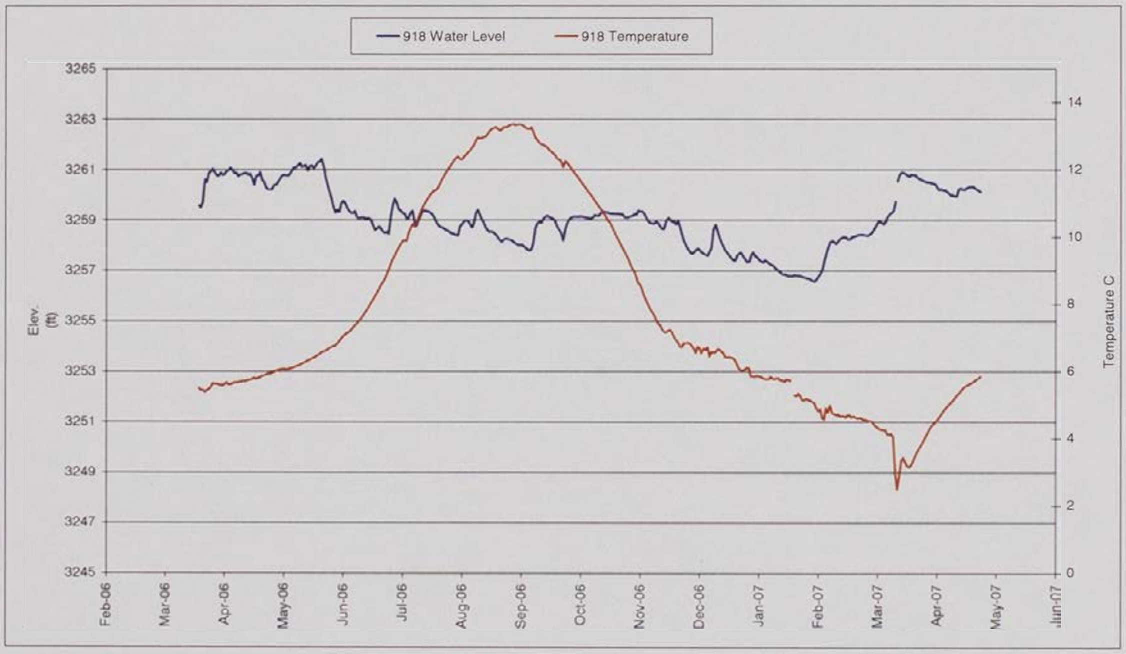

918 Water Level
918 Temperature
Elev. (ft)
Temperature C
3265
3263
3261
3259
3257
3255
3253
3251
3249
3247
3245
14
12
10
8
6
4
2
0
Feb-06
Mar-06
Apr-06
May-06
Jun-06
Jul-06
Aug-06
Sep-06
Oct-06
Nov-06
Dec-06
Jan-07
Feb-07
Mar-07
Apr-07
May-07
Jun-07

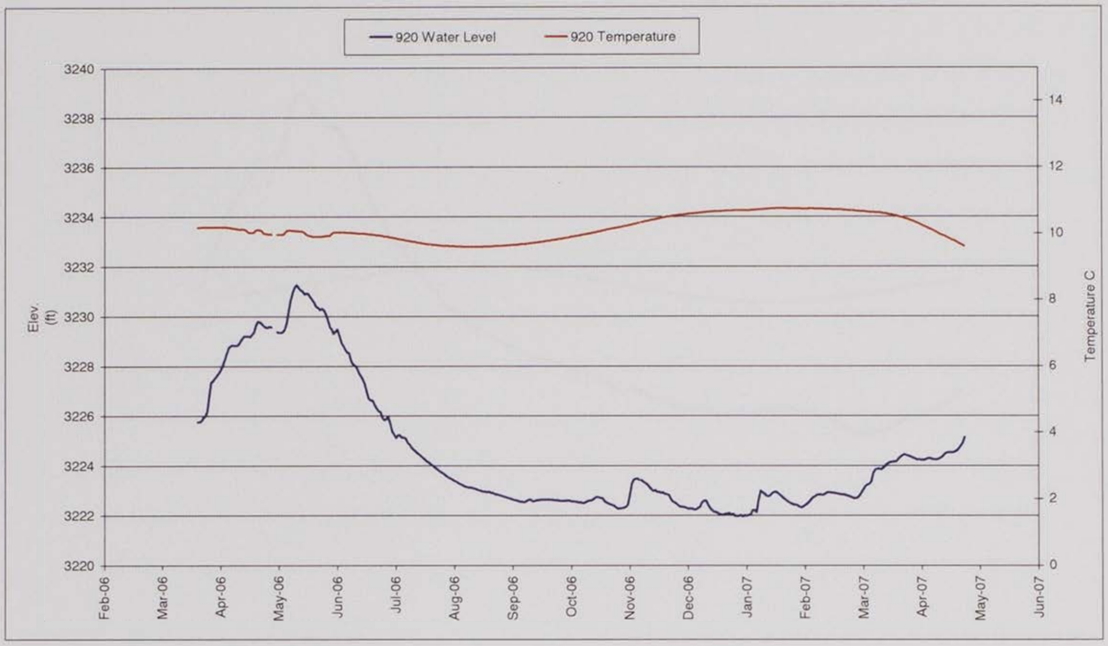

920 Water Level
920 Temperature
Elev. (ft)
Temperature C
3240
3238
3236
3234
3232
3230
3228
3226
3224
3222
3220
14
12
10
8
6
4
2
0
Feb-06
Mar-06
Apr-06
May-06
Jun-06
Jul-06
Aug-06
Sep-06
Oct-06
Nov-06
Dec-06
Jan-07
Feb-07
Mar-07
Apr-07
May-07
Jun-07

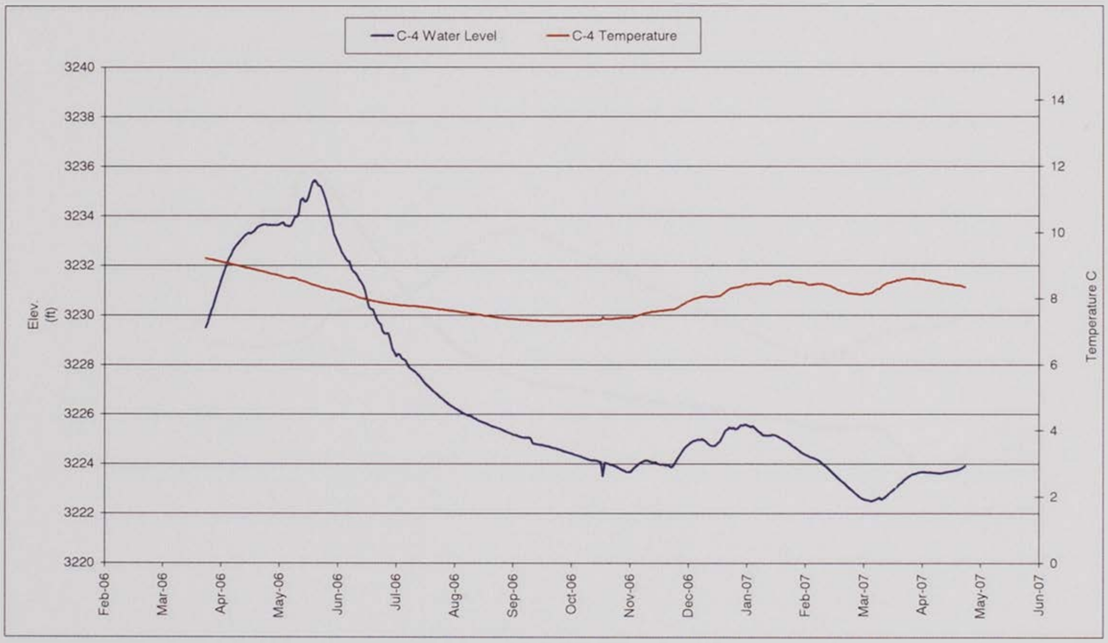

C-4 Water Level
C-4 Temperature
Elev. (ft)
Temperature C
3240
3238
3236
3234
3232
3230
3228
3226
3224
3222
3220
14
12
10
8
6
4
2
0
Feb-06
Mar-06
Apr-06
May-06
Jun-06
Jul-06
Aug-06
Sep-06
Oct-06
Nov-06
Dec-06
Jan-07
Feb-07
Mar-07
Apr-07
May-07
Jun-07

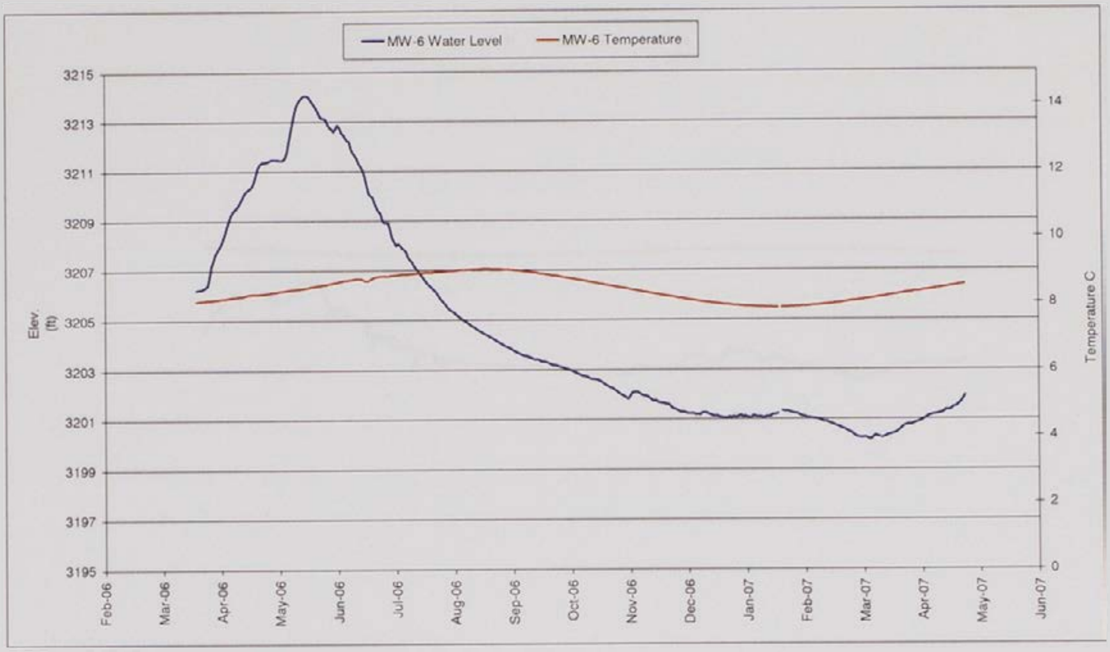
MW-6 Water Level
MW-6 Temperature
Elev. (ft)
Temperature C
3215
3213
3211
3209
3207
3205
3203
3201
3199
3197
3195
14
12
10
8
6
4
2
0
Feb-06
Mar-06
Apr-06
May-06
Jun-06
Jul-06
Aug-06
Sep-06
Oct-06
Nov-06
Dec-06
Jan-07
Feb-07
Mar-07
Apr-07
May-07
Jun-07

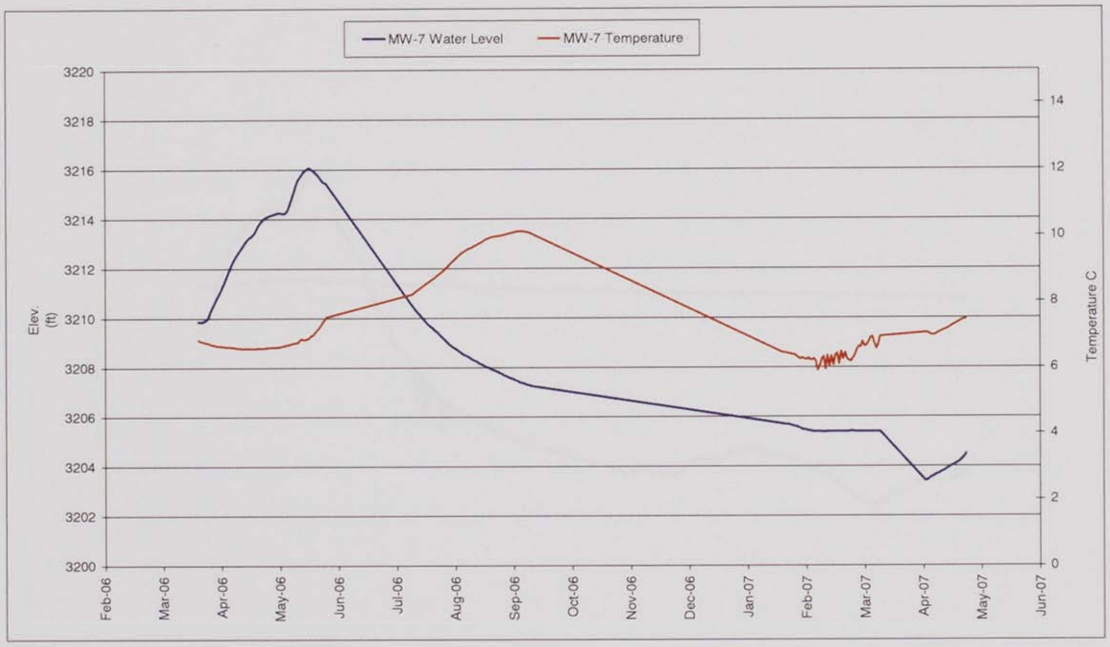
MW-7 Water Level
MW-7 Temperature
Elev. (ft)
Temperature C
3220
3218
3216
3214
3212
3210
3208
3206
3204
3202
3200
14
12
10
8
6
4
2
0
Feb-06
Mar-06
Apr-06
May-06
Jun-06
Jul-06
Aug-06
Sep-06
Oct-06
Nov-06
Dec-06
Jan-07
Feb-07
Mar-07
Apr-07
May-07
Jun-07

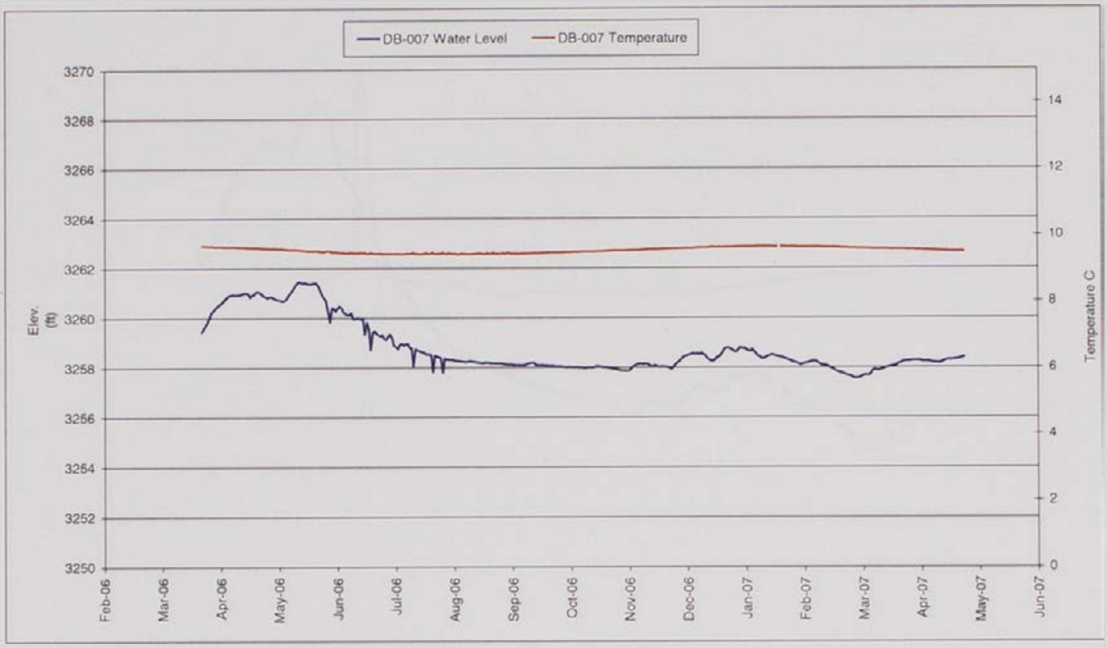

DB-007 Water Level
DB-007 Temperature
Elev. (ft)
Temperature C
3270
3268
3266
3264
3262
3260
3258
3256
3254
3252
3250
14
12
10
8
6
4
2
0
Feb-06
Mar-06
Apr-06
May-06
Jun-06
Jul-06
Aug-06
Sep-06
Oct-06
Nov-06
Dec-06
Jan-07
Feb-07
Mar-07
Apr-07
May-07
Jun-07

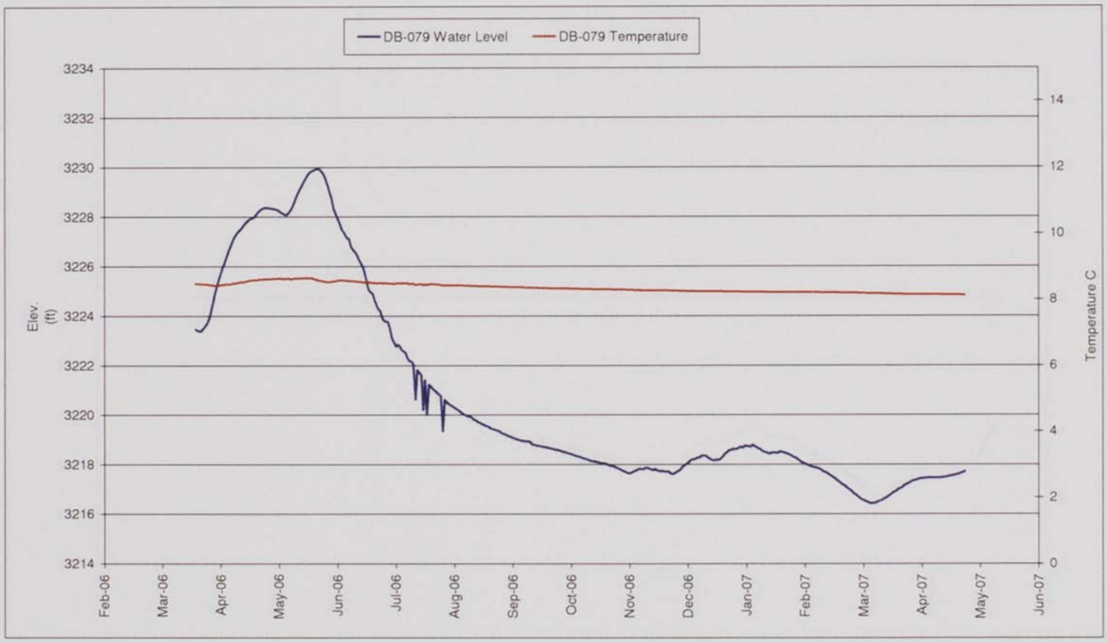

DB-079 Water Level
DB-079 Temperature
Elev. (ft)
Temperature C
3234
3232
3230
3228
3226
3224
3222
3220
3218
3216
3214
14
12
10
8
6
4
2
0
Feb-06
Mar-06
Apr-06
May-06
Jun-06
Jul-06
Aug-06
Sep-06
Oct-06
Nov-06
Dec-06
Jan-07
Feb-07
Mar-07
Apr-07
May-07
Jun-07

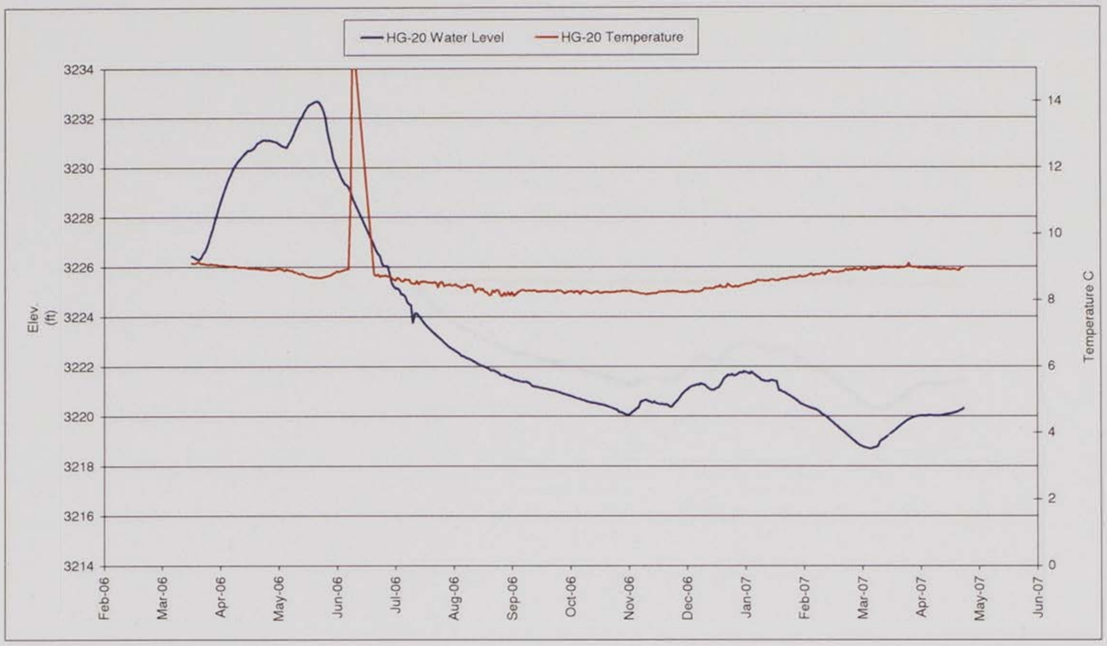

HG-20 Water Level
HG-20 Temperature
Elev. (ft)
Temperature C
3234
3232
3230
3228
3226
3224
3222
3220
3218
3216
3214
14
12
10
8
6
4
2
0
Feb-06
Mar-06
Apr-06
May-06
Jun-06
Jul-06
Aug-06
Sep-06
Oct-06
Nov-06
Dec-06
Jan-07
Feb-07
Mar-07
Apr-07
May-07
Jun-07

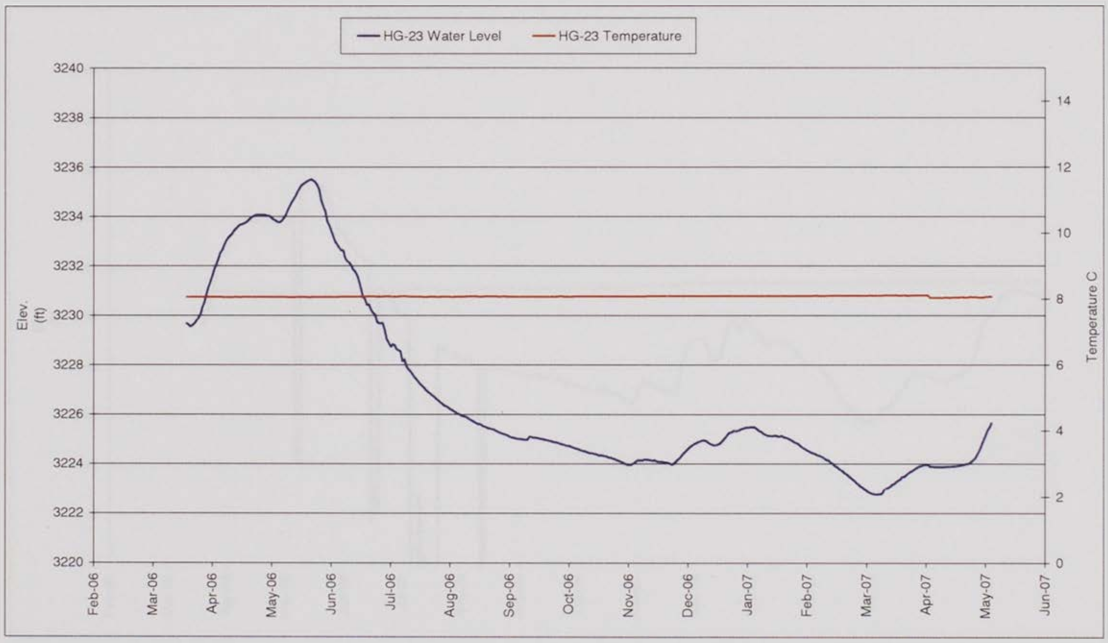

HG-23 Water Level
HG-23 Temperature
Elev. (ft)
Temperature C
3240
3238
3236
3234
3232
3230
3228
3226
3224
3222
3220
14
12
10
8
6
4
2
0
Feb-06
Mar-06
Apr-06
May-06
Jun-06
Jul-06
Aug-06
Sep-06
Oct-06
Nov-06
Dec-06
Jan-07
Feb-07
Mar-07
Apr-07
May-07
Jun-07

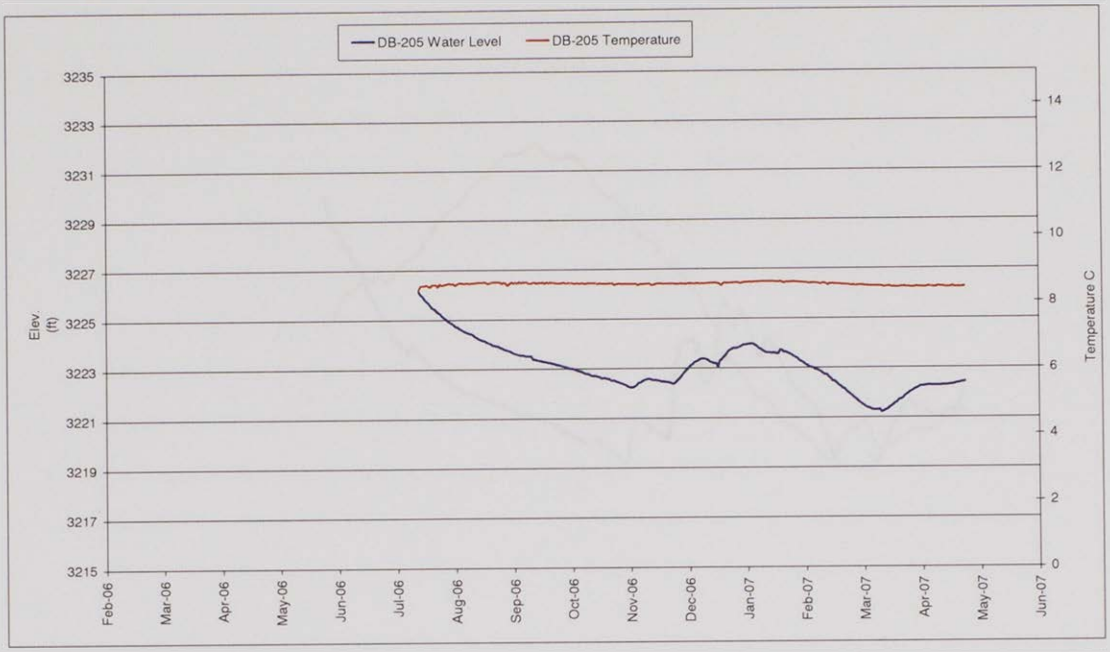
DB-205 Water Level
DB-205 Temperature
Elev. (ft)
Temperature C
3235
3233
3231
3229
3227
3225
3223
3221
3219
3217
3215
14
12
10
8
6
4
2
0
Feb-06
Mar-06
Apr-06
May-06
Jun-06
Jul-06
Aug-06
Sep-06
Oct-06
Nov-06
Dec-06
Jan-07
Feb-07
Mar-07
Apr-07
May-07
Jun-07

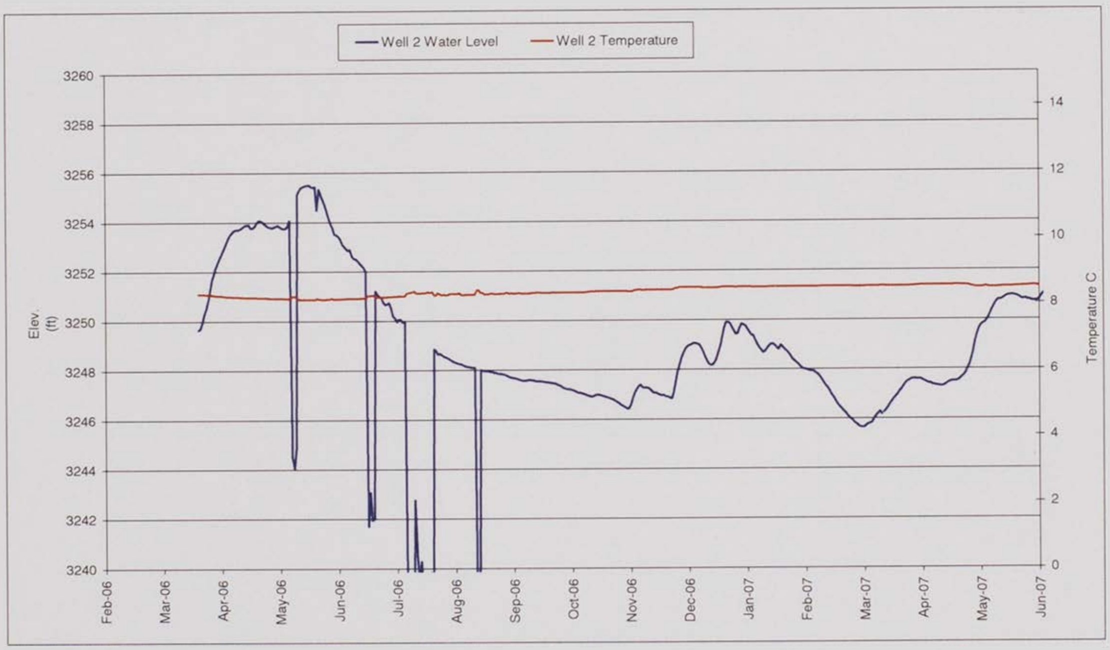
Well 2 Water Level
Well 2 Temperature
Elev. (ft)
Temperature C
3260
3258
3256
3254
3252
3250
3248
3246
3244
3242
3240
14
12
10
8
6
4
2
0
Feb-06
Mar-06
Apr-06
May-06
Jun-06
Jul-06
Aug-06
Sep-06
Oct-06
Nov-06
Dec-06
Jan-07
Feb-07
Mar-07
Apr-07
May-07
Jun-07

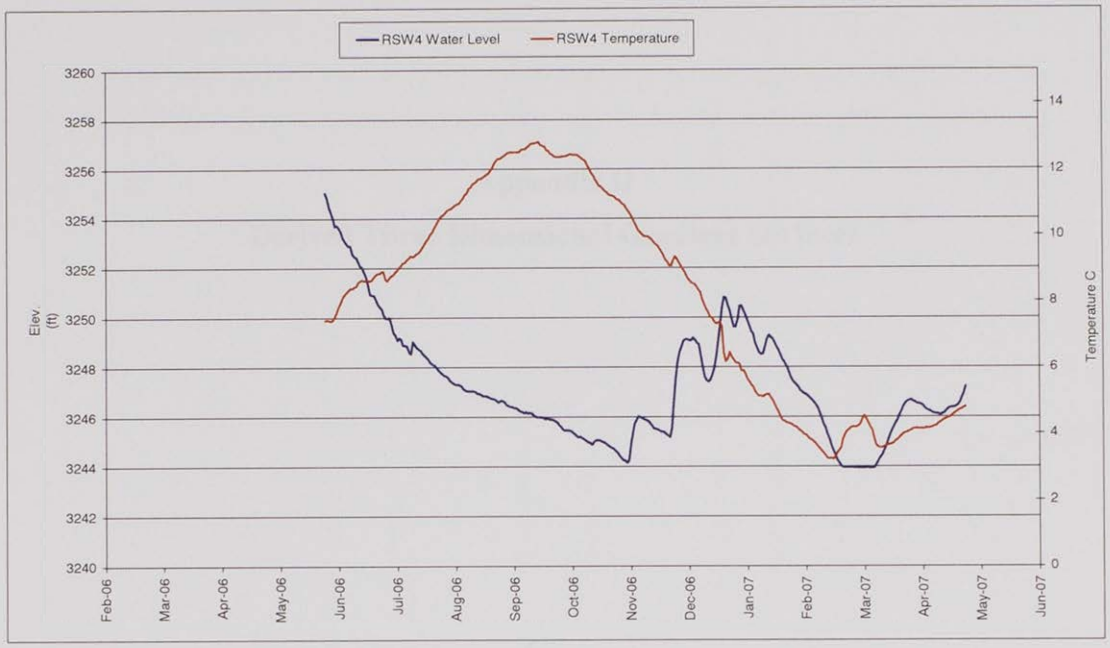
RSW4 Water Level
RSW4 Temperature
Elev. (ft)
Temperature C
3260
3258
3256
3254
3252
3250
3248
3246
3244
3242
3240
14
12
10
8
6
4
2
0
Feb-06
Mar-06
Apr-06
May-06
Jun-06
Jul-06
Aug-06
Sep-06
Oct-06
Nov-06
Dec-06
Jan-07
Feb-07
Mar-07
Apr-07
May-07
Jun-07

Appendix D
Derived Three Dimensional Gradient Surfaces

To establish gradients at exact depths of 1, 2 and 3 ft below the river bed, linear regressions were completed to establish estimated gradients. The data used to make correlations are attached on the CD-ROM.

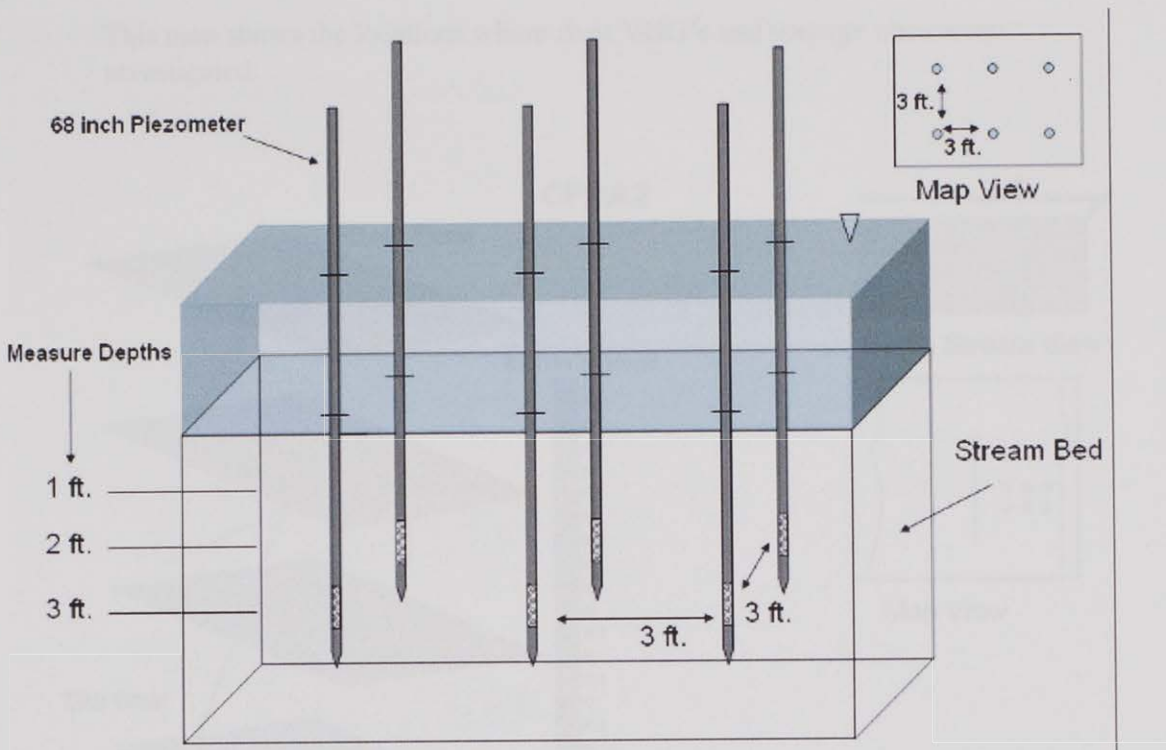
68 inch Piezometer
Map View
3 ft.
3 ft.
Measure Depths
1 ft.
2 ft.
3 ft.
3 ft.
3 ft.
Stream Bed

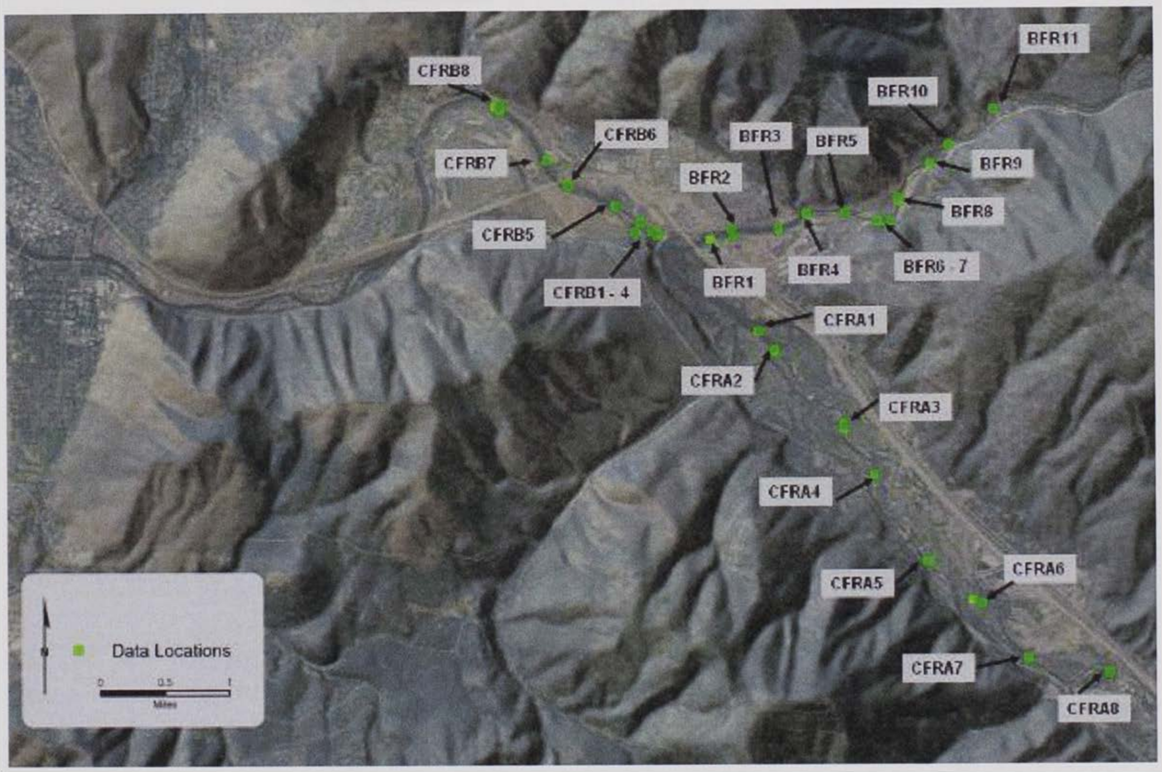
CFRB8
CFRB7
CFRB6
CFRB5
CFRB1 - 4
BFR1
BFR2
BFR3
BFR4
BFR5
BFR6 - 7
BFR8
BFR9
BFR10
BFR11
CFRA1
CFRA2
CFRA3
CFRA4
CFRA5
CFRA6
CFRA7
CFRA8
Data Locations

This map shows the locations where river VHG's and seepage rates were investigated.

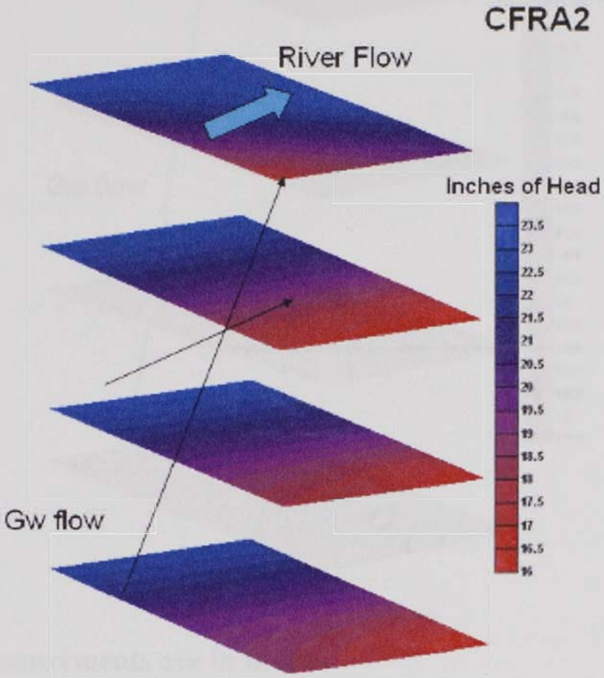

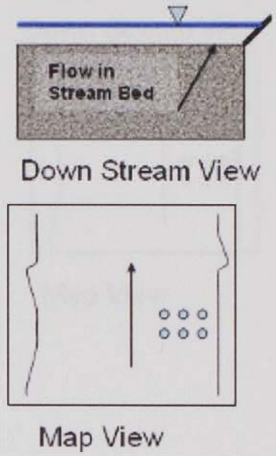

Measurements are in Inches

CFRA2											
1a		1b		1c		2a		2b		2c	
depth	wl	depth	wl	depth	wl	depth	wl	depth	wl	depth	wl
8.75	42.25	9.25	38.5	13	31.75	10.75	41.25	8.75	39.25	11	34
20.25	30.75	18.25	29.5	20.75	24.25	20.5	31.25	21.5	26.25	22.25	22
38	10.5	35.5	12	37	7.5	36.5	15	35.25	12.5	37	7.5

Normalized Depths			
	12	24	36
1a	39.10	26.02	12.93
1b	35.76	23.64	11.51
1c	32.91	20.75	8.58
2a	39.95	27.72	15.50
2b	35.93	23.81	11.70
2c	32.78	20.57	8.36

CFRA3

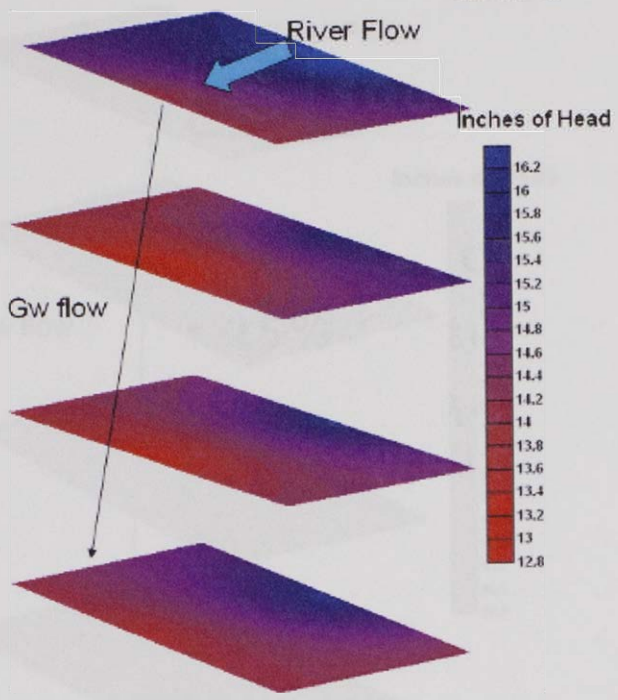

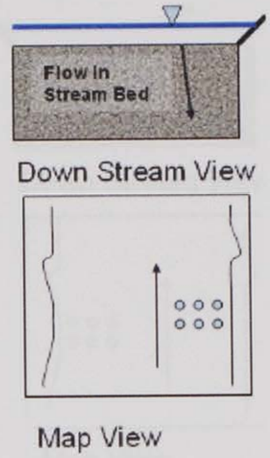

Measurements are in Inches

CFRA3											
1a		1b		1c		2a		2b		2c	
depth	wl	depth	wl	depth	wl	depth	wl	depth	wl	depth	wl
14.5	39.25	12	40.25	14	39	12	42	14.5	41.25	13.5	40
24	29.5	20	31.5	25	28	24	30	22	32.5	21	32.5
35.5	17.5	33.5	18.5	36	18	37	17	37	17.75	36	18

Normalized Depths			
	12	24	36
1a	41.87	29.44	17.01
1b	39.98	27.90	15.83
1c	40.74	29.29	17.84
2a	42.00	30.00	18.00
2b	43.45	31.02	18.59
2c	41.39	29.68	17.96

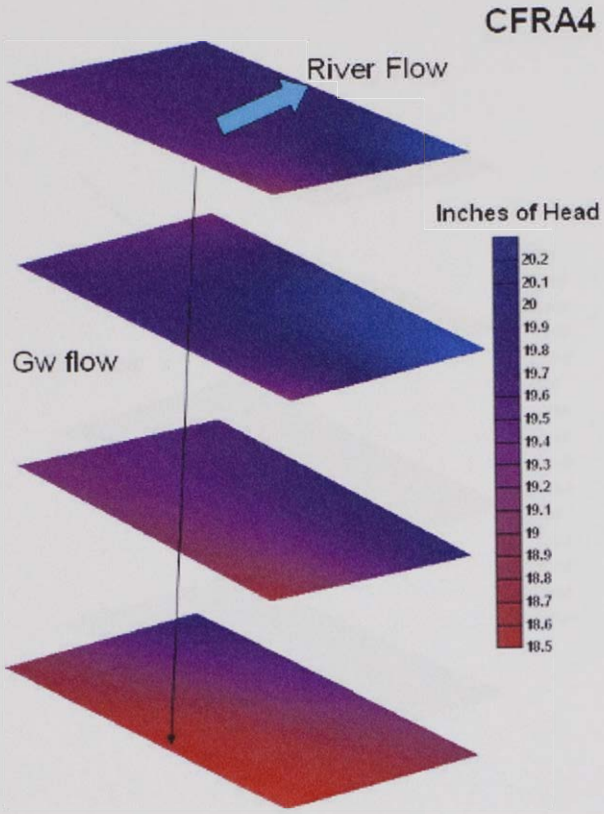

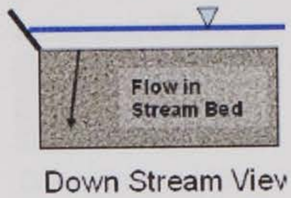

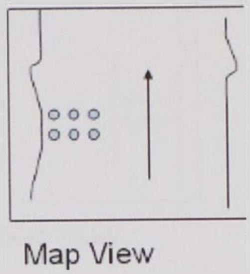

Measurements are in Inches

CFRA4											
1a		1b		1c		2a		2b		2c	
depth	wl	depth	wl	depth	wl	depth	wl	depth	wl	depth	wl
19.75	29.5	17.5	31	17.5	31	20	27.5	21	27	19.5	29
30	19.75	29.5	20	28	21			30.5	17.5	27.5	20.75
39	11.25	37	12.75	36.5	12.75	38.5	10.75	38	10.75	36	12

Normalized Depths			
	12	24	36
1a	36.84	25.46	14.08
1b	36.20	24.99	13.78
1c	36.31	24.78	13.26
2a	34.74	23.88	13.01
2b	35.50	24.00	12.51
2c	36.72	24.36	12.00

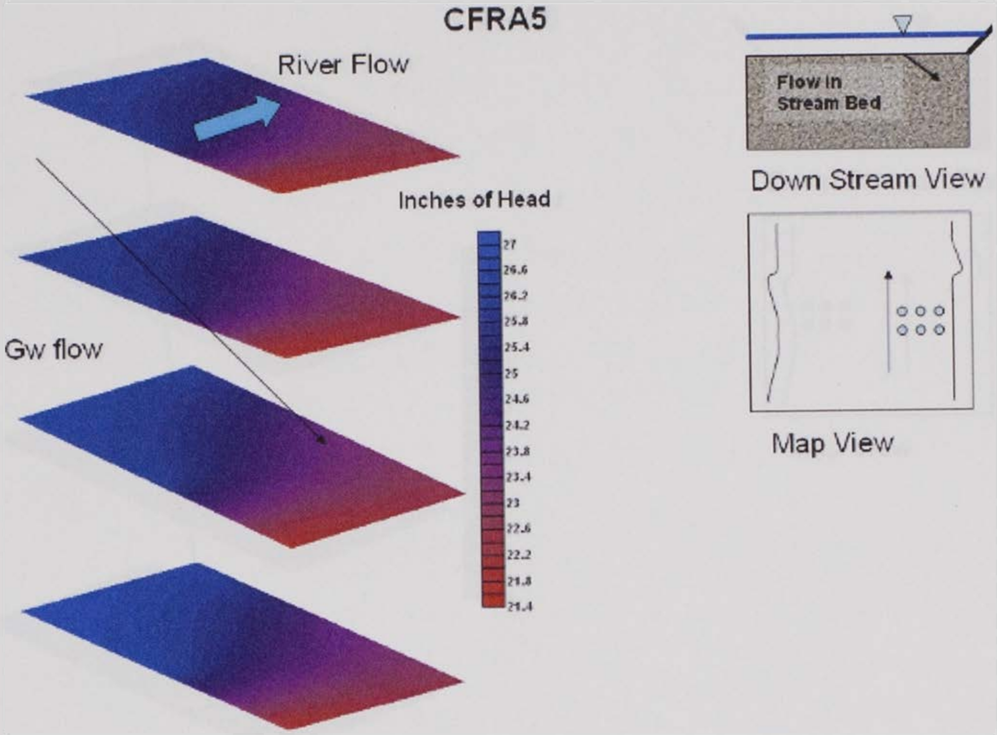

Measurements are in Inches

CFRA5											
1a depth	wl	1b depth	wl	1c depth	wl	2a depth	wl	2b depth	wl	2c depth	wl
11.75	34.75	11	31	12	29.5	9.5	36	14	30.5	12.5	29.5
22	24.5	17.25	24.75	16	25.5	23.25	22.25	23.25	21.25	20.25	21.75
35.25	11	30.5	11	29	12	33.5	11.75	32.5	11.5	31.25	10.25

Normalized Depths			
	12	24	36
1a	34.54	22.41	10.27
1b	30.04	17.71	5.38
1c	29.56	17.18	4.80
2a	33.52	21.40	9.28
2b	32.64	20.31	7.99
2c	30.09	17.76	5.42

CFRA6

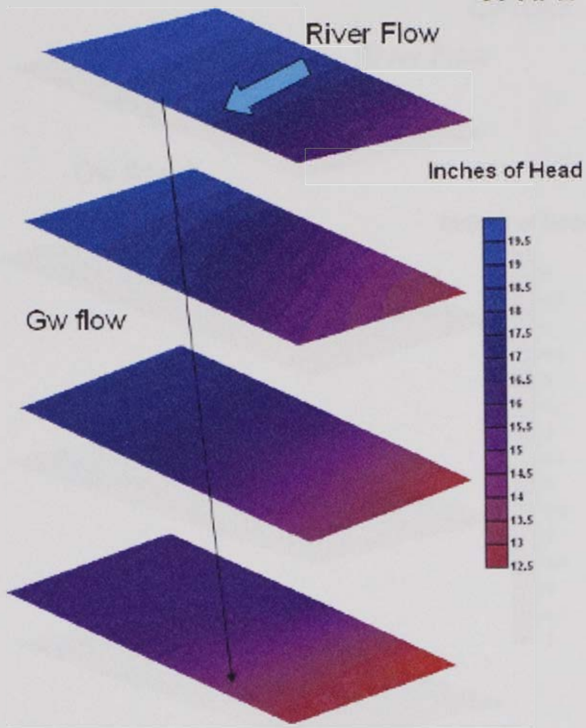

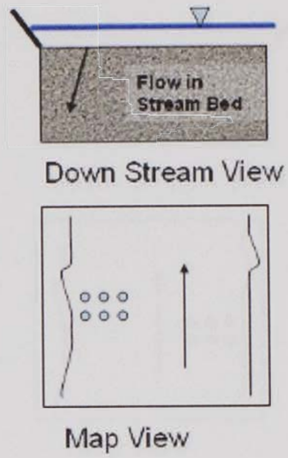

Measurements are in Inches

CFRA6											
1a		1b		1c		2a		2b		2c	
depth	wl	depth	wl	depth	wl	depth	wl	depth	wl	depth	wl
12.5	40.25	9.5	39.75	10.5	37.75	15.5	39.75	12	39.25	11	37
24.5	30.5	20	31.75	22	29.25	25.5	31.25	22.5	31	22	29
35.5	19.75	34.5	17.5	35	16.25	38	19	37.5	13.75	32.25	18.75

Normalized Depths			
	12	24	36
1a	41.00	30.32	19.63
1b	38.03	27.28	16.53
1c	36.99	26.43	15.87
2a	43.25	32.16	21.06
2b	40.12	28.00	15.88
2c	36.61	26.32	16.04

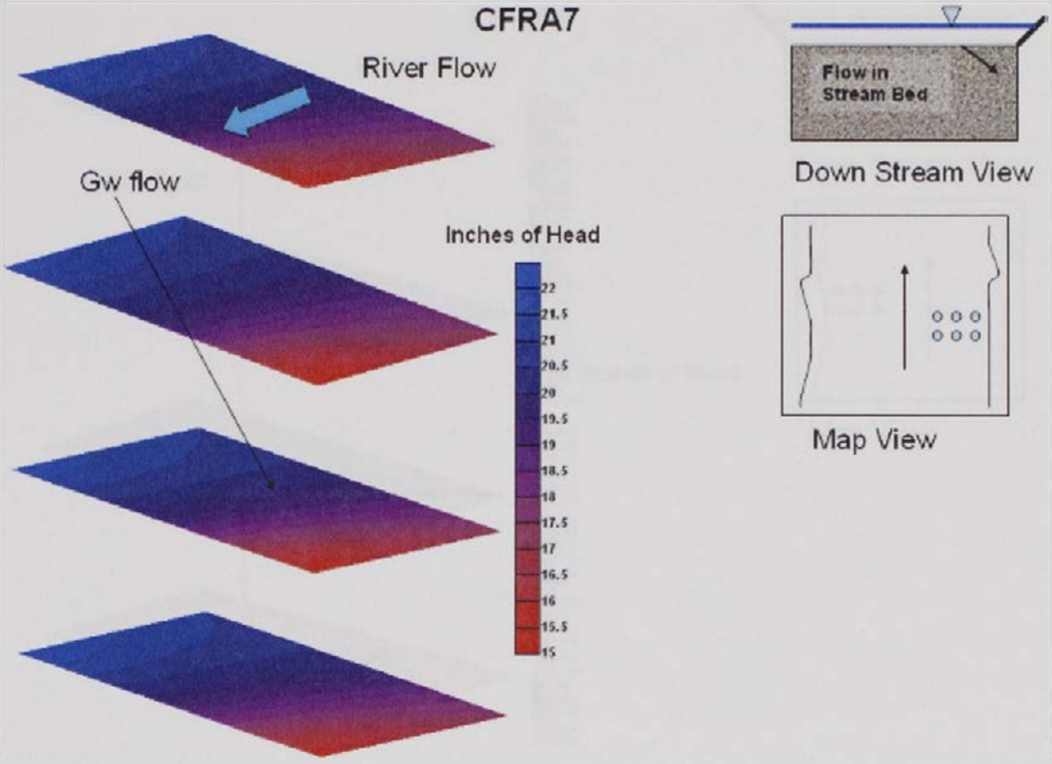

Measurements are in Inches

CFRA7											
1a		1b		1c		2a		2b		2c	
depth	wl	depth	wl	depth	wl	depth	wl	depth	wl	depth	wl
19.5	33.5	14.5	34	13	33.25	18.75	31.75	16	32	13.5	33.5
33.25	19.75	27.5	21	25.5	20.5	30	20.75	27	21	26.5	20.5
37.5	15	35	13.5	35.5	10.5	38.5	12	37	10.75	36.5	10.5

Normalized Depths			
	12	24	36
1a	41.21	28.96	16.71
1b	36.50	24.50	12.50
1c	34.23	22.09	9.95
2a	38.56	26.58	14.59
2b	36.09	23.95	11.81
2c	35.00	23.00	11.00

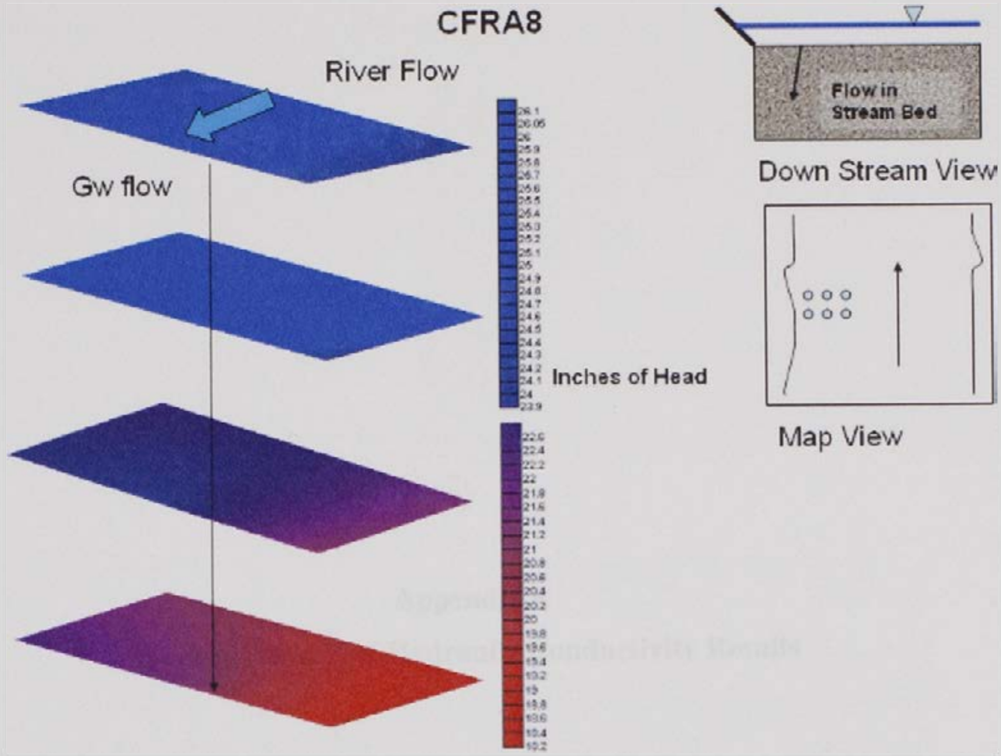

Measurements are in Inches

CFRA8											
1a		1b		1c		2a		2b		2c	
depth	wl	depth	wl	depth	wl	depth	wl	depth	wl	depth	wl
11.5	32	12	30.5	13.5	30.5	12	31.75	12.5	30.25	13.5	30.75
24	20	21	21.75	26	23.5	24.5	19.75	23.5	20.25	28.5	18.75
35	10.75	29.75	16	36	11.75	33.5	13.5	37.25	11.5	38	12.5

Normalized heads @ depths			
	12	24	36
1a	31.33	20.46	9.60
1b	30.04	20.23	10.42
1c	32.74	22.88	13.01
2a	31.37	21.10	10.83
2b	30.01	20.98	11.95
2c	31.66	22.67	13.67

Appendix E

Falling Head Test Hydraulic Conductivity Results

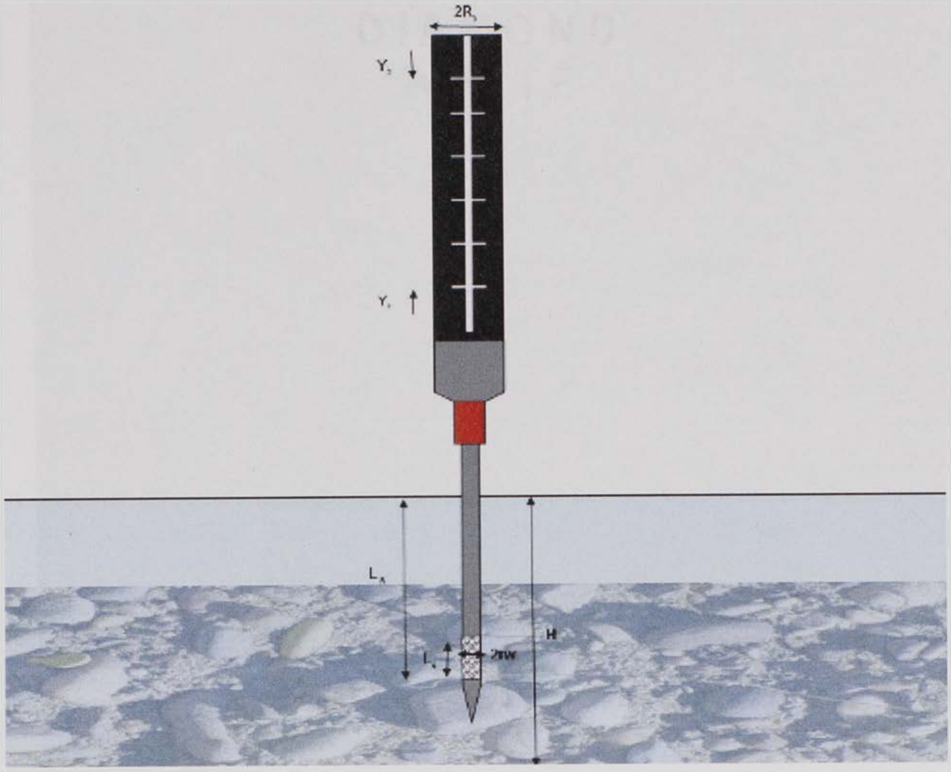

$$K = \frac{r_c^{\,2} \ln\left(\frac{R_e}{R_w}\right)}{2L_e} \frac{1}{t} \ln\left(\frac{y_o}{y_t}\right)$$

where:

$$\ln\left(\frac{R_e}{R_w}\right) = \left[\frac{1.1}{\ln\left(\frac{Lw}{rw}\right)} + \frac{A + B \ln\left[\frac{(H - Lw)}{rw}\right]}{\frac{L_e}{rw}} \right]^{-1}$$

The terms A and B are dimensionless numbers determined from a chart and are a function of L_e/rw.

All Values are in Meters.

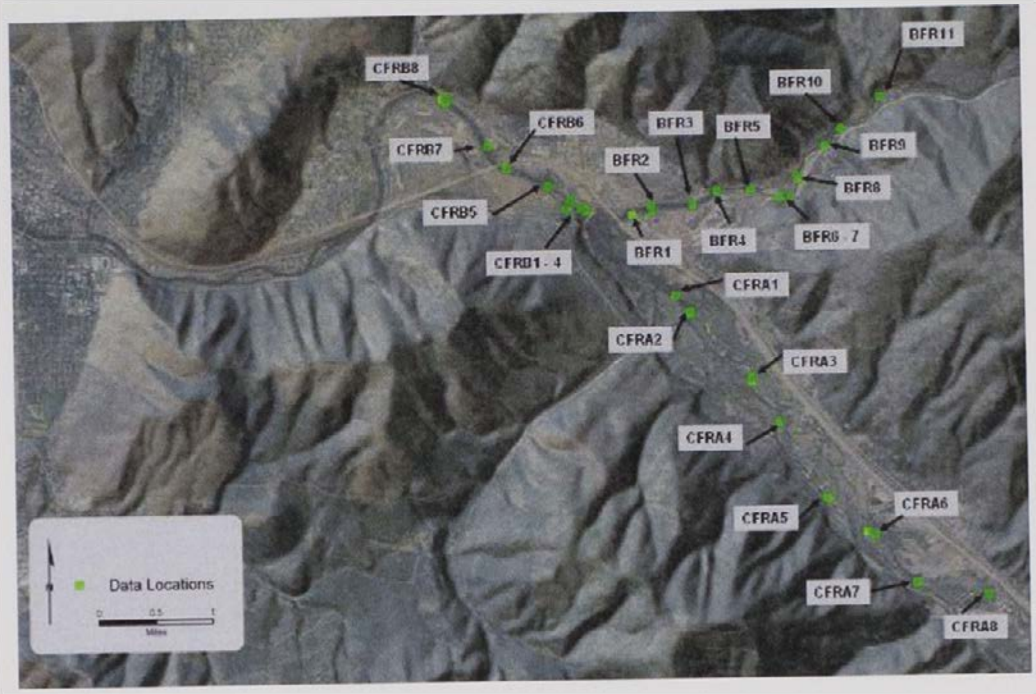

A map illustrating the locations where river VHG's and seepage rates were investigated.

Location cfra2

		Site 1	Run 1		Site 1	Run 2
		Ho		1.30	Ho	1.30
		Hi		0.60	Hi	0.60
		L		0.10	L	0.10
		t1		0.00	t1	0.00
		rc		0.10	rc	0.10
		Le		0.10	Le	0.10
		ln(re/r)		0.32	ln(re/r)	0.32
		lw		1.00	lw	1.00
		R e		0.06	R	0.06
		a		1.75	a	1.75
		b		0.50	b	0.50
		h		2.44	h	2.44
		le/r		1.60	le/r	1.60
Kh	m/day			8.12		12.18
Kh	ft/day			26.64		39.96
	Average		33.30			
Kv			3.33			

Location
cfra3

		Site 1	Run 1	Site 1	Run 2
		Ho	1.53	Ho	1.53
		Hi	0.83	Hi	0.83
		L	0.10	L	0.10
		t1	0.00	t1	0.00
		rc	0.10	rc	0.10
		Le	0.10	Le	0.10
		ln(re/r)	0.31	ln(re/r)	0.31
		lw	0.77	lw	0.77
		R	0.06	R	0.06
		a	1.75	a	1.75
		b	0.50	b	0.50
		h	2.67		2.67
		le/r	1.60	le/r	1.60
Kh	m/day		24.20		154.47
Kh	ft/day		79.40		506.82
	Average	293.11			
Kv		29.31			

		Site 2	Run 1
		Ho	1.58
		Hi	0.83
		L	0.10
		t1	0.00
		rc	0.10
		Le	0.10
		ln(re/r)	0.26
		lw	0.72
		R	0.06
		a	1.75
		b	0.50
		h	15.00
		le/r	1.60
Kh	m/day		9.14
Kh	ft/day		29.98
Kh	Average	29.98	
Kv	Average	3.00	

average of 2 sites 16.15

Location

cfra4		Site 1	Run 1	Site 1	Run 2
		Ho	1.34	Ho	1.34
		Hi	0.74	Hi	0.74
		L	0.10	L	0.10
		t1	0.00	t1	0.00
		rc	0.10	rc	0.10
		Le	0.10	Le	0.10
		ln(re/r)	0.32	ln(re/r)	0.32
		lw	0.91	lw	0.91
		R	0.06	R	0.06
		a	1.75	a	1.75
		b	0.50	b	0.50
		h	2.48	h	2.48
		le/r	1.60	le/r	1.60
Kh	m/day		153.85		199.38
Kh	ft/day		504.80		654.17
	Average	579.48			
Kv		57.95			
		Location 2	Run 1		
		cfra4			
		Ho	1.54		
		Hi	0.94		
		L	0.10		
		t1	0.00		
		rc	0.10		
		Le	0.10		
		ln(re/r)	0.26		
		lw	0.80		
		R	0.06		
		a	1.75		
		b	0.50		
		h	15.00		
		le/r	1.60		
Kh	m/day		4.84		
Kh	ft/day		15.87		
Kh	Average	15.87			
Kv	Average	1.59			

average of 2 sites 29.77

Location
cfra5

		Site 1	Run 1
		Ho	1.87
		Hi	1.17
		L	0.10
		t1	0.00
		rc	0.10
		Le	0.10
		ln(re/r)	0.30
		lw	0.61
		R	0.06
		a	1.75
		b	0.50
		h	3.01
		le/r	1.60
Kh	m/day		4.56
Kh	ft/day		14.97
	Average	14.97	
Kv		1.50	

		Site 2	Run 1	Site 2	Run 2
		Ho	1.58	Ho	1.58
		Hi	1.17	Hi	1.17
		L	0.10	L	0.10
		t1	0.00	t1	0.00
		rc	0.10	rc	0.10
		Le	0.10	Le	0.10
		ln(re/r)	0.25	ln(re/r)	0.30
		lw	0.61	lw	0.61
		R	0.06	R	0.06
		a	1.75	a	1.75
		b	0.50	b	0.50
		h	15.00	h	2.72
		le/r	1.60	le/r	1.60
Kh	m/day		4.21		4.97
Kh	ft/day		13.82		16.31
Kh	Average	15.06			
Kv	Average	1.51			

average of 2 sites 1.50

Location
cfra6

		Site 1	Run 1
		Ho	1.34
		Hi	0.64
		L	0.10
		t1	0.00
		rc	0.10
		Le	0.10
		ln(re/r)	0.32
		lw	0.96
		R	0.06
		a	1.75
		b	0.50
		h	2.48
		le/r	1.60
Kh	m/day		3.21
Kh	ft/day		10.52
	Average	10.52	
Kv		1.05	

		Site 2	Run 1
		Ho	1.36
		Hi	0.64
		L	0.10
		t1	0.00
		rc	0.10
		Le	0.10
		ln(re/r)	0.26
		lw	0.93
		R	0.06
		a	1.75
		b	0.50
		h	15.00
		le/r	1.60
Kh	m/day		6.43
Kh	ft/day		21.11
Kh	Average	21.11	
Kv	Average	2.11	

average of 2 sites 1.58

Location
cfra7

		Site 1	Run 1
		Ho	1.34
		Hi	0.64
		L	0.10
		t1	0.00
		rc	0.10
		Le	0.10
		ln(re/r)	0.31
		lw	0.80
		R	0.06
		a	1.75
		b	0.50
		h	2.48
		le/r	1.60
Kh	m/day		7.55
Kh	ft/day		24.78
	Average	24.78	
Kv		2.48	
		Site 2	Run 1
		Ho	1.50
		Hi	0.64
		L	0.10
		t1	0.00
		rc	0.10
		Le	0.10
		ln(re/r)	0.26
		lw	0.96
		R	0.06
		a	1.75
		b	0.50
		h	15.00
		le/r	1.60
Kh	m/day		3.34
Kh	ft/day		10.95
Kh	Average	10.95	
Kv	Average	1.09	

average of 2 sites 1.79

Location
cfra8

		Site 1		Run 1
		Ho		1.26
		Hi		0.56
		L		0.10
		t1		0.00
		rc		0.10
		Le		0.10
		ln(re/r)		0.32
		lw		0.85
		R		0.06
		a		1.75
		b		0.50
		h		2.40
		le/r		1.60
Kh	m/day			17.93
Kh	ft/day			58.81
	Average		58.81	
Kv			5.88	

		Site 2		Run 1
		Ho		1.33
		Hi		0.56
		L		0.10
		t1		0.00
		rc		0.10
		Le		0.10
		ln(re/r)		0.26
		lw		0.80
		R		0.06
		a		1.75
		b		0.50
		h		15.00
		le/r		1.60
Kh	m/day			3.78
Kh	ft/day			12.39
Kh	Average		12.39	
Kv	Average		1.24	

average of 2 sites 3.56

Location
cfrb2

		Site 1	Run 1	Site 1	Run 2
		Ho	1.55	Ho	1.55
		Hi	0.85	Hi	0.85
		L	0.10	L	0.10
		t1	0.00	t1	0.00
		rc	0.10	rc	0.10
		Le	0.10	Le	0.10
		ln(re/r)	0.27	ln(re/r)	0.27
		lw	1.50	lw	1.50
		R	0.06	R	0.06
		a	1.75	a	1.75
		b	0.50	b	0.50
		h	15.00	h	15.00
		le/r	1.60	le/r	1.60
Kh	m/day		5.22		5.22
Kh	ft/day		17.14		17.14
Kh	Average	17.14			
Kv	Average	1.71			

Location
cfrb7

		Site 1	Run 1	Site 1	Run 2
		Ho	1.63	Ho	1.63
		Hi	0.93	Hi	0.93
		L	0.10	L	0.10
		t1	0.00	t1	0.00
		rc	0.10	rc	0.10
		Le	0.10	Le	0.10
		ln(re/r)	0.27	ln(re/r)	0.22
		lw	1.50	lw	0.18
		R	0.06	R	0.06
		a	1.75	a	1.75
		b	0.50	b	0.50
		h	15.00		15.00
		le/r	1.60	le/r	1.60
Kh	m/day		4.88		4.07
Kh	ft/day		16.01		13.36
Kh	Average	14.68			
Kv	Average	1.47			

Location
bfr5

		Site 1	Run 1		Site 1	Run 2
		Ho	1.99		Ho	1.99
		Hi	1.29		Hi	1.29
		L	0.10		L	0.10
		t1	0.00		t1	0.00
		rc	0.10		rc	0.10
		Le	0.10		Le	0.10
		ln(re/r)	6.39		ln(re/r)	6.39
		lw	1.50		lw	1.50
		R	0.06		R	0.06
		a	1.75		a	1.75
		b	0.50		b	0.50
		h	15.00		h	15.00
		le/r	1.60		le/r	1.60
Kh	m/day		90.82			90.82
Kh	ft/day		297.98			297.98
Kh	Average	297.98				
Kv	Average	29.80				

Location
bfr6

		Site 1	Run 1	Site 1	Run 2
		Ho	1.64	Ho	1.64
		Hi	0.94	Hi	0.94
		L	0.10	L	0.10
		t1	0.00	t1	0.00
		rc	0.10	rc	0.10
		Le	0.10	Le	0.10
		ln(re/r)	6.39	ln(re/r)	7.18
		lw	1.50	lw	0.18
		R	0.06	R	0.06
		a	1.75	a	1.75
		b	0.50	b	0.50
		h	15.00		15.00
		le/r	1.60	le/r	1.60
Kh	m/day		116.60		131.13
Kh	ft/day		382.58		430.22
Kh	Average	406.40			
Kv	Average	40.64			

Location
bfr8

		Site 1	Run 1	Site 1	Run 2
		Ho	1.60	Ho	1.60
		Hi	0.90	Hi	0.90
		L	0.10	L	0.10
		t1	0.00	t1	0.00
		rc	0.10	rc	0.10
		Le	0.10	Le	0.10
		ln(re/r)	6.39	ln(re/r)	7.18
		lw	1.50	lw	0.18
		R	0.06	R	0.06
		a	1.75	a	1.75
		b	0.50	b	0.50
		h	15.00		15.00
		le/r	1.60	le/r	1.60
Kh	m/day		120.54		135.55
Kh	ft/day		395.50		444.75
Kh	Average	420.12			
Kv	Average	42.01			

Location

bfr9

		Site 1	Run 1	Site 1	Run 2
		Ho	2.07	Ho	2.07
		Hi	1.37	Hi	1.37
		L	0.10	L	0.10
		t1	0.00	t1	0.00
		rc	0.10	rc	0.10
		Le	0.10	Le	0.10
		ln(re/r)	6.39	ln(re/r)	7.18
		lw	1.50	lw	0.18
		R	0.06	R	0.06
		a	1.75	a	1.75
		b	0.50	b	0.50
		h	15.00		15.00
		le/r	1.60	le/r	1.60
Kh	m/day		86.47		97.24
Kh	ft/day		283.71		319.04
Kh	Average	301.38			
Kv	Average	30.14			

Location
bfr11

		Site 1	Run 1	Site 1	Run 2
		Ho	1.66	Ho	1.66
		Hi	0.96	Hi	0.96
		L	0.10	L	0.10
		t1	0.00	t1	0.00
		rc	0.10	rc	0.10
		Le	0.10	Le	0.10
		ln(re/r)	6.39	ln(re/r)	7.18
		lw	1.50	lw	0.18
		R	0.06	R	0.06
		a	1.75	a	1.75
		b	0.50	b	0.50
		h	15.00		15.00
		le/r	1.60	le/r	1.60
Kh	m/day		114.73		129.02
Kh	ft/day		376.44		423.32
Kh	Average	399.88			
Kv	Average	39.99			

Appendix F

Temperature Monitoring and Modeling Data

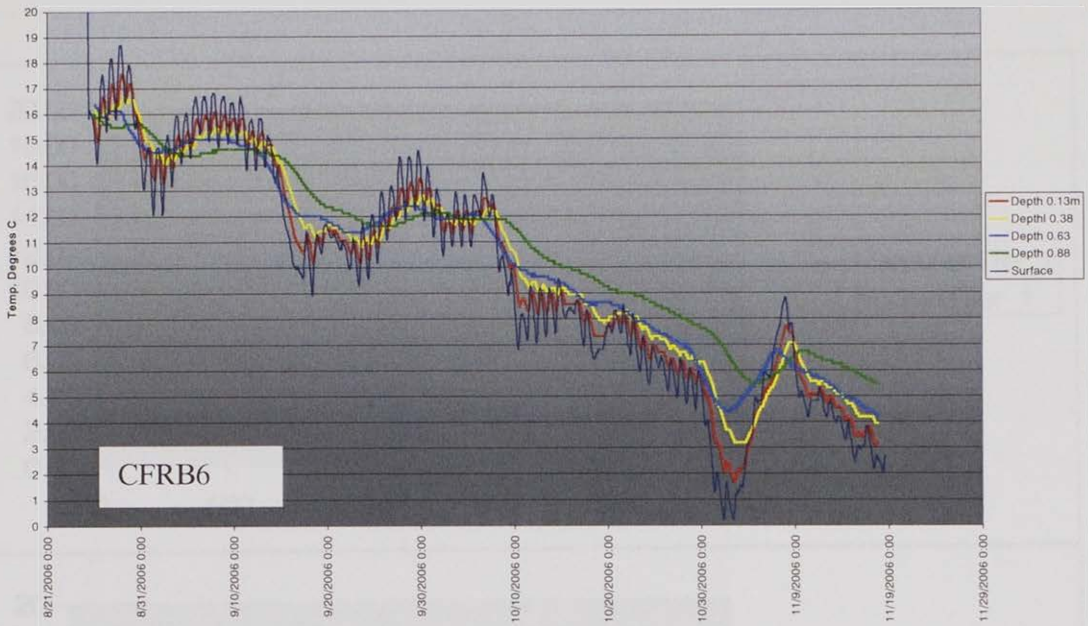
CFRB6
Temp. Degrees C
Depth 0.13m
Depthl 0.38
Depth 0.63
Depth 0.88
Surface
8/21/2006 0:00
8/31/2006 0:00
9/10/2006 0:00
9/20/2006 0:00
9/30/2006 0:00
10/10/2006 0:00
10/20/2006 0:00
10/30/2006 0:00
11/9/2006 0:00
11/19/2006 0:00
11/29/2006 0:00

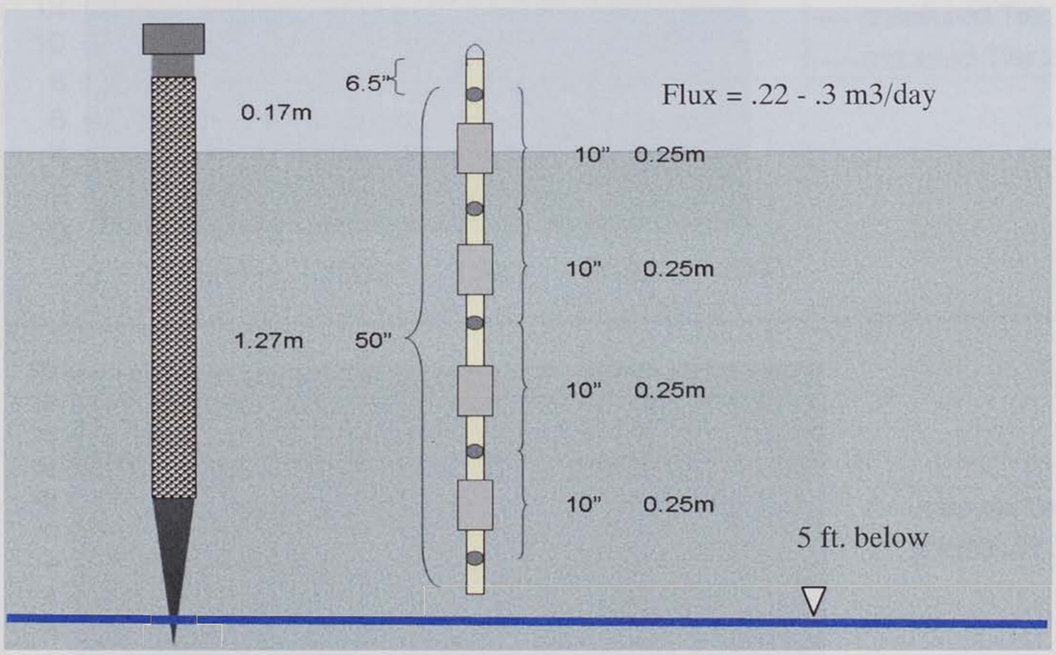
6.5"
0.17m
Flux = .22 - .3 m3/day
10" 0.25m
10" 0.25m
1.27m 50"
10" 0.25m
10" 0.25m
5 ft. below

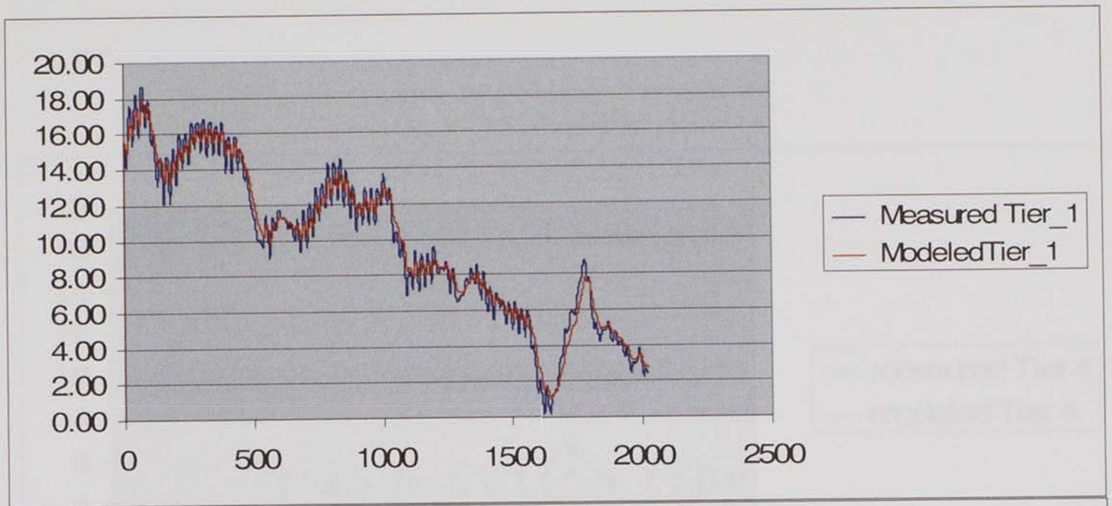

20.00
18.00
16.00
14.00
12.00
10.00
8.00
6.00
4.00
2.00
0.00
0
500
1000
1500
2000
2500
Measured Tier_1
ModeledTier_1

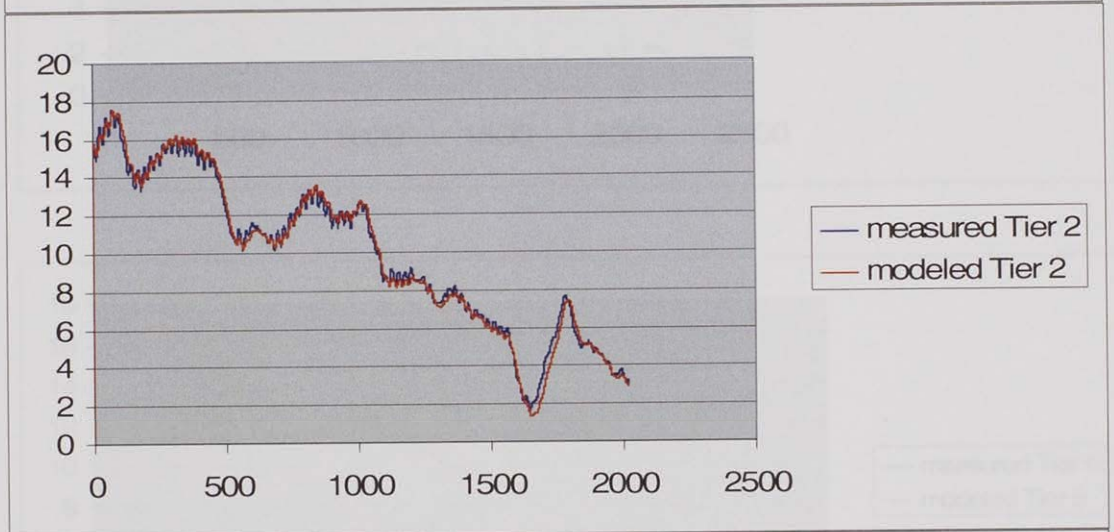

20
18
16
14
12
10
8
6
4
2
0
0
500
1000
1500
2000
2500
measured Tier 2
modeled Tier 2

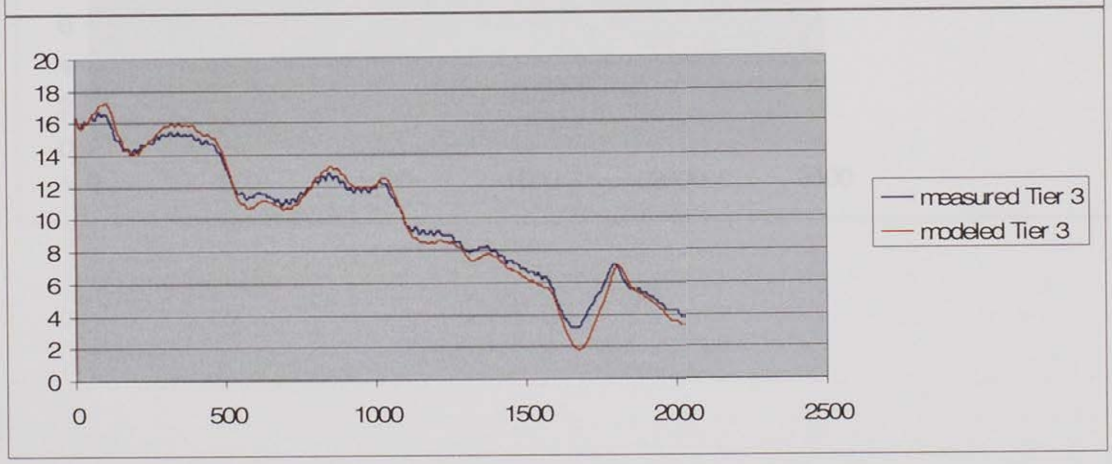

20
18
16
14
12
10
8
6
4
2
0
0
500
1000
1500
2000
2500
measured Tier 3
modeled Tier 3

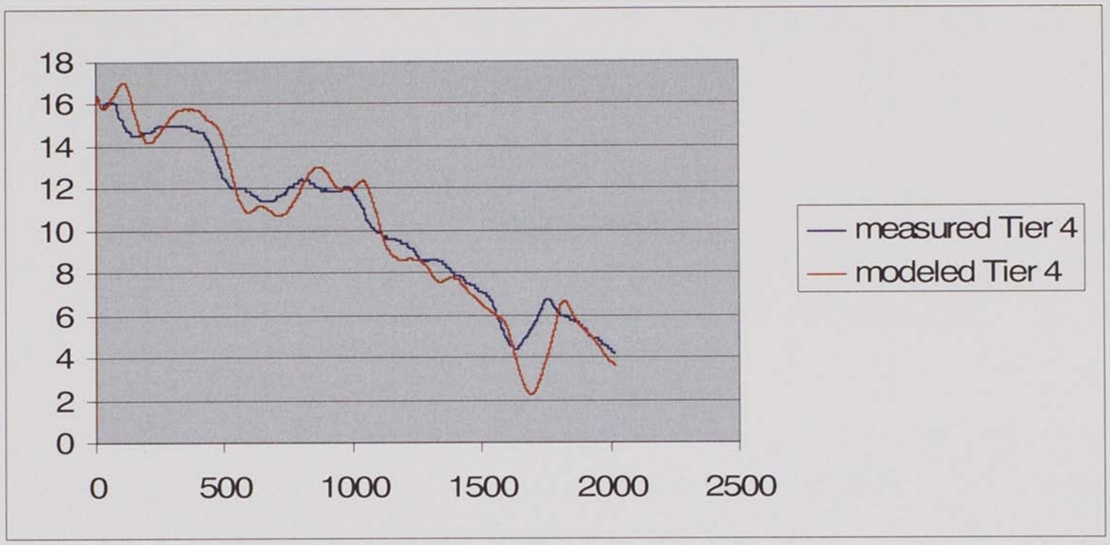
18
16
14
12
10
8
6
4
2
0
0
500
1000
1500
2000
2500
measured Tier 4
modeled Tier 4

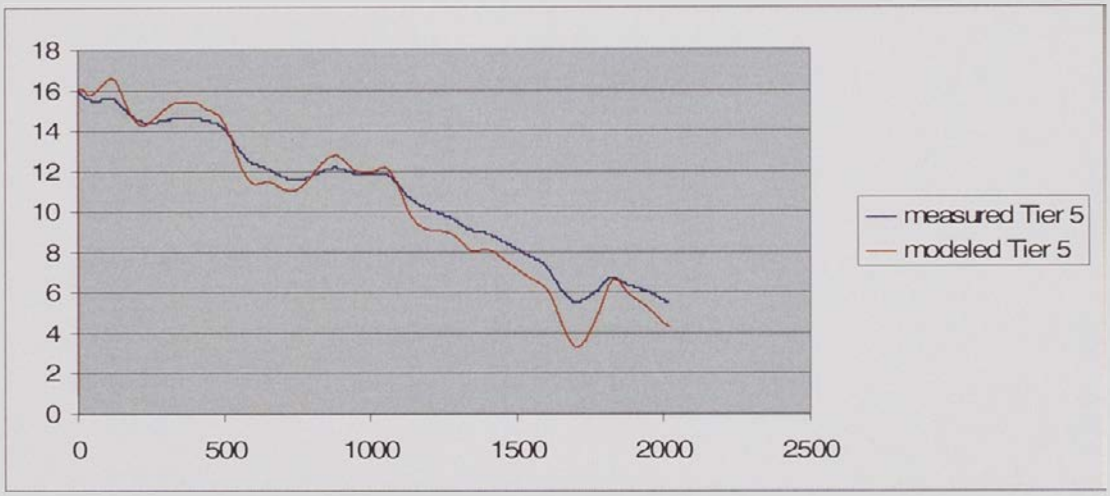
18
16
14
12
10
8
6
4
2
0
0
500
1000
1500
2000
2500
measured Tier 5
modeled Tier 5

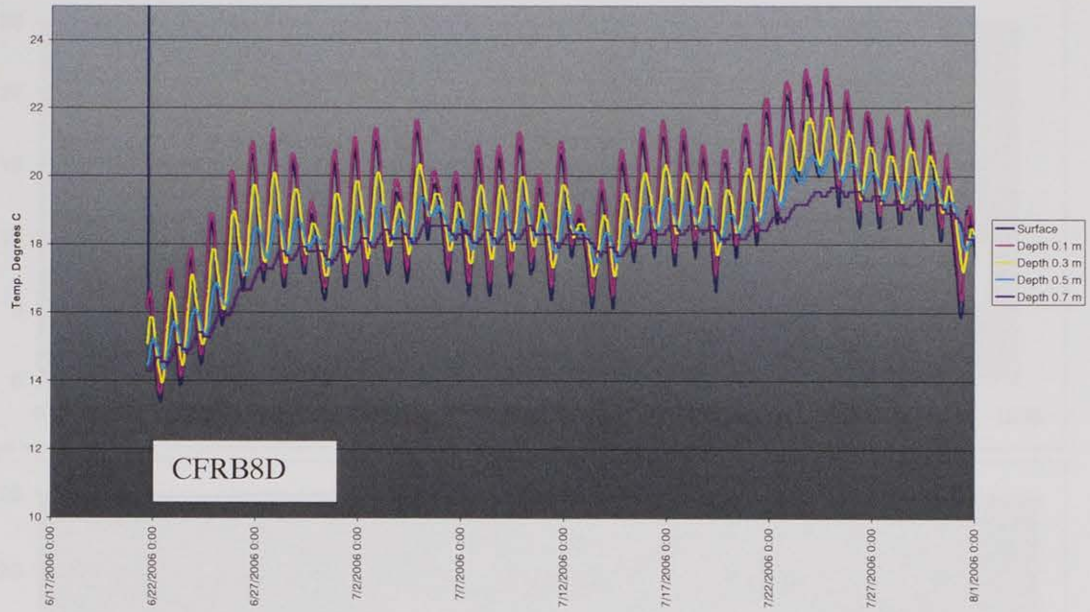
CFRB8D
Temp. Degrees C
24
22
20
18
16
14
12
10
6/17/2006 0:00
6/22/2006 0:00
6/27/2006 0:00
7/2/2006 0:00
7/7/2006 0:00
7/12/2006 0:00
7/17/2006 0:00
7/22/2006 0:00
7/27/2006 0:00
8/1/2006 0:00
Surface
Depth 0.1 m
Depth 0.3 m
Depth 0.5 m
Depth 0.7 m

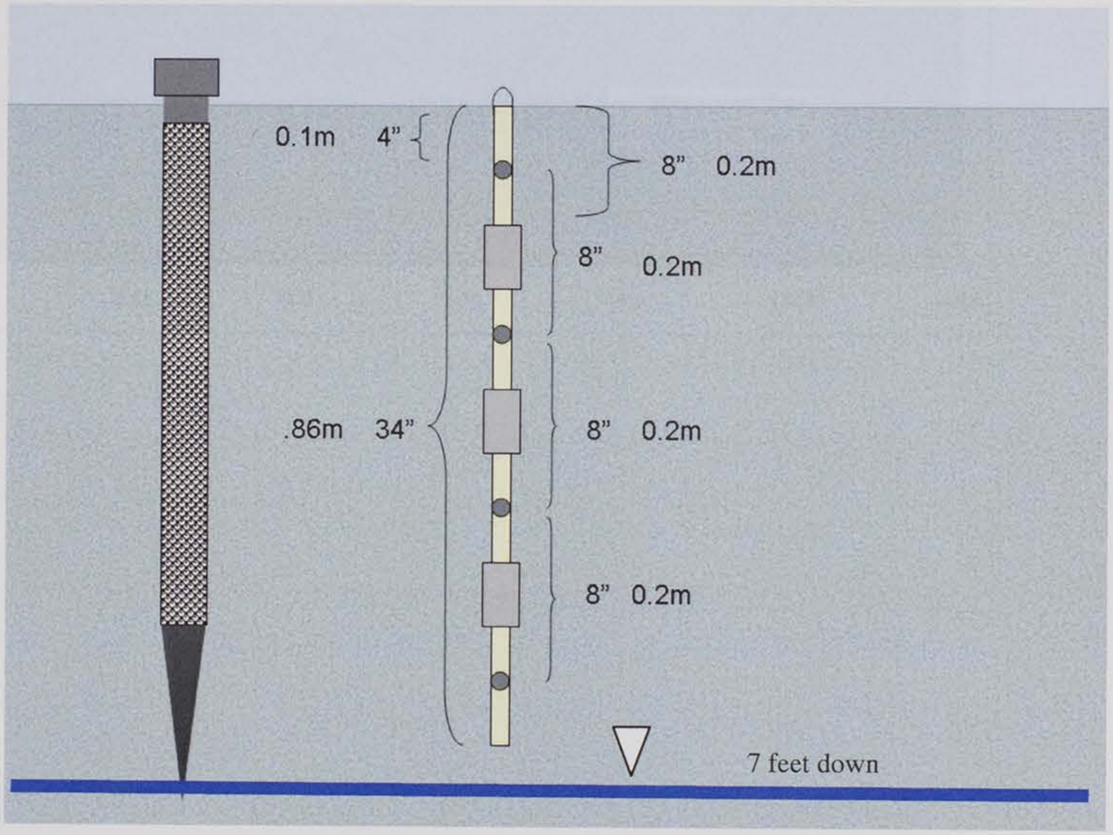
0.1m 4"
8" 0.2m
8" 0.2m
.86m 34"
8" 0.2m
8" 0.2m
7 feet down

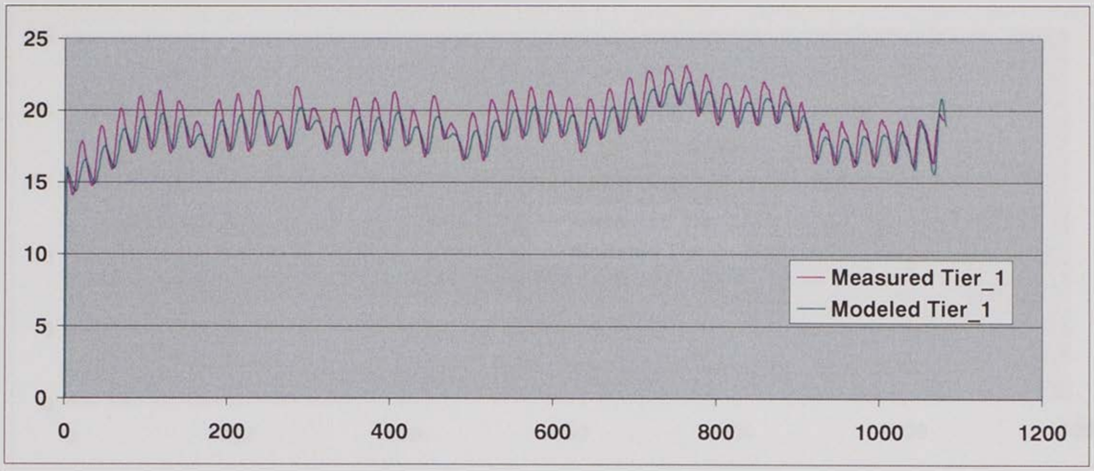

25
20
15
10
5
0
0
200
400
600
800
1000
1200
Measured Tier_1
Modeled Tier_1

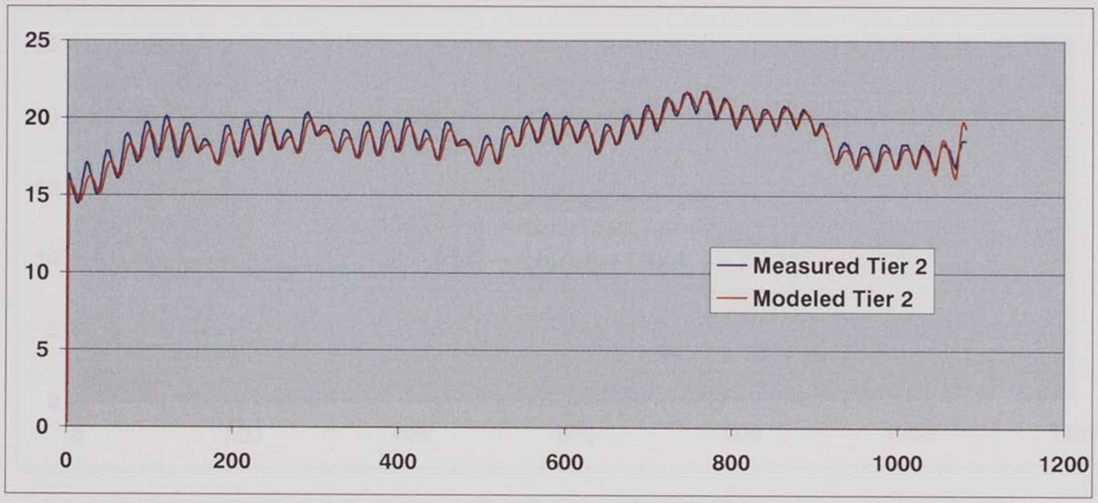

25
20
15
10
5
0
0
200
400
600
800
1000
1200
Measured Tier 2
Modeled Tier 2

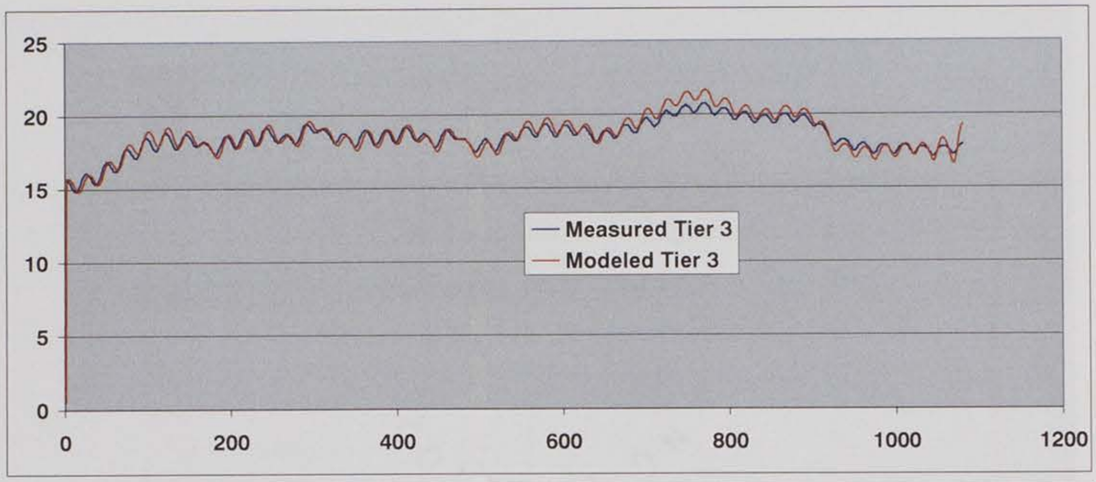
25
20
15
10
5
0
0
200
400
600
800
1000
1200
Measured Tier 3
Modeled Tier 3

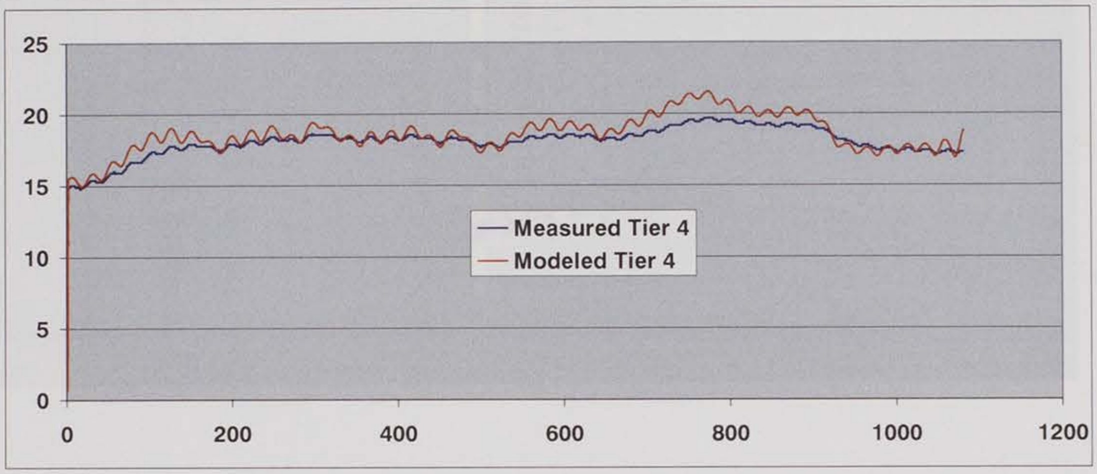
25
20
15
10
5
0
0
200
400
600
800
1000
1200
Measured Tier 4
Modeled Tier 4

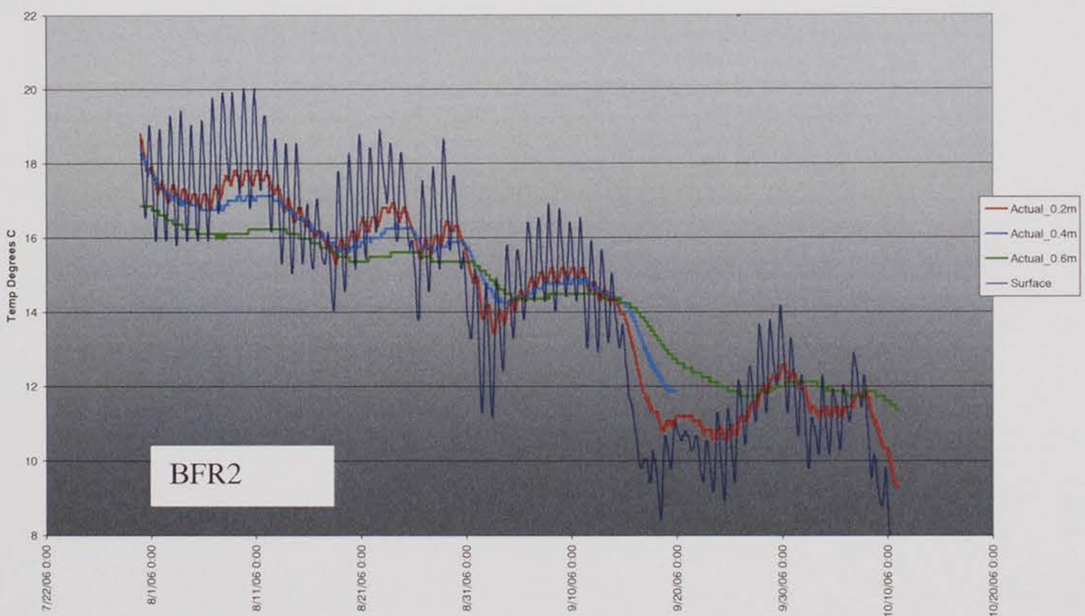
22
20
18
16
14
12
10
8
Temp Degrees C
7/22/06 0:00
8/1/06 0:00
8/11/06 0:00
8/21/06 0:00
8/31/06 0:00
9/10/06 0:00
9/20/06 0:00
9/30/06 0:00
10/10/06 0:00
10/20/06 0:00
Actual_0.2m
Actual_0.4m
Actual_0.6m
Surface
BFR2

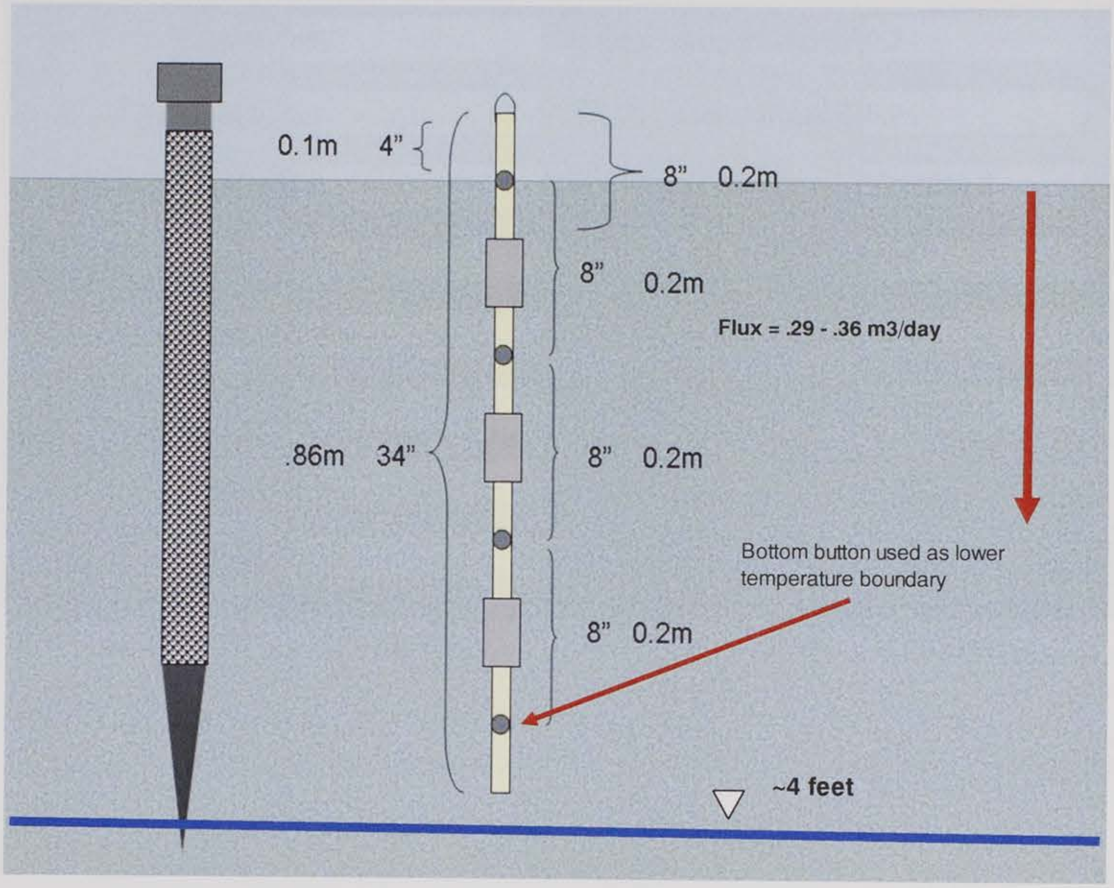
0.1m 4"
8" 0.2m
8" 0.2m
Flux = .29 - .36 m3/day
.86m 34"
8" 0.2m
Bottom button used as lower temperature boundary
8" 0.2m
~4 feet

name	bfr2	Long. disp.	0.2
Kzz/Khh	0.1	Trans. disp.	0.2
saturated Khh	7.0	Cs	3200000.0
specific storage	1.0E-6	KTr	0.85
porosity	0.275	KTs	1.4
RMC	0.045	Cw	4186000.0
alpha	3.0		
beta	5.0		

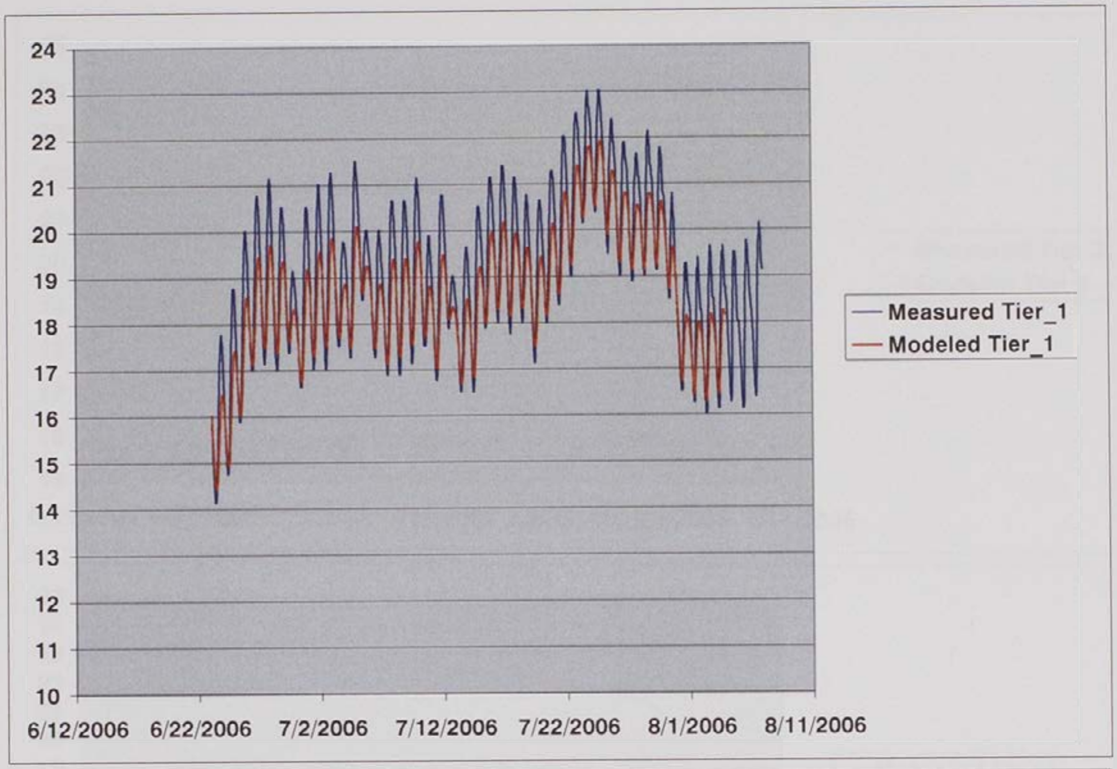
24
23
22
21
20
19
18
17
16
15
14
13
12
11
10
6/12/2006
6/22/2006
7/2/2006
7/12/2006
7/22/2006
8/1/2006
8/11/2006
Measured Tier_1
Modeled Tier_1

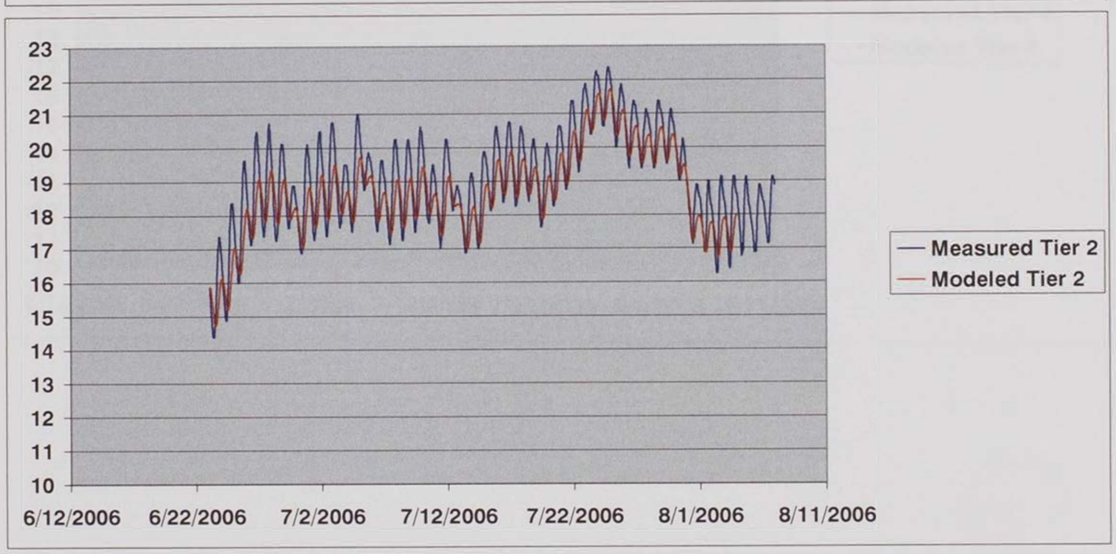
23
22
21
20
19
18
17
16
15
14
13
12
11
10
6/12/2006
6/22/2006
7/2/2006
7/12/2006
7/22/2006
8/1/2006
8/11/2006
Measured Tier 2
Modeled Tier 2

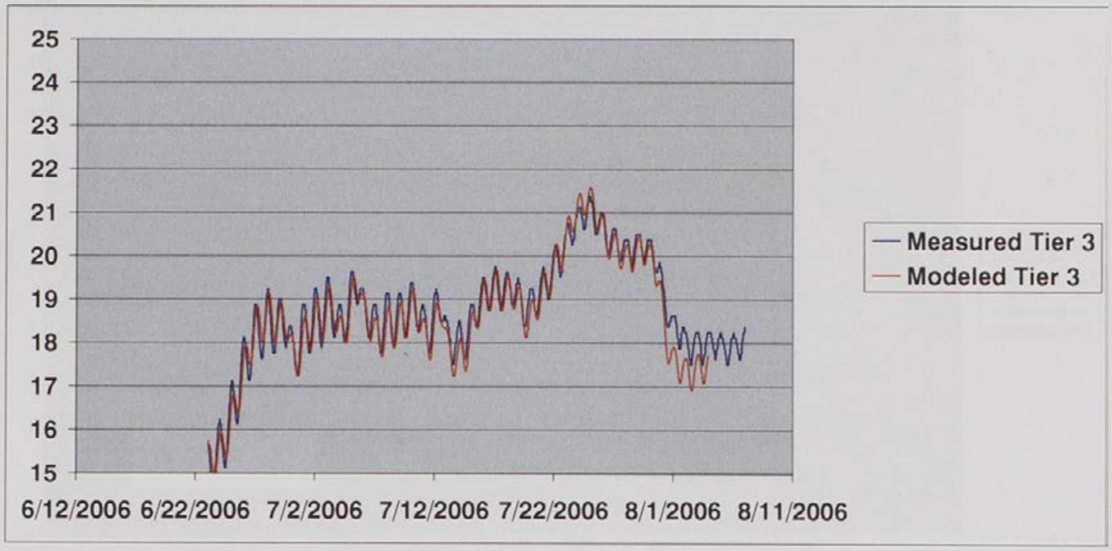
25
24
23
22
21
20
19
18
17
16
15
6/12/2006 6/22/2006 7/2/2006 7/12/2006 7/22/2006 8/1/2006 8/11/2006
Measured Tier 3
Modeled Tier 3

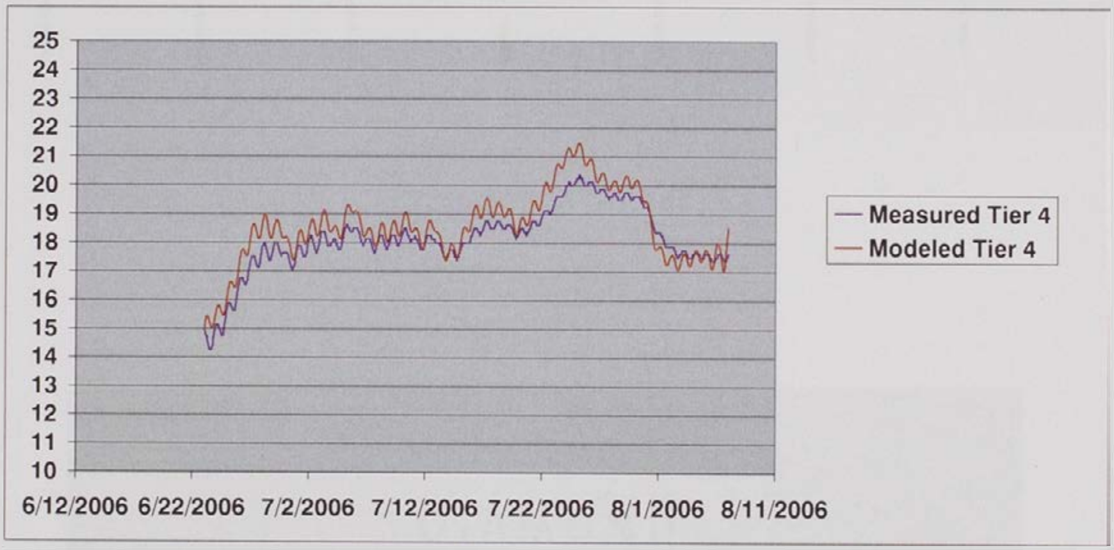
25
24
23
22
21
20
19
18
17
16
15
14
13
12
11
10
6/12/2006 6/22/2006 7/2/2006 7/12/2006 7/22/2006 8/1/2006 8/11/2006
Measured Tier 4
Modeled Tier 4

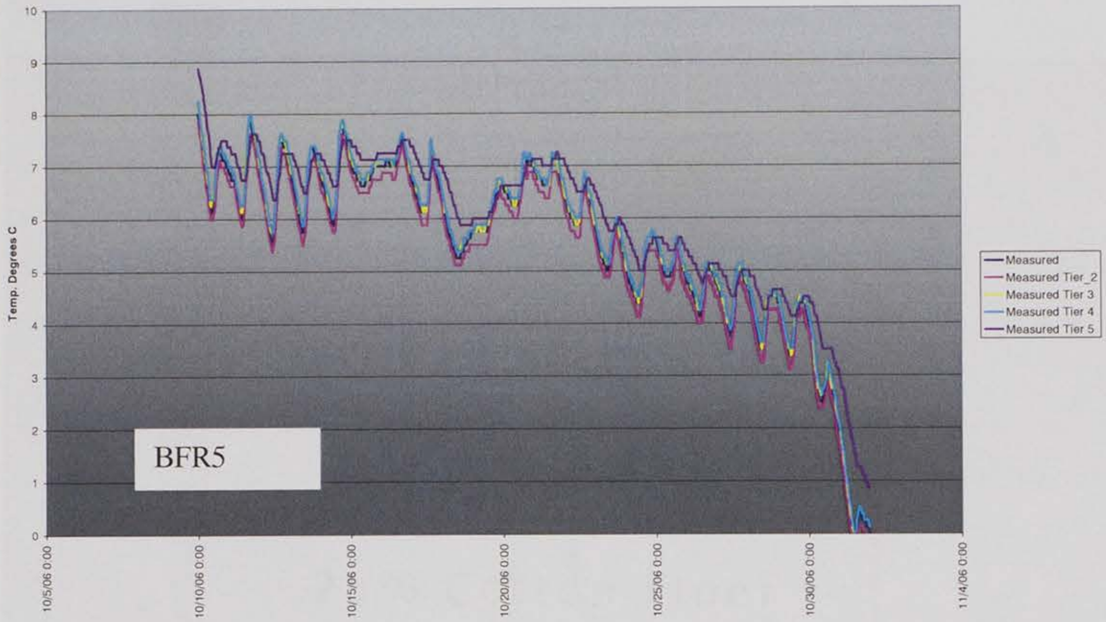
Temp. Degrees C
BFR5
Measured
Measured Tier_2
Measured Tier 3
Measured Tier 4
Measured Tier 5
10/5/06 0:00
10/10/06 0:00
10/15/06 0:00
10/20/06 0:00
10/25/06 0:00
10/30/06 0:00
11/4/06 0:00

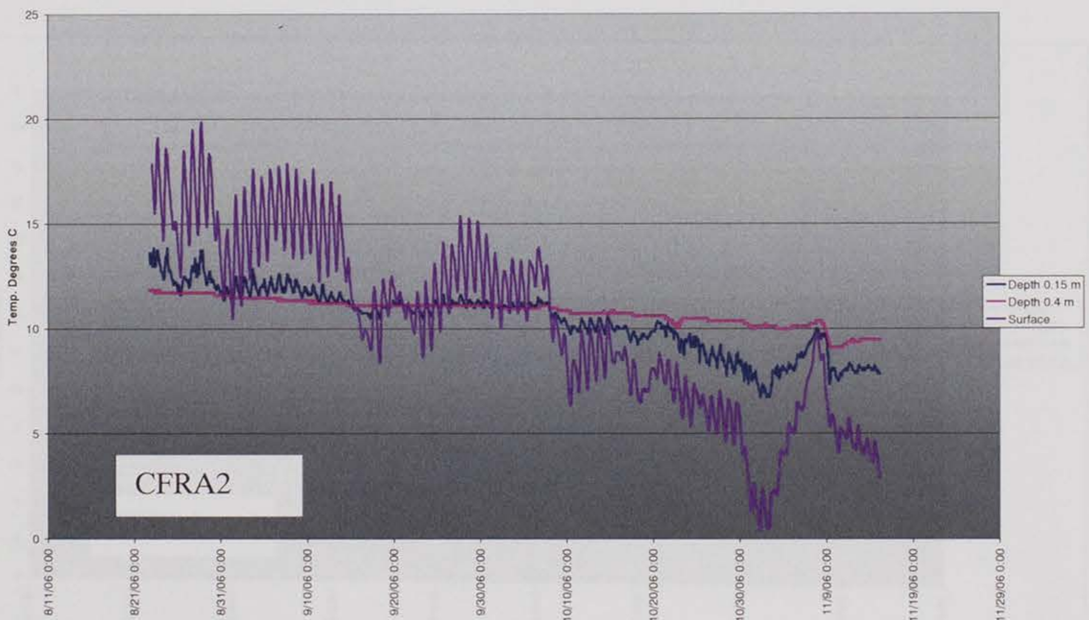
Temp. Degrees C
CFRA2
Depth 0.15 m
Depth 0.4 m
Surface
8/11/06 0:00
8/21/06 0:00
8/31/06 0:00
9/10/06 0:00
9/20/06 0:00
9/30/06 0:00
10/10/06 0:00
10/20/06 0:00
10/30/06 0:00
11/9/06 0:00
11/19/06 0:00
11/29/06 0:00

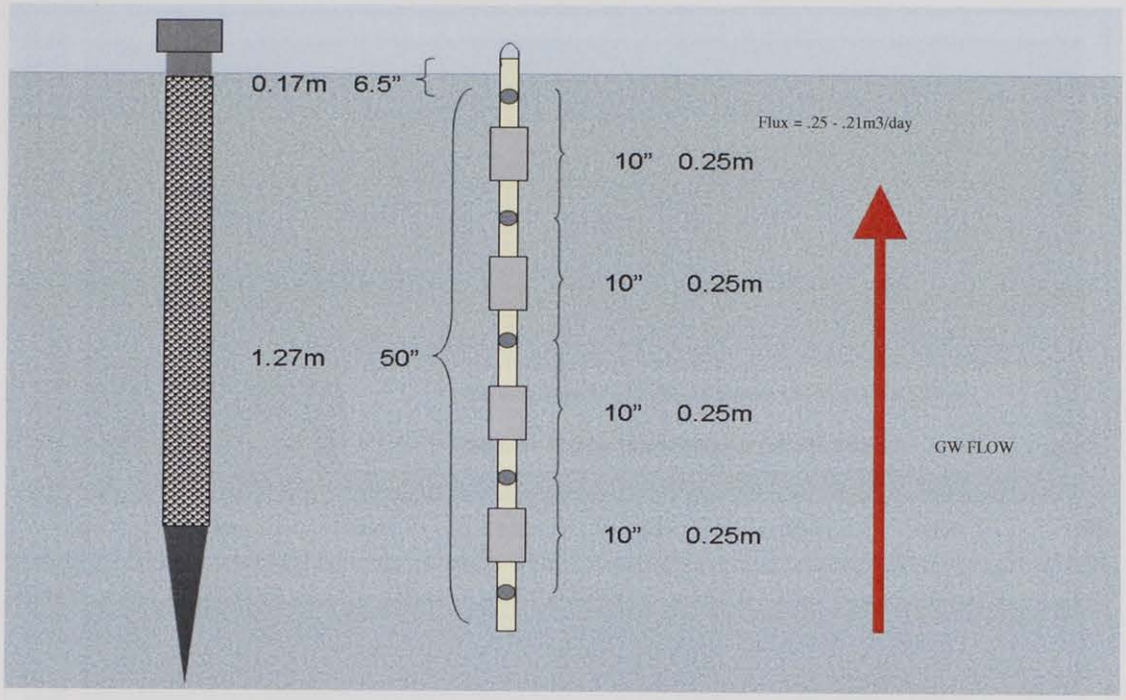
0.17m 6.5"
Flux = .25 - .21m3/day
10" 0.25m
10" 0.25m
1.27m 50"
10" 0.25m
GW FLOW
10" 0.25m

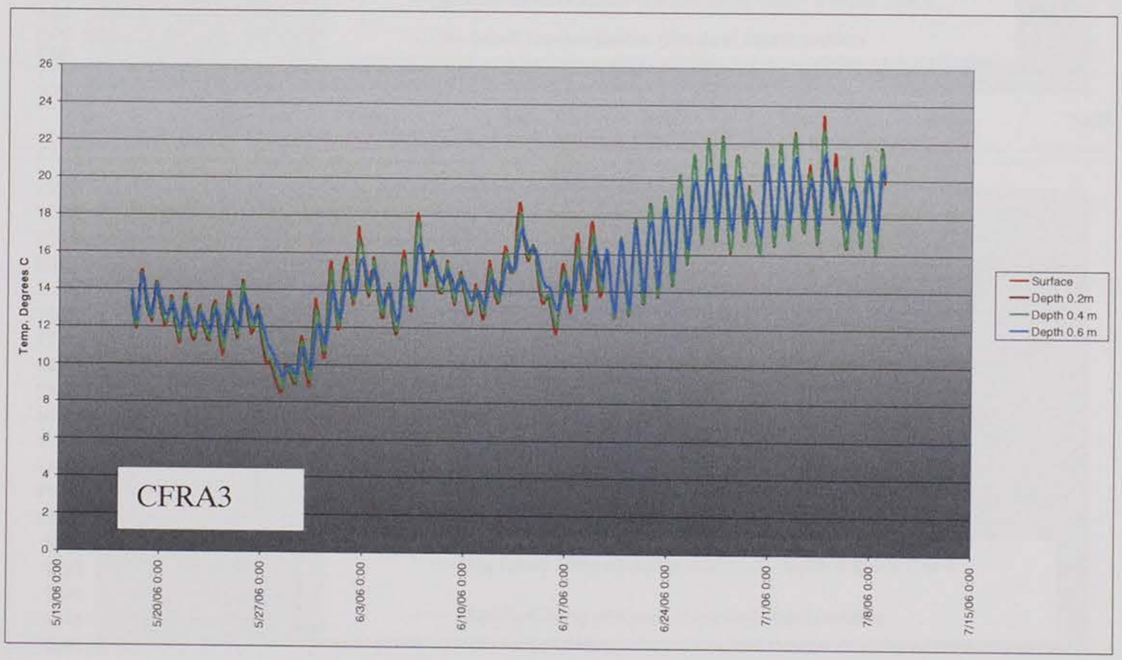
Temp. Degrees C
26
24
22
20
18
16
14
12
10
8
6
4
2
0
CFRA3
5/13/06 0:00
5/20/06 0:00
5/27/06 0:00
6/3/06 0:00
6/10/06 0:00
6/17/06 0:00
6/24/06 0:00
7/1/06 0:00
7/8/06 0:00
7/15/06 0:00
Surface
Depth 0.2m
Depth 0.4 m
Depth 0.6 m

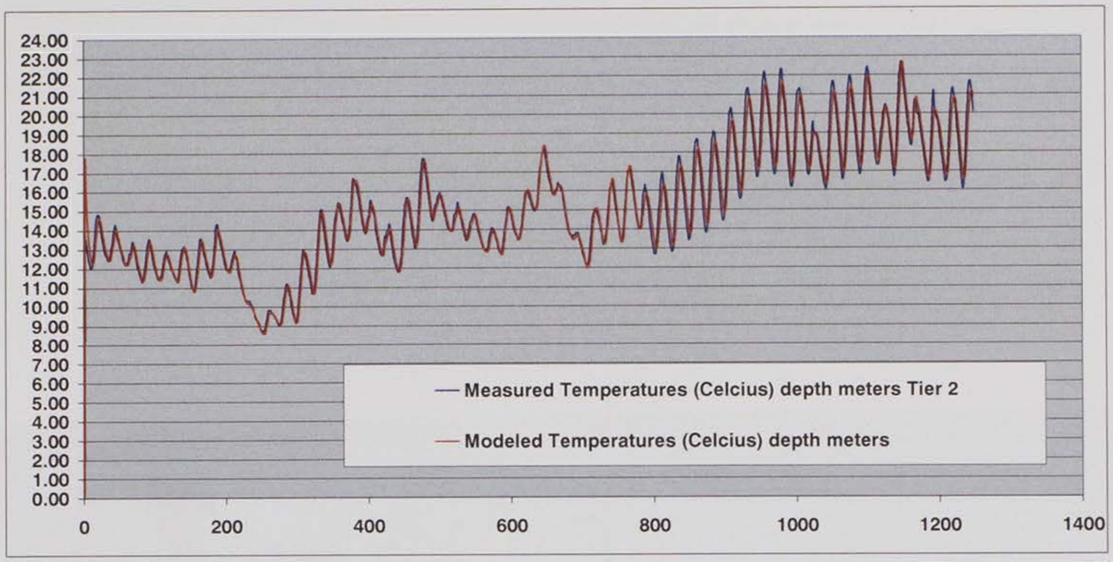
Measured Temperatures (Celcius) depth meters Tier 2
Modeled Temperatures (Celcius) depth meters
24.00
23.00
22.00
21.00
20.00
19.00
18.00
17.00
16.00
15.00
14.00
13.00
12.00
11.00
10.00
9.00
8.00
7.00
6.00
5.00
4.00
3.00
2.00
1.00
0.00
0
200
400
600
800
1000
1200
1400

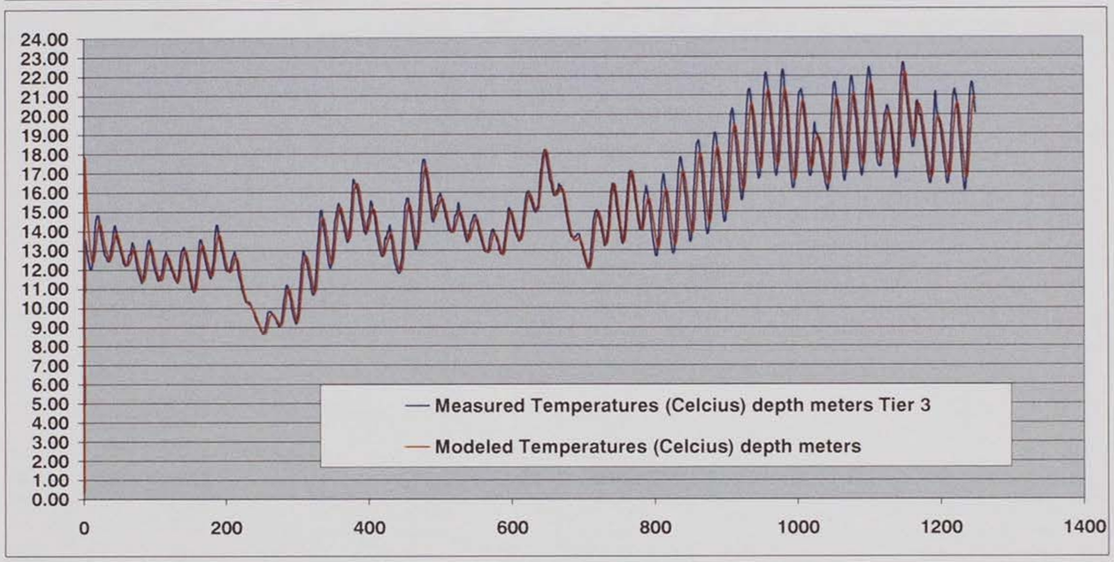
Measured Temperatures (Celcius) depth meters Tier 3
Modeled Temperatures (Celcius) depth meters
24.00
23.00
22.00
21.00
20.00
19.00
18.00
17.00
16.00
15.00
14.00
13.00
12.00
11.00
10.00
9.00
8.00
7.00
6.00
5.00
4.00
3.00
2.00
1.00
0.00
0
200
400
600
800
1000
1200
1400

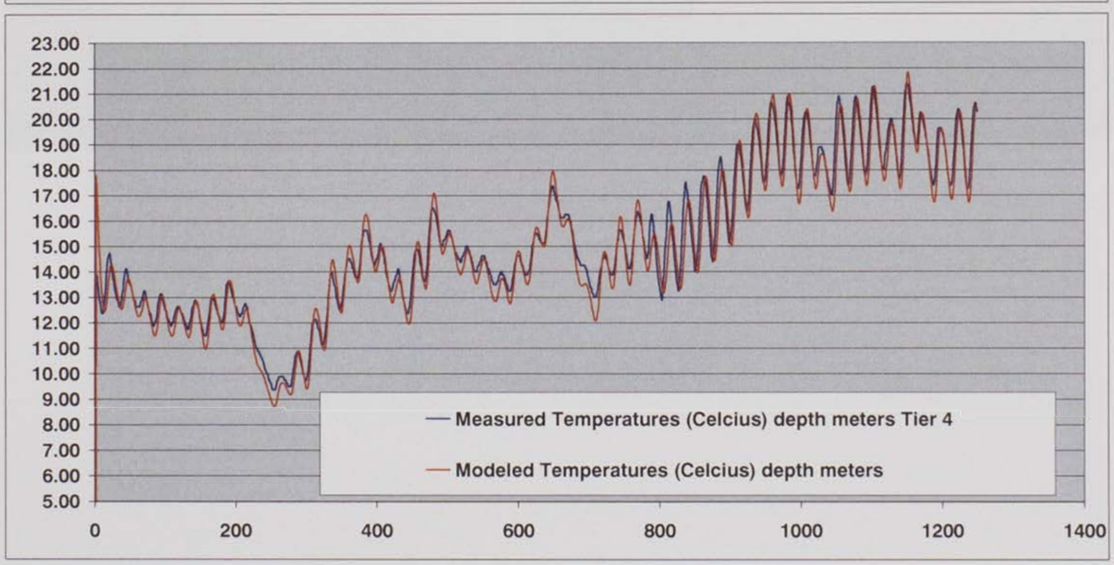
Measured Temperatures (Celcius) depth meters Tier 4
Modeled Temperatures (Celcius) depth meters
23.00
22.00
21.00
20.00
19.00
18.00
17.00
16.00
15.00
14.00
13.00
12.00
11.00
10.00
9.00
8.00
7.00
6.00
5.00
0
200
400
600
800
1000
1200
1400

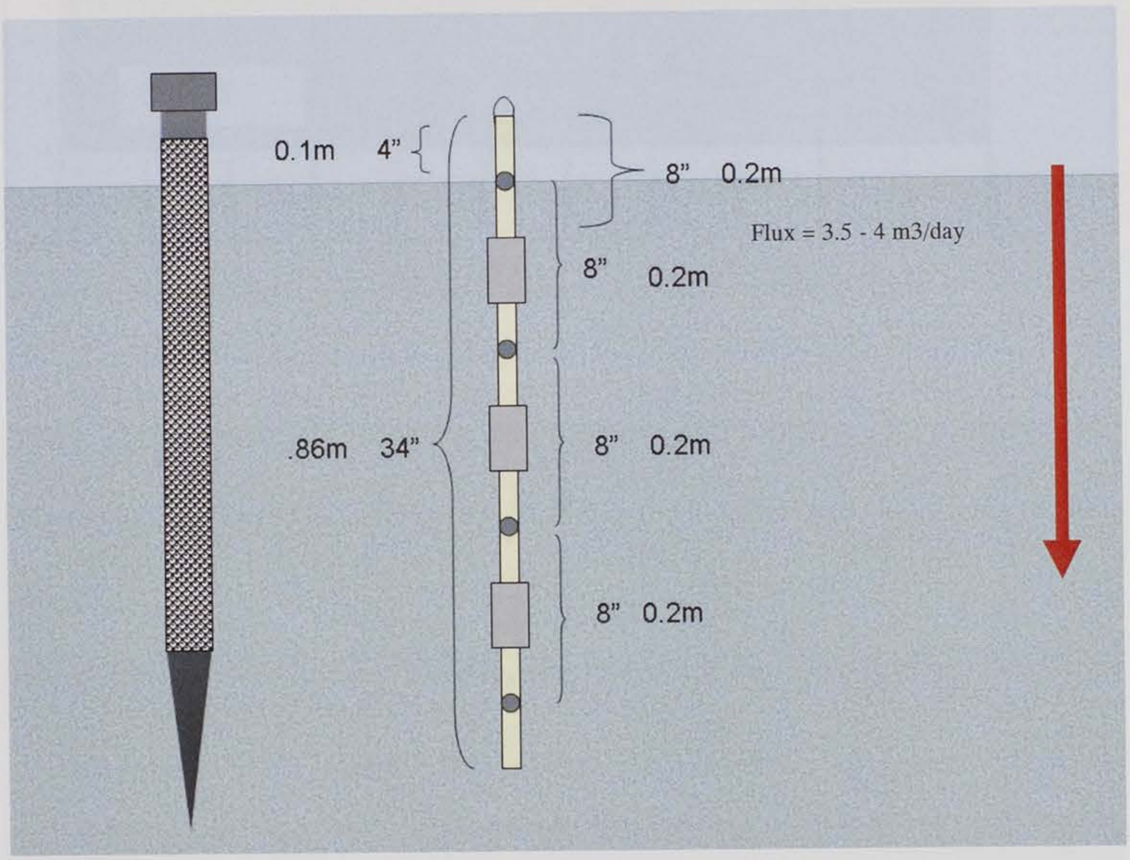
0.1m 4"
8" 0.2m
Flux = 3.5 - 4 m3/day
8" 0.2m
.86m 34"
8" 0.2m
8" 0.2m

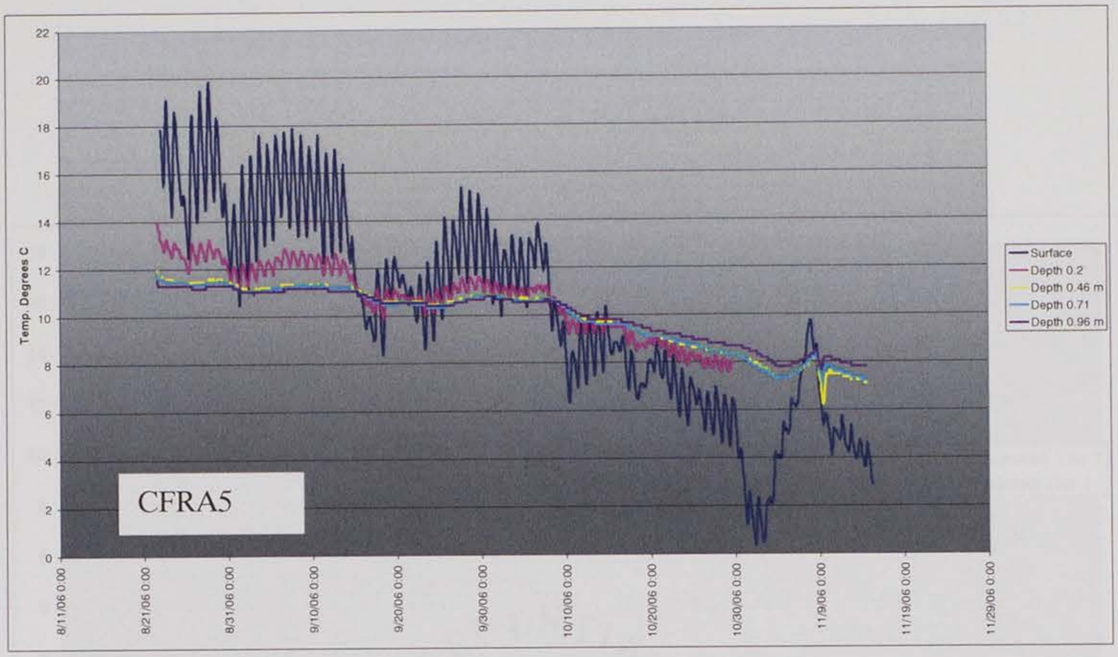

CFRA5
Temp. Degrees C
Surface
Depth 0.2
Depth 0.46 m
Depth 0.71
Depth 0.96 m
8/11/06 0:00
8/21/06 0:00
8/31/06 0:00
9/10/06 0:00
9/20/06 0:00
9/30/06 0:00
10/10/06 0:00
10/20/06 0:00
10/30/06 0:00
11/9/06 0:00
11/19/06 0:00
11/29/06 0:00

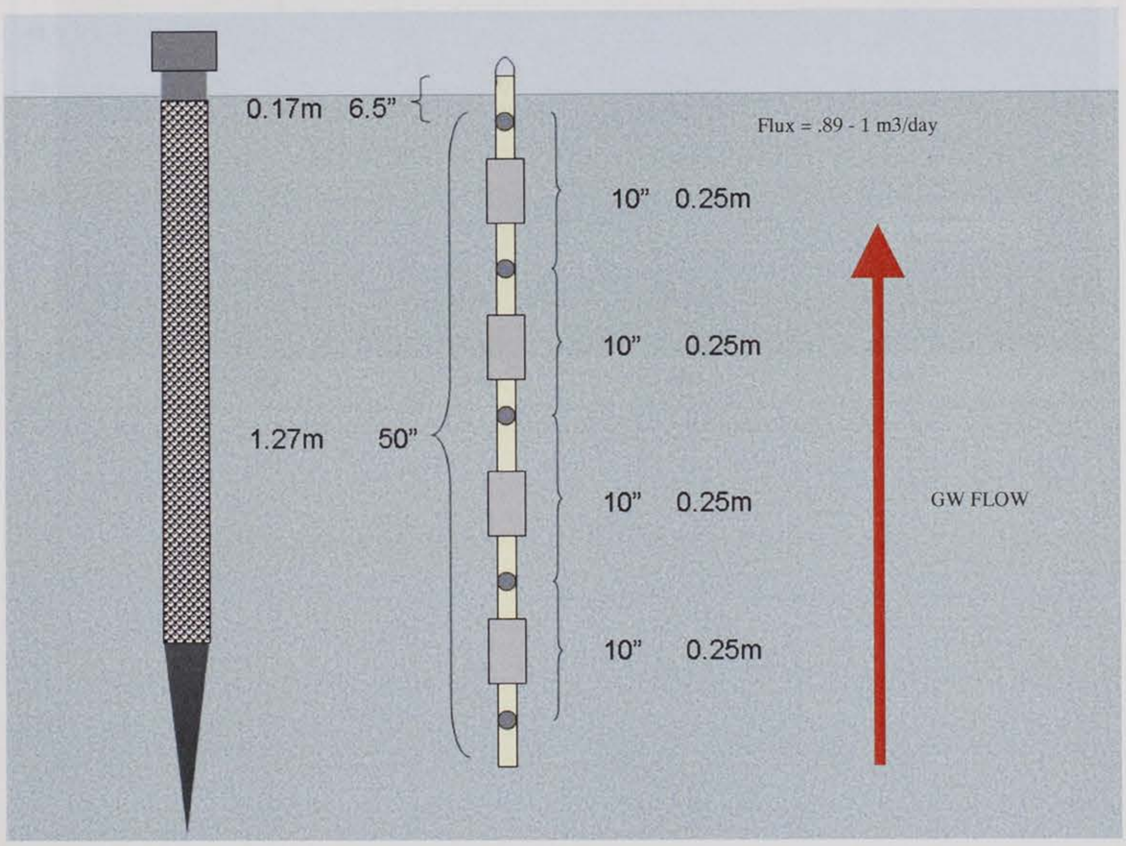

0.17m 6.5"
Flux = .89 - 1 m3/day
10" 0.25m
10" 0.25m
1.27m 50"
10" 0.25m
GW FLOW
10" 0.25m

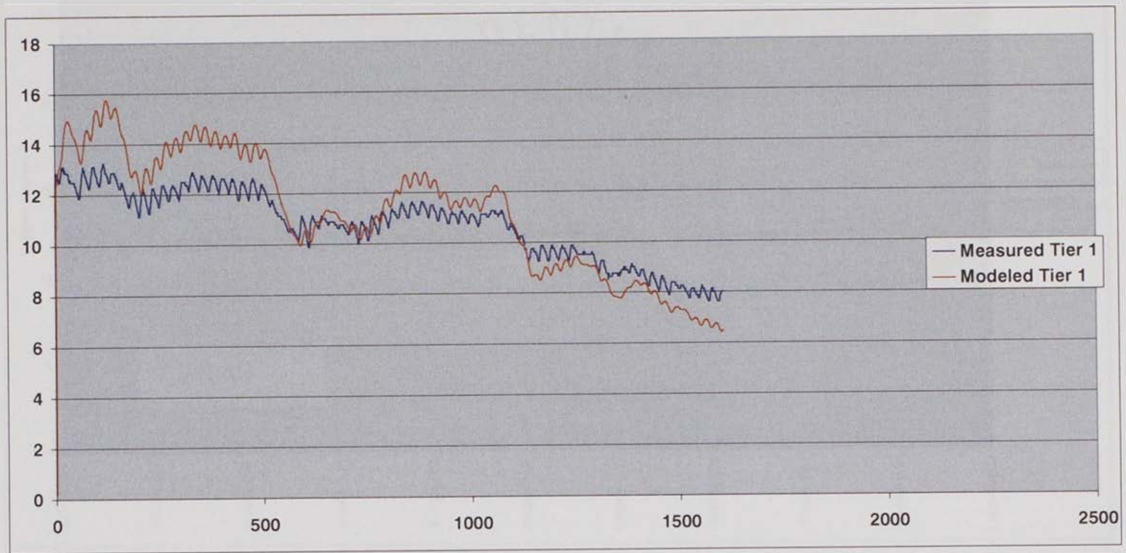

18
16
14
12
10
8
6
4
2
0
0
500
1000
1500
2000
2500
Measured Tier 1
Modeled Tier 1

14
12
10
8
6
4
2
0
0
500
1000
1500
2000
2500
Measured Tier 2
Modeled Tier 2

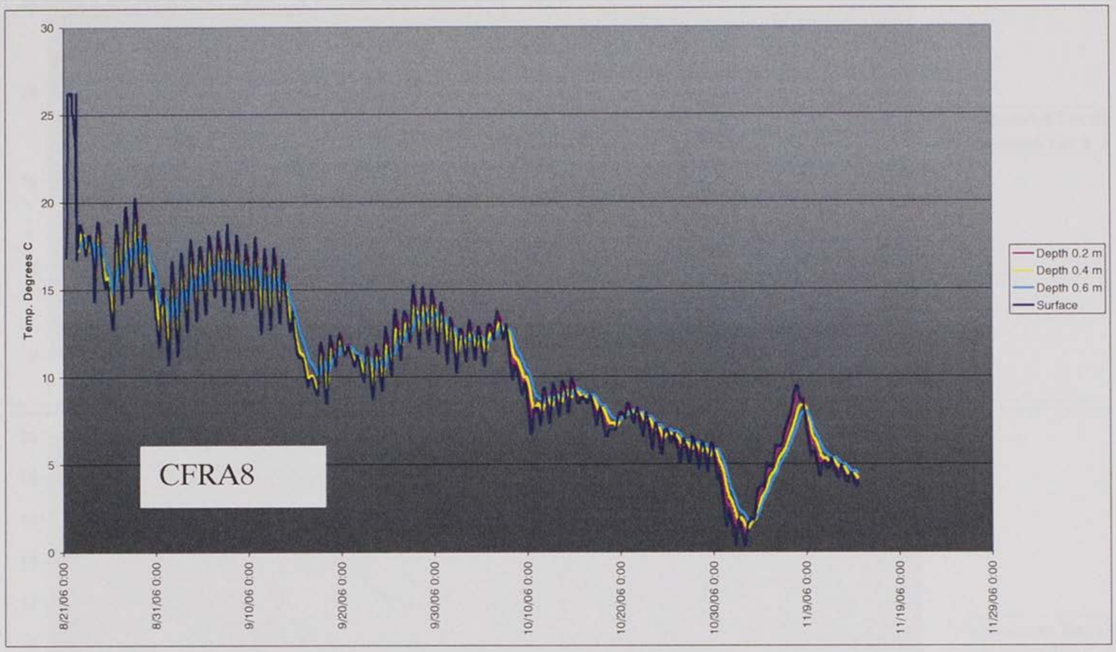
CFRA8
Temp. Degrees C
Depth 0.2 m
Depth 0.4 m
Depth 0.6 m
Surface
8/21/06 0:00
8/31/06 0:00
9/10/06 0:00
9/20/06 0:00
9/30/06 0:00
10/10/06 0:00
10/20/06 0:00
10/30/06 0:00
11/9/06 0:00
11/19/06 0:00
11/29/06 0:00

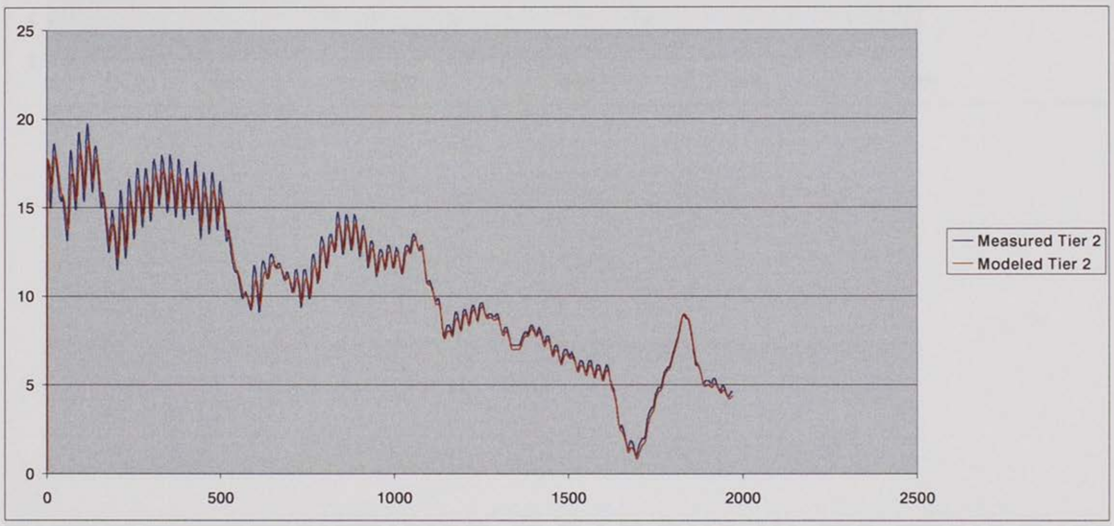
Measured Tier 2
Modeled Tier 2

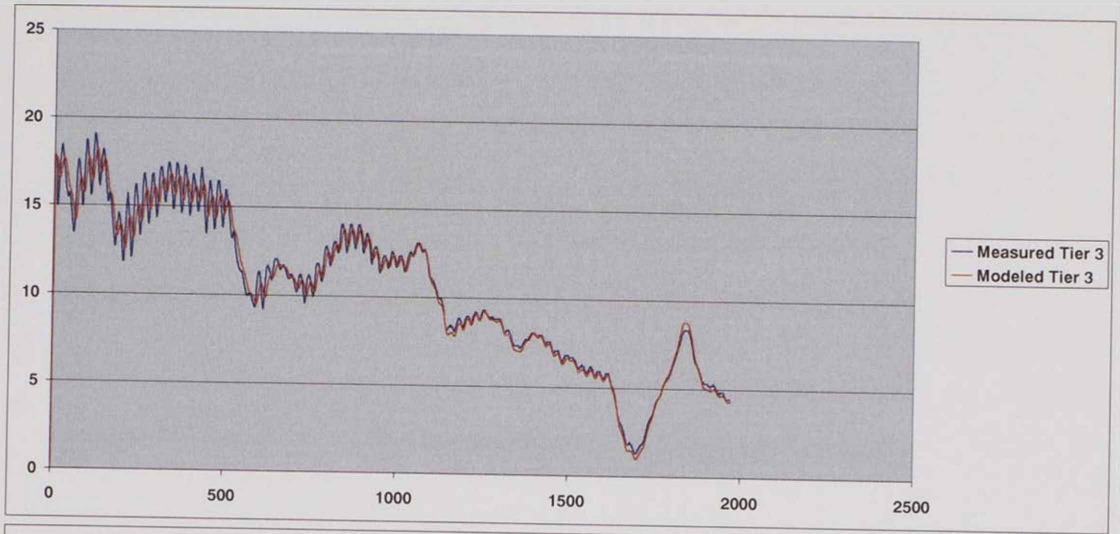
25
20
15
10
5
0
0
500
1000
1500
2000
2500
Measured Tier 3
Modeled Tier 3

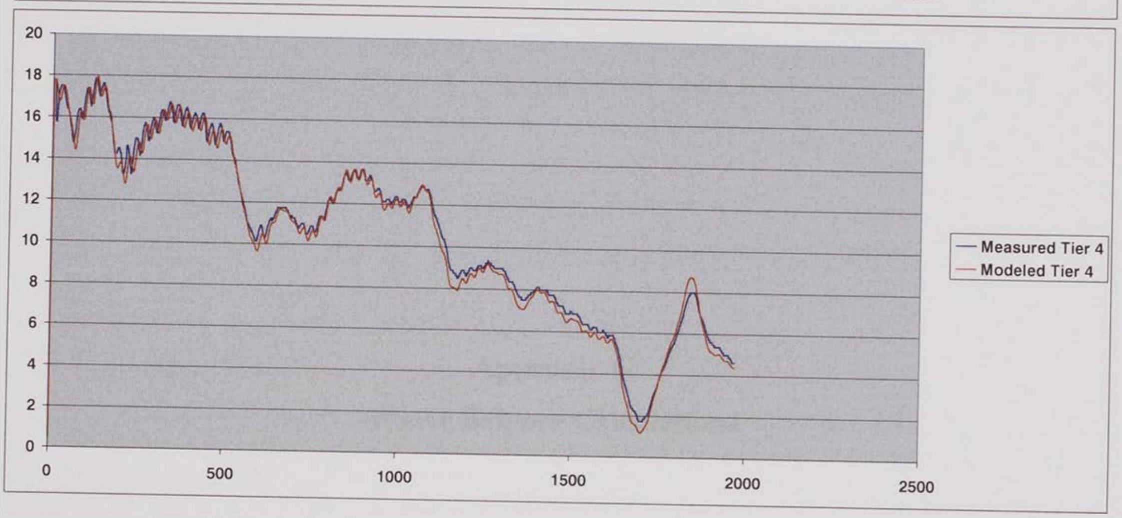
20
18
16
14
12
10
8
6
4
2
0
0
500
1000
1500
2000
2500
Measured Tier 4
Modeled Tier 4

Appendix G
Water Balance Calculations

Water Balance Calculations

Below is a detailed description explaining how each component of the estimated steady state water balance was estimated for low flow conditions. An annual groundwater balance for the project area was formulated as follows:

$$GW_{inCFU} + GW_{inBFU} + GW_{inDC} + GW_{inSC} + GW_{inBFR} + CFR_{leak} + Res_{leak} = GW_{outHGU} + GW_{ConsP} + GW_{outCFR} +/- \Delta \text{Storage}$$

Where:

GW_{inCFU} is lateral groundwater underflow at Turah Bridge

GW_{inBFU} is lateral groundwater underflow from the Blackfoot River valley,

GW_{inSC} is lateral groundwater underflow from side canyons including Deer Creek (DC), Marshall Creek (MC) and Crystal Creek (CC)

GW_{inMC} is lateral groundwater underflow from Marshall Creek,

GW_{inBFR} is seepage (recharge) from the Blackfoot River channel,

CFR_{leak} is seepage (recharge) from the Clark Fork River Channel,

Res_{leak} is seepage (recharge) from Milltown Reservoir,

GW_{outHGU} is lateral groundwater underflow at Hellgate Canyon,

GW_{ConsP} is consumed groundwater pumped from wells,

GW_{outcfr} is groundwater seepage into the Clark Fork River,

and Δ Storage is the net change in groundwater storage (net annual water level changes).

Blackfoot Canyon Underflow

Underflow estimates were determined using Darcy's law. The area of the Blackfoot canyon was estimated using the saturated thickness map to obtain a cross section of the valley (132610 ft^2). The saturated thickness map was created from the interpolated bedrock surface discussed in Berthelote (2007) and summarized in this report, and with the September 2006 groundwater surface. The horizontal hydraulic gradient was estimated to be 0.0013 from the September 2006 groundwater measurements. Nearby hydraulic conductivity suggest that the hydraulic conductivity of the aquifer is between 500 ft/day and 3,500 ft/day.

Clark Fork Canyon Underflow

The area of the Clark Fork canyon at Turah bridge was estimated using the same saturated thickness map as the one used to estimate the cross sectional area of the Blackfoot canyon. The area of the Clark Fork canyon at Turah was approximately 411650 ft^2, the horizontal hydraulic groundwater gradient was estimated to be 0.0025 and the hydraulic conductivity range of 500 ft/day to 1,500 ft/day.

Hellgate Canyon Underflow

The cross sectional area in Hellgate Canyon was estimated to be 115,000 ft^2 using Bethelote's bedrock elevation map and the water table from September 2006. The cross sectional area determined by Tallman (2005) of 319,000 ft^2 was determined to be overestimated. The hydraulic gradient was estimate using water table maps from September 2006 (0.023) and the hydraulic conductivity was estimated to range between 4,500 and 35,000 ft/day. Estimates of flux ranged from $2.7x10^6$ to $9.3x10^6$ ft^3/day. Tallman (2005) estimated flow through Hellgate Canyon to be $3.8x10^6$ ft^3/day to $7.6x10^6$ ft^3/day and estimated hydraulic conductivity in the canyon to be lower. Gestring estimated underflow through Hellgate Canyon ranging from $3.8x10^6$ to $7.5x10^6$ ft^3/day ; his numerical flow model was calibrated to an underflow of $6.1x10^6$ ft^3/day. Brick's [2003] model of the Milltown Dam Reservoir calculated a down gradient outflow through Bandman Flats of 4.6×10^6 ft^3/day. The values determined in this study for flow through Hellgate Canyon do bracket the values determined to flow through Bandman Flats. Therefore, the estimated range of discharge through Hellgate Canyon appears reasonable.

River Seepage Estimates

Surface water and groundwater exchanges were derived from the conceptual distributions of gaining and losing reaches and the flux rates determined by temperature modeling. Conceptual distributions are shown on Figures 56, 57 and 58. The distribution of these gaining and losing areas was assumed to extend halfway between measured points. The river flux estimates were estimated using data collected in the fall of 2006 during the initial drawdown. River flux estimates were made outside of the area of influence of the reservoir drawdown at this time with the exception of the flux estimates made in the BFR arm of the reservoir, which because of this may be underestimated.

CFR above the dam

Seepage from the Clark Fork River above the dam was estimate for 4 separate areas of river. The two reaches were gaining reaches and two reaches were losing reaches.

The first reach was the losing reach along Chuck Erickson's property. It was measured to have an approximate area of 823,771 ft^2. The seepage rates in this area were estimated for this reach from the Darcy's Law calculations and ranged from 0.8 to 0.16 $ft^3/day/ft^2$. Seepage data from temperature data was not used in this calculation because no data from baseflow conditions was retrieved as the temperature instruments were not found after the initial retrieval.

The second losing river segment (near Turah) was estimated to be 733296 ft^2. The seepage rate in this area was measured to be approximately 2.9 to 3.2 $ft^3/day/ft^2$ during baseflow conditions in the fall of 2006.

Groundwater flow into the Clark Fork River above Milltown Dam was estimated above the dam in two different areas. The first area was just upgradient of the duck bridge with an estimated area of 1,762,711 ft^2. Some of this area included the ditches and drainage network that suddenly appear as river channels in this area. The flux rate was measured at 0.82 to 0.7 $ft^3/day/ft^2$. The second area is the gaining reach along Crystal Creek Ranch property. The estimated area of this reach is 316,296 $ft^3/day/ft^2$. The flux rate in this area was estimated to be 2.9 to 3.2 $ft^3/day/ft^2$.

CFR below the dam

The Clark Fork River Below the dam has one river reach that was designated as gaining that extends from the dam to approximately 600 ft downgradient and a losing reach that extends the rest of the way down into Hellgate Canyon. The gaining reach below the dam was estimated to have an area of approximately 596,168 ft^2 and flux rates that were estimated from Darcy's Law to be 0.7 to 6 $ft^3/day/ft^2$ using a measured hydraulic conductivity range of 2 to 20 ft/day for river bed sediments and a measured gradient of 0.33.

The losing reach below the dam has an approximate area of 3,258,591ft^2 with estimated seepage rates from temperature monitoring that range between 0.72 and 3.0 $ft^3/day/ft^2$ during baseflow conditions measured in August 2006.

Blackfoot River

The Blackfoot River within the study area a losing river. The seepage from the river into the groundwater was estimated as one reach from where the Blackfoot River enters the Clark Fork River upgradient to station BFR6. The surface area of the Blackfoot River was estimated from maps to be 1,574,991 ft^2 with seepage rates estimated at 0.98 to 1.2 $ft^3/day/ft^2$

Reservoir

The flux from the reservoir area was estimated using Darcy's law. The estimated area of the reservoir was 3,571,390 ft^2 and the hydraulic conductivity was estimated to range between 0.019 and 0.2 and the hydraulic gradient was estimated at 0.25.

Appendix H

Summary of Error Estimates

The table below presents the errors estimated for each method used.

Technique	Method / Equipment	Error	References
Single Point Survey	Trimble XPS Survey Grade GPS	0.02 m	(Trimble, 2008)
River Stage	USGS Gage	0.003 m	(USGS,2008)
	Study Installed Staff Gage	0.003 m	(Berthelote et al., 2007; Gestring, 1994; Tallman, 2005)
	Study Installed Continuous Data Recorder	0.07 m	(Berthelote et al., 2007; Gestring, 1994; Tallman, 2005)
Groundwater Levels	Steel or Electronic Tape	0.03 m	(Berthelote et al., 2007; Gestring, 1994; Tallman, 2005)
	Solinst Data Recorder	0.07 m	(Berthelote et al., 2007; Gestring, 1994; Tallman, 2005)
Vertical Hydraulic Gradients	Peizometer	0.02	(Caldwell and Bowers, 2003; Tallman, 2005)
	VS2DHI	0.02	(Hsieh et al., 2000; Johnson et al., 2005)
Stream Bed Conductivity	Falling Head Test	3 %	(Landon et al., 2002)
Aquifer Conductivity	Peak Lag Analysis	6 %	(Pinder et al., 1969)
	Flow Tube Analysis	7.6 %	(Fetter, 2001)
	Historical Pump Tests	6.4 %	(Jahns, 1966; Land and Water Consulting, 2005; Walton, 1987)
Porosity & Specific Yield	Literature	- %	(Fetter, 2001)
Storativity	Literature		(Land and Water Consulting, 2004; Newman, 1996; Newman, 2005; Woessner W.W. and Popoff W.A., 1982; Woessner et al., 1984)
Numerical Modeling	Modflow with Groundwater Vistas	1.5 m	(Anderson and Woessner, 1992; Doherty, 2000; Environmental Simulations Inc. (ESI), 2004; Harbaugh, 2005; Harbaugh et al., 2000; Hill M.C., 1990; Hill, 1992; Hill, 1998; Hill and Tiedeman, 2007)
Bedrock-Alluvium Boundary	Well Logs	1.5 m	(GWIC, 2008)
	Slope Projections	- m	(Brick, 2003; Janiszewski, 2007; Nyquest, 2001)
	Bore Holes	0.6 m	(Janiszewski, 2007; Nyquest, 2001)
	Seismic Lines	4.5 m	(Gradient Geophysics, 1991; Janiszewski, 2007)
	Constrained Gravity	9 m	(Cordell and Henderson, 1968; Croft B., 2006; Evans, 1998; Gradient Geophysics, 1991; Hennes A., 2002; Janiszewski, 2007; Nyquest, 2001)

Appendix I
Summary of Model Calibration

Summary of Model Calibration

The following sections provide a detailed summary explaining the calibration process and results of the numerical groundwater model developed for this study. The model is further described in Berthelote et al. (2007).

Groundwater Model Execution and Calibration

The three-dimensional model was constructed and parameterized based on field observed water levels, measured and interpolated river and aquifer properties and geometries, and application of basic hydrogeologic principals. The calibration process consisted of performing an iterative process comparing model results with set calibrations targets. Targets included water levels measured at monitoring points, a historical water budget, the locations and rates of surface water groundwater exchanges, and lumping statistics that include all values such as the mean absolute error (Anderson and Woessner, 1992. Targets were specified for both steady state and transient calibrations (Table I-1). Qualitative calibration evaluations were applied including the general match of measured and modeled water table maps, and in transient simulations, the similarity of simulated verses measured hydrographs at monitoring points. In addition, modeled parameter values are expected to fall within estimated values based on field measurements and literature values, and within the known and interpreted geologic settings.

Calibration Parameter	Calibration Target	Target Type
Groundwater Levels	Absolute residual mean error +/- 4.5 ft	Quantitative
Water Balance Underflow	Within estimated range (Tables 4a & 4b)	Quantitative
River and Reservoir Leakage	Within estimated range (Tables 4a & 4b)	Quantitative
Location of Gaining and Losing River Reaches	+/- 0.5 mile	Qualitative
Match of Simulated and Measured Water Table Maps and Hydrographs (transient)	Observed closeness of fit	Qualitative
Aquifer Parameter Distribution	Supported by field data and geologic data sets	Qualitative

Table I-1 Listing of Calibration Parameters and Targets.

Initial calibration was formed on a steady state model. The calibrated steady state heads and fluxes were then input as initial conditions in a transient simulation. Once again an iterative calibration process was used to calibrate the transient model. The calibrated parameters and model structure of the transient model were then fed back into the steady state model to check to see if the new parameter distributions generated during transient calibration fit the steady state calibration. This process was repeated until both the steady state and transient models were considered calibrated with a common set of parameters. As a further evaluation the calibrated model was then applied to an independent data sets (not used for calibration), Gestring's 1992-1993 measurements. These data only include information for the Milltown area to Hellgate Canyon (Figure I-1).

Calibrated Groundwater Flow Model

The model calibration effort resulted in a supportable three-dimensional representation of the groundwater conditions within the region of investigation. The calibrated parameter distributions and calibration statistics related to steady state, transient and history match conditions are presented in the next sections.

Calibrated Parameter Distributions

The calibrated hydraulic conductivity distribution ranged from 75 to 60,000 ft/day (Figure I-1). Areas of low hydraulic conductivities are proximal to the confluence of the Clark Fork and Blackfoot River rivers. Regions of high conductivity are located in West Riverside and near the mouth of Hellgate Canyon. Initial assignment of reported field derived aquifer hydraulic conductivity underwent slight modifications during model calibration. The final distribution of parameters is shown in Figure I-1. These distributions area supported by well log interpretations, basic sediment depositional process theory, observed water level responds, and measured and interpreted flux rates. A storativity value of $1e^{-6}$ was assigned to cells in layers 2 through 6. Layer one was modeled as an unconfined aquifer and was assigned a specific yield of 0.15. Modeled porosity was assigned as 0.2 throughout. All storage and porosity values remained constant for all model runs. Reported aquifer hydraulic conductivity values in this work ranged from 300 to 90,000 ft/day.

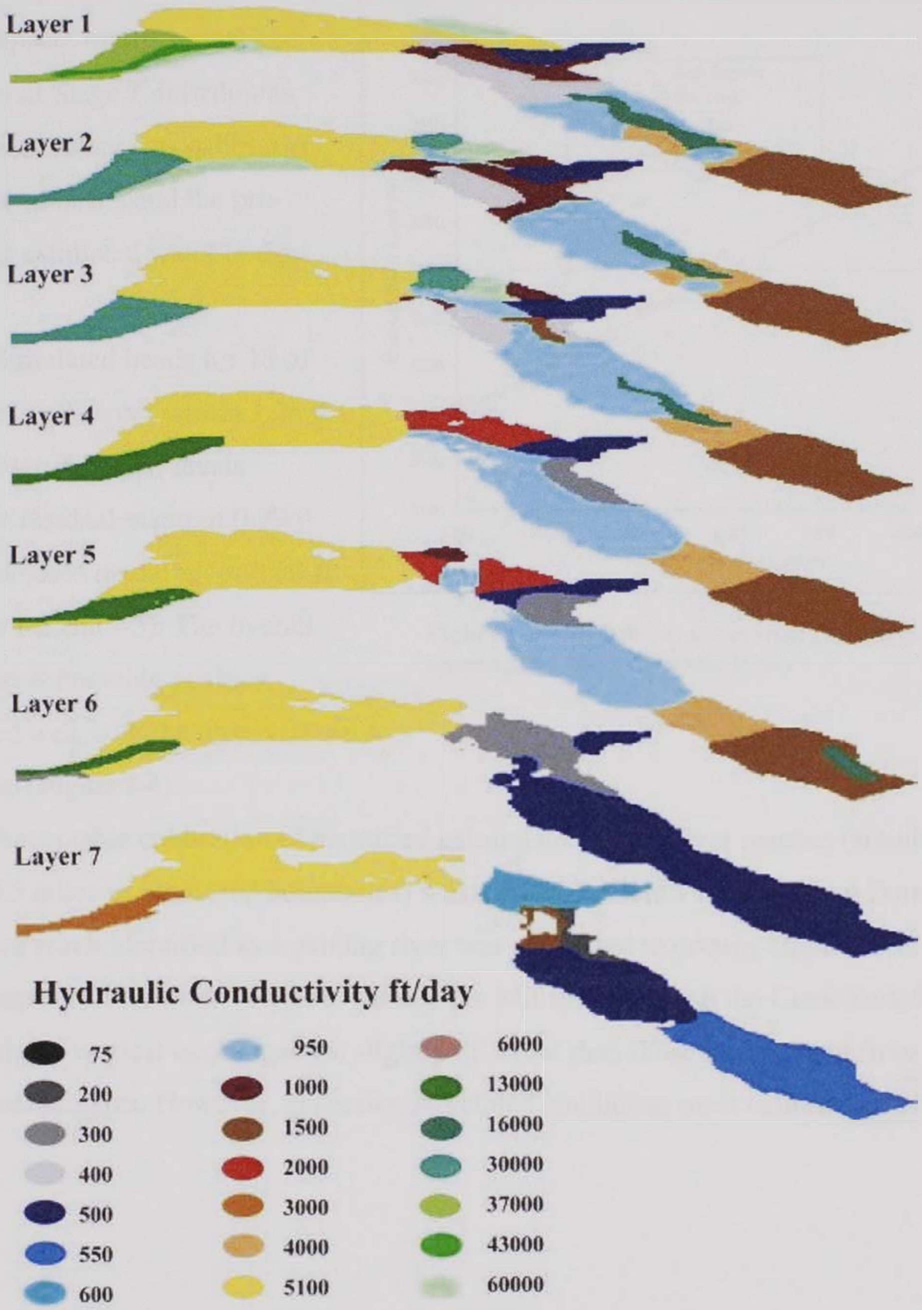

Figure I-1 Calibrated hydraulic conductivity distributions for each layer of the numerical model. Conductivities less than 500 ft/day are in grayscale with the Milltown Dam (K=75) being black. Conductivities between 500 and 950 ft/day are in blue scale, between 1000 and 10000 ft/day are in red scale, and between 10000 and 60000 ft/day are in green scale.

Steady State

The steady state model simulated conditions for March 31, 2006 which was the first new full data set collected prior to spring runoff events and initiation of Stage 1 drawdowns (June). The model was calibrated to measured heads and the pre-modeling estimated water budget terms.

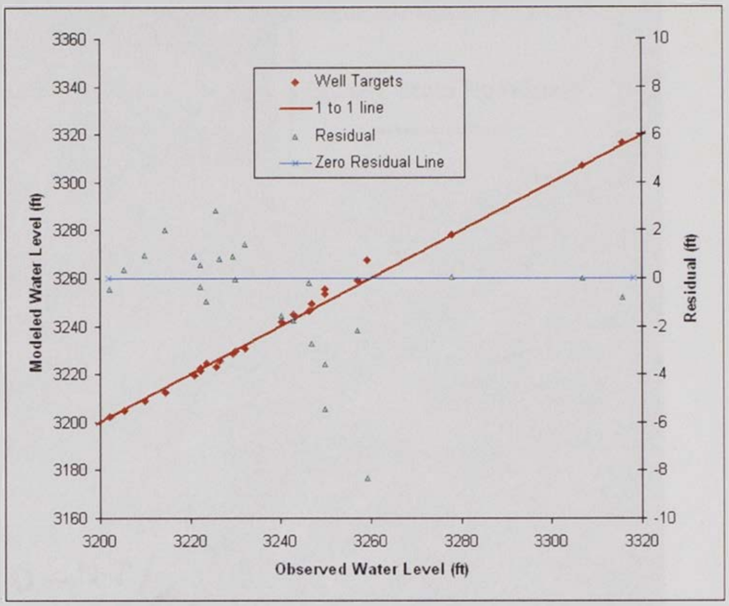

Figure I-2 Graph showing the steady state residuals and measured vs. observed water levels

Simulated heads for 18 of the target wells were within 1.75 ft of the observed water levels (absolute residual mean of 0.79 ft with a standard deviation of 0.60 ft) (Figure I-2 and I-3). The overall simulated water table position compared well with the observed water table map (Figure I-4).

Acceptable calibration of identified gaining and losing river reaches (simulated within 0.5 miles of measured boundaries) was achieved. Below the Milltown Dam the short river reach identified as a gaining river was simulated to occupy slightly less river reach length than the observed area. Above the Milltown Dam on the Clark Fork River the simulated vertical exchanges are slightly different than those interpolated from point field measurements. However, generally, simulated conditions meet calibration criteria.

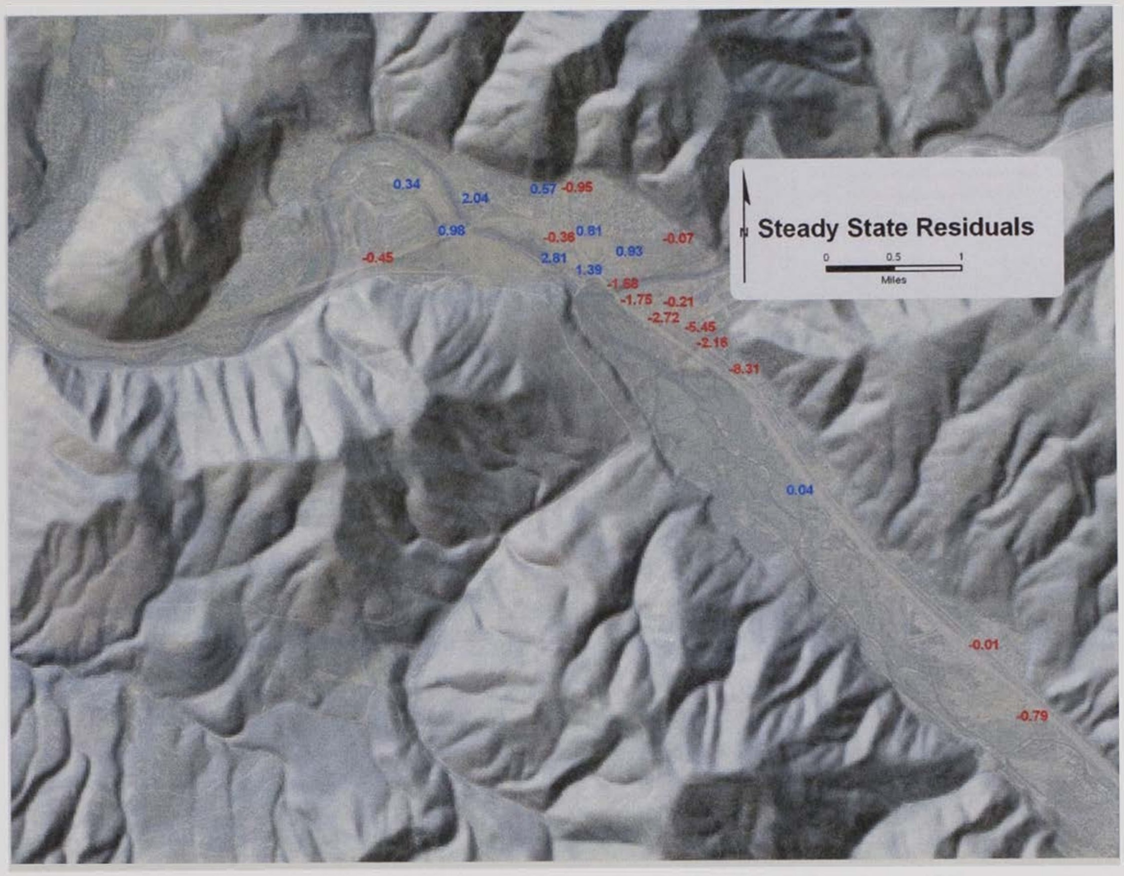

Figure I-3 Final distribution of residuals after steady state calibration. The numbers indicate the head difference from the observed water level to the simulated water level. Positive numbers (blue) indicate areas where the simulated water table is higher than observed values. Negative numbers indicate areas where the simulated water table is lower than observed values.

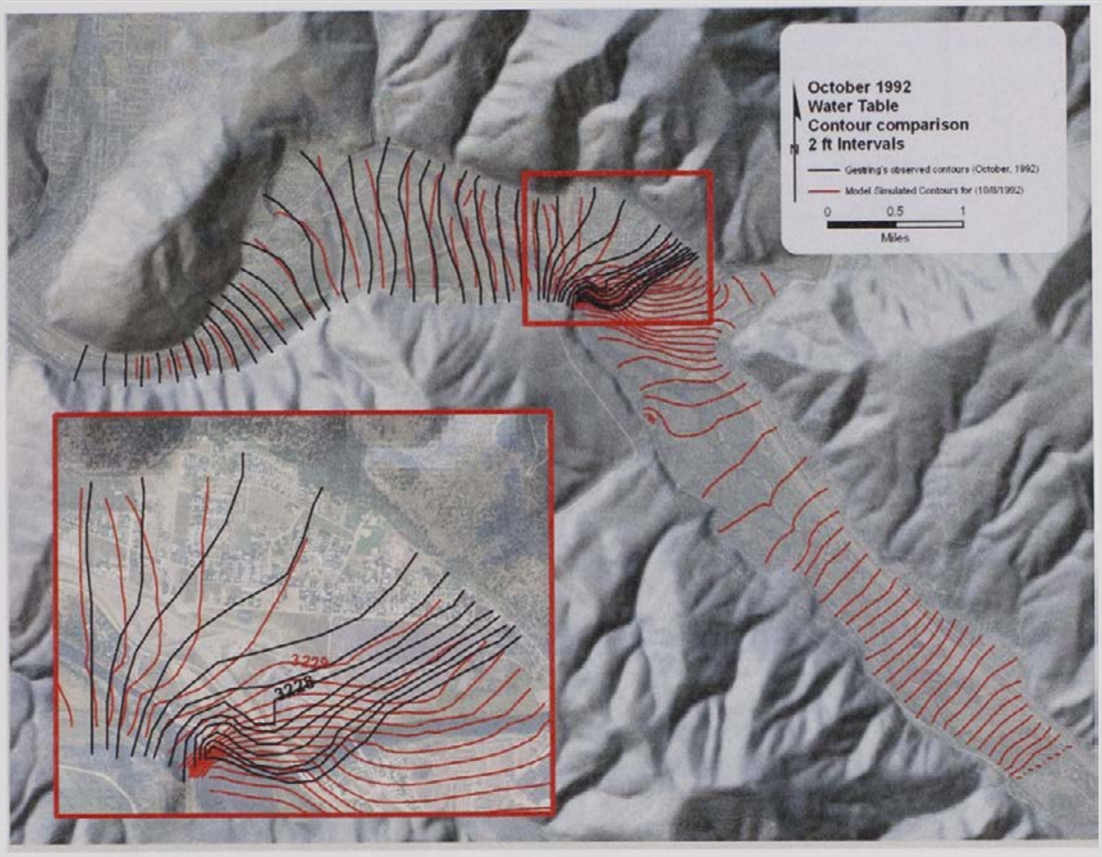

Figure I-4 Water table map for the March 31, 2006 head distribution (black lines have a 2 ft even contour intervals) and the simulated steady state heads (red lines have 2 ft odd numbered contour intervals).

The simulated steady state water budget (Table I-2) compared favorably with the pre-model estimated steady state budget. At first, the simulated water budget appears to have slightly underestimated the groundwater discharge from the aquifer into the Clark Fork River. This value is likely underestimated as the model underestimated groundwater discharging to the river below the dam.

	Steady State Model Value		Estimated Range	
			min	max
	Net flow		Net flow	Net flow
	ft^3/day	%	ft^3/day	ft^3/day
CFR above dam	-6.8E+05	-8	-8.00E+04	3.34E+06
Reservoir	1.7E+06	21	1.80E+05	3.20E+06
CFR below dam	3.1E+06	37	2.01E+06	6.10E+06
BFR arm	1.8E+06	22	1.50E+06	1.90E+06
GWinCFU	1.3E+06	16	5.20E+05	1.50E+06
GWinBFU	5.8E+05	7	8.60E+04	5.20E+05
GWoutHGU	-8.3E+06		-2.70E+06	-9.30E+06

Table I-2 Comparison of the pre-model estimated and simulated steady state water balance. Values shown in red fell outside of the estimated pre-model range.

Transient

The calibrated steady state heads, boundaries and fluxes were used as initial conditions during transient model calibration. The comparison of simulated heads to observed heads (March 31, 2006 to April 21, 2007), and the pre-modeling estimated water balance revealed the model does a reasonable job of simulating observed conditions under this more demanding evaluation. The results show the head match during the initial few stress periods was poorer than in later periods of the modeling effort (Figure I-5). This is most likely partly a result of an incomplete representation of flow and head conditions during spring runoff when river stages and groundwater levels were changing rapidly. However, residuals did stabilize as time progressed suggesting general transient conditions are appropriately represented.

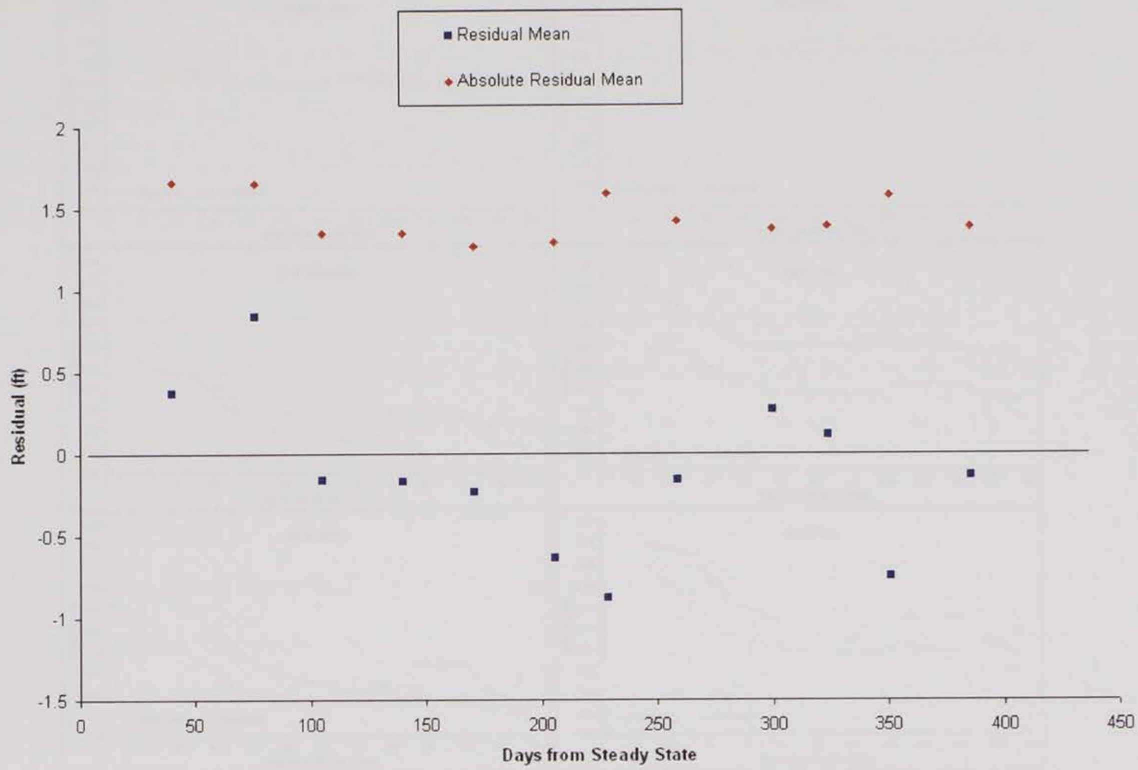

Figure I-5 Plot of the residual mean and absolute residual mean for each modeled stress period (varying length is days, see the accompanying table for stress period ending time (time) and computed statistics).

The comparison of observed and simulated heads over time at calibration targets provides an additional method with which to assess the representativeness of the numerical model (Figure I-6). Results show relatively good fits at most sites with simulated water levels following observed levels and trends.

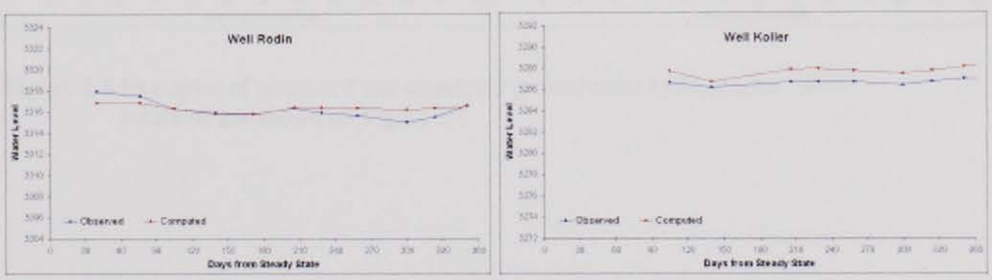

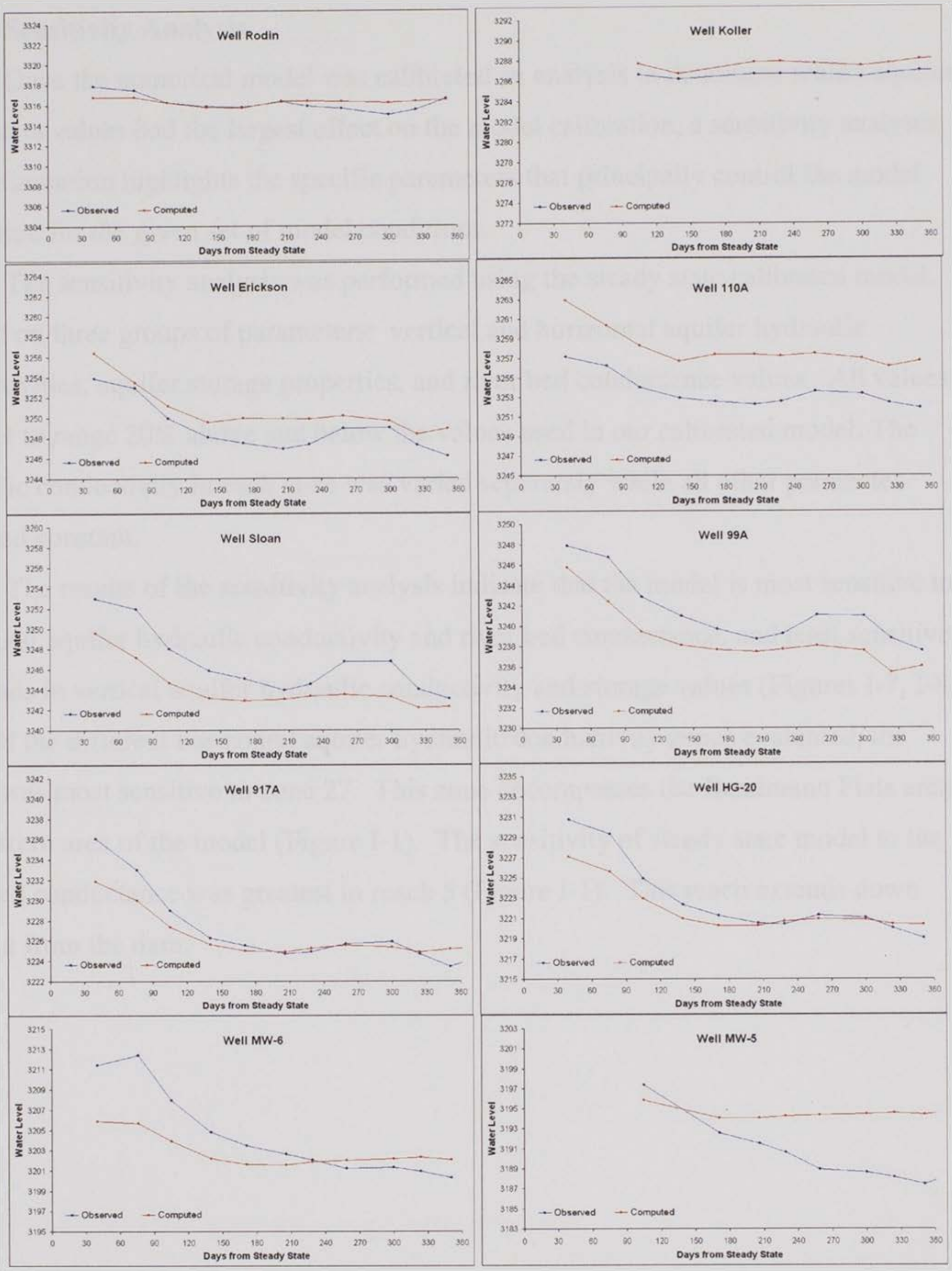

Figure I-6 Examples of measured and simulated groundwater hydrographs. Well locations are shown on Figure 10.

Sensitivity Analysis

Once the numerical model was calibrated an analysis to determine which aquifer parameters values had the largest effect on the model calibration, a sensitivity analyses. This information highlights the specific parameters that principally control the model calibration for the given set of model conditions.

The sensitivity analysis was performed using the steady state calibrated model. It focused on three groups of parameters: vertical and horizontal aquifer hydraulic conductivities, aquifer storage properties, and river bed conductance values. All values were set to range 20% above and below the values used in our calibrated model. The hydraulic conductivity in each zone was varied separately while all other parameter remained constant.

The results of the sensitivity analysis indicate that the model is most sensitive to horizontal aquifer hydraulic conductivity and river bed conductance, and least sensitive to variations in vertical aquifer hydraulic conductivity and storage values (Figures I-7, I-8, I-9). Of the different horizontal aquifer hydraulic conductivity zones evaluated, the model was most sensitive to zone 27. This zone encompasses the Bandmann Flats area in the western area of the model (Figure I-1). The sensitivity of steady state model to the river bed conductance was greatest in reach 5 (Figure I-1). This reach extends down gradient from the dam.

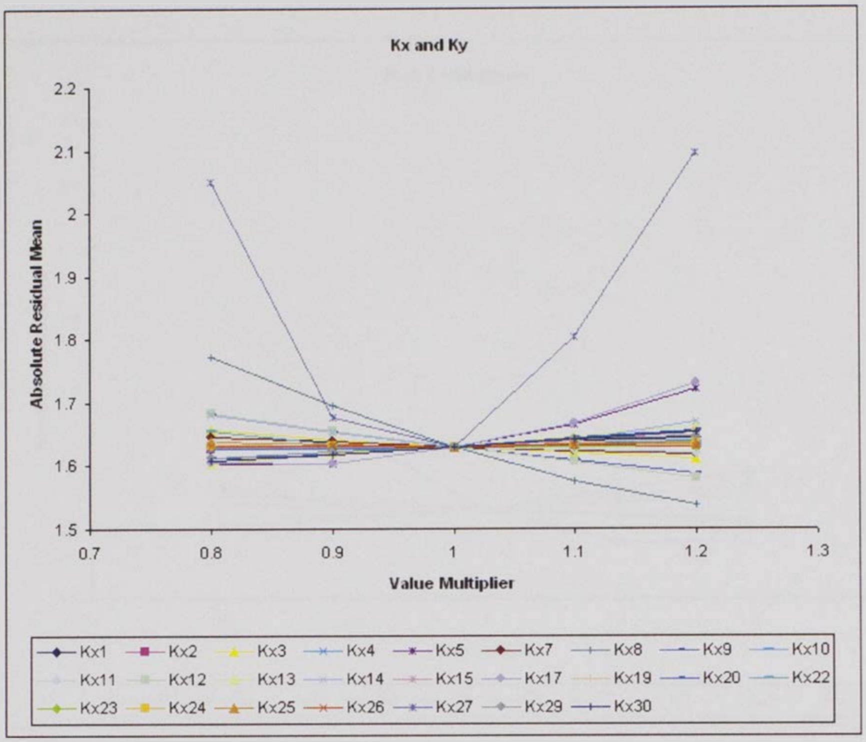

Figure I-7 The sensitivity results show how the model is sensitive to different horizontal conductivity zones. The Kx values represent different conductivity zones within the model.

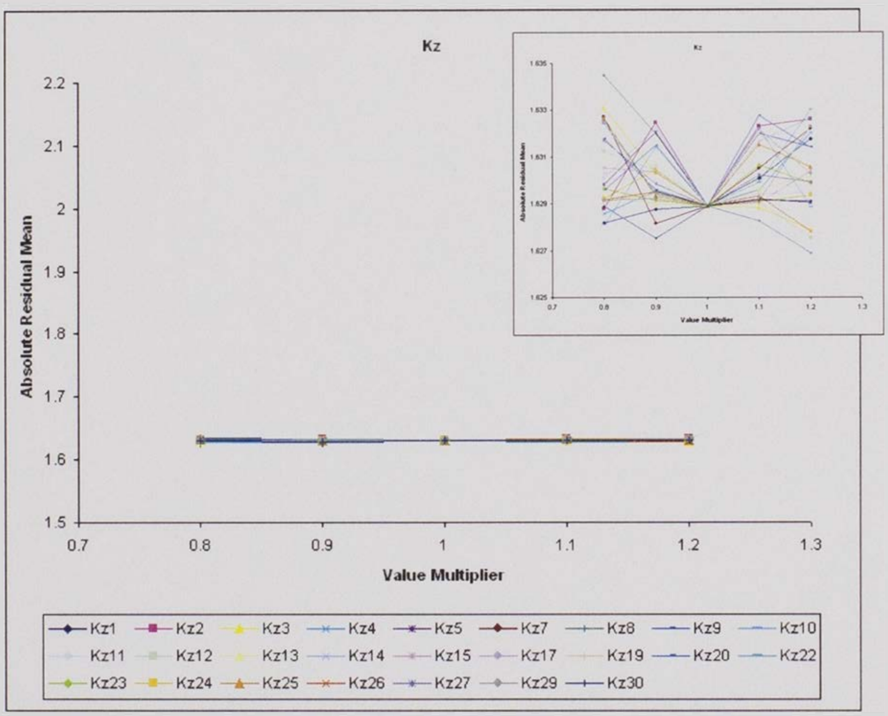

Figure I-8 The sensitivity results show how the model is not very sensitive to different vertical conductivity zones. The Kz values represent different vertical conductivity zones within the model. Each vertical conductivity zone is 0.10 of the horizontal conductivity.

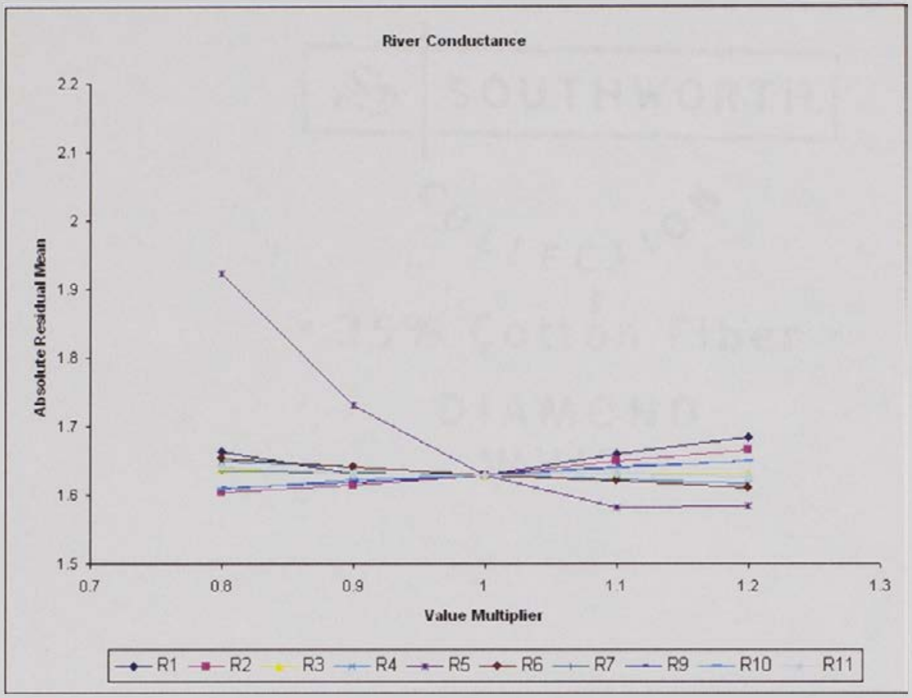

Figure I-9 Simulated drawdown. Illustration created by differencing the March 2006 steady state and predicted modeled water tables.